The completion of this thesis
was supported by the
Randy Seeling Award
given, in his memory, to another
outstanding graduate student
of the Geology Department,
University of Minnesota, Duluth.

STRATIGRAPHY, PHYSICAL VOLCANOLOGY, AND HYDROTHERMAL ALTERATION OF THE FOOTWALL ROCKS TO THE WINSTON LAKE MASSIVE SULFIDE DEPOSIT, NORTHWESTERN ONTARIO

A Thesis Submitted to the Faculty of the Graduate School

of the University of Minnesota

by

STEVEN ARVID OSTERBERG

In Partial Fulfillment of the Requirements

for the Degree of

Doctor of Philosophy

September, 1993

"Every mine manager, mine geologist, and every prospector in the field who appraises the future of mining properties does so on the basis of a theory of ore deposition whether he recognizes this fact or not."

R.H. Sales, May, 1954

ABSTRACT

The Winston Lake Zn-Cu-Ag massive sulfide deposit is situated above a sequence of metamorphosed Archean calc-alkaline volcanic and volcaniclastic rocks. A detailed mapping, petrographic, and chemical study was undertaken to evaluate the stratigraphic and hydrothermal development of the footwall rocks with regard to depositional environment and spatial controls on metasomatism and mineralization.

The footwall rocks are dominated by interlayered successions of metamorphosed volcaniclastic and volcanic rocks that have been extensively intruded and block faulted. Volcaniclastic-sediments were deposited at the base of the stratigraphy where they were interlayered with felsic pyroclastic deposits and/or their turbiditic equivalents. Locally massive sulfide and cherty exhalative beds were deposited.

A relatively thick section of interlayered felsic and mafic lava flows were erupted and deposited above the basal volcaniclastic rocks; minor interflow clastic and base metal-poor exhalative sediments accumulated during pauses in mafic volcanism. An upper clastic succession accumulated above the lava flows; basinal volcaniclastic-sediments were deposited and were overlain in part by felsic pyroclastic material that was erupted from a distant, extraneous source. Interlayered mafic lava flows and volcaniclastic rocks cap the footwall stratigraphy and host the Winston Lake deposit and stratigraphically equivalent mineralized occurrences.

Facies analysis of lava flows, along with the basinal distribution of volcaniclastic-sediments indicates the Winston Lake footwall stratigraphy developed

in a subsiding, subaqueous rift environment. Subsidence was focussed in the rift axis; associated stresses resulted in development of synvolcanic faults within and distal to the rift axis. The dominance of passive eruption products indicates volcanism occurred in relatively deep water beneath the volatile fragmentation depth.

Approximately 50% of the footwall stratigraphy has been hydrothermally altered in subconcordant to cross-stratal zones. Interaction of the rocks with metasomatic fluids, followed by isochemical metamorphism has resulted in unusual modal abundances of tremolite/actinolite, biotite, sillimanite, staurolite, anthophyllite/gedrite, chlorite, and quartz relative to metamorphosed primary compositions. Microprobe analyses indicate extreme Fe/Mg enrichment of ferromagnesian silicates near the base of the stratigraphy.

Mass balance analysis indicates variable enrichment of MgO, Fe_2O_3T, and K_2O, and depletion of CaO and Na_2O in altered rocks; TiO_2 and Al_2O_3 were relatively immobile. Overall mass losses, indicative of metasomatic leaching, dominate alteration towards the base of the stratigraphy, whereas both gains and losses occurred in the upper portions of the section.

Mg enrichment occurred in stratiform zones through shallow circulation of seawater-based hydrothermal fluids during progressive stratigraphic growth. Minor associated base metal-poor exhalites developed during intermittent pauses in volcanism and sedimentation. Substratiform zones of iron-aluminous-potassic alteration developed as chemically evolved fluids, which originated at depth, interacted with permeable lithologic units through which they buoyantly migrated.

The distribution of alteration indicates that chemically-evolved fluids rarely reached the sea floor environment but were generally confined beneath impermeable stratigraphic units. Metalliferous fluids periodically passed through the footwall rocks to the sea floor; no distinct chemical or mineralogical fingerprint of their passage is evident in the rocks, suggesting the metalliferous fluids were similar to chemically-evolved fluids except in metal content. The metalliferous fluids reached the sea floor during at least two stages of stratigraphic growth in which metals were deposited as massive sulfides. The first stage was at the Pick Lake deposit, near the base of the stratigraphy and the second stage was at the Winston Lake deposit at the top of the section.

The distribution and composition of alteration and associated base metal sulfide and cherty exhalative occurrences indicates the Winston Lake hydrothermal system was multistaged and involved multiple hydrothermal fluids. Stratigraphic development in a subsiding rift environment spatially controlled the movement of buoyant hydrothermal fluids through permeable lithologic units. Periodic synvolcanic faulting released metalliferous fluids to the sea floor where base metal sulfides were deposited.

ACKNOWLEDGEMENTS

This project would not have been possible without the support of numerous people, to all of whom my gratitude is herein extended. It is impossible to mention all individually, however, several deserve distinct recognition.

Ron Morton acted as a capable and most helpful thesis adviser. He first suggested the project and cheerfully provided direction and wise council throughout.

Minnova, Inc. gave me permission to work at Winston Lake and provided financial and logistical support for field work and provided me summer employment. Frank Balint, Gord Glenn, Rob Sim, Dan Courtney, and especially Ian Morrison deserve credit for providing discussion and technical assistance, and for willingly sharing of their knowledge of Winston Lake. Dave Thomas freely provided his geochemical data for my use. Paul Severin, now of Falconbridge Corp., was instrumental in initiating this project.

Jim Franklin of the Geological Survey of Canada gave insightful direction, and made analytical services of the G.S.C. available to me. Dr. Ingrid Karsgaard is gratefully acknowledged for her skillful microprobe analysis of my samples at the G.S.C.

Drs. James Grant, and W.E. Seyfried of the Geology Departments of the University of Minnesota at Duluth, and Minneapolis, respectively, and Paul Siders and J.C. Nichol of the UMD Chemistry Department served as committee members. All are thanked for there critical reviews of the dissertation.

The staff and students of the Department of Geology at UMD provided an enjoyable atmosphere to do graduate work. Joan Hendershot and Mary Nash cheerfully resolved numerous problems I brought to them and deserve recognition for their efforts. Numerous fellow graduate students provided on-going camaraderie. My fellow early morning coffee drinkers provided open ears to which I periodically vented my frustrations; I thank them. George Hudak was a co-worker throughout this project who without I likely would not have succeeded beyond several exams, and difficult courses. Nancy Nelson shared of her excellent editing skills and greatly improved the text.

M.J. Leone of the Graduate School has my appreciation for her efforts in solving numerous registration difficulties related to Ph.D. study on the Duluth campus.

I owe a long-standing debt of gratitude and respect to Professor Gene LaBerge of UW-Oshkosh. His enthusiasm directly led me to a career in geology, and he continues to willingly coach me.

Financing this project came by several means. The Department of Geology at UMD provided support as Teaching and Research Assistanceships and as the Ralph W. Marsden and Randy Seeling Scholarships. Scholarship support was also provided by the Midwest Federation of Mineralogical Societies. The Graduate School provided grant support to cover travel expenses to Minneapolis and elsewhere. The support of all is gratefully acknowledged.

BHP Minerals is thanked for providing me liberty in work scheduling and for technical support during the final stages of the project.

Finally, a most special thank you is due to my best friend, Sarah, for her patience with me, and for tolerating me during this project. She helped me to persevere to the end.

TABLE OF CONTENTS

Page

Page

Page

Page

LIST OF FIGURES

LIST OF TABLES

LIST OF PLATES

Plate #

I. INTRODUCTION

I.1 Introduction

Recent studies of ancient and modern volcanogenic massive sulfide (VMS) systems suggest a genetic connection between the massive sulfide deposits, hydrothermal systems, and morphology and method of emplacement of the associated volcanic rocks (Morton and Franklin, 1987; Franklin, 1986; Gibson et al., 1989; Kappel and Franklin, 1989; Koski et al., 1988). Unlike previously investigated areas, the host rocks to Minnova, Inc.'s Winston Lake Zn-Cu-Ag deposit exhibit unusual lithological diversity including the presence of abundant volcaniclastic rocks and unusual alteration styles. Good preservation of many primary textures and abundant outcrop makes Winston Lake an excellent place to study the association of volcanic processes and the development of hydrothermal systems. Furthermore, the unusual occurrence of high grade metamorphic minerals, without accompanying widespread penetrative deformation, makes Winston Lake a good site to study the mineralogical effects of metamorphism of hydrothermally altered rocks.

I.2 Purpose

Minnova, Inc., and its predecessor Corporation Falconbridge Copper (CFC), has historically focused considerable effort upon exploration of its mineral properties through detailed geological reconstruction of the oreforming environment. Therein, this research project was initiated in 1987 during the development stage of the Winston Lake Mine.

The purpose of this project is to study the volcanic, hydrothermal, and metamorphic evolution of the host rocks to the Winston Lake VMS deposit. Specific problems to be addressed include:

(1) What was the volcanic environment at Winston Lake with regard to volcanic deposit types and morphologies, depositional environment, and lithological diversity?

(2) How did the hydrothermal system develop within the volcanic environment with regard to spatial and genetic relationships to various rock types and stratigraphic controls?

(3) What controlled the localization of sulfide mineralization?

I.3 Location, Access, and Physiography

The Winston Lake deposit is located ~20km inland from the north shore of Lake Superior, immediately northwest of the village of Schreiber, approximately 145km northeast of Thunder Bay, Ontario (Figure 1). The property is reached by travelling north on a gravel road constructed by Minnova, Inc., which branches off Trans-Canada Highway 17 approximately 8km west of Schreiber (Figure 1).

The relief of the project area varies greatly and is typified by high hills (≤300m) with steep slopes, low-medium (≤50m) knob-like hills, and low (≤10m), broad ridges. Swamps and lakes are found between the hills and ridges and constitute 5% and 10% of the area, respectively.

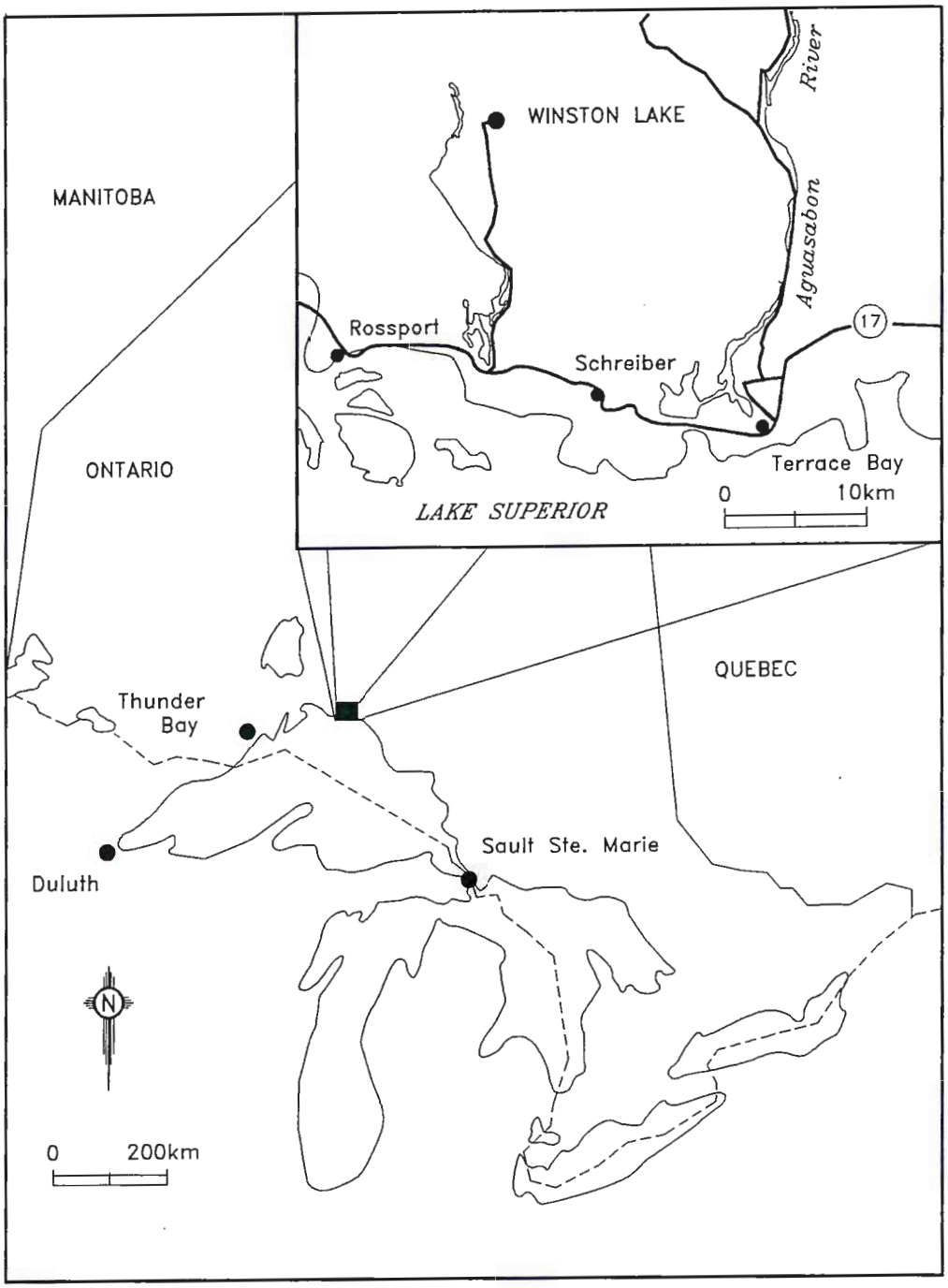

Figure 1. Location of the Winston Lake massive sulfide deposit, northwestern Ontario.

Total bedrock exposure averages 60% on the property. Of this, due to inaccessibly steep topography and abundant lichen cover, only about 30% is favorable for detailed mapping.

I.4 Methods

I.4.1 Field Methods

Geologic mapping and rock sampling was conducted for a total of nine months over the summers of 1987 through 1990. Mapping was done on old, but functional, cut grid lines established by CFC. The 1:5000 scale CFC Winston Lake geology map (Balint et al., 1984) was used for delineation of basic stratigraphic units and for selection of areas to be mapped in greater detail. Detailed mapping at scales of 1:1000, and 1:500 was completed in areas as shown in Figure 2. In addition, a 1:5000 field review of areas not detail-mapped was completed.

Approximately 26,000m of drill core from sixty-one diamond drill holes was reviewed for identification of down-dip variations in geology and for correlation to surface geology.

I.4.2 Laboratory Methods

Over 1000 representative hand samples were collected; 619 thin sections prepared from these samples were studied for identification of mineralogy, textures, alteration, and metamorphism. Two hundred and seventeen additional thin sections from a previous worker (Morton, 1984) were also examined. The modal mineralogy

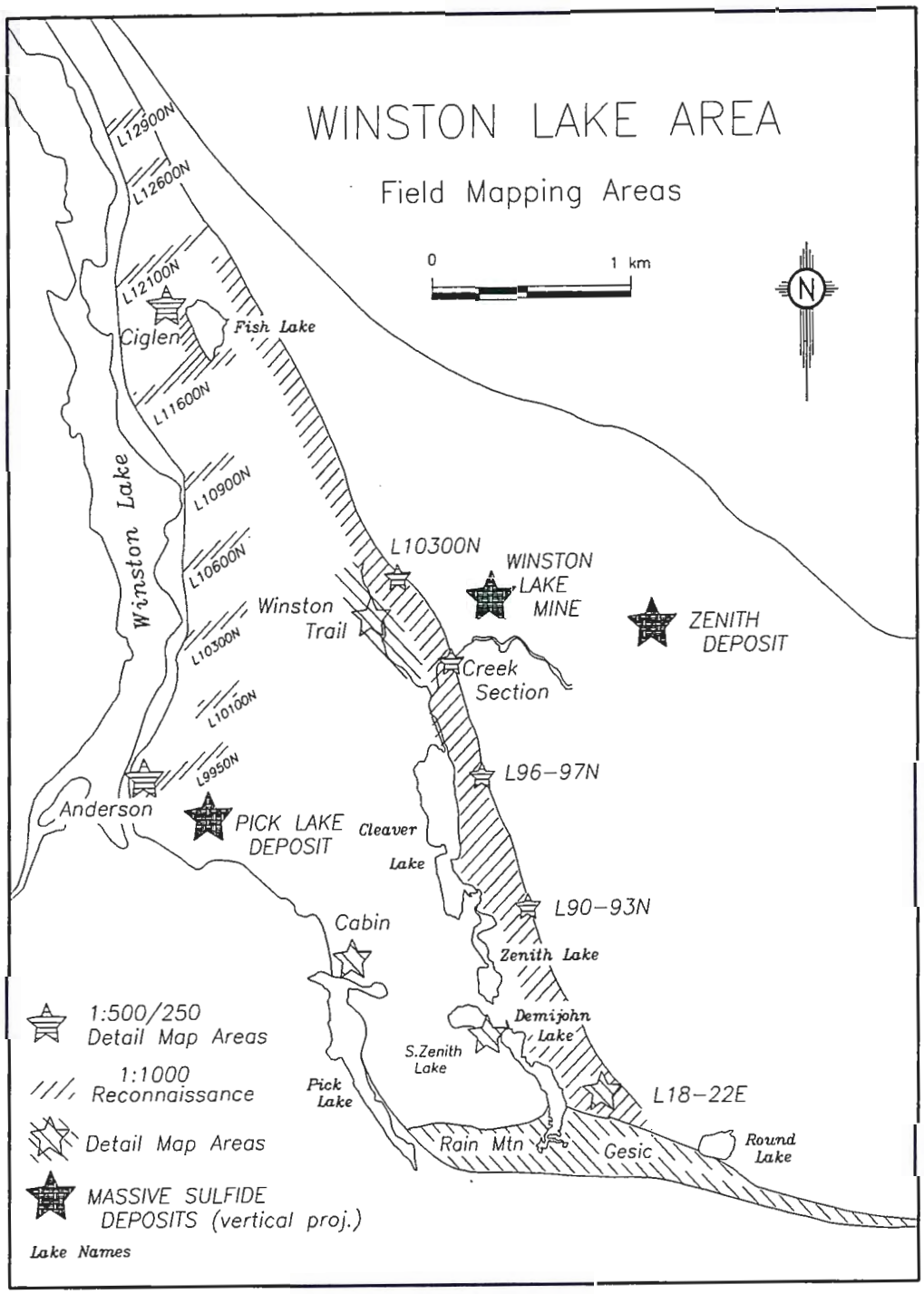

Figure 2. Geographic location of field mapping areas, lakes, and massive sulfide deposits, Winston Lake property.

of all thin sections studied is tabulated in Appendix I.

Two hundred and forty-five rock samples were analyzed for major oxides and trace elements by the Geological Survey of Canada. Analytical methods used and sample results are tabulated in Appendix II.

Microprobe mineral analyses were made on 16 polished thin sections to determine variations in the mineral compositions of biotite, chlorite, cordierite, garnet, and anthophyllite/ gedrite throughout the study area. This data was supplemented by analyses from 19 polished thin sections from the mineral chemistry study of Winston Lake altered rocks by Thomas (1991). Microprobe mineral analyses are tabulated in Appendix III.

Locations of thin section, polished thin section, and samples collected for chemical analyses are shown on Plates 1-3.

I.5 Previous Work

I.5.1 Geological Surveys

Several organized geological studies have been conducted in the Winston Lake-Big Duck Lake area, the first of which was Collins' (1909) reconnaissance mapping between the Nipigon and Pic Rivers.

Hopkins' (1915) survey outlined the general geology of the Big Duck Lake area. Hopkins (1921) supplemented his earlier work by a reconnaissance study of the Schreiber-Big Duck Lake area.

Bartley (1942) examined the Big Duck Lake-Aguasabon Lakes area and sub-divided the stratigraphy into Keewatin, post-Keewatin (Algoman?) and Keweenawan strata (Table 1). He interpreted the rocks to form the south limb of an overturned anticline.

Pye (1964) studied the general, structural, and economic geology of the Big Duck Lake area. He redefined Bartley's Early and Late Post-Keewatin rocks as pre-Algoman(?) and Algoman, respectively (Table 1), and subdivided the Keewatin rocks immediately east of Winston Lake into (1) Lower Metasediments, (2) Metavolcanics, and (3) Upper Metasediments. On the basis of pillow and graded bedding top-indicators, he interpreted (in contrast to Bartley, 1942) the Big Duck Lake area stratigraphy to form the south flank of a major syncline. Pye's survey also studied mineralization in the area, and he classified it as massive sulphide, disseminated sulphide, or vein deposits.

I.5.2 Mineral Exploration

The earliest known mineral exploration in the Winston Lake area occurred in 1879 when an Indian discovered massive Zn sulfide mineralization within gabbroic rocks near Kenebec Lake (The Mining Review, 1899).

Exploration activities continued sporadically over the next 70-80 years with the discovery of several base metal showings in the Winston Lake area (Pye,1964). No significant development activities took place until the 1960's when Zenmac Metal Mines, Ltd. mined 181,830 tons of 16.5% Zn from the Kenebec Lake discovery

Table 1.

Stratigraphic Subdivisions of Bartley (1942) and Pye (1964).

Bartley (1942)		Pye (1964)	
Quaternary		Cenozoic	
Pleistocene	sand and gravel	Recent and Pleistocene	glacial drift, gravel, sand, silt
		-great unconformity-	
Pre-Cambrian		Precambrian	
Keweenawan	diabase dikes and sills	Keweenawan	diabase
-intrusive contact-		-igneous contact-	
Post-Keewatin (Algoman?)		Algoman	quartz porphyry, quartz-feldspar porphyry
Late:	granite, syenite, granite gneiss; quartz and feldspar porphyry and pegmatite	-contact indeterminate-	
-intrusive contact-			granite (gneiss), porphyritic granite, migmatite, pegmatite
Early:	diorite, gabbro, pegmatitic diorite	-igneous contact-	
-intrusive contact-		Pre-Algoman	diorite, gabbro, amphibolite
		-igneous contact-	
Keewatin:	Volcanic Group Sedimentary Group	Keewatin	Upper Metasediments Metavolcanics Lower Metasediments

(Zenith Mine). Production ceased in early 1970 (Balint and Severin, 1984).

Geologists with CFC recognized the unusual occurrence of massive Zn sulfides in gabbroic rocks at the Zenith Mine and in 1978 initiated a reconnaissance geological and lithogeochemical survey of the area (Balint and Severin, 1984). The survey resulted in reinterpretation of Pye's (1964) Lower Metasediments (Table 1) as metamorphosed hydrothermally-altered volcanic and volcaniclastic rocks and interpretation of the Zenith deposit as a large xenolith of massive sulphide. The property was acquired in 1978 and detailed geology, lithogeochemical, and geophysical surveys identified VMS-style characteristics. Follow-up diamond drilling resulted in the discovery of the Winston Lake orebody in June of 1982 (Balint and Severin, 1984).

Exploration on the Winston Lake property by CFC and Minnova, Inc. has continued since 1982. Geological studies on the property included 1:1000 scale detailed mapping, extensive diamond drilling (Balint and Severin, 1984), an optical petrology study (Buchan, 1983), a preliminary volcanology and alteration study (Morton, 1984), Sm-Nd age-dating by Schandl and Gorton (1991), and a mineral chemistry study of hydrothermally-altered rocks (Thomas, 1991).

I.6 Regional Geology

I.6.1 Introduction

The Winston Lake deposit lies near the northern boundary of the Shebandowan-Wawa Subprovince within the Superior Structural Province of the

Canadian Shield (Figure 3). The subprovince is bordered to the north by the Quetico Metasedimentary Gneiss Belt and to the south by Proterozoic-aged rocks (Figure 3). As is typical of most Archean granite-greenstone complexes, the subprovince is composed of metavolcanic and metasedimentary rocks and associated granitic plutons.

I.6.2 Big Duck Lake Belt

In the vicinity of Winston Lake, the metavolcanic, metasedimentary and associated intrusive rocks form a 15km by 3-4km belt of rocks informally known as the Big Duck Lake greenstone belt (Balint and Severin, 1984). This succession of rocks forms an east-west trending, north-facing sequence bounded by granitic plutons and cut by Keweenawan diabase dikes (Figure 4) (Pye, 1964). Balint and Severin (1984) outlined three principal lithological components, which are best revealed near the west end of the belt (Figure 4). From oldest to youngest these include:

(1) The Winston Lake Sequence comprises calc-alkaline felsic and mafic metavolcanic rocks and lesser metasedimentary rocks. Lava flows dominate and are accompanied by subordinate pyroclastic lithologies.

(2) The Big Duck Sequence overlies the Winston Lake Sequence and is dominated by tholeiitic mafic lava flows. The flows are intruded by quartz porphyry and quartz-feldspar porphyry sills in the vicinity of Big Duck Lake. The Big Duck is separated from the Winston Lake by a series of differentiated tholeiitic mafic-ultramafic sills.

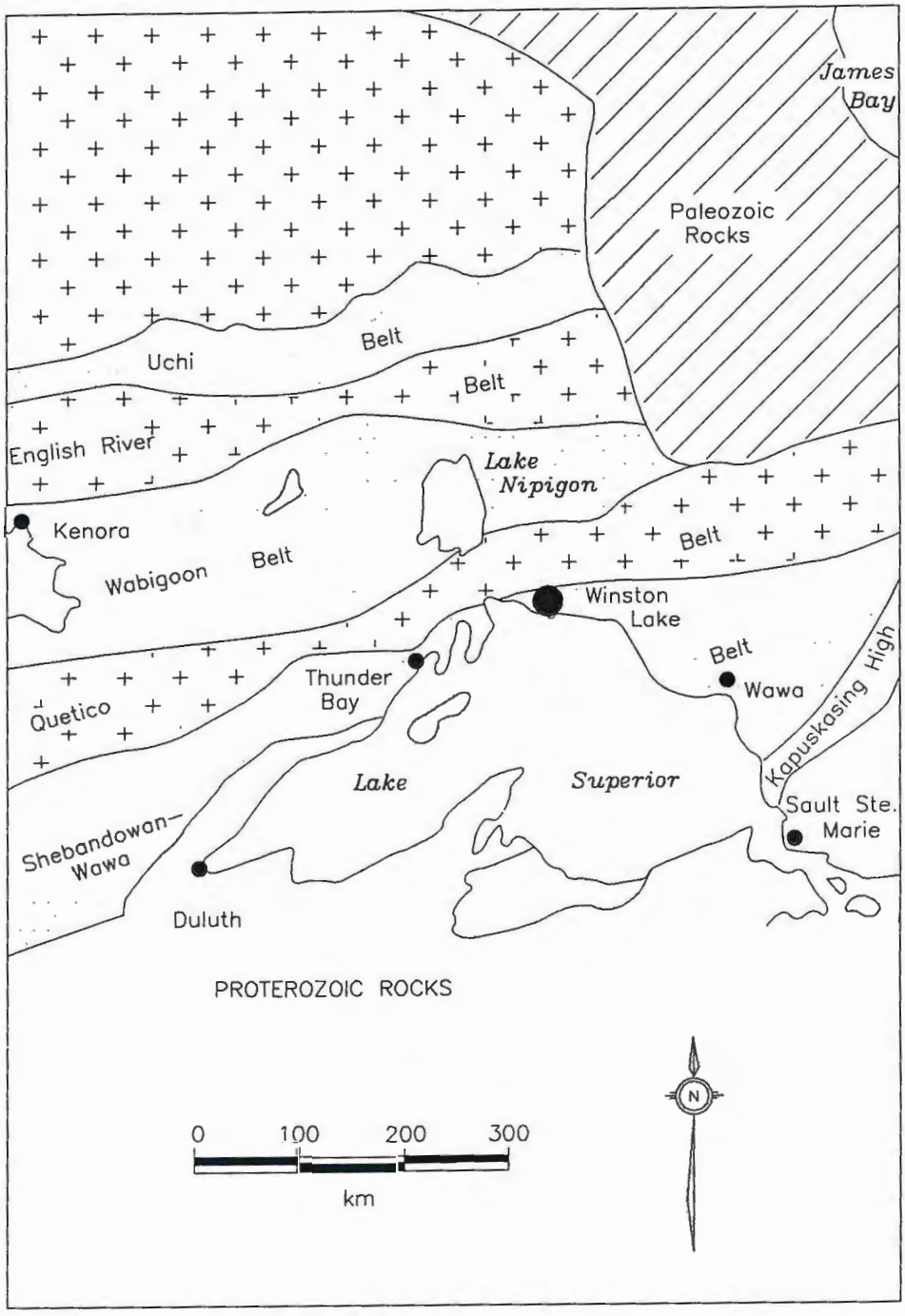

Figure 3. Location of Minnova, Inc.'s Winston Lake property within the Shebandowan-Wawa Subprovince of the Superior Structural Province.

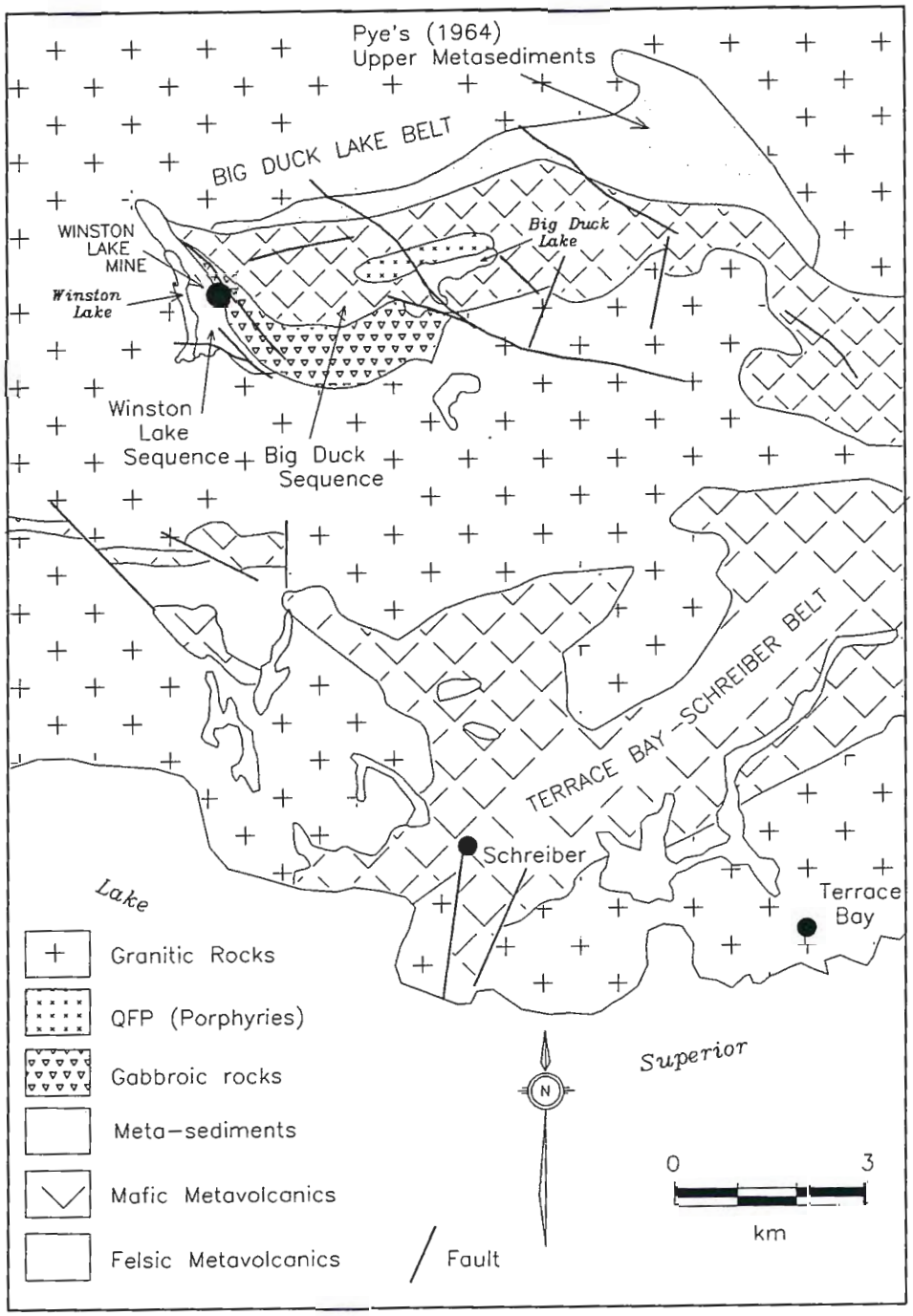

Figure 4. General geology of the Big Duck Lake Belt (after Severin and Balint, 1984).

(3) The Upper Metasediments of Pye (1964) overlie the Big Duck Sequence and form the north side of the Big Duck Lake Belt. Metasedimentary rocks are dominated by biotite-quartz-feldspar ± garnet schists and gneisses; minor iron formation occurs within the sequence.

Three prominent fault sets occur within the Big Duck Lake belt including NW, NE, and E-NE sets (Pye, 1964). The faults locally displace Keweenawan diabase dikes and are therefore thought to have had recurrent motion, at least locally (Pye, 1964).

Rocks towards the margins of the Big Duck Lake Belt have been subjected to upper greenschist-amphibolite grade metamorphism; garnet and hornblende are common. Toward the core of the belt greenschist grade metamorphism predominates with quartz-chlorite-actinolite-albite assemblages common (Pye, 1964).

Apart from the Zenith and Winston Lake base metal mines, no economic deposits have been found to date in the belt. Several Au ± Mo-base metal occurrences associated with quartz porphyry or quartz-feldspar porphyry intrusions have been recognized in the vicinity of Big Duck Lake (Pye, 1964).

II. LITHOLOGY AND STRATIGRAPHY

II.1 Introduction

The distribution of rock units within the study area is shown on Plate 1, which is a 1:5000 scale compilation of field mapping from this study and previous mapping by CFC. Modal mineral abundances are listed in Appendix I.

Most of the rocks of the Winston Lake Sequence have undergone amphibolite grade metamorphism. In addition to metamorphism many have undergone relatively intense, premetamorphic hydrothermal alteration; anomalous modal abundances of muscovite, biotite, chlorite, cordierite, garnet, actinolite/tremolite, anthophyllite/gedrite, and sillimanite reflect this alteration.

In spite of metamorphism and hydrothermal alteration, numerous primary textures and structures are preserved on outcrop; these permit recognition of some primary lithologic types and interpretation of depositional environments. For the sake of brevity, the prefix meta is herein discontinued for the remainder of the text.

II.2 Descriptive Subdivision

For descriptive purposes, the Winston Lake Sequence has been divided into two parts based upon geographic location. These include the Winston Footwall Block, and the Rain Mountain-Gesic Block. The Winston Footwall Block includes north-south striking, east dipping (45-60°) volcanic and associated volcaniclastic rocks north of the Pond Fault area; east-west striking, north-dipping (45-60°) rocks to the

south of the fault are described as the Rain Mountain-Gesic Block (Figure 5). Stratigraphic correlations between the two areas are described in detail in section III.2.1.

The Winston Footwall and Rain Mountain-Gesic Blocks are further subdivided into successions and units on the basis of lithologic types and stratigraphic position as illustrated in Table 2 and Figure 5. Intrusive rocks (Table 3) associated with the stratigraphy are described separately. In the naming of units current mine terminology has been adopted and used when possible and redefined or appended as necessary. Unit names are generally based upon local geographic or salient descriptive features. For brevity, unit abbreviations (Tables 2 and 3) are used in the remainder of the text.

In the following sections (II.3 and II.4), successions named on Table 2 are described generally on a unit by unit basis from oldest to youngest. Descriptions of each succession are followed by a brief interpretation of primary deposit types and volcanological setting.

II.3 Winston Footwall Block

II.3.1 Introduction

The Winston Footwall Block has been subdivided into four successions referred to as the Lower Clastic, Middle Flows Upper Clastic, and the Winston Lake Horizon Successions (Table 2).

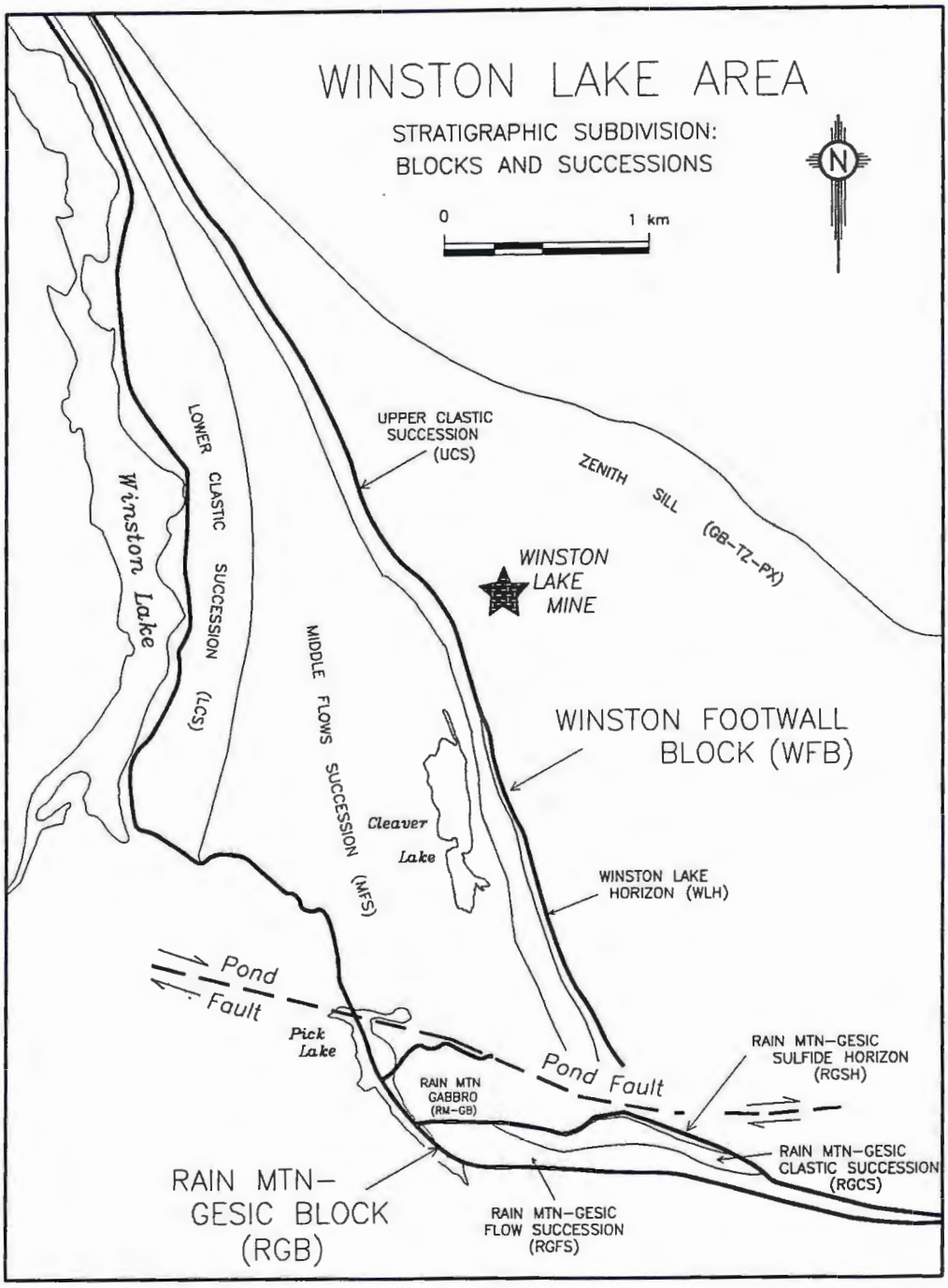

Figure 5. Subdivision of the Winston Lake Sequence into stratigraphic blocks and successions.

Table 2.

Descriptive Subdivision of the Winston Lake Sequence.
Successions and units listed from youngest (top) to oldest (bottom)
except as noted[1]; units numbered in order of description.

WINSTON FOOTWALL BLOCK (WFB)

Succession
units, (codes)

*Winston Lake Horizon (WLH)
(4) -Winston Lake VMS Deposit (WLH-MS)
(3) -Mafic Volcanic and Intrusive
Feeder Rocks (WLH-FR)
(2) -Mixed Laminated Ash and
Exhalative Sediments (WLH-CRT)
(1) -Mafic Lava Flows (WLH-MA)
-Footwall Flow (WLH-FWF)

Upper Clastic Succession (UCS)
(2) -Clotted Rhyolite (CLR)
(1) -Volcaniclastic and Associated Rocks (SIV)
**(1b) -Felsic Tuffs (SIV-FT)
**(1a) -Intermediate Volcaniclastics (SIV-VC)

Middle Flows Succession (MFS)
**(6) - Synvolcanic Felsic-Derived Volcaniclastic
Sediments and/or Tuffs (CT)
**(5) -Undivided Mafic Rocks (MA)
(4) -Middle Mafic Flow and Assoc. Rocks (MMF)
(3) -Camp Flow Rhyolite and
Assoc. Feeder Dikes (QFF)
(2) -Ladder Flow (LF)
(1) -"Main" QFP (QFP)

*Lower Clastic Succession (LCS)
(4) -Chemical Precipitates (CRT, MS)
(3) -Pick Clotted Rhyolite (PCLR)
(2) -Ciglen Clotted Rhyolite (CCLR)
(1) -Pick-Ciglen Clastics (PCC)

RAIN MOUNTAIN-GESIC BLOCK (RGB)

Succession
units, (codes)

Rain Mountain-Gesic Sulfide Horizon (RGSH)
(2) -Mixed Volcaniclastic, Cherty Tuffs,
and Sulfidic Rocks (RG-CRT)
(1) -Mafic Lava Flows (RG-MA)

Rain Mountain-Gesic Clastic Succession (RGCS)
(2) -Rain Mountain
Clotted Rhyolite (RMCLR)
(1) -Rain Mtn-Gesic Volcaniclastic Rocks (RGSIV)

Rain Mountain-Gesic Flow Succession (RGFS)
(2) -Rain Mtn-Gesic Ladder Flow (RGLF)
(1) -Rain Mtn-Gesic QFP (RGQFP)

[1]No relative age relationship
*of units within succession implied
**of unit with respect to others
implied.

Table 3.

Intrusive Rocks within and overlying the Winston Lake Sequence. Groups listed from youngest (top) to oldest (bottom) except as noted.

INTRUSIVE ROCKS
groups/ rock types
-units, (codes)

Keweenawan
-Diabase (DB)

Granitic Rocks (GR)

Miscellaneous Intrusions
**Felsite Sill (FD) --Gesic area
**Feldspar ± Quartz Porphyry (F(Q)P)

**Big Duck Sequence-Related
*Mafic to Ultramafic Sills (GB, TZ, PX)
-Zenith Sill (GB, TZ, PX)
-Rain Mountain Gabbro (RM-GB)
-Contact Lake Sill (GB, TZ, PX)
-Ciglen Road Sills (GB)
-plug-like intrusions (GB, PX)

*No relative age relationship of Gabbro occurrences is implied.

**Relative age unknown.

II.3.2 Lower Clastic Succession (LCS)

Introduction

The Lower Clastic Succession (LCS) forms the base of the Winston Footwall Block; it is bounded to the west by granitic rocks and to the east is conformably overlain by QFP of the Middle Flow Succession (Table 2). On surface the succession extends from near the south end of Winston Lake, north to beyond L13000N and ranges from 75-300m in map width (Plate 1). Exploration drilling has traced the succession to approximately 1 km down-dip. Drill holes collared in granite immediately northwest of Pick Lake (Plate 1) have also intersected the LCS implying a southerly plunging attitude to the granite-clastic contact.

Primary textures in the clastic rocks are generally poorly preserved. A strong north-south foliation is prominent and the rocks are locally intensely sheared and boudinaged; granitic diking is common, especially near the contact with the granite. Nevertheless, on a compositional basis, four mappable subdivisions of the LCS have been made. These include (1) Pick-Ciglen Clastics (PCC): a texturally variable sequence of volcaniclastic-sedimentary rocks; and intercalated (2) Ciglen Clotted Rhyolite (CCLR) and (3) Pick Clotted Rhyolite (PCLR): felsic pyroclastic or turbiditic equivalent rocks; and (4) Chemical Precipitates (CRT and MS).

Pick-Ciglen Clastics (PCC)

Volcaniclastic-sedimentary rocks designated as the Pick-Ciglen Clastics (PCC) volumetrically (70%) dominate the Lower Clastic Succession (LCS). These rocks

extend the full length of the LCS and attain a maximum preserved stratigraphic thickness of approximately 340m. Extensive recrystallization, lack of preserved primary textures other than plane parallel bedding, and extensive hydrothermal alteration preclude recognition of primary clastic protoliths.

On outcrop and in drill core the rocks range from medium gray to dark gray-green and vary from fine to medium grained. Garnet porphyroblasts, up to 3 cm in diameter or ≤5 cm aggregates of mm-scale garnets, are common and, along with silica clumps, weather positively giving the rocks a knobby appearance. Fragments are rare (<<1%) and have only been recognized near the northwest corner of Contact Lake. Here clasts are flattened and stretched ranging up to 3x10cm and are composed dominantly of recrystallized quartz and feldspar. Fragment protoliths were felsic but are otherwise unknown.

Garnet porphyroblasts and siliceous fragments are set in a quartzo-feldspathic groundmass. Layering thought to represent relict bedding is locally distinct in the groundmass; individual layers can be discontinuous to lens-shaped due to deformation. Variably well-layered rocks are complexly intercalated and, although subdivisions are not mappable, a continuum from well-laminated to thin-thickly banded or bedded to relatively massive, fine grained clastic rocks can be distinguished.

Thin-thickly banded or bedded rocks dominate (60%) the PCC unit. On outcrop, layering is coarser than in laminated rocks, ranging from 3cm to >1m, and is generally defined by alternating mafic and quartzofeldspathic layers.

Well-laminated rocks are fine grained, compose 15% of the PCC, and occur locally throughout the sequence. They are most conspicuous north of Fish Lake where they occur interlayered with felsic pyroclastic rocks. Laminations vary from 1-5cm and are generally dark gray to gray-green reflecting variation in biotite and/or hornblende abundance (Figure 6). Garnet (3-8%) porphyroblasts (1-2cm) are common along laminations. Fine grained (< 1 mm), dark grayish-green clastic rocks with abundant (5-30%) ≤2 cm garnet porphyroblasts occur intercalated throughout and compose 25% of the PCC unit. They are most conspicuous near the stratigraphic top of the unit as observed in drill core from south of Contact Lake. The rocks are generally massive and show only broad-scale (5-25m), subtle compositional variation defined by changes in garnet abundance.

In thin section the clastic rocks range widely in mineralogy depending upon degree of premetamorphic hydrothermal alteration. Least altered rocks, regardless of layering style, are dominated by prismatic hornblende (0-25%), flakes and clumps of biotite (0-20%) and muscovite (0-8%), subidioblastic to ragged or flowery garnet (0-40%), and blocky magnetite (0-2%) set in a very fine grained (< 0.2 mm) groundmass of granoblastic-polygonal quartz (20-60%) and plagioclase (10-45%). Plagioclase is locally albite twinned and is usually incipiently sericitized. With increased alteration, hornblende diminishes in abundance and is replaced by acicular actinolite (0-5%), bow-tie to radial "sprays" of anthophyllite (0-10%), xenoblastic-blocky staurolite (0-3%), porphyroblastic garnet (0-50%) with rotational inclusion

structures and growth zoning, and local bundles of fine grained, needle-like sillimanite (0-2%).

Ciglen Clotted Rhyolite (CCLR)

Felsic rocks of the Ciglen "Clotted" Rhyolite (CCLR) occur interlayered with the PCC toward the north end of the property (Plate 1). Volcanic facies (after Cas and Wright, 1987) defined in the field as proximal flow sets, coupled with thickness variation, fragment distribution and character, and a distinctly felsic nature suggest the rocks represent deposits of felsic pyroclastic flows. CCLR rocks compose 15% of the LCS and form a thick (50m) sequence best exposed along L12900N (Plate 1). The sequence thins southward and down dip where it becomes interlayered with PCC, and eventually pinches out immediately south of the Ciglen strip (Plate 1).

Along L12900N the CCLR deposits can be subdivided into 2-3 individual flow sets; these consist of relatively thick (15-25m) massive, fine grained, light gray to bluish-gray siliceous, variably fragment-rich basal units overlain by thin (1-3m) well-bedded ash deposits of similar composition, color, and grain size (Figure 7). Bedding in ashy deposits is defined by subtle color and/or grain size variation. In general the number and thickness of basal beds decreases quickly to the south and down-dip; subdivision of flow units becomes impossible south of ~L12600N.

Black to greenish black lithic fragments, locally with 1-3mm light gray-pinkish rims, compose 10-30% of basal beds. Balint and Severin (1984) described such fragments as "clots"; their terminology has been continued in this study for

Figure 6. Well laminated volcaniclastic-sediments of the PCC unit.

Figure 7. CCLR felsic pyroclastic unit showing relatively massive basal portion (bottom) overlain by well-laminated upper ashy beds (top).

consistency sake. The fragments are typically flattened, range from 1-25cm in length and have length: width ratios varying from 1:1 up to 12:1. No vertical sorting of fragments has been recognized, and, in general, the abundance and size of fragments decrease laterally towards the unit's southern and down-dip extent. Rare digitated terminations are preserved on clots and similarity in shape to better preserved, partially altered fragments in other pyroclastic units up-section suggests the clots may represent pervasively replaced juvenile fragments. Alternatively, the clots could represent intermediate to mafic accidental fragments. Ashy zones typically contain fewer (0-5%) fragments and those present are typically smaller (≤3 cm long) than in basal beds.

In thin section the clots are dominated by fine grained (<0.5mm) prismatic hornblende (70-98%), minor epidote (tr), recrystallized quartz (2-15%), and plagioclase (tr-15%). Rims, where present, are composed of distinctly coarser grained (0.5-1mm) recrystallized plagioclase (60%) and quartz (40%). Near the southern, distal extent of the deposits, where the rocks have been hydrothermally altered, fragments become increasingly biotitic (0-80%).

"Clot" fragments are set in a very fine grained (0.2mm) groundmass of recrystallized quartz (60-85%) and plagioclase (10-30%) mosaics with accessory fine grained (<1mm) prismatic hornblende (5%), epidote (tr), and minor biotite (0-10%).

Pick Clotted Rhyolite (PCLR)

A second felsic pyroclastic unit, the Pick "Clotted" Rhyolite (PCLR) has been delineated and occurs interlayered with PCC rocks near the southern end of the LCS. These rocks are similar in grain size and color to the CCLR, but are distinguished by their location and facies analysis. The rocks are typically massive to well laminated, but no individual pyroclastic flow sets have been recognized. PCLR rocks compose 14% of the LCS and are best visible in drill core south of Contact Lake (Plate 1). They are poorly exposed on surface and generally cannot be correlated between outcrops; correlation between drill cores is better, but is locally not possible. Several individual PCLR units are present, the number and thickness (from 0-80m) of which generally decrease in an up-dip and a northerly direction. An exception occurs near DDH WL-26 (Plates 1) where faulting has displaced the lower portions of the stratigraphic section.

Dark green-black lapilli-sized "clot" fragments similar in shape to those of the CCLR compose 0-15% of the rock and generally decrease in abundance towards the north and up-dip. The fragments are typically lens-shaped, 1-5cm long, and have length to width ratios up to 5:1. Unlike the CCLR, the fragments are dominantly biotitic; pyrrhotite is locally present as ≤4mm blocky grains in irregular clumps near the core of the fragments. One to two cm ragged to subidioblastic pink garnet porphyroblasts, or aggregates of red mm-scale idioblastic garnets (0-7%) locally overgrow fragments. Excellent examples are found in DDH's WL-10, WL-25, and WL-26.

In thin section, fragments show no preserved primary texture and consist dominantly of fine grained biotite (65-95%), pyrrhotite (0-2%), recrystallized quartz (0-5%) and plagioclase (0-5%). The fragments and garnet porphyroblasts are set in a very fine grained (<0.2mm) foliated matrix of quartz (60-90%) and plagioclase (15-25%) mosaics, and biotite (5-20%); unlike the CCLR, hornblende is not present. Overall, the felsic tuffs seem to be less susceptible to hydrothermal alteration than the PCC volcaniclastic rocks, but where altered biotite, garnet, anthophyllite, and cordierite are locally abundant.

Chemical Precipitates (CRT, MS)

Rocks formed through chemical precipitation form a relatively minor (1%) portion of the LCS and are interlayered with PCC, PCLR, and CCLR lithologies. The rocks have been examined in considerable detail by Balint and Severin (1984) and Minnova staff (Morrison, pers.comm.) and therefore only a cursory review was completed in this study. The rocks range from recrystallized cherts (CRT) to massive sulfide (MS) deposits and occur in two general areas, the Ciglen occurrence, and the Anderson showing-Pick Lake deposit area (Plate 1).

Balint and Severin (1984) describe zinc rich exhalites within altered clastic rocks (PC-Clastics and CCLR) at the Ciglen showing as "a train of lenses or pods of bedded sulfides occurring over a strike length of 75m." Individual pods are typically 1.5m long by 20-30cm thick and consist of 1-5cm sulfidic layers associated with relatively coarse grained light gray quartz thought to represent recrystallized chert.

Sulfide layers are composed dominantly of brownish, fine grained to medium grained sphalerite (30-100%), with associated pyrrhotite (10-20%), pyrite (≤5%), quartz, a green silicate, and magnetite. The mineralized siliceous pods are hosted by variably siliceous, biotitic, and garnetiferous altered volcaniclastic rocks thought to be metamorphosed hydrothermally altered rocks (Balint and Severin, 1984). The mineralization and alteration is spatially associated with the Ciglen fault (Plate 1) which likely represents a reactivated synvolcanic structure.

Cherty rocks and massive sulfides are present near the southern extent of the LCS at the Anderson showing and the down-dip stratigraphically equivalent Pick Lake deposit (Plate 1). At the Anderson a broad (30x150m) rusty sequence of extensively altered, sulfidic clastic rocks contains rare (2%) siliceous and garnetiferous pods which may represent recrystallized chert. Pods are typically ≤30cm x 2m and consist of reddish-brown, extensively oxidized sulfides, recrystallized quartz, and ≤1cm garnet (0-15%) porphyroblasts.

Drilling in volcaniclastic and pyroclastic rocks down-dip of the Anderson has intersected numerous, narrow (≤30cm) highly siliceous zones thought to represent recrystallized chert (Morrison and Sim, 1989). The rocks are typically light grayish, fine grained and vary from massive to vaguely laminated. Contacts with host rocks are typically gradational.

Morrison and Sim (1989) briefly describe the Pick Lake massive sulfide deposit as a broad, steeply north-plunging sheet-like deposit within altered felsic pyroclastic rocks. Mineralization extends for approximately 200m along strike, and

to a depth of at least 1km; the deposit is typically ≤ 1.5m thick but locally reaches up to 14m (Morrison, pers. comm.). Sulfide mineralization consists mainly of brownish, fine grained to medium grained sphalerite (50-90%), with pyrrhotite (5-40%), chalcopyrite (0-5%), pyrite (0-2%) quartz (tr-5%), and biotite (tr-2%). The massive sulfides are typically in sharp contact with the host rocks.

Interpretation

Although extensive hydrothermal alteration and recrystallization precludes a detailed sedimentological analysis of the PC-Clastic succession, the dominance of quartz and feldspar in the rocks suggests detritus derivation from a felsic source terrane. Deposition of PCC rocks was periodically interrupted by pyroclastic volcanism from two distinct sources. Facies variation suggests relatively distal emplacement of CCLR rocks as multiple south-directed pyroclastic flows from an eruptive center somewhere north of L13000N. The distribution and character of PCLR rocks suggest they also are relatively distal pyroclastic deposits, but were derived from a source south of the Contact Lake area.

The interlayered nature of PCLR with PCC rocks indicates they can be used, in a general way, as marker horizons within the LCS. As such, although the LCS is presently bordered to the immediate west by granitic rocks, the distribution of clastic rocks suggests an original south-thickening geometry to the LCS.

Breaks in clastic deposition are reflected, at least locally, by chemical precipitates; stratigraphic and temporal implications of other chemical rocks will be discussed in a later section.

II.3.3 Middle Flow Succession (MFS)

Introduction

The Middle Flow Succession (MFS) comprises approximately 80% of the Winston Footwall Block and consists of mafic and felsic lava flows and volcaniclastic rocks. The MFS is in conformable contact with the underlying Lower Clastic Succession (LCS) and the overlying Upper Clastic Succession (UCS) (Figure 5).

A prominent north-south trending foliation is common in rocks of the MFS; local crenulation textures are present, especially near faults. In spite of structural fabrics, primary volcanic structures are locally well-preserved and recognizable. However, finer scale primary volcanic textures are generally not preserved.

Based upon lithologic types, stratigraphic position, and phenocryst size and abundance five mappable subdivisions of the MFS have been made (Table 2). These include in order of description: the "main" QFP (QFP), the Ladder Flow (LF), the Camp Flow (QFF), Middle Mafic Flow (MMF), Undivided Mafic Rocks (MA), and mostly Felsic-derived Volcaniclastic Sediments and/or Tuffs (CT).

"Main" QFP (QFP)

Quartz-feldspar porphyritic rocks (QFP) form the base of, and volumetrically dominate (75%), the Middle Flow Succession (MFS). The QFP conformably overlies the volcaniclastic (LCS) rocks to the west and is conformably overlain by mafic lava flows (LF) and, locally, by volcaniclastic rocks (CT) to the east.

The QFP extends over 4600m along strike, reaches a maximum apparent map thickness of about 1000m near its southern extent, and thins northward to about 50m near the north end of the study area. The unit is bounded to the south by several NW-SE trending faults, movement along which has probably structurally thickened the unit. Diamond drilling has traced the QFP down-dip to approximately 1.5 km with no apparent appreciable thickness variation relative to surface widths.

North of L9500N and, locally, in the Cabin area (Plate 1) gabbroic intrusive rocks dilate the QFP. Granitic sills and dikes are locally common in the Cabin area.

In outcrop the QFP varies widely from tan to pinkish gray to gray-brown in color (Figure 8). Most (95%) of the QFP is massive and homogeneous except for a characteristic "ribbony-appearing" cleavage; internal morphological subdivisions are very rare. Locally, especially north of Fish Lake, the cleavage is less conspicuous but the massive QFP gradationally acquires a color banded appearance. Individual bands range up to 3 cm in thickness and reflect variable biotite content. The bands are typically lens-shaped and pinch out within 15-50cm; the shape of bands and lack of

associated fragmental textures suggests the banding probably reflects metamorphic or structurally-induced layering.

The QFP locally exhibits a thicker (5-10cm) layering also defined by variable biotite content. The thicker bands locally exhibit broad, outcrop-scale wavy fold patterns and these may represent a primary flow banding.

Unequivocal autoclastic textures such as hyaloclastite and flow breccias have not been recognized. However, fragments have been observed in one outcrop near grid location 8890N, 9255E. Relatively massive QFP is separated by a 1-2 m -wide zone with rare (10%), subangular block-sized (10-20 cm) felsic fragments semisupported in a light gray to brownish biotitic matrix. These fragments appear lithologically identical to massive QFP and may represent autoclastic flow breccia or alteration- induced pseudofragment structures.

Cloudy gray quartz phenocrysts are generally easily visible in outcrop and in drill core and are typically oval to augen-shaped where strained. The phenocrysts range up to 3x15mm in diameter, constitute 5-30% of the rock, and are generally uniformly distributed. Where relatively fresh, blocky to tabular plagioclase phenocrysts are present (5-20%) and range from 2-6mm in diameter. Where altered, feldspar phenocrysts are typically not preserved.

Garnet porphyroblasts are locally present (0-5%) in the QFP. Near the base of the unit, euhedral red garnets (≤3mm) occur locally within weakly biotitic feldspar-phyric rocks. Balint and Severin (1984) suggest the garnet may reflect clastic detritus incorporated into the base of the QFP and later metamorphosed. In intensely

altered rocks garnet porphyroblasts are typically coarse grained (≤2cm), range from pink to reddish in color, compose from 0-20% of the rock and, along with quartz, weather positively to give the rock a knobby appearance.

In thin section quartz phenocrysts are typically recrystallized and consist of mosaics of interlocking quartz crystals which are distinctly coarser grained (0.05-0.1mm) than groundmass quartz. Primary grain shapes and textures of phenocrysts are never preserved. Where present, plagioclase phenocrysts are variably sausseritized; grain margins are commonly recrystallized to very fine grained (<0.01mm) feldspar. Albite, and local Carlsbad and Pericline twinning is usually preserved. Sericite pseudomorphs feldspar phenocrysts to varying degrees, generally increasing in abundance in proximity to alteration zones.

In thin section it can be seen that garnet porphyroblasts range widely from very fine grained (≤0.01mm) isolated idioblastic crystals, to 1-2cm irregular clumps of fine grained garnets, to coarse grained (≤1cm) anhedral crystals showing multiple growth zones.

Porphyroblasts and phenocrysts are set in a very fine grained (≤0.01mm) matrix dominated by recrystallized quartz (23-57%) and plagioclase (5-30%) mosaics. In least altered rocks, accessory minerals include foliated muscovite (1-20%) and biotite (1-22%), which is locally retrograded to chlorite (0-20%); trace amounts of zircon, apatite, and epidote are also typically present. Hornblende is notably absent in the QFP. With increased hydrothermal alteration biotite generally increases in abundance and is accompanied by bundle-like knots of sillimanite (0-20%), fine

grained to relatively coarse grained (0.02-0.5mm), variably pinitized cordierite (0-30%) porphyroblasts which contain inclusions of staurolite (0-15%) and quartz, and local prismatic to radial clumps of anthophyllite (0-35%). Fine grained (0.02mm), subhedral spinel is rarely present (0-3%).

Ladder Flow (LF)

Mafic lava flows of the Ladder Flow Unit (LF) comprise approximately 10% of the MFS and are found in three general areas. First, mafic lavas conformably overlie QFP and extend from near the south end of Cleaver Lake to near the north end of the property. The flows are locally separated from the QFP by, and are interlayered with, volcaniclastic rocks. The flows reach a maximum thickness of about 75m near their southern extent and thin northward to 0m near L12400N. Diamond drilling has intersected the flows at down-dip depths of up to 1 km with thicknesses consistent with surface variation.

A second occurrence of LF rocks is between Pick and Zenith Lakes where fault-bounded slices of mafic lava flows up to 100x700m are structurally intercalated with QFP.

In the third occurrence similar mafic lava flows lie between the Pond Fault and the Rain Mountain Gabbro (Plate 1). The rocks are in fault contact with and/or are intruded by gabbro to the south.

On outcrop the mafic lavas vary from fine grained, dark grayish green, to medium-coarse grained greenish-brown where intensely altered. Massive and

pillowed morphologies dominate and are accompanied by lesser sheet-flow and autobrecciated forms. The thickness and lateral extent of flow types is difficult to determine due to discontinuous exposures; no obvious discernable facies relationships exist between flow morphologies. Morphological varieties are typically in relatively sharp contact with adjacent types, suggesting the LF unit represents compound lava flows (Cas and Wright, 1987).

Massive and pillow lavas occur throughout the unit and comprise 30 and 60%, respectively of the LF. Pillows vary from oval and bulbous, to elongate tube-like and rare mattress forms, and range from 10cm-2m in dimension (Figure 9). Local budded forms with moderate to well-preserved re-entrant selvedges have been observed along the Winston Trail, and the north edge of Rain Mountain. Pillows and tubes are generally very tightly packed and are outlined by 1-5 cm thick, black, fine-grained, hornblende-rich selvedges. Rare, $\leq$7mm garnet porphyroblasts are found along the selvedges. Selvedge material locally forms relatively long ($\leq$1.5m) wedge-shaped (0-10cm thick) domains separating flow lobes or tubes. Interpillow material is rare and typically consists of rusty, siliceous material (recrystallized chert?) in $\leq$10 cm triangular patches.

Morton (1983) recognized local sheet flow lavas near L10000N, 9535E. These lavas appear as multiple (2-4) sheet-like parallel layers ranging from 3cm-2m in thickness and up to 3m in length; thicker layers could represent flow lobes. Sharp contacts typify the sheets and are marked by 1-3cm selvedges lithologically identical to pillow rinds. Hyaloclastite tops and bottoms to sheet flows reported by Morton

Figure 8. Tan to pinkish-grey, massive main QFP; white specks are plagioclase phenocrysts.

Figure 9. Well pillowed mafic lava flow of the LF unit.

(1983) were not recognized in this study.

Flow breccias have been unequivocally recognized only in the Winston Trail detail area near 10250N, 9500E (Plate 2). A zone of broken pillow breccia up to 3.5m thick and 8m long occurs at the base of the LF and is composed of 20%, 10-40cm subround to subangular pillow/lobe fragments supported within a pervasively altered matrix. Fragments are lithologically identical to associated massive to pillowed LF material.

Hyaloclastite is extremely rare and has been recognized only in the Winston Trail detail area (Plate 2). Here 10-20cm wide and 1-5m long discontinuous zones separate pillow lobed and massive flows. Blocky-angular fragments are typically $\leq$2cm in diameter and compose 80-90% of the zones; fragment interstices are filled by fine grained chloritic material. Rare sinusoidal-shaped chloritic fractures suggest the fragmental zones may, in part, represent brittle deformation of mafic lava along minor fault zones.

The LF can be subdivided into four main lithologic parts: (1) feldspar phyric, (2) aphyric, (3) aphyric semimassive hornblende-rich rocks, and (4) extensively altered flows.

Feldpar-phyric rocks comprise 40% of the LF and are distinguished by 2-6mm blocky-lath-like, pink-chalky white plagioclase phenocrysts which comprise 5-60% of the rock. In distribution there is a general increase in abundance of phenocrysts towards the south, and phenocrysts are especially abundant (40-60%) along the north side of Rain Mountain. On a given outcrop no vertical zoning in phenocryst

distribution has been recognized in massive or pillowed flows; however, Morton (1983) suggested phenocrysts within sheet flow lavas are gradationally concentrated in the lower 1/3 of the flow.

In thin section plagioclase phenocrysts are typically seriate and locally glomerophyric in distribution. Albite twinning is generally well-preserved except where phenocrysts have been extensively sausseritized or pseudomorphed by sericite. Grain boundaries are typically recrystallized to very fine (<0.01mm) grains.

The phenocrysts are set in a fine grained (<0.01mm) matrix dominated by very fine grained (<0.1mm), recrystallized, variably sausseritized plagioclase (35-40%) and fine grained, (0.1-1mm) subidioblastic, prismatic hornblende (30-55%). Accessory tremolite-actinolite (0-10%), retrograde chlorite (0-10%), sericite (0-15%), epidote (0-20%), quartz (0-12%), opaques (0-10%), and rare carbonate (tr) are also present.

Petrographically pillow and tube selvedges are dominated by fine grained (≤0.2mm) subidioblastic hornblende (40-70%), with plagioclase (15-30%), epidote (2-7%), and chlorite (1-8%).

Relatively fresh aphyric mafic lava flows comprise 10% of the LF. Aphyric rocks are most commonly, although not exclusively found at or near the base of the LF unit; they are typically in sharp contact with overlying feldspar-phyric flows. The aphyric rocks are, in general, texturally featureless; no primary flow structures have been recognized. Conformability with and separation from overlying and underlying

rocks by volcaniclastic material indicates the aphyric rocks are probably lava flows although they may, in part, represent massive tuffaceous deposits or sills.

Immediately southeast of South Zenith Lake (Plate 2) aphyric mafic rocks locally contain (1-5%) light gray to tan oval, to lens-shaped felsic structures up to 1cm x 5cm in dimension. In thin section, the felsic structures are comprised of very fine grained ($\leq$0.01mm) mosaics of recrystallized quartz and feldspar; feldspar is typically dusty in appearance due to incipient sausseritization. Although no internal structure is recognized, these structures may represent strained, recrystallized variolites. Under the microscope the aphyric rocks are mineralogically similar to the matrix of the feldspar-phyric lavas (Appendix I).

A second variety of aphyric mafic material has been locally exposed by outcrop stripping near the north end of the Winston Trail detail area (10345N, ~9475E) (Plate 2). Massive, very dark green-black, fine grained hornblende-rich rock forms a 0-3 m thick zone partially enveloping a zone of typical feldspar-phyric LF. In outcrop and petrographically the hornblende-rich material is similar in appearance and mineralogy to pillow and tube selvedges (Appendix I).

Based upon its geometrical distribution, and mineralogical and chemical similarity to selvedge material, the aphyric, hornblende-rich rock may represent an originally glassy carapace to an enclosed feldspar-phyric flow. Alternatively, the rock could represent aphyric, irregular-shaped dikelike intrusion.

Approximately 50% of the LF is comprised of mafic volcanic rocks which have been extensively hydrothermally altered; primary flow morphologies are generally

very well-preserved, but where massive, original lithologic character is not evident. Feldpar phenocrysts are only very rarely preserved and the rocks are dominated by needle-like, fine-medium-grained tremolite/actinolite (0-40%), coarse-grained bow-tie to radial anthophyllite (25-45%) with associated coarse-grained cordierite (10-55%) and garnet (0-25%) porphyroblasts. Minor staurolite (0-10%) and quartz (0-25%) occurs, usually as inclusions within cordierite and garnet. Foliated "mats" of fine-coarse-grained biotite (tr-10%) and chlorite (tr-10%) are also commonly present.

Camp Flow Rhyolite (QFF)

Felsic rocks, which have been called the Camp Flow Rhyolite (QFF) are thought to represent lava flow(s) and comprise 40% of the MFS. This unit is laterally extensive (>5km), yet relatively thin (50-200m) (Plate 1), and drilling has intersected the unit at down-dip depths of up to approximately 1500m. The QFF overlies mafic lava flows of the LF or, more locally, volcaniclastic rocks; the basal contact is conformable except where locally faulted. Diamond drilling (DDH GO-3) has intersected QFF near the extreme southeast edge of the WFB immediately north of the Pond Fault. Unlike all other drill intersections and surface exposures found further north, three descrete zones ranging from <10 to approximately 50 feet in thickness are interlayered with and overlain by volcaniclastic rocks.

Rocks of the QFF are similar in appearance to those of the main QFP. Phenocrysts of quartz (7-20%) and plagioclase (0-20%) are similar in shape and texture, but are distinctly finer grained (1-3mm) than in the QFP. Phenocrysts are

also similar in distribution and texture to those of the QFP and are set in a fine-medium grained recrystallized quartzo-feldspathic matrix.

On outcrop, thin section, or on a chemical basis no subdivision of the QFF into individual flows has been recognized except for minor associated flow breccias. Compound flow units could be present but local shearing, recrystallization, and hydrothermal alteration make delineation of such impossible.

On outcrop the rocks vary from tan-pale gray where fresh, to bright white to medium brownish where extensively altered. Massive flows dominate (35%) and are most conspicuous south of Cleaver Lake where the rocks are relatively fresh. Where extensively weathered they acquire a sugary to granular texture reflecting recrystallization.

Compositional banding is more common in the QFF than in the QFP. Fresh rocks exposed between Cleaver and Demijohn Lakes locally display up to 50cm wide zones with discontinous, dark colored hornblende ± biotitic streaks and bands (Figure 10); rare tight folds (possibly synvolcanic) are evident. Balint and Severin (1984) suggest the zoning may represent primary flow banding. Alternatively, the banding may reflect an incipient stage of hydrothermal alteration. A comparably-thick mineralogical zoning is locally recognized in intensely hydrothermally altered QFF in a single exposure along the Winston Trail (near 10050N, 9620E). Garnet (5%) porphyroblasts are concentrated in broad (50-70cm) parallel zones which may reflect selective alteration along primary compositional heterogeneities (flow bands).

A finer scale layering is well-developed in biotite-rich QFF exposed along the Ciglen Road and is similar, but generally more pronouncedm than thin banding in the QFP. A continuum exists locally between well-developed banding, lensy, lapilli- to block-sized pseudofragments, amoeboid-shaped alteration patches, and cross-cutting biotitic alteration veins suggesting at least some of the banding may be of a transposed structural origin.

Primary fragmental structures are rare and have been recognized only where the rocks are relatively fresh. DDH GO-3, in the L18-22E area, intersected a 2.1m-thick zone at the top of the QFF in which ≤20cm fragments are supported in a light gray felsic tuffaceous, locally cherty matrix. Fragments appear lithologically identical to the underlying massive QFF.

Flow bottom fragments have been recognized in only one outcrop (L8600N, 9330E). A poorly exposed ≤3m thick zone of undeterminable lateral extent contains rare (5%), stretched, block-sized (≤30cm), subangular felsic and feldspar-phyric mafic fragments set in an ashy felsic matrix.

Hyaloclastite has not been observed in the QFF, however fine grained tuffs are locally associated with relatively fresh rocks and may represent recrystallized accumulations of fine grained hydroclastic material. Thin (≤20cm) discontinuous color laminated white-gray-tan zones are locally present at the top of the QFF between L8500N and L9100N. The tuffs are clearly felsic and contain rare cherty interlaminae.

Petrographically, the QFF also appears very similar to the QFP with regard to texture and mineralogy (Appendix I).

QFF-related Dikes

In the South Zenith Lake area (Plate 2), south of the Pond Fault, aphyric, and feldspar-phyric mafic lava flows of the LF are locally intruded by quartz-feldpar porphyritic dikes lithologically similar in outcrop and thin section to the QFF. The dikes range widely in width (3-28m) and cross-cut the host rocks at a high angle (70-80°). No chill margins have been noted. Quartz and plagioclase phenocrysts within the dikes are zoned in distribution from 0%, adjacent to wall rocks, to 15%, and 12%, respectively, approximately 5m inward from the contact.

Well-preserved 2-60cm diameter xenoliths are locally present (10%) within the QFF dikes and include mafic volcanic (80%) and volcaniclastic (19%) lithologies; rare (1%) 2-10cm rusty patches are also present and may represent oxidized sulfidic fragments (Figure 11). The xenoliths are concentrated away from dike margins, are typically elongate, and are aligned at approximately 90° to the local foliation direction. Xenolith and phenocryst distribution is believed to reflect flow segregation processes.

Minor felsic dikes intrude aphyric mafic lava immediately southeast of South Zenith lake. Where exposed dikes are ≤ 50cm thick and appear identical to marginal, aphyric portions of dikes described above. Local intrusive textures are present but large xenoliths were not observed.

Figure 10. QFF felsic lava flow showing well-developed hornblende-biotite flow(?) bands.

Figure 11. QFF feeder dike containing mafic volcanic xenoliths (dark colored).

Middle Mafic Flow and Associated Rocks (MMF)

Mafic lava flows and sill-like intrusions of the Middle Mafic Flow and Associated Rocks (MMF) cap the MFS between L8700N and approximately L10200N and have been intersected in drilling to depths of ~1km. Hydrothermal alteration makes delineation of the unit's exact northern extent difficult. The MMF reaches a maximum thickness of ~60m, comformably overlies the QFF, is interlayered with volcaniclastic rocks to the south, and is underlain by similar rocks down-dip beneath the Winston Lake orebody (Balint and Severin, 1984).

In outcrop, the rocks are dark gray to greenish black in color and range from fine to medium grained. Most of the MMF is aphyric with ≤3mm blocky plagioclase phenocrysts locally composing up to 5% of the rock. The rocks vary in morphology from massive, to rare pillowed morphologies; autoclastic structures have not been recognized.

Massive rocks dominate (99%) the MMF and consist of both intrusions and, based upon a broad conformable nature, massive lava flow(s). Subgabbroic, massive, semiconformable sills 0.5-5m thick are well-exposed and distinguishable in road-cuts along the northeast shore of Cleaver Lake. Elsewhere intrusions are not mappably distinguishable from massive lava flows.

Unequivocal pillow-structures have been recognized in only one outcrop (~L8900N, ~8450E). Massive lava passes relatively abruptly into a 2 m± thick pillowed zone exposed over ~10m of strike length. Pillows are typically long and lensy (0.5-2m x ≤20cm) and are outlined by relatively thin (≤1cm), dark grey-black,

hornblende-rich selvedges. Pillows are tightly packed and inter-pillow material is absent.

Mafic tuffaceous rocks have not been conclusively recognized, however the basal contact of the MMF is locally marked by a ≤ 1m-thick very well-foliated zone. The rocks are typically dark gray-green, exhibit a very fine color lamination, and grade into adjacent massive mafic or volcaniclastic rocks. Layering may reflect a thin primary bedding or a secondary fabric. No associated fragmental or clastic textures have been recognized.

Petrographically, where fresh, rocks of the MMF appear similar to aphyric lavas of the LF. Hornblende and plagioclase dominate the rock and are accompanied by minor epidote, chlorite, quartz, and opaques. Where hydrothermally altered, tremolite/actinolite, biotite, chlorite, cordierite, anthophyllite, and garnet are variably present (Appendix I).

Undivided Mafic Rocks (MA) - Cabin Area

Mapping by CFC geologists and detailed follow-up by this study in the Cabin area (Figure 2) has outlined a 100-125m wide by 125-150m thick sequence of mafic volcanic and intrusive rocks. The mafic rocks are abruptly bounded to the north by QFP and are transected to the south by the Pond Fault. Granite intrudes the sequence to the west and granitic and gabbro sills are found within this mafic sequence (Plates 1 and 2).

The mafic rocks can be subdivided into aphyric (80%) and feldspar-phyric (20%) portions which appear lithologically identical in outcrop and in thin section to rocks of the MMF, and LF (Appendix I). Although distinct on outcrop, mappable units have not been delineated because actual contacts are typically not exposed, or because of complex distribution patterns.

In overall distribution (Plate 1 and 2) the mafic rocks appear to cross-cut the QFP. On a local scale, 1-3m thick sill or dike-like intrusions of fresh MA into altered QFP and rare ≤30cm elongate QFP xenoliths within feldspar-phyric mafic rocks have been observed near the QFP-MA contact. Such features suggest an intrusive emplacement of the mafic sequence. However, near the top of the sequence, detailed mapping has outlined a local 10m(±) thick zone of aphyric pillowed lava flows (Figure 12). The lateral extent of the pillowed zone and contact relationship with massive rocks is uncertain as exposure is limited. Pillows are typically oval to bun shaped, tightly packed with no interpillow material, and have notably thin (5mm ±) black hornblende-rich selvedges.

Synvolcanic Felsic-Derived Sediments and/or Tuffs (CT)

As defined by Balint and Severin (1984) synvolcanic felsic-derived sediments and/or tuffs (CT) represent accumulations of finely bedded sulphide-rich rocks. The rocks are intimately associated with volcanic rocks of the MFS and occur as lens-like accumulations of volcaniclastic material up to 15m thick, extending from <1m to 100m laterally; their thickness and extent probably reflect paleotopography (Balint

and Severin, 1984). In the subsurface they can only rarely be traced between adjacent drill holes.

Figure 12. Pillowed mafic lava flow in the Cabin area.

In distribution the rocks are typically found in four stratigraphic positions: (1) intra QFP, (2) at the top of the main QFP, (3) intra LF, and (4) at the top of the LF. In addition, local fault bounded slices of similar rocks are present in the Cabin area (Plates 1 and 2).

The CT deposits generally appear as fine-medium grained, light gray (where fresh) to dark green-gray (where altered) color laminated rocks. No discrete clasts

have been recognized. Compositional layering reflects modal variability of mafic minerals and ranges from fine cm-scale laminations to thick (10-20cm) bedding.

Recrystallized clastic portions of the CT are dominantly felsic but include variable (up to 50%) mafic material and probably represent QFP and LF-detritus. A siliceous (cherty?) chemical exhalative component comprises 0-5% of the CT and is locally interlayered with sulfide-rich beds which contain pyrrhotite, pyrite, chalcopyrite, and sphalerite up to 10% total (Balint and Severin, 1984).

Mineralization associated with CT rocks is most notably developed at the Trail and Cabin occurrences both of which are described in detail by Balint and Severin (1984) and are only briefly summarized here. The Trail occurrence (Plate 2) is found in several exposures between L10000N and L10500N and consists of anomalous Cu in bedded rusty clastic rocks and in adjacent associated LF. Weakly anomalous base metal mineralization at the Cabin occurrence occurs at the base of garnet-bearing CT and consists of an approximately 1m-thick highly siliceous pyrrhotite-pyrite-rich zone exposed intermittently over approximately 150m(±) of strike length.

Near the north end of the Winston Trail detail area (~10315N, ~9495E)(Plate 2) a 7m-thick pocket of altered pink, garnet-rich CT is present between QFP and LF volcanic rocks. The upper 2-3m of the deposit contains several (20%) matrix-supported, generally oval (≤25cm) to elongate (25x40cm) structures outlined or filled by relatively coarse grained (1-4cm) subidioblastic garnet crystals. The origin of the structures is problematic. Considering the shape of the garnet-

iferous structures and proximity to the basal contact of a mafic lava flow they may represent lava blobs or pillow fragments and lava tubes which tumbled, or were injected into wet, saturated CT from an advancing lava flow. Alteration and metamorphism of the mafic rock and enclosing sediment carapace resulted in growth of garnet crystals. Similar-shaped structures have been reported elsewhere by Snyder and Fraser (1963), Allen (1980a, 1982), Busby-Spera and White (1987), Dixon, (1990), and Branney and Suthren, (1988), and are thought to represent peperite structures resulting from interaction of mafic magma and wet ash or sediment. Poorer examples of similar structures are present up section (~10350N, ~9495E) where garnet crystals are concentrated within CT as 4 x 10cm elongate clumps and oval pods at the base of another LF flow (Plate 2). Alternatively, as suggested by Galley (1991, pers. comm.), the pods may represent dome and basin interference folds of narrow (≤5cm veins) garnetiferous veins.

In thin section the CT consists of variable fine-medium grained, recrystallized quartz (5-60%), and plagioclase (0-35%), foliated biotite (0-20%) and chlorite (0-15%), and subidioblastic hornblende (0-50%). With increased alteration anthophyllite (0-40%), cordierite (0-15%), sillimanite (0-12%), staurolite (0-12%), garnet (0-30%), spinel (0-tr), and opaques (0-4%) become volumetrically important.

Interpretation- MFS

The MFS is dominated by alternating felsic and mafic volcanic and associated intrusive rocks. Volcanism was intermittent; pauses are marked by the local occurrence of volcaniclastic deposits as noted by Balint and Severin (1984).

The presence of pillows, lava tubes, and rare hyaloclastite clearly indicate the LF and MMF units were deposited in a subaqueous environment (Cas, 1987; Jones, 1968; Moore, 1975). Flow breccias (although rare), conformability and interlayering with sedimentary rocks and mafic lava flows, possible flow banding, and chemical and lithologic homogeneity, suggest the QFF, and in part, the QFP represent subaqueous felsic lava flow deposits.

If structural thickening, dilation by gabbroic sills, and subsidence is considered, it is conceivable that the QFP deposit of the MFS had a relatively gentle (10-20°) paleoslope similar to that of the rhyolitic shield or plateau deposits of the Millenbach D-68 Lava Dome of Noranda (Gibson, 1989). It is notable that Gibson (1989) found that massive portions of lava lobes at Noranda were identical in structure, texture and amygdule content regardless of proximity to source; massive portions of the QFP at Winston Lake are similarly identical regardless of location. The paucity of flow breccia and lobe-hyaloclastite at Winston Lake, similar to that found in Noranda, may reflect partial endogenous growth of the QFP and destruction of delicate glassy textures during anealment immediately after emplacement or during metamorphic recrystallization. Furthermore, it is possible that the banding in the QFP, which is relatively well-developed north of Fish Lake, may have formed preferentially in

hyaloclastite-rich rocks. The effects of hydrothermal alteration may have contributed to destruction of original lobe-hyaloclastite structures.

The abundance of lava flows (mafic and felsic), and the lack of pyroclastic flow, hyalotuffs, or extensive hyaloclastite deposits, suggests volcanism was relatively passive in character. Fisher and Schmincke (1984) indicate volcanism is relatively passive in subaqueous environments beneath the volatile fragmentation depth (VFD), that depth at which exsolving magmatic volatiles contribute to explosive volcanic eruptions. The VFD depends principally on the type and amount of dissolved volatiles and thus on magma composition, and is generally <500m (Fisher and Schmincke, 1984). Beneath the VFD, confining pressure of the overlying water column prohibits rapid volatile exsolution. Eruptions are principally effusive and magmatic in origin as water-magma interactions are relatively nonexplosive. Superheating of water is minimized and contributes negligibly to the eruption process (Sheridan and Wohletz, 1981).

The relatively large length:thickness ratio (25:1-100:1) of the QFF also suggests eruption and deposition beneath the VFD. Cas (1979) demonstrated deep water, subaqueously erupted and emplaced silicic lavas may behave fluidly and be highly mobile because of the inability of volatiles to escape under the high hydrostatic pressure of the deep water environment. The notable lack of amygdules and gas cavities in the lava flows of the MFS supports this idea.

The eruption vents to lava flows were possibly elongate and fissure-like in form and were probably located towards the south end of the MFS. Several features

when considered together suggest this. Thickness variation along strike at various down-dip depths is comparable to surface thickness variation suggesting an elongate feeder morphology. All units, with the exception of the MMF, are northward thinning or terminating in distribution suggesting vents were located in a southward direction. Vague modal and size zoning of feldspar phenocrysts in LF support this facies analysis. Localized QFF feeder dikes in the South Zenith Lake area and field relations in the Cabin area also suggest a southern source direction.

In the Cabin area the overall cross-cutting distribution of mafic rocks, and localized mafic intrusive and closely associated lava flows may represent an axial trough-like feeder complex to mafic lavas of post-QFP deposition. Undistinguishable map relations of lithologically variable (feldspar phyric vs. aphyric) rocks may reflect complex multiple magmatic pulses and episodes in the feeder environment. Anomalously thin pillow selvedges and tight pillow packing suggests high temperatures, and low viscosity both consistent with proximity to source vents.

Post magmatic fault movement along the Pond Fault and NW-SE fault structures and late stage intrusion of the Rain Mountain Gabbro resulted in relocation of feeder structures from original to present geographic positions.

II.3.4 Upper Clastic Succession (UCS)

Introduction

The Upper Clastic Succession (UCS) overlies the Middle Flow Succession (MFS), comprises approximately 7% of the WFB, and ranges from 75-200m in

thickness (Figure 5). The UCS caps the northern 1/3 of the WFB and to the south is conformably overlain by the Winston Lake Horizon (WLH). Based upon composition the UCS can be subdivided into two 1:5000 scale mappable components (Plate 1): (1) Volcaniclastic and Associated Rocks (SIV), and (2) Clotted Rhyolite (CLR): felsic pyroclastic deposits (Table 2).

Volcaniclastic and Associated Rocks (SIV)

Undivided Volcaniclastic and Associated Rocks (SIV) comprise approximately 35% of the UCS (Plate 1). The rocks are similar in character to those of the PCC unit, but, in general, primary bedding structures are better preserved and hydrothermal alteration is minor. SIV rocks dominate the southern extent of the UCS and are concentrated primarily south of L9100N; minor occurrences are found further north stratigraphically above and below the MMF. SIV deposits reach a maximum thickness of ~200m and at their southern extent they terminate abruptly against mafic volcanic rocks. Very minor occurrences are found on surface immediately south of the mafic rocks and are intruded by gabbro. The SIV unit thins northward and terminates between L8800N and L9100N where it is interlayered with MMF. The SIV is in conformable contact with underlying QFF and with overlying pyroclastic rocks. Diamond drilling (DDH: GO-3, WL-6, WL-8, WL-15) in the L18-22E and immediately north of the Pond Fault suggests the SIV deposits extend at depth another 300m southeast than as observed on surface.

Detailed mapping in the L18-22E (Plate 2) area has allowed the SIV sequence to be subdivided into two components (Table 2). In order of decreasing abundance these are (1) Intermediate Volcaniclastics (SIV-VC), and (2) Felsic Tuffs (SIV-FT).

Intermediate Volcaniclastics (SIV-VC)

Intermediate Volcaniclastics (SIV-VC) dominate the SIV (95%) sequence. On outcrop the rocks are generally tan-medium gray in color, fine grained, and sugary in texture. The rocks appear intermediate to felsic in composition with minor (5%) mafic interbeds; cherty interlaminae are locally present. Crystal clasts are rare and typically <2mm in diameter. Cloudy gray quartz, and blocky, cream-gray plagioclase crystals locally compose up to 8% and 7% of the rock, respectively. Reddish-brown garnet porphyroblasts are rare, but reach 10% in some outcrops. The porphyroblasts typically have irregular to corroded grain boundaries and are ≤ 1cm in diameter.

Most (80%) SIV-VC rocks are massive; bedded varieties (Figure 13) are subordinate (35%) and are best developed towards the base of the unit in outcrops beneath the powerlines immediately northeast of Demijohn Lake (Plate 1). Where present bedding ranges from 1cm-30cm in thickness. Bedding is generally defined by color variation with lighter colored basal portions grading to darker upper parts. Dark beds are typically hornblende ± biotite-rich and alternate with lighter colored quartzo-feldspathic beds. Local graded zones, soft-sedimentary flame structures, and rare lithic clasts are well-preserved near the base of the unit. Clasts are rare (tr) and

typically ≤5cm in diameter, but locally reach up to 20cm in diameter; mafic (volcanic or intrusive), QFF, and volcaniclastic varieties are present.

In thin section crystal clasts appear as oval-round structures of relatively coarse-grained (0.05-0.1mm) recrystallized quartz. Plagioclase crystals are generally blocky, albite twinned, and variably sericitized or sausseritized. Garnet porphyroblasts are typically monocrystalline with irregular margins and minor (<5%) inclusions of quartz.

Crystal clasts and garnet porphyroblasts are enclosed by a very fine grained (≤0.2mm) groundmass dominated by recrystallized quartz (5-55%) and plagioclase (5-45%) mosaics, variable subidioblastic hornblende (0-40%) and tremolite/ actinolite (0-10%). Foliated flakes of muscovite (0-6%), biotite (0-6%), and chlorite (0-5%), with accessory epidote, opaques, minor apatite, and zircon are also present. In thin section bedding is reflected by variability in modal percent of hornblende and/or biotite.

Felsic Tuffs (SIV-FT)

The second component of the SIV sequence is denoted SIV-FT for felsic tuffs which are distinguishable on surface only in the L18-22E map area (Plates 1 and 2). The tuffs are restricted in distribution to the extreme south end of the SIV sequence where they are in sharp lateral contact with mafic volcanic rocks. The deposits reach a maximum ~80m in thickness at their southern end and, to the north, grade into SIV-VC rocks.

Diamond drilling in the L18-22E immediately north of the Pond Fault has intersected similar rocks to the southeast of those in outcrop. Here the SIV-FT deposits thin from 100 to ~35m in thickness towards the southeast, and are interlayered with SIV-VC and mafic lava flows.

SIV-FT rocks are distinctly tan-light gray, fine grained, aphyric, sugary-textured, and quartzo-feldspathic. The rocks are generally massive; bedding and individual pyroclastic flow sets have not been recognized.

Apart from color the SIV-FT can be distinguished from SIV-VC rocks by the occurrence of black to greenish- black lensy fragments much like those in the CCLR and PCLR. The fragments comprise 0-5% of the rock and are typically ≤ 1mm x ≤4cm in dimension; most are ≤5mm x ≤2cm and exhibit no size zoning. As in the CCLR and PCLR, fragments are composed of hornblende and/or biotite with rare associated sulfide grains or rare ≤2mm red-brown garnets at the cores of fragments.

The groundmass of the fragments is similar to that of the SIV-VC but contains only minor (<5%) hornblende and biotite.

Clotted Rhyolite (CLR)

Deposits of the Clotted Rhyolite (CLR) overlie the QFF lava flow unit in the northern part of the property and MMF or SIV to the south and compose 65% of the UCS. Based on facies mapping the rocks are thought to be felsic pyroclastic flow deposits similar to, but better preserved than, those of the CCLR. The CLR generally decreases in thickness southward from a maximum ~100m between L10900N and L12500N, where it is subconcordantly intruded by gabbro, to ~0m at

its extreme southern extent. Local variations in the general thickness do occur (Plate 1) and probably reflect mantling of irregular paleotopography. Down-dip thickness variations are consistent with surface variations.

Volcanic facies are recognized, as in the CCLR, on the basis of unit thickness variation, fragment size and percent variation, and locally by subdivision of deposits into recognizable pyroclastic flow sets (Cas and Wright, 1987). As such, the proximal facies direction is northward and grades southward into distal facies deposits. In the proximal environment up to four individual flow sets are recognizable in the L11450N-L11600N areas on surface and in DDH WL-14 (L11900N). The flow sets consist of relatively thick, massive "basal" beds separated by thinly bedded, ashy beds. Thickness of basal beds decreases up-section from ~22 to 16m. The basal beds are lithologically similar to those of the CCLR and are typically fragment-rich (Figure 14). The ashy beds vary from 2.1-7.5m in thickness (increasing up-section), are typically finely (≤5mm) color laminated from tan to bluish-gray, and are similar to ashy beds of the CCLR. Distinction of flow sets is generally not possible south of ~L11000N; the lack of flow sets probably reflects development of distal facies characteristics. Fragments, where present, are locally concentrated but mappable zones and flow sets are not delineable in the distal facies. The CLR deposits are generally aphyric although quartz and feldspar crystal fragments are locally present up to 10 and 15% respectively. No mappable pattern of crystal distribution has been recognized, perhaps due to incomplete exposure. Crystals are generally ≤3mm in diameter and appear similar to those in the SIV-VC deposits.

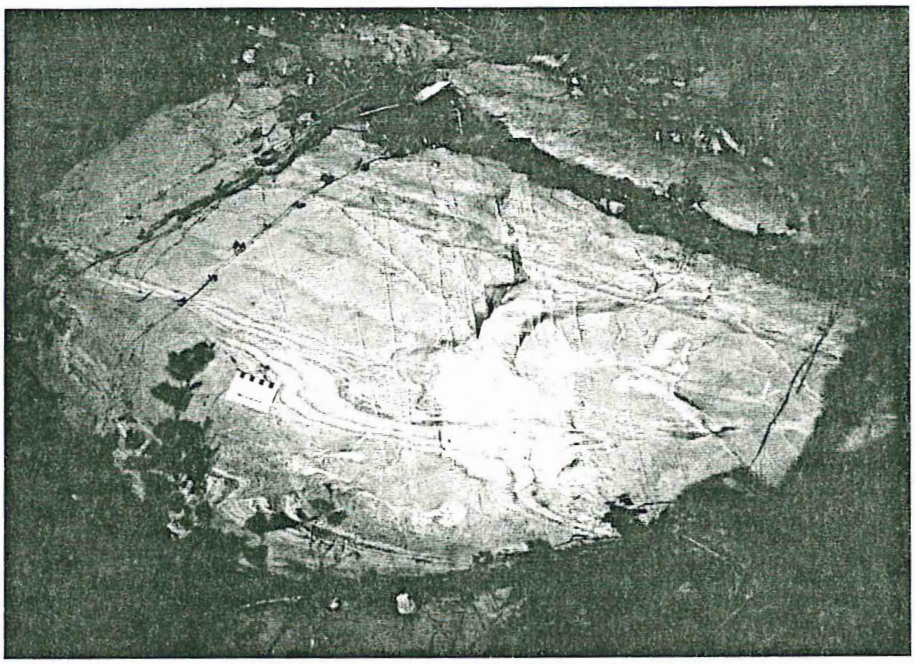

Figure 13. Bedded intermediate volcaniclastic rocks of the SIV-VC unit.

Figure 14. Relatively massive, "clot" fragment-rich basal bed of the CLR felsic pyroclastic unit.

Lithic fragments are common in the CLR and generally decrease in size and abundance southward. Where flow sets are distinguishable fragments are restricted to basal beds. Three general fragment types have been recognized. Clot fragments identical to those of the CCLR dominate, and compose 0-70% of the rock. They are lensy to oval in shape, ≤0.7cm x 1-2cm in diameter and rarely reach up to 3cm x 15cm. Digitated terminations are well-preserved locally.

As in the CCLR, hornblende dominates (≥50%) most clots but ranges widely (5-100%). Light gray-tan, quartzofeldspathic-rich clots with similar size and shape characteristics to hornblende-rich clots have been recognized and are best preserved near L11500N. The wide variation in hornblende content and digitated terminations suggest at least some clots may be pseudomorphed juvenile fragments; however, some may also represent intermediate-mafic accidental fragments within felsic pyroclastic flow deposits.

Rare (1%) siliceous accessory lithic fragments are also present and these are similar in size and shape to the clot fragments. They are typically tan, very fine grained (<<1mm), and aphyric.

Mafic accidental fragments occur locally (1%) and are observed only in proximal facies deposits. Fragments are fine-medium grained, feldspar and hornblende-rich, and appear similar to mafic volcanic or gabbroic rocks. Feldspar content is conspicuously greater than in the hornblende-rich clot fragments. The mafic fragments are typically oval to lens-shaped and are ≤3cm x ≤5cm along their axis; one elongate ~20cm x ~40cm block fragment has been recognized near

11550N, 9425E. On outcrop surface CLR rocks, particularly south of ~L10000N, locally contain negatively weathered (in relief), lens-shaped pits. Similar size, shape, and distribution to associated clot fragments suggests the pits probably represent weathered-out fragments.

In thin section quartz and plagioclase crystal fragments are variably recrystallized and, although generally smaller and locally angular, appear similar to phenocrysts in the QFP and QFF deposits. Hornblende-rich clots observed under the microscope appear similar to those in the CCLR and contain up to 95% hornblende depending upon proximity to alteration zones. Hornblende-poor clot fragments consist dominantly of recrystallized quartz (42-46%) and plagioclase (50%), with accessory hornblende, biotite, chlorite, epidote, opaques, apatite, and zircon; Morton (1983) found rare (0-3%) quartz phenocrysts locally within such fragments. Quartz and plagioclase in hornblende-poor clots is notably coarser-grained (0.5-1mm) than in the fragment matrix and appears very similar to that in pinkish rims noted around clot fragments in the CCLR.

Mafic accessory fragments appear basaltic in thin section and are dominated by plagioclase (58%) and hornblende (30%) with accessory quartz, biotite, chlorite, epidote, and opaques (Appendix I).

Crystal and lithic fragments are enclosed in a fine grained (0.1-0.2mm), recrystallized-granular matrix dominated by quartz (25-49%), plagioclase (15-57%), and subidioblastic hornblende (0-20%), with accessory epidote, biotite, and chlorite where relatively fresh. Where hydrothermally altered hornblende is replaced by

variable amounts of cordierite, biotite, chlorite, tremolite/actinolite, garnet, staurolite, sillimanite, and anthophyllite (Appendix I).

Locally felsic rocks, similar to those of the CLR, are exposed in roadcuts along the northeast shore of Cleaver Lake. Stratigraphically the felsic rocks lie immediately above the Camp Flow (QFF) and are overlain and subconcordantly intruded by rocks of the Middle Mafic Flow (MMF); minor SIV volcaniclastic rocks are associated with these felsic deposits. Chemically (Appendix II) and lithologically these rocks appear similar to the CLR. Hornblende-rich clot fragments are present (0-15%) and locally show symmetrical grading over widths of two meters. No other mappable zoning has been recognized.

Faint, tan-light gray color variations within the felsic rocks locally define 2mm-10cm, thick laterally consistent bedding planes. In one roadcut near 9250N bedding outlines a large 2m scale, relatively tight Z-fold, which is especially conspicuous when the outcrop is wet. Lack of associated folding in adjacent rocks and an inconspicuous nonaxial planar foliation to bedding relationships suggests the fold may be of soft-sedimentary origin. The rocks are typically aphyric except for rare, fine grained ($\leq$ 1mm) quartz and feldspar crystals as in the main CLR deposit. One subrounded, elongate 7x15cm aphyric felsic accessory fragment has been noted near 9250N.

In spite of its stratigraphic position the chemical and lithological character of this deposit suggests it is genetically related to the CLR unit.

Interpretation

Deposition of the UCS marks a temporal pause and change in style of volcanism following deposition of the MFS. Volcaniclastic sedimentation and pyroclastic volcanism replaced the passive emplacement of lava flows and associated intrusion of the MFS. Although much less hydrothermally altered, several lithologic similarities suggest the UCS and LCS were probably deposited in similar fashions.

On surface, volcaniclastic rocks (SIV) of the UCS form a south-thickening sequence similar to that of the PCC unit. Compositionally the rocks range from felsic to mafic-rich suggesting a mixed detritus source terrane. As in the LCS, deposition of SIV volcaniclastic rocks was locally interrupted by felsic pyroclastic volcanism, although tuffs (SIV-FT) are much less extensive than the PCLR deposits in the LCS. Lateral extent, thickness and clot size variation suggests the SIV-FT rocks were deposited from locally erupted pyroclastic flows.

Deposition of volcaniclastic material ended with emplacement of CLR pyroclastic flows. Unlike the stratigraphically underlying QFF and QFP deposits, facies variations in the CLR suggest deposition as south-directed pyroclastic flows. Such variation, in addition to relatively abundant matrix hornblende, suggests a volcanic source north of the property that was unrelated to the QFF and QFP source. In contrast, facies and compositional similarities between CLR and CCLR deposits of the LCS suggest episodic volcanic eruptions from a common source.

II.3.5 Winston Lake Horizon Succession (WLH)

Introduction

To avoid confusion with past usage the WLH is herein considered to be those volcanic and volcaniclastic rocks that cap the WFB and are situated between the stratigraphically underlying CLR and overlying feldspar porphyritic tholeiitic mafic lava flows of the Big Duck Sequence. The WLH is intruded or dilated by, or locally enclosed within gabbro of the Big Duck Sequence (Table 3). In situ portions of the WLH on surface extend for approximately 2.5km along strike; isolated remnants have been mapped as far north as L11700N. Exploration drilling and mine development have traced the WLH to down-dip depths of up to ~1km. Drilling has also intersected similar rocks in the L18-22E area subsurface immediately north of the Pond Fault where they extend at least 300m further along strike than surface exposures. In thickness the WLH ranges widely from 10-100m, but is generally <30m thick. Sections >30m thick are restricted to the L18-22E area (Plates 1 and 2); elsewhere thicknesses are generally uniform both laterally and with dip.

Detailed mapping (1:500 scale) in several areas (Plate 3), previous mapping by CFC geologists, and mine development have resulted in subdivision of the WLH into four parts. These include: interlayered (1) mafic lava flows (WLH-MA, WLH-FWF) and (2) mixed laminated ash and exhalative sediments (WLH-CRT), (3) mafic volcanic and intrusive (?) feeder rocks (WLH-FR), and (4) the Winston Lake VMS deposit (WLH-MS). Field relations suggest the present distribution as well as the

preservation of these various rocks reflects intrusion of the hangingwall gabbro as well as pre-WLH paleotopography and paleostructures.

Mafic Lava Flows (WLH-MA, -FWF)

Mafic lava flows compose 45% of the WLH and are regularly interlayered with WLH-CRT deposits (Figure 15). Up to six individual lava flows are present but only 1-3 are typically preserved, reflecting the level of intrusion by the overlying gabbro sill. The upper flows have been previously interpreted by CFC geologists (Balint, pers. comm.) as gabbroic sills, but lateral continuity and conformability with CRT deposits as well as chemical affinity to the WFB indicate an extrusive origin.

Balint and Severin (1984) denote the basal mafic unit as the footwall flow (WLH-FWF) reflecting its relationship to most of the Winston Lake deposit. Apart from hydrothermal alteration the WLH-FWF is lithologically identical to successively younger lavas in the WLH. The WLH-FWF is somewhat more extensive to the north than the younger flows, reflecting paleodistribution, and or removal of upper flows by gabbro intrusions. However, no WLH-FWF-equivalent basal mafic lava flow is present in the Gesic area subsurface north of the Pond Fault.

Individual lava flows range in thickness from 2-33m; most are between 4 and 10m thick and are fairly uniform in thickness (Plates 2 and 3). On average the FWF is the thickest, but no other systematic variation amongst flows has been recognized. Although relatively thin, the flows are laterally continuous, and individual lava flow units can be traced on outcrop north from ~L8000N for approximately 2km. North

of ~L10000N the lavas are laterally less continuous reflecting outcrop distribution, gabbroic intrusion, and paleotopography or paleostructures.

In outcrop mafic lavas of the WLH appear similar to those of the MMF. The rocks are typically fine-medium grained, aphyric, dark green-gray to black where fresh, and intensely greenish-gray where altered. Most (99%) of the flows are massive deposits. Pillows, sheet structures, and hyaloclastite are extremely rare; no autoclastic textures were recognized. Apart from rare primary structures, no internal flow subdivisions were recognized, suggesting the deposits are simple lava flows (Cas and Wright, 1987). Contacts with adjacent rock types (CLR, CRT) are typically sharp, straight to locally irregular.

Pillow-like structures have been recognized in two outcrops near Selim Creek (Plate 3) within otherwise massive mafic lava flow. The structures are long and lensy (15 x 50cm) and are outlined by ≤ 1cm dark greenish-gray, hornblende-rich selvedges. No associated hyaloclastite or interpillow material is present.

Sheet flow lavas have been recognized in one outcrop within the L18-22E detailed map area (Plate 2) at 7900N, ~9900E. Sheet-like parallel layers 5-10cm thick by 1-2m long are separated by ≤4-7mm hornblende(?) -rich, dark gray selvedges. The sheets pinch-out and tightly overlap laterally; no associated hyaloclastite is present.

In thin section, where fresh, the mafic lavas are indistinguishable from aphyric portions of the LF and the MMF. In close proximity to the Winston Lake ore body

the WLH-FWF is extremely chloritic (≤60%) with associated biotite, cordierite, anthophyllite and garnet (Appendix I).

Mixed Laminated Ash and Exhalative Sediments (WLH-CRT)

As defined by Balint and Severin (1984) WLH-CRT deposits are mixed laminated ash and exhalative sediments near the top of the WFB. The CRT comprises 45% of the WLH and occurs as discrete deposits interlayered with and separating mafic lava flows (WLH-MA)(Figure 15). Individual deposits are typically 3-5m thick, but range from 0.5-27m locally. Local, relatively abrupt thickness variation of CRT units in the vicinity of the Winston Lake ore body may reflect paleotopography.

In composition, bedding character, and color, the deposits vary both laterally and vertically although no systematic trends have been recognized. No clasts or fragments have been recognized either.

On outcrop and in drill core the CRT deposits generally appear as fine grained recrystallized rocks which range in color from white to creamy yellow, light green and dark green.

The deposits are dominated by felsic to mafic volcaniclastic or tuffaceous rocks with a minor cherty exhalative component (5%). Throughout the CRT deposits minor sulfide-rich beds are present (Balint and Severin, 1984). Pyrite and pyrrhotite dominate and form up to 20% of the rock locally. Near the Winston Lake deposit

sphalerite-rich beds have been noted and massive magnetite locally comprises up to 50% of a 5m section of CRT (Balint and Severin, 1984).

Plane-parallel bedding is well-preserved and common, particularly in clastic and cherty rocks, and typically ranges from mm-scale laminations to 15cm thick beds defined by color variation; local thickly bedded (>1-2m) to massive sections also occur. Normally graded beds are locally present. Soft-sedimentary flame structures and slump brecciation-textures are locally preserved in drill core in relatively unaltered rocks immediately up-dip of the Winston Lake deposit near L10000N. Cross- and wavy-bed-forms reported by Balint and Severin (1984) were not observed in this study.

In thin section the CRT deposits range widely in mineralogy depending upon the degree of hydrothermal alteration and primary composition. Recrystallized quartz (0-50%) and plagioclase (24-67%), and subidioblastic hornblende (0-50%) typically dominate and are accompanied by variable tremolite/ actinolite, muscovite, biotite, chlorite, epidote, sphene, and apatite (Appendix I). Garnet is locally abundant (10%) in the Gesic subsurface CRT intersections.

Mafic Volcanic and Intrusive Feeder Rocks (WLH-FR)

Detailed mapping in the L18-22E area (Plate 2) immediately northeast of Demijohn Lake has delineated a 100-150m-wide by 150m-thick sequence of mafic rocks, which on outcrop and in thin section are lithologically identical to lavas of the WLH. The sequence can be mapped up-section to the stratigraphic level of the

WLH where mafic lavas become laterally extensive to the north as the WLH-FWF. The distribution of mafic rocks and lithologic similarity to WLH-lava flows suggests the sequence represents vent facies deposits of WLH mafic rocks.

In overall distribution the mafic rocks appear to cross-cut the SIV volcaniclastic sequence; however, on outcrop no mappable dikes have been recognized. The base of the section is truncated by the Pond Fault. Most (65%) of the rocks are massive in character and probably represent both laterally limited lava flows and intrusive rocks. Contacts are relatively sharp and the mafic rocks interfinger over strike lengths of 25-100m with SIV rocks to the north. To the south, on surface, gabbroic intrusions displace much of the original stratigraphic section and only minor SIV is preserved in situ. However, primary stratigraphy is present in drill core north of and adjacent to the Pond Fault, where mafic lavas are interlayered with SIV rocks. Pillowed lavas, peperitic flows, and sheet flows are recognizable and are locally separated by thin SIV deposits; no autoclastic structures have been found.

Individual pillowed lava flows vary from 3-20m thick and can be traced a maximum of 100m laterally. Pillows are typically concentrated near the margins of more massive lava flows. Abundant pillows mark the terminus of one ~7m thick flow exposed at ~7880N, ~9695E, and the flow passes relatively abruptly along strike into SIV-FT deposits (Figure 16). Pillow structures are typically bulbous and bun-like to elongate in form and from 20-50cm in dimension. Very small, yet discrete pillows ranging from 1x3 cm to egg-size are locally well-preserved on the margins of lava flows. Budded forms with re-entrant selvedges are also locally preserved.

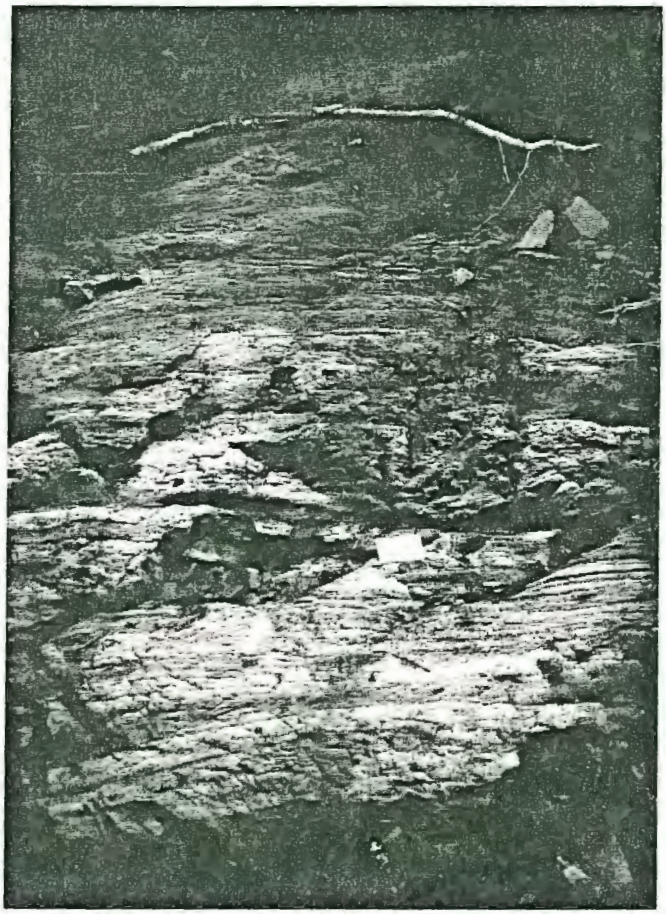

Figure 15. Photograph of a portion of the WLH showing mafic lava flows (WLH-MA) separated by laminated ashy sediments (WLH-CRT).

Figure 16. Photograph showing the pillowed terminous of a mafic lava flow (WLH-FR) in contact with bedded volcaniclastic-sediment (SIV-VC).

Pillows and buds are outlined by thin (≤5mm), fine grained, dark, hornblende(?)-rich selvedges. Rare, feldspar-filled, oval white amygdules(≤3mm) are locally present.

Pillows vary widely from tightly spaced structures with no interpillow material, to loosely-spaced, globule-like lava pods isolated within contorted bedded SIV (Figure 16). Near the margins of flows, pillows appear somewhat similar in shape to peperite structures associated with the LF deposits. The abrupt lateral termination of some lava flows and isolation of pillows within contorted, laminated clastic rocks suggests the mafic lavas may have been injected into or deposited on wet unconsolidated clastic material (Busby-Spera and White, 1987).

Sheet-flow lavas are relatively rare and appear as ≤2m-thick zones with 1-10cm thick by 40cm-2m long, overlapping, coalesced mafic sheets. Layering is conformable to bedding in associated CRT deposits and is typically marked by dark gray ≤7mm selvedge-like bands. No hyaloclastite was recognized in the rocks.

Winston Lake Volcanogenic Massive Sulfide Deposit (WLH-MS)

The Winston Lake massive sulfide deposit (WLH-MS) composes approximately 10% of the WLH. Apart from its relationship to the WLH stratigraphy, the WLH-MS has not been examined in this study. Morrison and Sim (1989), Balint and Severin (1984), and Sim et al. (1990) give more detailed descriptions of the orebody.

Total preproduction mineable reserves as of November, 1987 were 3,076,339 tonnes at 1% Cu, 15.60% Zn, 30.87 g/t Ag, and 1.02 g/t Au (Morrison and Sim,

1989). Two main ore types are known (Morrison and Sim, 1989) : (1) Low-grade ore consisting of 10-20% xenoliths in "massive-locally banded, fine to medium grained homogenous mixtures of sphalerite, pyrrhotite, pyrite, and chalcopyrite"; and (2) High grade ore (up to 54% Zn) comprised of massive to locally banded, medium to coarse-grained sphalerite, with chalcopyrite and/or pyrrhotite.

Approximately 30% and 70% of the WLH-MS is underlain by altered WLH-FWF and altered CLR, respectively (Balint and Severin, 1984). To the east gabbro comprises about 40% of the deposit's hangingwall. From 1 to 20m of laminated cherty CRT overlies the remainder of the WLH-MS; most of the CRT overlies the central vicinity of the deposit. Contacts with host rocks are typically sharp, and disseminated ore is rare (Balint and Severin, 1984).

Balint and Severin (1984) describe the massive sulfide deposit as a gently north-plunging succession of numerous thin, intercalated sheets with overall dimensions of 700-800m long by 300-400m wide with thickness from 2-~20m, but averaging ~4.3m. The thickest portions appear as elongate, mound-like sulfide accumulations (Sim, pers. comm.) and may be analogous to sulfide mounds of modern sea floor deposits (Davies et al., 1987; Kappel and Franklin, 1989). Locally up to 20% of the ore body consists of xenoliths or "rafts" of altered WLH enveloped within massive sulfide. Xenoliths range widely from 1cm to 15m in diameter.

Recent work by mine geologists suggests that zoning in Cu and Au distribution is present (Sim, pers. comm.). Detailed analytical work and mine development drilling has outlined two moderately north-plunging lineaments defined by Cu and

Au enrichment in the sulfides; cross-structures oriented approximately orthogonally to the lineaments may also be present.

Mine development has exposed a growth fault with ≤2m of displacement in the footwall rocks; no displacement is evident in the hangingwall to the sulfide deposit. The fault is sulfide-enriched and thought to represent a metal-bearing fluid conduit. Cu-enriched stringer-mineralization has been locally intersected by development drilling and typically underlies Cu-enriched zones.

Interpretation

Deposition of the WLH lava flows marked a return to volcanism after volcaniclastic deposition of the Upper Clastic Succession (UCS). The volcanism was periodic as reflected by intercalation of lavas with WLH-CRT and WLH-MS rocks.

Lithologic and chemical similarity, and laminated nature suggests the felsic components of the CRT represent fine ashy CLR material which settled from the water column after deposition of the main body of CLR. The subordinate mafic component of the CRT may represent fine grained reworked, granulated flow material or hyaloclastite associated with mafic lava flows. Cherty CRT reflects chemical precipitation and at least localized breaks in clastic deposition.

Similarities in character as well as general lack of hydrovolcanic deposits and amygdules suggests relatively passive volcanism beneath the VFD similar to that of mafic lavas of the MFS. Lack of flow breccia, sparsity of pillow structures, and the

laterally extensive, yet relatively thin nature suggest the lava flows were relatively fluid, low viscosity deposits.

Comparable thickness near the surface to deposit thicknesses at depth suggests the WLH lava flows were erupted from an elongate feeder similar to that of the MFS. Map relationships indicate lava flows probably emanated from a feeder source in the L18-22E area where a laterally limited, yet relatively thick section of mafic rocks is comparable in distribution to mafic rocks in the Cabin area. Mafic rocks in the L18-22E area may thus also represent an axial trough-like paleostructure; however, unlike the Cabin sequence, host deposits were largely unconsolidated volcaniclastic deposits. Growth faults probably developed contemporaneously with eruption of lava and confined the lateral distribution of the lava flows until the axial trough structure was filled. Subsequently erupted lava flows then became laterally extensive. Restriction of the WLH-FWF to the north and absence of it in the Gesic subsurface to the southeast, suggests a north-facing paleoscarp growth fault. Sheet-flow lavas, thin pillow selvedges, and local intrusive relationships is consistent with vent proximity in the L18-22E area.

The WLH-MS represents a stratigraphic break within the WLH. Sim, Balint, and Morrison (pers. comm.) suggest CRT xenoliths within, and CRT deposits above the massive sulfide deposit indicates inflationary and/or replacement processes similar to those of modern sea floor deposits of the Escanaba Trough (Koski et al., 1988) and Middle Valley (Franklin et al., 1990) were responsible for formation of the WLH-MS.

Growth faults, metal zoning, and paleolineaments in the massive sulfide deposit; soft-sedimentary textures and slump breccias in the footwall CRT deposits; and focused alteration in the footwall rocks suggest synvolcanic structures are present in the immediate footwall region of the ore body. The general observation of less continuous distribution of lava flows north of this region supports this conclusion as north-directed lavas would be partially or entirely dammed by south-facing fault scarps.

Localization of synvolcanic structures in the deposit area will be further described in a later section.

II.4 Rain Mountain-Gesic Block (RGB)

II.4.1 Introduction

The Rain Mountain-Gesic Block (RGB) includes a 50-200m thick section of rocks extending eastward approximately 3km from the south end of Pick Lake. The block is bordered to the south by granitic intrusive rocks and to the north by a gabbro sill and/or the Pond Fault. In the Rain Mountain area, drilling (ZO-71) indicates the gabbro sill becomes discordant at depth and has displaced and removed the primary stratigraphy. Detailed (1:1000) mapping in the Rain Mountain and Gesic areas (Figure 2) has allowed subdivision of the stratigraphy into three successions (Figure 5). These include from oldest to youngest: (1) Rain Mountain-Gesic Flow Succession (RGFS), (2) Rain Mountain-Gesic Clastic Succession (RGCS), and (3) the Rain Mountain-Gesic Horizon Succession (RGSH).

II.4.2 Rain Mountain-Gesic Flow Succession (RGFS)

Introduction

The Rain Mountain-Gesic Flow Succession (RGFS) forms the base of and comprises 50% of the preserved stratigraphy in the Rain Mountain-Gesic Block (RGB) (Figure 5). The flow succession is comformably overlain and locally inter-layered with clastic rocks and can be subdivided into Rain Mountain-Gesic (1)-QFP (RGQFP), and (2) -Ladder Flow (RGLF) (Plate 1) which are similar to the QFP and LF units of the WFB.

Rain Mountain-Gesic QFP (RGQFP)

QFP forms the base of the stratigraphy in the RGB. To the north the RGB-QFP is conformably overlain by mafic lava flows and intruded by granitic rocks. The QFP is locally exposed immediately east of the south end of Pick Lake (Plates 1 and 2). Diamond drilling in the Gesic area has intersected up to 170m of QFP at depths of up to 1300m down-dip of the surface; drill holes terminate within QFP indicating a greater actual thickness exists.

On outcrop RGQFP is similar in character to the QFP of the WFB. The rocks are tan to pinkish grey, massive, and contain a poorly to moderately well-developed ribbony-appearing cleavage; no autoclastic textures have been recognized. Unlike the QFP in the WFB, a well-developed banded appearance is not present in the RGQFP.

The rocks have been extensively recrystallized and are typically quartzofeldspathic; quartz (5-18%) and, where not extensively hydrothermally altered, plagioclase (0-13%) phenocrysts are present. Where altered, variable biotite (tr-20%), chlorite (0-10%), muscovite (tr-25%), garnet (0-13%), and cordierite (0-22%) are present along with rare tremolite/actinolite, anthophyllite, and staurolite.

Rain Mountain-Gesic Ladder Flow (RGLF)

Mafic lava flows of the RGLF are lithologically similar to flows of the Ladder Flow (LF) unit of the Winston Footwall Block (WFB). The RGLF overlies RGB-QFP and is generally overlain by volcaniclastic rocks (Plates 1 and 2). East of approximately Rain Mountain L17S on surface, the lavas are bordered to the south by granitic rocks. Diamond drilling in the Gesic area has intersected the mafic unit over 30-70m sections at down-dip depths of 400-600m where it overlies RGQFP. The mafic rocks extend the entire length of the RGB and range in thickness from 130m near Pick Lake to 30m immediately east of Round Lake. Individual lava flows have not been recognized anywhere in the RGB.

Unlike LF rocks of the WFB, the RGLF rocks are dominantly massive. Pillows are rare and have been recognized only in the Gesic area near L4+50E. The pillows are lensy and range from 5-25cm in thickness to 15-60cm in length; dark green hornblende-rich selvedges are typically ≤ 1cm thick. Sheet-like lavas up to 3-4m long occur locally near Rain Mountain L15S and consist of 1-2cm wide dark green parallel selvedges separated by 10-15cm massive zones. Autoclastic textures,

amygdules, or gas cavities have not been recognized. Where not hydrothermally altered the mafic rocks are dominated by plagioclase (5-50%) and hornblende (35-72%). Plagioclase phenocrysts vary from 0-25% in abundance and 2-5mm in diameter and are strongly concentrated towards the west. Porphyritic rocks dominate (80%) in the Rain Mountain area whereas aphyric to weakly porphyritic varieties are concentrated (80%) on surface exposures in the Gesic area. Gesic area drill intersections contain approximately 50% feldspar-phyric rocks. Where hydrothermally altered, hornblende decreases and is modally replaced by variable tremolite/actinolite (0-30%), biotite (0-22%), chlorite (0-28%), garnet (0-35%), anthophyllite (0-40%), cordierite (0-35%), staurolite (0-3%), and rare spinel (0-tr).

Interpretation

As with volcanic deposits of the WFB, the dominance of lava flows, and the lack of autoclastic structures, amygdules, or gas cavities suggests relatively deep water passive volcanism. The decrease in phenocryst content and unit thickness to the east suggests a westward proximal direction for the lava flow deposits. No eruptive vents have been recognized for volcanic deposits.

II.4.3 Rain Mountain-Gesic Clastic Succession (RGCS)

Introduction

The Rain Mountain-Gesic Clastic Succession (RGCS) composes 45% of the Rain Mountain-Gesic Block (RGB) and overlies the RGFS (Figure 5). The

succession can be subdivided into volcaniclastic (RGSIV) and pyroclastic components (RMCLR) (Plates 1 and 2), which are described below from oldest to youngest.

Rain Mountain-Gesic Synvolcanic Volcaniclastic Rocks (RGSIV)

Volcaniclastic (RGSIV) rocks comprise 95% of and form the base to the RGCS (Plates 1 and 2). The rocks are locally interlayered with mafic lava flows (RGLF), especially towards the west end of Rain Mountain. On the surface RGSIV deposits are approximately 120m thick near the west end of Rain Mountain and extend approximately 1500m east where they pinch-out within mafic volcanic rocks near Gesic L5E (Plate 1). Diamond drill hole GO-1, in the Gesic area, has intersected 35m of similar rocks approximately 300m downdip of surface.

On outcrop the volcaniclastic rocks appear tan to medium gray in color and vary from massive to bedded; bedding ranges from 1cm to 40cm in thickness and is generally less-well preserved than in volcaniclastic rocks of the WFB. The deposits vary from fine to coarse-grained; the coarser rocks are generally hydrothermally altered deposits.

Relatively fresh rocks are concentrated in the upper 20m of the Rain Mountain area and are dominated by recrystallized quartz and feldspar. Red-brown, $\leq$ 1cm, flowery-shaped garnet porphyroblasts locally accentuate bedding and constitute up to 20% of the rock. Quartz and feldspar crystal clasts have been found only rarely, and no lithic clasts have been noted.

Medium to coarse grained hydrothermally altered rocks dominate (85%) the stratigraphy and are most abundant in the Gesic area. Large (1-4cm) red garnet porphyroblasts (0-15%) accentuate compositional layering that may also reflect a primary layering.

In thin section fresh rocks are dominated by recrystallized quartz (20-43%), plagioclase (20-42%), and hornblende (12-40%) with accessory garnet, biotite, chlorite, muscovite, and opaques. Garnet (0-40%), tremolite/actinolite (10-30%), anthophyllite (7-40%), biotite (7-25%), and staurolite (tr-9%) are present where the rocks are more altered. Garnet porphyroblasts, in altered rocks, are typically growth zoned and may contain abundant quartz inclusions.

Rain Mountain Clotted Rhyolite (RMCLR)

Intermediate-felsic tuffaceous rocks are preserved near the east end of Rain Mountain where they compose approximately 5% of, and cap, the RGCS (Plates 1 and 2). Exposures of the tuffs are best as moderate to steep cliffs near grid location 1+80W between 13+30S and 13+60S. The unit is faulted-off at its west end near L15S where it reaches a maximum thickness of approximately 8m. No correlative rocks have been recognized east of Rain Mountain in the Gesic area.

On outcrop the tuffs are very well foliated and are distinctly blue-gray in color. They are typically ashy to fragment-rich and contain rare fine grained (1-2mm) quartz (0-2%) and plagioclase (0-1%) phenocrysts. Black lithic fragments locally compose 20% of the deposit, are typically lens-shaped, and range from 2mm

x 1cm to 8mm x 5cm in diameter. Hornblende dominates (80%) cores to the fragments and is accompanied by quartz and plagioclase which is concentrated in 1-3mm light grayish-white rims. Red-brown flowery-shaped garnet porphyroblasts (1-5%), ranging from 1-3mm in diameter, are locally overgrown on both fragment and matrix portions of the rock.

In thin section garnets appear similar to those of underlying fresh volcaniclastic (RGSIV) rocks. They are generally monocrystalline grains set in a matrix dominated by recrystallized quartz (30-39%), plagioclase (34-40%), and subidioblastic hornblende (0-12%). Tremolite/actinolite and biotite are locally present.

Interpretation (RGCS)

The quartz, feldspar, hornblende-rich character of unaltered RGSIV deposits suggests erosional derivation from a mixed mafic to felsic terrane.

By comparison to similar rocks (CLR) of the WFB, the RMCLR is thought to represent a pyroclastic flow deposit. The eastward thinning character of the tuffs suggests a westward proximal source.

II.4.4 Rain Mountain-Gesic Sulfide Horizon (RGSH)

Introduction

The Rain Mountain-Gesic Sulfide Horizon (RGSH) forms approximately 5% of and caps the Rain Mountain-Gesic Block (RGB) (Figure 5). The RGSH is

intruded and overlain by gabbro in the Rain Mountain area and by a felsite sill in the Gesic area (Plate 1). Contacts with the felsite appear gradational, probably due to shearing and structural intercalation. The sulfide horizon directly overlies Rain Mountain Clotted Rhyolite (RMCLR) at Rain Mountain, and at Gesic it is in gradational contact with underlying volcaniclastic deposits (Plates 1 and 2). Seven old trenches and two recent outcrop strips expose the sulfide horizon in the Gesic area. Where exposed, the horizon is 2-5m thick; however immediately west of Demijohn Lake it is up to 15m thick where preserved beneath the hangingwall gabbro intrusion. In the Gesic area diamond drilling intersected the RGSH in only one drill hole (GO-1) where it is 22m thick. All evidence indicates that faulting has displaced the down-dip extension of the mineralized horizon.

Lithologically the RGSH consists of two interlayered components that are in sharp contact: (1) mafic lava flows (RG-MA), and (2) mixed volcaniclastics, cherty tuffs, and sulfidic rocks (RG-CRT).

Mafic Lava Flows (RG-MA)

Mafic lava flows (RG-MA) are locally preserved in the Rain Mountain-Gesic Sulfide Horizon (RGSH). East of Gesic L5E lavas overlie and are separated from sulfidic rocks, volcaniclastics, and cherty tuffs (RG-CRT) by a felsite sill (Plates 1 and 2). Immediately west of Demijohn Lake, mafic lavas are locally interlayered with RG-CRT units and reach up to ~20m in thickness. The lavas are typically fine to medium grained, dark green-grey massive rocks. No amygdules, gas cavities, or

autoclastic textures have been recognized however, poorly preserved pillow structures are locally present. The mafics are typically aphyric but are locally feldspar phyric, especially at Rain Mountain. Phenocrysts are typically 1-3mm in diameter and are set in a fine grained matrix of hornblende and plagioclase. At Rain Mountain phenocrysts compose 2-8% of the rock, whereas at Gesic they are 0-3% of the rock.

Mixed Volcaniclastic, Cherty Tuffs, & Sulfidic Rocks (RG-CRT)

Mixed volcaniclastics, cherty tuffs, and sulfidic rocks (RG-CRT) dominate (90%) the Rain Mountain-Gesic Sulfide Horizon (RGSH). They occur throughout as a 2-22m thick basal unit of the succession and are locally well mineralized at both the Rain Mountain and Gesic showings (Plates 1 and 2).

In outcrop the RG-CRT rocks are typically fine grained, extensively recrystallized to a sugary texture, and vary from massive to banded or bedded on a cm-scale. Oxidation imparts a rusty red-brown to orangish color to the rocks, which makes recognition and delineation of lithologic variation difficult. Where distinguishable, volcaniclastic components are compositionally variable and appear somewhat similar to RGB-SIV deposits except for the presence of cherty interlaminae. They are mineralogically similar to RGSIV deposits and consist dominantly of quartz and feldspar with variable associated hornblende, tremolite/actinolite, garnet, biotite, chlorite, anthophyllite, spinel, and opaques. Cherty sections typically appear as light gray, cm-scale interbeds within these volcaniclastic rocks. Gossanous, rusty, well mineralized zones, which typically contain ≤ 10%

sulfides as pyrrhotite ± pyrite, minor sphalerite, chalcopyrite, and gahnite are found at the Rain Mountain and Gesic occurrences. Disseminated magnetite (0-8%) is locally present as 1-4mm subhedral grains. Semimassive sulfides are present in the Gesic area (Plate 2) where trench exposures and talus locally contain up to 45% sphalerite. Hydrozincite is locally present as diffuse white to gray chalky patches or thready seams on outcrop surfaces. Balint and Severin (1984) discuss the occurrences in further detail.

Interpretation (RGSH)

Volcaniclastic rocks of the Rain Mountain-Gesic Sulfide Horizon (RGSH) indicate continued sedimentation after deposition of the RMCLR pyroclastic unit. Mafic lavas mark a renewal of volcanic activity. Based upon compositional similarity to RGSIV deposits, the volcaniclastics probably represent a continuation of RGSIV-related sedimentation. The presence of stratiform cherty, sulfidic, and gossanous zones imply exhalative discharge contemporaneous with sedimentation.

II.5 Intrusive Rocks

Intrusive rocks make up approximately 65% of the rocks in the Winston Lake area when including the footwall stratigraphy and the immediate hangingwall to the Winston Lake deposit. They have not been examined specifically in this study except where observed in the course of detailed mapping. The distribution of intrusions was

outlined principally by CFC geologists and is recorded by Balint and Severin (1984) and Balint et al. (1984) from which the following descriptions are taken.

Four major groups of intrusions (Table 3) can be distinguished including: (1) those related to the Big Duck Sequence, (2) miscellaneous intrusions of unknown origin, age, or magmatic association, (3) granitic rocks, and (4) diabase dikes.

II.5.1 Big Duck Sequence-Related (GB-TZ-PX)

Intrusions chemically related to the Big Duck Sequence (Balint and Severin, 1984) are the most abundant intrusions within the Winston Lake area (Plate 1). The intrusions are differentiated mafic to ultramafic sills with lesser plug-like bodies.

Balint and Severin (1984) describe the mafic rocks (GB) as gabbroic to dioritic sills consisting dominantly of plagioclase and hornblende with minor K-feldspar and quartz. Accessory ilmenite (or leucoxene), magnetite, sphene, and Fe-sulfides are also present. Five textural varieties have been noted by Balint and Severin (1984) including:

(1) massive to weakly foliated gabbro,

(2) blotchy, mottled, or knobby gabbro,

(3) banded gabbro,

(4) coarse grained gabbro, and

(5) feldspar porphyritic or glomeroporphyritic gabbro.

The ultramafic rocks typically occur in a semicontinuous layer at the base of individual differentiated sills or in plug-like bodies. Balint and Severin (1984) subdivide the ultramafic rocks into transition (TZ), and pyroxenite (PX) zones.

Rocks of the ultramafic transition zone (TZ) typically occur between gabbroic rocks and pyroxenitic cumulate rocks and consist of 90-100% amphibole, ≤10% feldspar, and 5-10% phlogopite (Balint and Severin, 1984). Where present, the zone is typically ≤5m thick and is in gradational contact with underlying pyroxenite and overlying gabbro.

Pyroxenitic rocks (PX) occur as a relict cumulate phase at the base of the differentiated sills. The rocks typically consist of 60-90% blue-green amphibole, which is variably altered to chlorite or talc-chlorite. The base of the unit is typically marked by a shear zone (Balint and Severin, 1984). Five occurrences of mafic to ultramafic intrusive rocks have been noted at the Winston property. These include: the Zenith Sill, Rain Mountain Gabbro Sill, Contact Lake Sill, Ciglen Road Sill, and plug-like intrusions.

Zenith Sill

Mafic to ultramafic rocks of the Zenith Sill are the dominant intrusive rocks within the volcanic stratigraphy in the Winston Lake area and stratigraphically separate the Winston Lake and the Big Duck sequences. In map distribution the sill increases over ~8km of strike length from 0m to ~2500m in thickness from the northwest to southeast ends of the Winston property (Plate 1). Regional government

zone. No evidence of mafic volcanic rocks or gabbroic gneiss as mapped by Balint et al. (1984) was found during detailed mapping.

Contact Lake Sill (GB)

The differentiated mafic to ultramafic Contact Lake sill occurs near the base of the main QFP and extends over approximately 4 km of strike length from near L13000N south to the Contact Lake area where it is cut off by granitic rocks (Plate 1). The sill is typically 100-150m in total map thickness and consists of a 0-100m thick basal ultramafic zone and an upper gabbroic phase. The gabbroic and ultramafic phases are identical to those of the Zenith Sill. Morrison (pers. comm., 1989) suggests the Contact Lake sill may represent the basal differentiated portion of the lowermost Zenith Sill and that at depth, the intrusions merge and underlie the upper portion of the Winston Lake stratigraphy.

Ciglen Road Sill (GB)

Narrow (0-40m), north-south trending gabbroic sills extend from north of Cleaver Lake approximately 3500m to approximately L13000N and generally parallel the Ciglen road. The sills can be mapped southward into a 200m ± diameter gabbroic plug at the north end of Cleaver Lake. Lithologically the rocks are identical to gabbroic phases of the Zenith Sill.

Plug-like Intrusions (GB-PX)

Small (≤ 100m dia) generally plug-like differentiated intrusions were outlined by CFC geologists (Balint et al., 1984) near Puddle Lake (~9550N, ~9250E), and near ~10500N, ~9550E (Plate 1). The intrusive bodies are lithologically identical to those of the Zenith Sill.

II.5.2 Miscellaneous Intrusions

Felsite Sill (FD)--Gesic Area

A felsite sill (FD) of unknown age was outlined in the Gesic area by CFC geologists (Balint et al., 1984). The sill occurs as a 1300m long by 0-60m thick intrusion located in the immediate hangingwall to the Gesic occurrence (Plates 1 and 2). At its western end the sill is bordered to the north by gabbro; east of the Round Lake area the sill is bordered by mafic lava flows.

On outcrop the rock is very fine grained, tan to light grey, and very massive except where locally sheared and rusty. Petrographically the felsite consists of ≥ 85% quartz-plagioclase, with minor K-feldspar, muscovite, biotite, chlorite, and opaques.

F(Q)P Intrusion (F(Q)P)--Gesic Area

A coarse grained plagioclase ± quartz porphyritic (F(Q)P) rock was noted during reexamination of Gesic area DDH GO-1 (Plate 1). The rock is not exposed at surface. It occurs as a 120m thick section which is in fault contact with overlying QFP, and is intruded by gabbro down-hole. Considering the massive and relatively

coarse grained character of the rock it is thought to be of probable intrusive origin. The rock typically consists of 20-40%, 1-6mm plagioclase, and 0-2%, 1-4mm quartz phenocrysts set in a matrix of quartz, plagioclase, hornblende (≤ 10%), and biotite (≤ 15%) with accessory opaques, sphene, and apatite. Whole rock data (Appendix II) indicates an intermediate (66% SiO_2) composition.

II.5.3 Granitic Rocks

Granitic rocks border the Winston Lake Sequence (WLS) to the west and south and occur locally as dikes and sills within the WLS (Plate 1). No systematic detailed study on these rocks has been done to date, and they were not examined in this study except for occurrences in the Gesic and Cabin map areas.

Balint and Severin (1984) recognize three granitic phases. First, granite gneiss generally occurs within 100-200m of the base of the WLS stratigraphy and is typically grey to pink, streaky, and weak to moderately foliated. The granite gneiss locally contains xenoliths of sediment, QFP, and mafic volcanic rocks, and is locally cut by brickwork style alteration veins (Morrison, 1989, pers. comm.). The presence of xenoliths and alteration veins suggests the gneiss may represent a synvolcanic intrusive phase (Balint and Severin, 1984; Morrison, 1989, pers. comm.).

Second, massive granite is found generally beyond the granite gneiss and is feldspar and quartz-rich, with ≤ 10% hornblende-biotite. The massive granite locally cuts the granite gneiss.

Third, pegmatitic rocks are found throughout the granitic bodies and locally as ≤5m dikes and sills within the WLS. The pegmatites are typically coarse grained, quartz-biotite-K-feldspar-rich, and massive.

Detailed mapping in the Cabin area (Plate 2) identified a fourth granitic occurrence. Here, granite occurs as a light grey to tan, fine grained, locally sugary-textured, relatively massive, magnetite-rich (tr-5%) rock dominated by quartz-feldspar-biotite. The granite forms sills and dikes up to 25m wide and locally contains mafic volcanic and gabbroic xenoliths.

II.5.4 Diabase Dike (DB)

A diabase dike (DB) occurs near the south end of the property at the east end of Rain Mountain and in the L18-22E areas (Plates 1 and 2). The dike is typically 20-30m wide and subvertical. It has been right-laterally displaced by the Pond Fault over approximately 200m.

On outcrop the diabase is typically rusty-brown, fine to medium grained, and very massive. Balint and Severin (1984) report mm to cm scale grey-green, flinty-looking chilled margins to the dikes.

On the basis of lithological similarity to other diabase dikes in the region (Pye, 1964), the dike is thought to be of Late Proterozoic age.

III. PHYSICAL VOLCANOLOGIC RECONSTRUCTION

III.1 Introduction

A reconstruction of the physical volcanologic setting for the Winston Lake area has been developed based on detailed field studies. The Winston Lake area is underlain by alternating stratigraphic successions which are dominated by lava flows and clastic deposits. These deposits are believed to have been cyclically emplaced in a deep-water rift environment. The rift axis was centered near the south-end of the Winston Footwall Block (WFB) and was intruded by gabbro following volcanism of the Big Duck Lake Sequence. Late stage block faulting disrupted the volcanic sequence into the Winston Footwall and Rain Mountain-Gesic Blocks, and dextral strike-slip movement transported the blocks into their present positions. The evidence that leads to these conclusions includes stratigraphic correlations and facies relationships, physical morphology of deposits, synvolcanic structures, and rift-associated post-volcanic intrusions.

The following sections discuss the evolution of the stratigraphy and the stratigraphic location of and controls on sulfide mineralization. Structural considerations, which support the conclusions, are described in chapter IV.

III.2 Discussion

III.2.1 Stratigraphic Correlations and Facies Relationships

Several factors, including lithologic similarities, consistent thickness variations and facies relationships between successions, and lithologic units indicates the

Winston Footwall (WFB) and Rain Mountain-Gesic (RGB) Blocks were once a continuous section of stratigraphy. Following deposition, the stratigraphy was intruded by gabbro, block faulted, and right laterally displaced into its present position.

Figure 17 is a schematic stratigraphic correlation section along and between the stratigraphic blocks. The diagram illustrates unit by unit correlations and unit thickness variation. Table 4 summarizes and illustrates that a direct correlation can be made between the WFB and RGB for each stratigraphic succession except the Lower Clastic Succession (LCS) of the WFB. No Rain Mountain-Gesic Block-equivalent has been recognized for the LCS; this may reflect displacement and removal by granitic intrusives. For all other successions correlations can be made. However, within the successions that are correlable, the Camp Flow (QFF) and Footwall Flow (WLH-FWF) units (Table 4) are not correlable between the stratigraphic blocks as they were principally north-directed lava flows. The controls on the distribution of these flows is discussed in a later section in the context of synvolcanic structures. Facies relationships of most volcanic units are consistent when correlating the WFB and RGB and suggest that the rift axis was centered in the vicinity of the Pond Fault (Figure 17). Proximal volcanic facies directions for lava flows and for SIV-FT and PCLR pyroclastic units are consistently towards the fault. Volcanic feeder structures in the Cabin, L18-22E, and South Zenith Lakes area are situated at various stratigraphic levels near the south end of the WFB in the proximal volcanic facies (Figure 17).

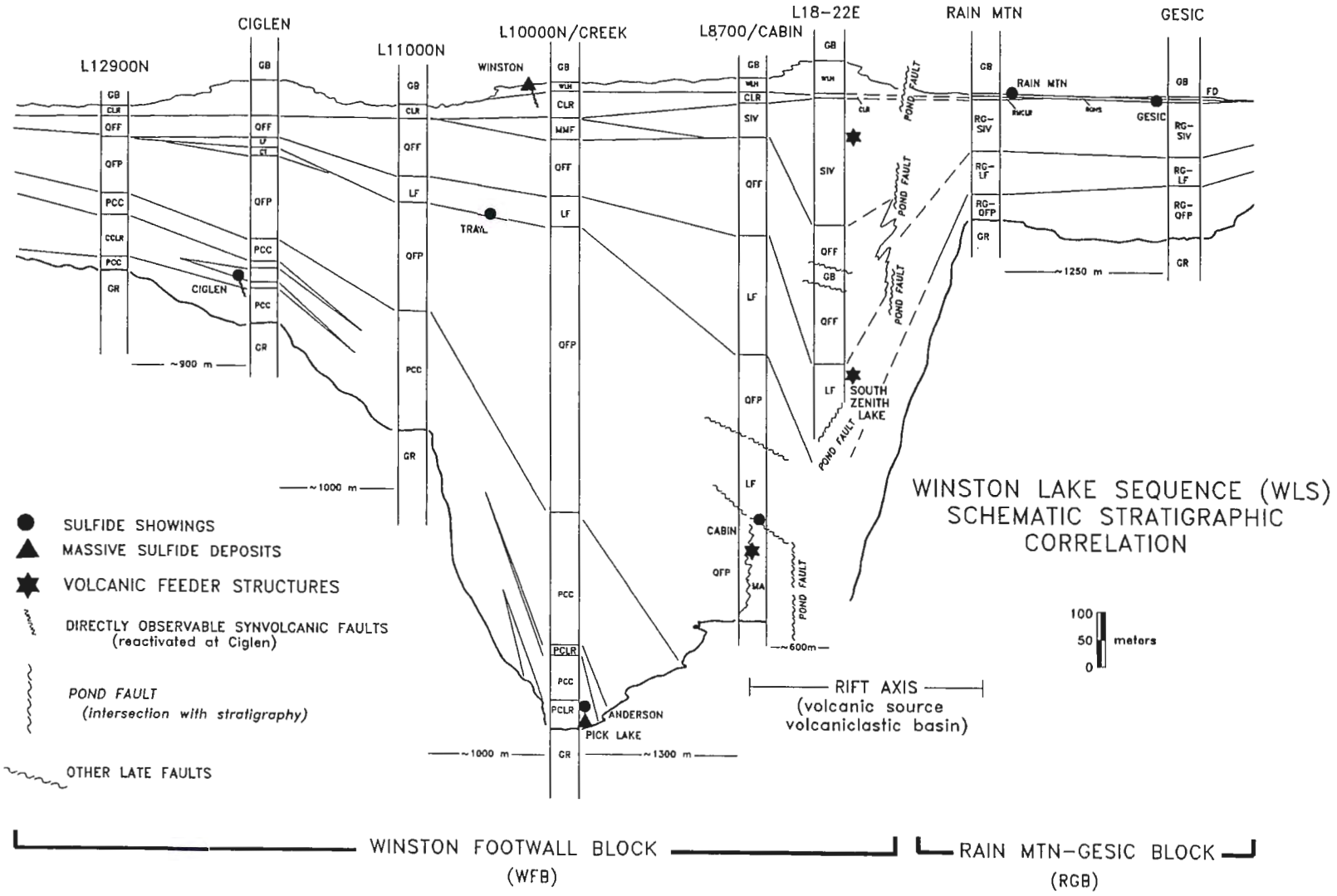

Figure 17. Unit thickness variation and schematic stratigraphic correlation of the Winston Footwall (WFB) and Rain Mountain-Gesic (RGB) Blocks. (modified from Balint and Severin, 1984, figure 8).

Table 4.

Summary of Stratigraphic Correlations between the Winston Footwall and Rain Mountain Blocks. Units listed from youngest (top) to oldest (bottom) except as noted[1].

WINSTON FOOTWALL BLOCK (WFB)		RAIN MOUNTAIN-GESIC BLOCK (RGB)
Succession units, (codes)		*Succession units, (codes)*
*Winston Lake Horizon (WLH)	----------	Rain Mountain-Gesic Sulfide Horizon (RGSH)
-Winston Lake VMS Deposit (WLH-MS)		----------
-Mafic Volcanic and Intrusive Feeder Rocks (WLH-FR)		----------
-Mixed Laminated Ash and Exhalative Sediments (WLH-CRT)	----------	-Mixed Volcaniclastic, Cherty tuffs, and Sulfidic Rocks (RGB-CRT)
-Mafic Lava Flows (WLH-MA)	----------	-Mafic Lava Flows (RGB-MA)
-Footwall Flow (WLH-FWF)		
Upper Clastic Succession (UCS)	----------	Rain Mountain-Gesic Clastic Succession (RGCS)
-Clotted Rhyolite (CLR)	----------	-Rain Mountain Clotted Rhyolite (RMCLR)
-Volcaniclastic and Associated Rocks (SIV)	----------	-Rain Mtn-Gesic Volcaniclastic Rocks (RGSIV)
**-Felsic Tuffs (SIV-FT)		----------
**-Synvolcanic Intermediate Volcaniclastics (SIV-VC)		----------
		----------
Middle Flows Succession (MFS)	----------	Rain Mountain-Gesic Flow Succession (RGFS)
**-Synvolcanic Felsic-Derived Sediments and/or Tuffs (CT)		----------
**-Undivided Mafic Rocks (MA)		
-Middle Mafic Flow and Associated Rocks (MMF)		----------
-Camp Flow Rhyolite and Assoc. Feeder Dikes (QFF)		----------
-Ladder Flow (LF)	----------	-Rain Mtn-Gesic Ladder Flow (RGLF)
-"Main" QFP (QFP)		-Rain Mtn-Gesic QFP (RGQFP)
*Lower Clastic Succession (LCS)		----------
-Chemical Precipitates (CRT, MS)		----------
-Pick Clotted Rhyolite (PCLR)		----------
-Ciglen Clotted Rhyolite (CCLR)		----------
-Pick-Ciglen Clastics (PCC)		----------

[1]No relative age relationship
*of units within successions implied
**of unit with respect to others implied

Thickness variation of correlated clastic deposits (SIV-RGSIV) suggests basinal accumulation centered between the Winston Footwall and Rain Mountain-Gesic Blocks. Thickening of the clastic deposits at the basin axis and of volcanic units in the proximal facies suggests subsidence of the stratigraphic pile coincident with volcanism and sedimentation. Although only preserved in the Winston Footwall Block (WFB), the southward thickened nature of the Lower Clastic Succession (LCS) is consistent with basinal accumulation and subsidence in the vicinity of the postulated rift axis. Subsidence was apparently relatively passive and gentle as slump/debris flow deposits associated with faulting are rare. Furthermore, subsidence was probably asymmetric with respect to the rift axis as discussed below.

III.2.2 *Physical Morphology of Deposits*

The dominance of lava flows, and the paucity of hydrovolcanic rocks indicates that volcanism throughout development of the stratigraphy was mostly passive and was characterized by deep water effusive eruptions. Feeders to the lavas were likely somewhat elongate based on the similarity of unit thicknesses at the surface and at depth.

Considering the dominance of lava flows and subsidence coincident with deposition, it is likely that major physiographic edifices were never present at Winston Lake. Instead a relatively low, broad gently-sloping elongate shield/plateau-like morphology was most likely.

III.2.3 Synvolcanic Structures in the Rift Axis Zone

Active rift environments are characterized in part as zones of synvolcanic faults (McKenzie et al., 1980). Such faults can be difficult to distinguish in ancient terranes where they have frequently been reactivated and are now the sites of late, post volcanic faults (Riverin, 1990, pers. comm.). At Winston Lake the Pond Fault, located near the south end of the WFB (Plate 1) probably represents, at least in part, a reactivated synvolcanic structure. The fault marks and transects the vicinity of the postulated rift axis and is in close proximity to and cuts off feeder structures in the Cabin, South Zenith Lake, and L18-22E areas. Movement related to development of the Pond Fault as presently positioned was likely focussed along stratigraphically weak synvolcanic fault zones.

Evidence of synvolcanic growth faulting in the present vicinity of the Pond Fault near the south is seen in the distribution of the Camp Flow (QFF) at its southernmost extent. DDH GO-3, collared near L8000N in the L18-22E area, intersected QFF material in three separate zones; all other drill intersections and surface exposures are characterized by one discrete body of the QFF material. In DDH GO-3 a lower, zone (≤50m thick) underlies two narrower (≤ 10m) sections of QFF that are interlayered with SIV-group volcaniclastic rocks. This interlayering with volcaniclastic rocks suggests growth faulting contemporaneous with eruption of the QFF unit. Except for minor southward flow, eruption was primarily north directed, likely due to the damming effect of a north-facing synvolcanic fault scarp. Minor backwards overflow of lava over the fault escarpment occurred coincident with

initial SIV volcaniclastic sedimentation and resulted in interlayering of the QFF and SIV deposits. Figure 18 schematically summarizes stratigraphic relationships and eruption history of the QFF unit in the proximal vent facies.

The distribution of mafic lava flows within the WLH, at the southernmost extent of the WFB, suggests the presence of a synvolcanic fault escarpment within the L18-22E feeder zone similar to that responsible for QFF distribution. North of the L18-22E mafic lava (WLH-FWF) forms the base of the WLH; in contrast, no stratigraphically equivalent lava flow deposit is present south of the feeder or in the Rain Mountain or Gesic areas. Instead, volcaniclastic rock (-CRT) forms the WLH and the base of the correlative RGSH. The selective distribution of the basal mafic lava flow is best explained by a north-facing fault escarpment that effectively dammed southward flow of mafic lava from its feeder zone until burial of the escarpment by subsequent deposition of the basal CRT unit.

Further evidence of synvolcanic faulting related to rift development is the overall greater thickness of volcanic and clastic deposits at the south end of the WFB in contrast to the correlative west end of the RGB. Greater thicknesses in the WFB may indicate that most active and greatest subsidence was on the northern, down-dropped side of growth faults in the axial zone. Alternatively, the comparative thickness differences may simply reflect a missing portion of stratigraphy from the west end of the RGB that was displaced or digested by subconcordant intrusion of the RM-GB.

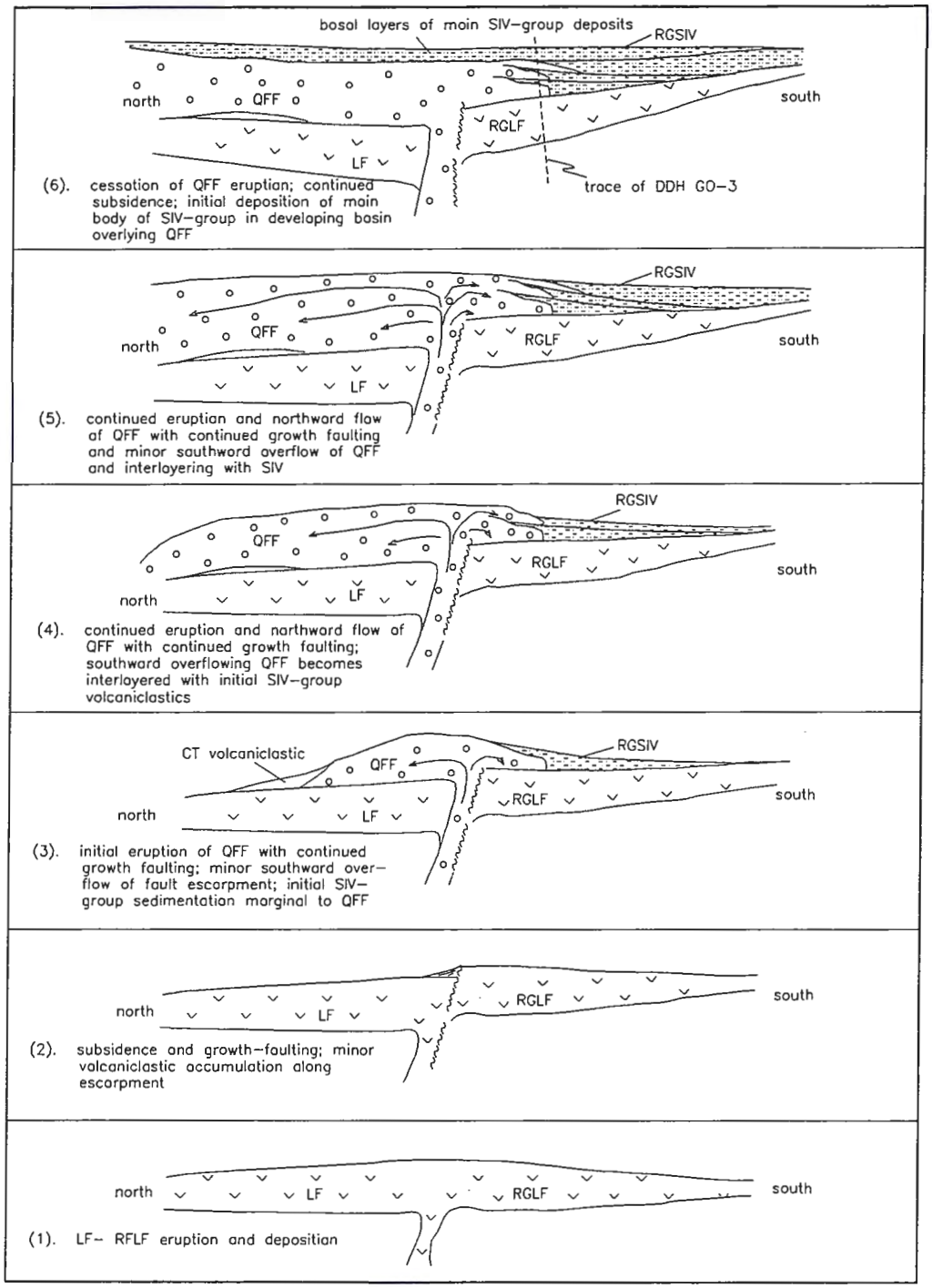

Figure 18. Schematic model of growth faulting, QFF eruption, subsidence, and associated SIV-group sedimentation near the rift axis.

III.2.4 Rift-Associated Post-Volcanic Intrusions

As noted previously the Winston Footwall and Rain Mountain-Gesic Blocks are separated in part by the Rain Mountain Gabbro (RM-GB) sill. As such the intrusion occupies a position in close proximity to the postulated axis of the paleorift. Lithologic and chemical similarities to the Zenith Sill indicate the intrusions are genetically related and, considering its location in the rift axis, it is likely that the RM-GB represents a feeder keel to the Zenith Sill. Intrusion was likely focussed in the rift axis along a zone of pre-existing synvolcanic weakness. Proximity of the RM-GB to the reactivated Pond Fault and feeder structures supports this conclusion. The intrusion may have displaced, or partially replaced, volcanic or volcaniclastic material in the axial feeder zone.

III.3 Stratigraphic Evolution

The stratigraphy of the WLS is dominated by interlayered volcanic rocks and clastic deposits. Volcanic rocks are dominantly lava flows that originated from passive eruptions in deep water beneath the VFD and were erupted from an axial rift. Volcaniclastic rocks were deposited mainly in subsiding basins that developed in the vicinity of the axial rift; clastic sedimentation was periodically interrupted by emplacement of pyroclastic flow deposits and/or their turbiditic equivalents. Pyroclastic volcanism was principally from extraneous source vent(s) to the north, but was rarely from episodically active vents within the rift axis. Pauses in volcanism and clastic deposition were marked by local chemical sedimentation and mineralization.

Deposition of the chemically distinct mafic volcanic rocks of the Big Duck Sequence (BDS) marked an end to construction of the Winston Lake Sequence. Emplacement of chemically related intrusions followed deposition of the BDS. The Zenith Sill was fed through a keel-like intrusion that transected the WLS and is represented by the Rain Mountain Gabbro. The keel was localized in a pre-existing zone of weakness centered along the WLS paleorift.

Late stage structural stresses reactivated synvolcanic structures within the rift axis and resulted mainly in dextral strike-slip motion.

Figure 19 schematically summarizes development of the Winston Lake area stratigraphy.

III.4 Stratigraphic Location of Mineralization

Mineralization in the WLS is localized in several stratigraphic positions; this probably, in part, reflects evolution of the WLS paleorift. Figure 17 illustrates the stratigraphic position of various surface showings and massive sulfide deposits. Apart from the Winston and Ciglen occurrences direct evidence for controls on localization of mineralization has not been recognized. Nevertheless several points can be made regarding the stratigraphic position and localization of the occurrences.

Synvolcanic growth faults have been recognized both beneath and within the Winston Lake deposit and at the Ciglen occurrence (Balint and Severin, 1984). Considering the thickening and subsidence of the stratigraphic pile in the postulated paleorift axis, it is plausible that most of the synvolcanic faults were south-dipping

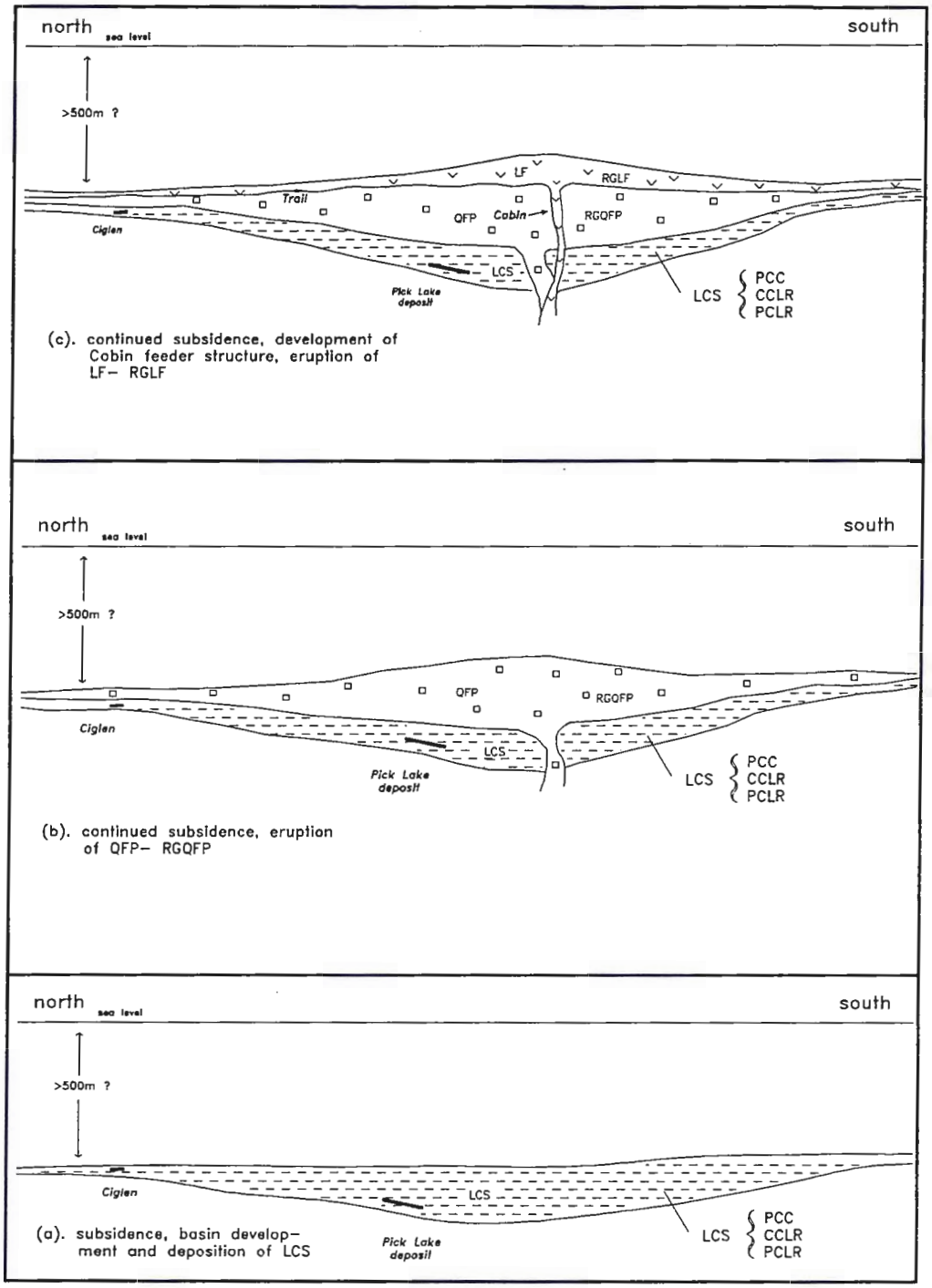

Figure 19. Schematic summary of stratigraphic development of the Winston Lake area stratigraphy.

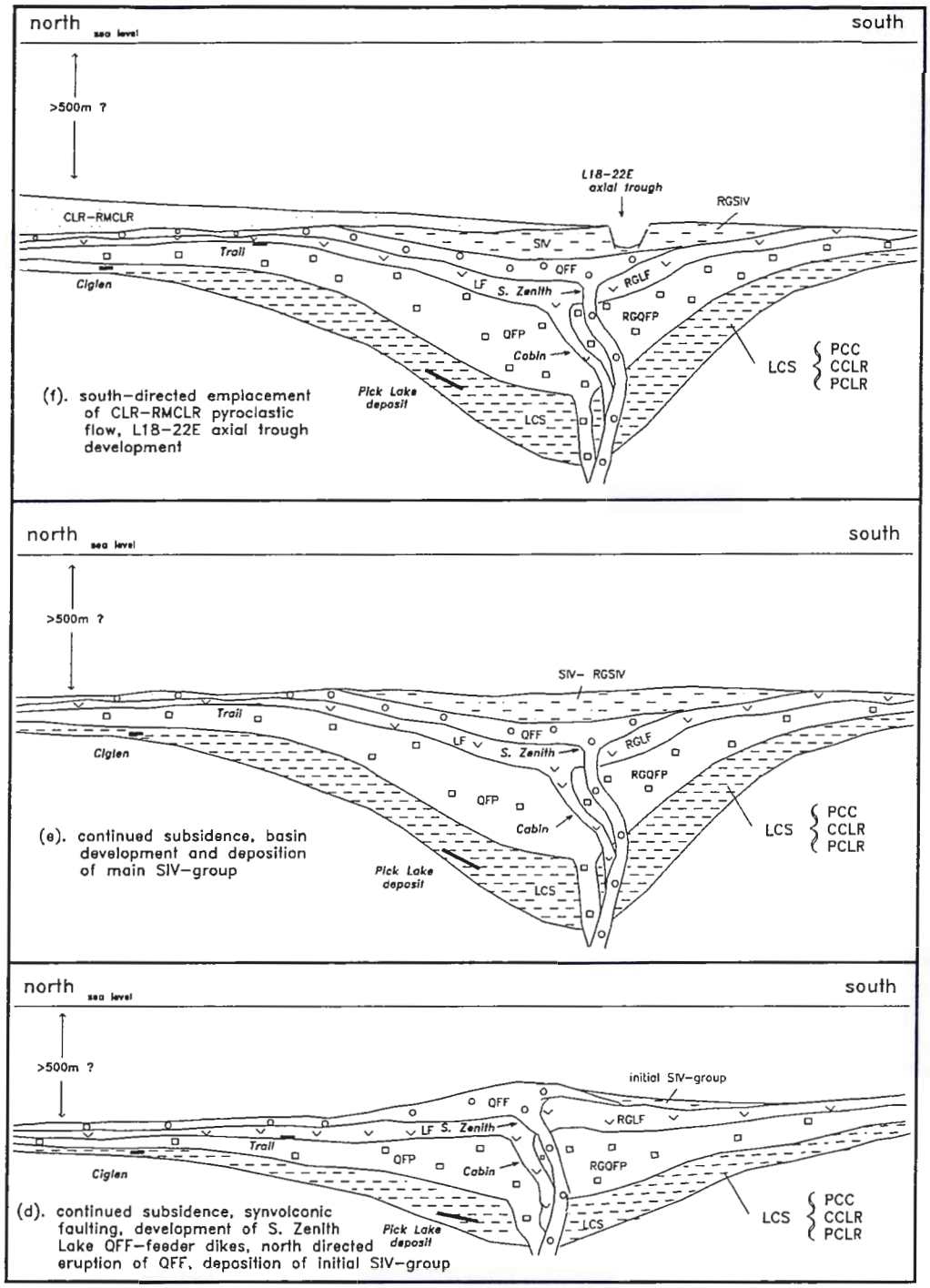

Figure 19. (continued)

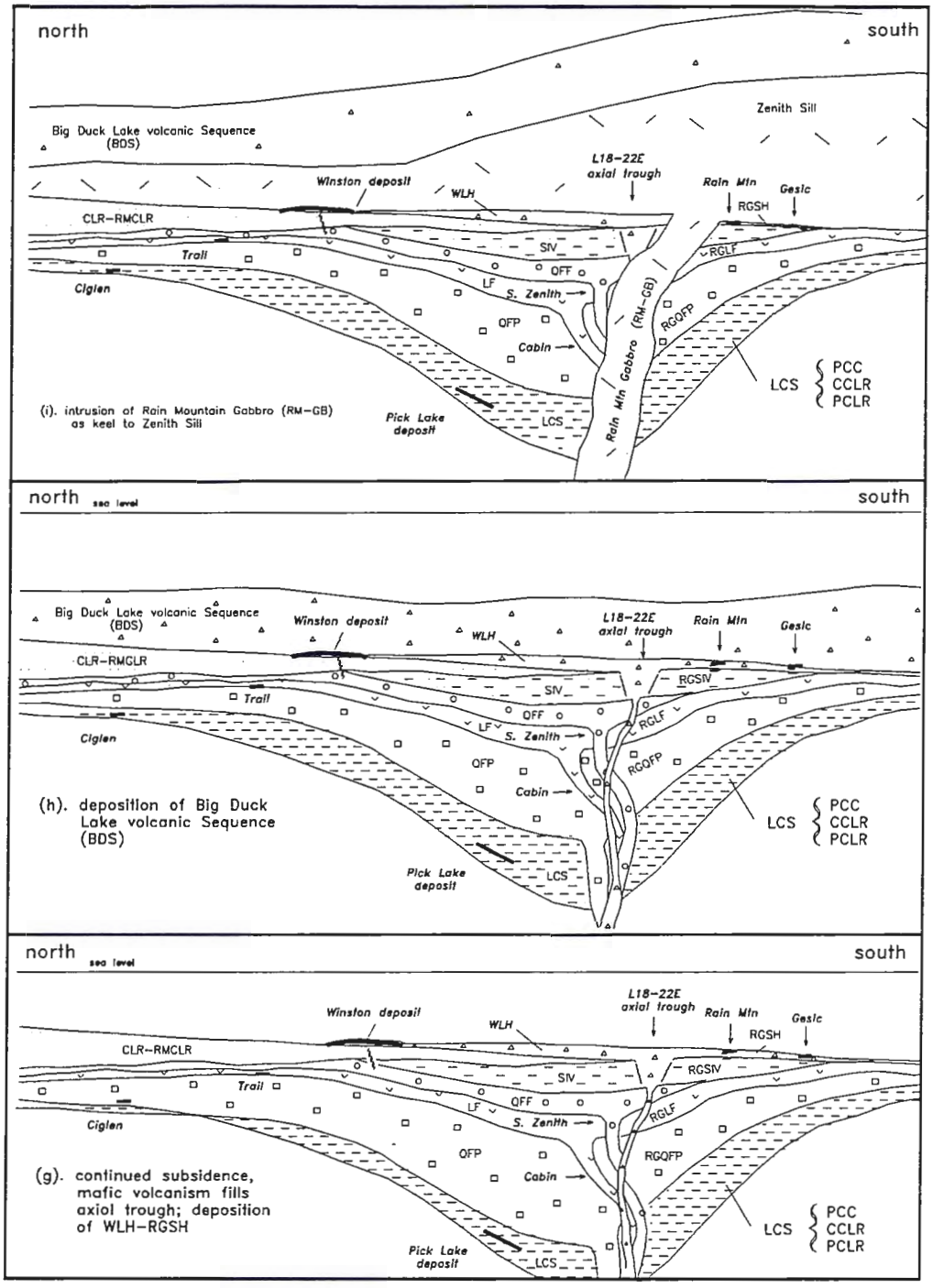

Figure 19. (continued)

normal structures that developed in response to subsidence-related stresses. The faults likely channeled metal-bearing hydrothermal fluids towards the seafloor where the metals were deposited.

Detailed review of diamond drill core from the Pick Lake Deposit area has outlined multiple felsic pyroclastic units (PCLR), some of which show relatively abrupt discontinuity in lateral distribution. Such discontinuity, along with steeply north-plunging thickness trends in the massive sulfide deposit (Morrison, 1991, pers. comm.) suggests synvolcanic faulting may have occurred and could have initiated mineralization. The location of the deposit, marginal to the postulated rift axis, would be a zone of active synvolcanic faulting, high heat flow, and high permeability, all favorable factors in development of massive sulfide deposits.

The Cabin occurrence, by association with volcaniclastic (CT) rocks and mafic lava flows (LF), is thought to have formed during pauses in volcanism. Proximity to the volcanic feeder structure recognized in the Cabin area and the Pond Fault indicates localization of mineralization near the axis of active rifting and volcanism.

Mineralization at the Trail showing is associated with local volcaniclastic (CT) deposits beneath and between individual flows of the LF unit; mineralization is also present within pillowed flows. Sulfide deposition occurred during pauses in flow deposition that likely reflect periods of subsidence and volcanic quiescence in the rift axis. Although not recognizably associated with synvolcanic faulting, the volcaniclastics and pillowed lava flows were likely highly permeable rocks that could focus migrating hydrothermal fluids and provide favorable hosts for mineralization.

Finally, the Rain Mountain and Gesic occurrences are located within the RGSH and are considered approximate stratigraphic equivalents of the Winston Lake deposit. If synvolcanic faults are present, they should mirror (across the rift axis) synvolcanic faults beneath the Winston deposit.

IV. STRUCTURAL GEOLOGY

IV.1 Introduction

The structural geology of the Winston Lake Sequence was not specifically examined in this study, but structural data were collected during the course of detailed mapping. The following sections summarize the data collected from minor folds, foliations, lineations, kinematic indicators, joints, and faults. These data, along with previous descriptions of Balint and Severin (1984), were used to reconstruct the deformation history of the WLS.

All of the rocks in the WLS have undergone some degree of structural deformation. The deformation was progressive; early megascopic structures are cut and displaced by faults. A Keweenawan diabase dike cuts the early structures and the displaced stratigraphy and is itself displaced indicating at least local reactivation of faults. No major folds have been recognized.

IV.2 Megascopic Structures

IV.2.1 Introduction

Megascopic structural elements present throughout the WLS include foliation, minor folds, and local lineations and kinematic indicators. Orientations of foliation and fold data are characteristically distinct between the Winston Footwall and Rain Mountain-Gesic Blocks.

IV.2.2 Winston Footwall Block (WFB)--Megascopic Structures

Foliation is present throughout the WFB and is best developed in clastic rocks. In felsic lava flows the foliation is developed to varying degrees and typically occurs as a ribbony-appearing cleavage. The foliation typically parallels primary layering and, on average, strikes ~160° and dips ~40-50° to the east. Strike varies to ~200° degrees in the Contact-Loon Lake area near the south end of the LCS. Lens-shaped lithic fragments and alteration pseudofragments are flattened parallel to the foliation plane. Crenulation cleavage is developed locally on the foliation. The trend of the cleavage varies widely, but is generally east-west and cleavage typically dips steeply to the south. The cleavage has only been recognized in close proximity to faults.

Numerous minor folds have been mapped in the L18-22E area at the south end of the WFB. The folds are best developed in WLH-CRT and SIV deposits and have a consistent Z-geometry. The folds are typically open to closed with a moderately inclined axial plane (~45°) and moderate plunge (~35°); fold axes have an average bearing of ~135°. The regional foliation is axial planar to the folds. Rare mineral lineations in the rocks are defined by hornblende and are parallel to fold axes.

Kinematic indicators have been recognized, although rarely, within the LCS near the western margin of the WFB. At the Ciglen showing a narrow granitic dike shows repeated left lateral offset of up to 0.5m along 20cm to 1m spaced foliation

planes. Clockwise rolled garnets indicating sinistral shear movement are present locally at the Anderson strip.

IV.2.3 Rain Mountain-Gesic Block (RGB)--Megascopic Structures

A limited amount of foliation and fold data were collected from the RGB. Foliation is well developed throughout the area; minor folds are rare. No crenulation cleavage or kinematic indicators were recognized.

The dominant structural element in the RGB is a well developed bedding parallel foliation. The foliation is parallel to primary layering. The attitude of the foliation is notably distinct from that in the WFB as strike and dip average ~270° and 45° to the north, respectively. As in the WFB, lens-shaped lithic fragments are elongated parallel to foliation.

Minor folds are rare in the RGB and are found only within RGSIV deposits. The folds are similar to those in the L18-22E area of the WFB; they have an open to closed Z-geometry and are moderately inclined and plunging. An average fold axis has a bearing of ~070° and dip of ~35°. As in the WFB foliation is axial planar to folds.

IV.3 Joints

Joints are present throughout the Winston Lake area in virtually all rock types. Conjugate sets are commonly discernible on individual outcrops, but no grouping of joint sets is recognized on an area-by-area or regional basis. Joints

range widely in strike and generally dip subvertically. Northeasterly-trending joints are most prominent and strike on average ~035°. No other concentrated orientation of joints is recognized.

IV.4 Faults

Faults are present throughout the Winston Lake area; they have been recognized by displacement of stratigraphy and by weak to pronounced topographic linears. They have been intersected in drilling and vary in appearance from narrow (≤ 10m) strongly foliated zones to narrow (≤ 10cm) to wide (10's of meters) zones of clay-chlorite-rich fault gouge or quartz-flooded brecciated zones. The faults are all considered to be late stage structures as they generally cut and offset primary layering, altered stratigraphy, and foliation trends.

Based on style and predominant attitude Balint and Severin (1984) classified faults into three groups: Contact, Splayed, and Northeast Trending types.

IV.4.1 Contact Faults

Balint and Severin (1984) defined Contact Faults as those faults which parallel formational contacts. Four such faults are recognized including the X-fault, Kenebec Lake Fault, Cleaver Lake Fault, and the Camp Flow Fault (Plate 1). The faults are characterized as highly foliated, schistose, micaceous or chloritic shears ranging from centimeters to meters in thickness (Balint and Severin, 1984). Displacement along the faults has not been resolved.

IV.4.2 Splayed Faults

Several splayed faults are present near the south end of the WFB. The structures are typically subparallel to stratigraphy and form arcuate trending faults that can sometimes be mapped laterally into Contact Faults. The faults typically strike 120-160° and dip eastward. Stratigraphy is most noticeably displaced along these structures between the Pick and Zenith lakes areas where fault-bounded slices of LF and QFF have been structurally intercalated primarily with QFP. Based on map relationships, movement was horizontal, but was locally along the dip plane direction. Balint and Severin (1984) resolved dextral displacement of stratigraphy on several of the Splayed Faults.

The Pond Fault located between the WFB and RGB is considered a special example of the Splayed Faults. The structure varies along strike from subparallel to locally discordant to stratigraphy. Stratigraphic correlations and volcanologic reconstruction indicates right lateral displacement of at least 1km.

IV.4.3 Northeast Trending Faults

Balint and Severin (1984) define NE Trending Faults as subvertical faults that strike ~020-060° and intersect the stratigraphy at high angles. The structures are reflected topographically as very weak linears along which stratigraphy has been offset less than 10's of meters. Balint and Severin (1984) postulated that NE faults in the vicinity of Puddle Lake and Selim Creek may represent reactivated ring faults that developed in the volcanic edifice beneath the Winston deposit and may have had a controlling influence on the distribution of alteration. No evidence to support this theory was observed in this study.

IV.5 Structural Interpretation

Based upon cursory examination and review of structural data it seems that deformation in the Winston Lake area occurred in multiple stages. Deformation was coincident with metamorphism and was related to intrusion of granite magma marginal to the WLS.

Development of foliation within the Winston Lake area was an early deformation possibly coincident with rotation of the stratigraphy. The stratigraphy underwent significant flattening during foliation as evidenced by elongation of fragments parallel to the foliation plane. Foliation axial planar to minor folds indicate that folds developed coeval with the foliation and are related to a regional folding of stratigraphy. Similarity in structural elements and in angular relationships of foliation to minor folds indicates co-development of the structures in the RGB and WFB prior to block faulting.

Stresses following foliation and fold development resulted in faults along which crenulation cleavage developed locally. Displacement was variable but dominantly dextral and resulted in transposition of the RGB at least 1km from the WFB along the Pond Fault. The Pond Fault was reactivated as evidenced by displacement of the primary stratigraphy and offset of granite and diabase that intrude the stratigraphy. Development of joints throughout the area was likely related to the same stress regime responsible for faulting.

V. ALTERATION

V.1 Introduction

During early reconnaissance mapping of the Winston Lake property, CFC geologists recognized certain metavolcanic rocks that contain cordierite and anthophyllite or sillimanite. Such rocks are unusual because there is no primary igneous rock of comparable composition that, upon metamorphism, would contain such minerals (Winkler, 1979; Yardley, 1989); thus, Balint and Severin (1984) concluded they were hydrothermally altered prior to metamorphism. Many of the rock units in the Winston Lake Sequence (WLS) have been metasomatically altered by hydrothermal solutions and subsequently metamorphosed to amphibolite grade. The alteration resulted in chemical changes to the rocks, but metamorphism was isochemical and resulted only in the growth of metamorphic minerals and development of metamorphic textures. The composition and distribution of the present mineralogy therefore reflects premetamorphic hydrothermal alteration of varying degrees; the distribution of alteration may have been modified somewhat by post-volcanic, post-hydrothermal structural transposition.

One of the primary purposes of this study is to describe the variability in mineralogy that reflects premetamorphic metasomatism. Such description is essential to geochemical characterization of the rocks and an understanding of the chemical changes that took place in these rocks during hydrothermal alteration.

V.2. Distribution of Alteration

In this study hydrothermally altered rocks are defined as those rocks containing muscovite, biotite, chlorite, hornblende, epidote, tremolite/actinolite, cordierite, anthophyllite/gedrite, sillimanite, andalusite, staurolite, or spinel in modal abundances inconsistent with metamorphosed primary igneous or sedimentary compositions (Winkler, 1976; Yardley, 1989). Altered rocks comprise approximately 50% of the Winston Lake Sequence (WLS) and occur principally as subconcordant zones. Surface alteration extends from near the southwestern edge of the Winston Footwall Block (WFB) north to the Fish Lake area (Plate 1). This alteration connects with a subconcordant zone near the stratigraphic top of the WFB that extends from ~L10000N to the north edge of the map area. Subconcordant alteration is also developed along approximately 2km of strike in the Rain Mountain-Gesic area. Through drill core studies, alteration of comparable extent has been recognized down-dip of the surface exposures, but the pervasiveness of alteration generally decreases with increasing depth.

Certain minerals characteristic of metamorphosed hydrothermally altered rocks are most abundant and extensively developed in certain protoliths and are absent or minor in others. For example, anthophyllite is best developed in mafic protoliths, and sillimanite and andalusite are best developed in felsic protoliths. Such associations indicate that the rocks buffered the fluids to varying degrees and that the composition of the altered rocks reflects, in part, the compositional character of protoliths. Experimental studies (Seyfried, 1987; Mottl, 1983) indicate that the final

bulk composition of rocks affected by hydrothermal alteration is a function of several factors including protolith composition, fluid chemistry, volume of reacting hydrothermal fluids, and the intensity and duration of chemical exchange between fluid and rock.

Figure 20. Photograph illustrating outcrop-scale substratiform biotitic alteration within bedded volcaniclastic-sedimentary rocks of the PCC unit. Alteration is evident as dark band across outcrop on which hammer is approximately centered.

The original porosity and permeability of the rocks was apparently an important factor in controlling the distribution of alteration. Alteration is laterally extensive and sub-stratiform in volcaniclastic-sedimentary rocks on both a unit, and outcrop-scale (Figure 20). Such units were likely to have been permeable when

deposited; the distribution of alteration fits well with this characteristic. On outcrop and in thin section, adjacent beds or bands are commonly composed of the same minerals but in widely differing modes. This represents variable alteration of beds or layers dependent upon differing primary mineral modal variation and composition, and/or permeability control on the volume of hydrothermal fluids available to react with a bed. Alternatively the layering could represent, in part, a metamorphic compositional differentiation.

The felsic pyroclastic units (CLR, CCLR, RMCLR, and PCLR) appear to be less pervasively altered than enclosing rocks suggesting that they had relatively low permeability. This may reflect recrystallization and self-sealing of the rocks immediately after emplacement due to latent heat of eruption.

Field observations indicate that primary lava flow morphology was an important factor in controlling the distribution of alteration within mafic lava flows. This is especially evident in the LF north of ~L10000N. On outcrop individual pillows, lobes, and lava tubes are intensely and pervasively altered and may be in sharp contact with very weakly or unaltered, massive flows of the same primary composition. The pillows, lobes, and lava tubes apparently focussed and channeled hydrothermal fluids because of relatively high permeability. Flow brecciated zones exhibit pervasive alteration in matrix material and variable alteration in fragments, suggesting relatively high permeability in the matrix.

Direct controls on the distribution of alteration minerals within felsic lava flows (QFF, QFP, and RGQFP) have not been recognized except for possible

selective alteration along primary flow banding-induced compositional heterogeneities.

V.3 Outcrop-scale Alteration Textures

On outcrop or in drill core, where alteration is not pervasive or controlled by primary flow morphology or layering, distinctive textures that reflect alteration can be recognized. Veins filled with hornblende or biotite ± cordierite-anthophyllite are present locally and have been described as "brickwork" style alteration by CFC geologists. The veins are typically ≤20cm wide and are subparallel to primary layering or cross-cut non-altered to weakly-altered rock.

Locally, in felsic volcanic rocks, a continuum of alteration textures can be observed from fresh rock to brickwork style veins to semipervasive alteration that surrounds domains of fresh to weakly altered rock (Figure 21). Where deformation is relatively minimal, fresh domains are highly irregular to amoeboid-like in shape, but where deformation is relatively strong, the fresh domains are lens-like, 2-20cm long, and are referred to as pseudofragments in local mine terminology (Figure 22). Altered portions of the rocks represent fractures or zones through which hydrothermal fluids moved.

V.4 Alteration Zones

Field mapping supplemented by petrographic study has allowed subdivision of the stratigraphy into eight zones (Plate 1) that developed in response to

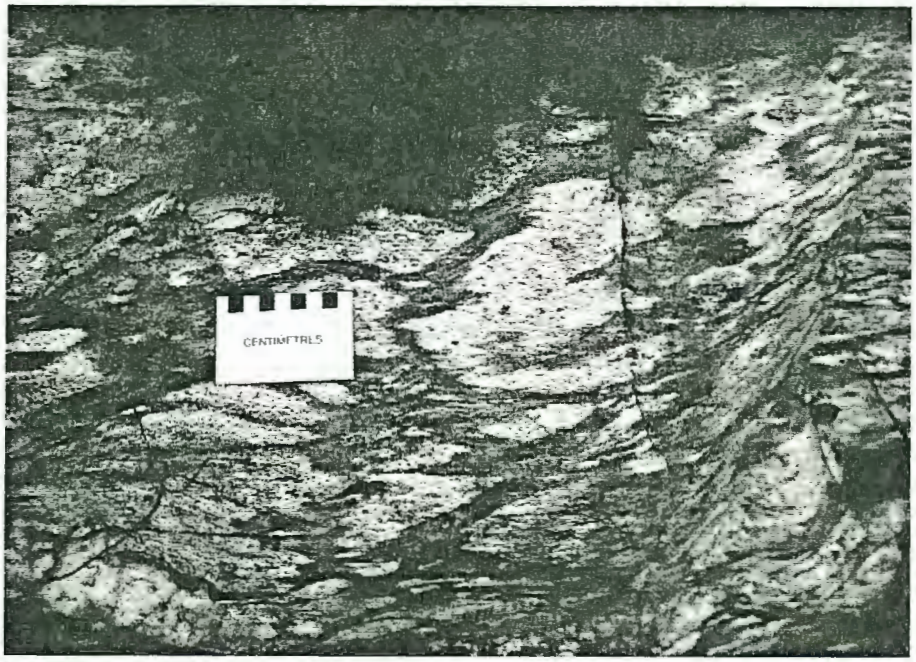

Figure 21. Irregular to amoeboid-shaped domains of relatively fresh rock (light colored) surrounded by intense, semipervasively altered matrix (dark colored).

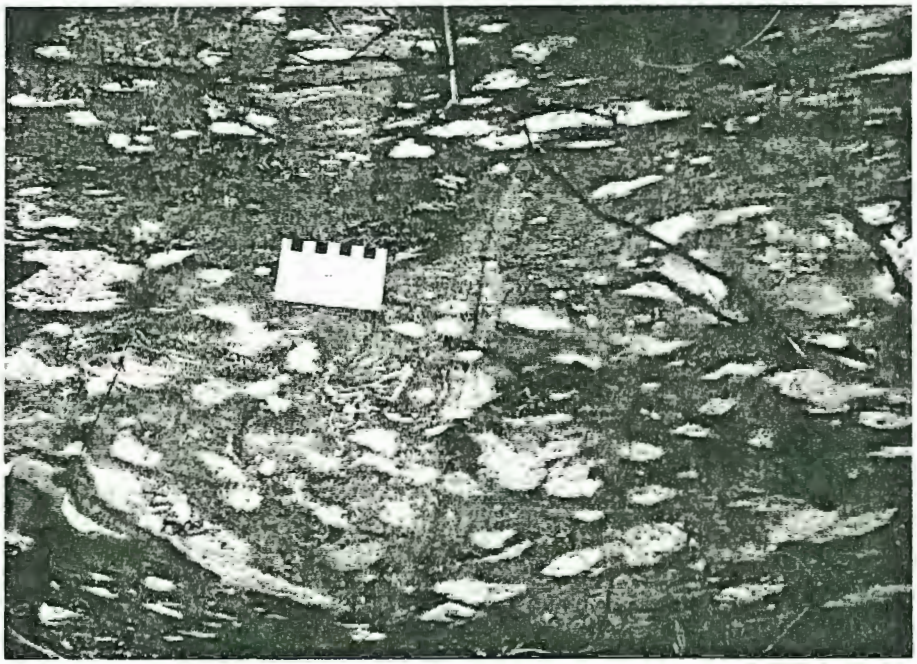

Figure 22. Lens-shaped alteration "pseudofragments" (light colored) surrounded by intensely-altered matrix.

metamorphism of variably hydrothermally altered rocks. The zones have been defined primarily on the presence of a characteristic mineral in an assemblage identifiable in rocks of the map area (Table 5). In delineating zones the modal abundance of the characteristic mineral is considered of subordinate importance to its presence, because at amphibolite grade the grain size is typically coarse and the modal abundance is largely dependent upon the specific position in a rock from which a thin section is cut. The alteration zones are named for the characteristic mineral(s) present and are: (1) least altered, (2) tremolite/actinolite, (3) biotite, (4) sillimanite, (5) sillimanite-staurolite, (6) anthophyllite/gedrite, (7) chlorite, and (8) quartz.

Mineral assemblages may differ slightly within a particular alteration zone depending upon primary lithologic composition. For this reason, to summarize the mineralogical composition of alteration zones, the rock units are divided into four general categories based on mineral assemblages: mafic volcanic rocks, volcaniclastic rocks, felsic lava flows, and felsic pyroclastic rocks (Table 5).

The subconcordant distribution of alteration zones makes delineation of temporal relationships among zones difficult. Locally, however, the distribution of and sharp contact relationships among zones suggest cross-cutting or overprinting of zones. Elsewhere contact relationships between zones are gradational and imply progressive, gradual variability in the effects of metasomatism.

In order to identify variations in composition of certain minerals between and within alteration zones, rock samples were studied by electron microprobe. A suite

Table 5.
Alteration Assemblages

ALTERATION ZONE	MAFIC VOLCANIC ROCKS: (LF,RGLF,MMF, FWF,MA)	VOLCANICLASTIC SEDIMENTARY ROCKS: (LCS,PCC,SIV,RGSIV,CT)	FELSIC LAVA FLOWS: (QFF, QFP, RGQFP)	FELSIC PYROCLASTIC ROCKS: (CLR,RMCLR, CCLR, PCLR, SIV-FT)
LEAST ALTERED (LA)	PL-HBL-OPA ± [1] PP-QTZ-T/A	QTZ-PL-HBL ± [1] QP-PP-KSP-GNT-OPA	QP-PP-QTZ-PL ± [1] KSP-HBL-GNT-CDT-OPA	QTZ-PL-HBL ± [1] QP-PP-KSP-T/A-GNT-OPA
TREMOLITE/ ACTINOLITE (T/A)	PL-T/A-OPA ± [2] PP-QTZ-HBL	QTZ-T/A ± [2] QP-PP-PL-HBL-BIO-GNT-OPA	none	QTZ-PL-T/A-BIO-OPA ± [2] QP-PP-GNT
BIOTITE (BIO)	QTZ-BIO-OPA ± [3] SP	QTZ-BIO ± [3] QP-PP-HBL-T/A-SP-OPA	QTZ-BIO ± [3] QP-PP-PL-KSP-OPA	QTZ-BIO-CHL-OPA ± [3] QP-PP-KSP-HBL-T/A-PIN
SILLI-MANITE (SIL)	none	QP-QTZ-MUSC-BIO-CHL-SIL ± [4] EPI-GNT-	QTZ-BIO-SIL ± [4] QP-MUSC-CHL-EPI-GNT-PIN	QTZ-PL-MUSC-BIO-CHL-SIL ± [4] PIN
SILLI-MANITE-STAUROLITE (SIL-ST)	none	QTZ-BIO-CHL-SIL ± [5] PIN	QTZ-CDT-SIL-ST-OPA ± [5] BIO-CHL-GNT	QTZ-CHL-SIL-ST ± [5] BIO
ANTHOPHYLL-ITE/GEDRITE (AN/GD)	AN/GD-OPA ± [6] QTZ-OPA	QTZ-AN/GD-OPA ± [6] QP-T/A	QTZ-AN/GD-OPA ± [6] QP-MUSC-SP	QTZ-CHL-AN/GD-OPA ± [6] QP-MUSC-SP
CHLORITE (CHL)	CHL-AN/GD-CDT-OPA ± BIO-SP-PIN	none	none	none
QUARTZ (QTZ) (SILICIF-ICATION)	none	QTZ-GNT ± AN-SIL-BIO-ST	none	none

footnotes:
[1] ± MUSC-BIO-CHL-EPI; [2] ± MUSC-CHL-EPI-CDT; [3] ± PL-MUSC-CHL-EPI-GNT-CDT-STAUR-PIN; [4] ± PL-CDT-PIN; [5] ± QTZ-PL-MUSC-GNT-CDT-PIN; [6] PL-BIO-CHL-EPI-GNT-CDT-STAU-PIN

mineral codes:
QP=quartz phenocrysts; PP=plagioclase phenocrysts; QTZ=quartz; PL=plagioclase; KSP=K-feldspar; HBL=hornblende; T/A=tremolite/actinolite; MUSC=muscovite/sericite; BIO=biotite; CHL=chlorite; EPI=epidote; GNT=garnet; AN/GD=anthophyllite/gedrite; CDT=cordierite; SIL=sillimanite; ST=staurolite; SP=spinel; OPA=opaques

of 16 polished thin sections was analyzed at laboratories of the Geological Survey of Canada in Ottawa in order to determine variations in chemical composition of biotite, anthophyllite/ gedrite, cordierite, plagioclase, spinel, hornblende, chlorite, staurolite, sillimanite, and garnet within the Lower Clastic Succession. These analyses were supplemented with data collected by Thomas (1991) from the LF, QFF, MMF, and WLH-FWF units. Appendix III lists the microprobe data used in this study and summarizes analytical techniques.

The mineralogy, textures, and distribution of the eight different alteration zones along with microprobe mineral compositions, where available, are summarized below in the general order of increasing alteration intensity.

Least Altered Zones

Approximately 50% of the rocks of the Winston Lake Sequence (WLS) contain mineral assemblages characteristic of the least altered zones (Plate 1). Least altered rocks are found primarily between the North Cleaver and Demijohn lakes areas and in the extreme northern and southern ends of the map area. Down-dip distribution is comparable.

On outcrop and in drill core least altered rocks are weakly foliated. Plagioclase phenocrysts and crystal fragments or clasts are well preserved and matrix grain size is distinctly finer than in more altered rocks. Primary volcanic and sedimentary textures are better preserved in rocks of the least altered zones than in rocks within other alteration zones.

In thin section least altered mafic volcanic, volcaniclastic sedimentary, and felsic pyroclastic rocks are characterized by the presence of hornblende and plagioclase (Appendix I). Microprobe data (Table 6) of Thomas (1991) from the LF, MMF, and WLH-FWF units indicates compositions from ferro- to magnesian-hornblende according to classification of Hawthorne (1981). Microprobe analyses from the PCC unit indicates a similar ferrohornblende composition. Plagioclase crystals in the PCC units were also analyzed and contain a Na_2O:CaO ratioo of 1.15:1. Minerals associated with hornblende and plagioclase include quartz, rare K-feldspar, tremolite/actinolite, muscovite, biotite, chlorite, epidote, garnet, and opaques. Because hornblende is absent in nearly all felsic lava flows (QFP, RGQFP, QFF) it cannot be used to delineate least altered zones within these units (Appendix I). However, plagioclase phenocrysts are well preserved in least altered felsic lava flows, and their presence is the primary criterion by which the least altered zone is recognized. The plagioclase phenocrysts are set in a matrix dominated by quartz and plagioclase.

Rocks within least altered zones locally contain hornblende-bearing brickwork style alteration veins. Roadcuts of felsic tuff along the east side of Cleaver Lake near 9250N contain 1-5cm wide subparallel to criss-crossing veins of massive hornblende (Figure 23). Apart from the veins, the felsic tuffs are similar to least altered felsic tuffs elsewhere on the property. Although plagioclase-hornblende-bearing assemblages in mafic rocks are indicative of amphibolite grade metamorphism (Winkler, 1976; Yardley, 1989), they may also be indicators of

Table 6. Summary of Microprobe Data for Alteration Zones.

Summary of Microprobe Data for Least Altered Zone

N	UNIT	ALTN[1]	MIN[2]	NA_2O	K_2O	MGO	FEO	AL_2O_3	SIO_2	CAO	TIO_2	MNO	CR_2O_3	ZNO	TOTAL	MG/FE
3	CLR	LA	HBL	1.68	0.34	6.50	23.04	9.61	43.29	10.53	0.83	0.19	0.02	0.03	96.06	0.28
3	CLR	LA	PLAG	9.52	0.11	0.01	0.11	22.11	67.16	2.88	0.02	0.02	0.02	0.04	102.32	0.05
2[3]	WLH-FWF	LA	HBL	1.41	0.50	11.03	16.96	11.46	44.49	11.67	0.54	0.18			98.32	0.65
2[3]	MMF	LA	HBL	1.55	1.28	4.94	24.79	11.97	40.04	11.05	0.84	1.25			97.73	0.20
1	LF*	LA	HBL	0.91	0.64	9.74	18.69	10.29	44.93	11.98	0.63	0.32			98.22	0.52
4	PCC	LA	HBL	1.60	0.23	7.05	21.67	14.60	41.35	10.16	0.55	0.31	0.02	0.07	97.59	0.33
5	PCC	LA	PLAG	7.71	0.36	0.01	0.15	26.00	60.83	6.68	0.05	0.01	0.01	0.04	101.84	0.07
5	PCC	LA	GNT	0.02	0.07	2.69	33.43	20.70	36.91	3.54	0.06	3.29	0.02	0.02	100.77	0.08

Summary of Microprobe Data for Biotite Zone

N	UNIT	ALTN[1]	MIN[2]	NA_2O	K_2O	MGO	FEO	AL_2O_3	SIO_2	CAO	TIO_2	MNO	CR_2O_3	ZNO	TOTAL	MG/FE
3[3]	QFF	BIO	BIO	0.37	9.24	20.81	6.01	17.52	40.00	0.01	0.79	0.02			94.78	3.47
1[3]	LF*	BIO	BIO	0.83	7.42	20.56	8.20	15.23	40.56	0.00	0.63	0.03			93.53	2.51
1[3]	WLH-FWF	BIO	BIO	0.27	8.70	18.28	11.60	16.03	37.90	0.03	0.88	0.02			93.81	1.58
4	PCC	BIO	BIO	0.20	8.42	6.35	24.48	19.38	32.87	0.17	1.69	0.02	0.02	0.11	93.69	0.26
1[3]	LF*	BIO	CHL	0.10	0.12	17.56	21.56	18.16	27.97	0.15	0.02	0.15			85.89	0.81
1[3]	LF*	BIO	CHL?	0.25	9.03	20.99	5.74	18.15	39.77	0.01	0.88	0.03			94.85	3.66
1	PCC	BIO	CHL	0.01	0.00	8.48	33.34	23.25	22.92	0.03	0.12	0.00	0.00	0.10	88.25	0.25
3	PCC	BIO	GNT	0.03	0.00	1.96	39.75	20.94	36.93	0.94	0.03	0.58	0.01	0.04	101.21	0.05
3	PCC	BIO	SPINEL	0.57	0.01	1.10	19.91	55.62	0.03	0.00	0.01	0.00	0.02	21.20	98.48	0.06

Summary of Microprobe Data for Sillimanite-Staurolite Zone

N	UNIT	ALTN[1]	MIN[2]	NA_2O	K_2O	MGO	FEO	AL_2O_3	SIO_2	CAO	TIO_2	MNO	CR_2O_3	ZNO	TOTAL	MG/FE
3	PCC	SIL-ST	BIO	0.37	8.21	9.55	21.06	18.71	35.52	0.05	1.21	0.02	0.02	0.05	94.75	0.45
3	PCC	SIL-ST	GNT	0.02	0.01	2.89	38.07	21.29	36.74	0.57	0.03	0.41	0.02	0.05	100.09	0.08
3	PCC	SIL-ST	ST	0.06	0.01	1.61	14.75	53.69	27.25	0.00	0.57	0.02	0.00	0.84	98.80	0.11

Summary of Microprobe Data for Anthophyllite/Gedrite Zone

N	UNIT	ALTN[1]	MIN[2]	NA_2O	K_2O	MGO	FEO	AL_2O_3	SIO_2	CAO	TIO_2	MNO	CR_2O_3	ZNO	TOTAL	MG/FE
1	CCLR	AN/GD	QTZ	0.89	0.01	0.08	0.55	0.03	99.94	0.01	0.04	0.00	0.01	0.01	101.56	0.15
6	CCLR	AN/GD	PLAG	10.19	0.05	0.01	0.05	22.95	64.92	3.50	0.01	0.01	0.00	0.04	101.72	0.16
5[3]	CCLR	AN/GD	GD	2.14	0.01	9.79	26.82	17.28	40.57	0.20	0.16	0.30	0.03	0.07	97.36	0.36
2[3]	LF*	AN/GD	AN	0.10	0.04	20.44	19.38	2.03	54.56	0.18	0.06	0.10			96.97	1.05
1[3]	MMF	AN/GD	AN	0.12	0.06	18.88	20.45	2.70	52.23	0.39	0.03	0.23			95.14	0.92
1[3]	WLH-FWF	AN/GD	AN	0.00	0.02	20.36	20.94	1.96	53.27	0.16	0.00	0.12			96.81	0.97
6	PCC	AN/GD	GD	1.97	0.01	9.81	26.61	18.69	40.08	0.23	0.20	0.39	0.02	0.09	98.09	0.37
1[3]	CCLR	AN/GD	BIO	0.41	7.64	12.55	19.04	17.05	35.66	0.24	1.05	0.10	0.00	0.09	93.83	0.66
2[3]	LF*	AN/GD	BIO	0.46	7.90	18.79	10.66	15.41	40.02	0.00	0.99	0.03			94.28	1.76
2[3]	WLH-FWF	AN/GD	BIO	0.37	7.66	17.00	12.47	15.95	38.52	0.03	0.87	0.08			93.09	1.36
5	PCC	AN/GD	BIO	0.29	8.25	12.26	17.85	18.20	36.52	0.07	1.19	0.04	0.02	0.12	94.81	0.69
2[3]	CCLR	AN/GD	CHL	0.04	0.08	11.04	29.67	20.73	25.88	0.12	0.10	0.13	0.04	0.11	87.94	0.37
1[3]	LF*	AN/GD	CHL	0.05	0.01	17.14	23.36	22.45	25.31	0.00	0.07	0.00			88.43	0.73
1[3]	MMF	AN/GD	CHL	0.00	0.04	22.38	16.60	22.93	26.92	0.02	0.03	0.02			88.96	1.35
1[3]	WLH-FWF	AN/GD	CHL	0.00	0.03	22.61	15.72	22.48	26.65	0.00	0.16	0.03			87.73	1.44
6	CCLR	AN/GD	GNT	0.02	0.01	3.81	35.46	21.02	37.09	1.05	0.03	1.23	0.01	0.07	99.78	0.11
5	PCC	AN/GD	GNT	0.04	0.03	4.33	34.86	22.05	36.75	1.21	0.03	1.60	0.04	0.08	101.00	0.12
8	PCC	AN/GD	CDT	0.26	0.00	8.52	7.21	33.22	48.91	0.01	0.02	0.09	0.01	0.08	98.34	1.18
5	PCC	AN/GD	ST	0.07	0.01	2.00	12.67	52.58	27.33	0.03	0.65	0.06	0.00	2.22	97.61	0.16

1ALTN = Alteration Zone; 2MIN = Mineral; 3representative data from Thomas (1991)
LF* Ladder Flow undivided (after Thomas, 1991)
see Tables 1 and 5 for unit and mineral codes, respectively

metamorphosed spilitic alteration resulting from the interaction of mafic rocks and seawater shortly after deposition (MacGeehan, 1977; Parry and Hutchinson, 1981; Gibson et al., 1983; Seyfried, 1984). For this reason and because of the local occurrence of hornblende in brickwork style veins, the rocks cannot, with complete certainty, be interpreted as unaltered, and are therefore classified as least altered.

Tremolite/Actinolite Zones

Tremolite/actinolite alteration zones are defined as areas within which rocks contain tremolite/actinolite-bearing mineral assemblages (Table 5); hornblende, anthophyllite, or biotite, if present, are subordinate to tremolite/actinolite in abundance (Appendix I). Tremolite/actinolite alteration zones are rare and make up only about 3% of the Winston Lake Sequence (WLS). They typically occur in gradational contact with hornblende and/or anthophyllite/gedrite alteration zones and are thought to be of intermediate intensity. Isolated tremolite/actinolite zones are found near the upper contact of the Lower Clastic Succession (LCS) and in mafic lava flows between L9900-L10400N (Plate 1). Zones within mafic lava flows are generally not distinguishable on the 1:5000 scale alteration map as they are mostly narrow (≤5m) and localized.

In outcrop and drill core, rocks containing tremolite/actinolite-bearing assemblages are difficult to distinguish from those containing least altered assemblages. Those from tremolite/actinolite zones may be lighter green in appearance and slightly coarser in grain size than those from least altered zones.

Tremolite/actinolite is characteristically found with plagioclase in altered mafic lava flows, with quartz in altered volcaniclastic rocks, and with quartz and plagioclase in felsic pyroclastic rocks (Appendix I). Relict plagioclase phenocrysts or crystal clasts are preserved locally. Tremolite/actinolite-bearing assemblages have not been recognized in felsic lava flows.

Biotite Zones

The biotite alteration zones are defined as domains of rock that contain biotite in amounts greater than the modal abundance of hornblende or tremolite/actinolite and contain no anthophyllite/gedrite or sillimanite (Table 5). These rocks comprise approximately 16% of the stratigraphic succession. The biotite zones are widely developed in felsic lava flows and pyroclastic rocks where they occur in gradational contact with least altered or tremolite/actinolite zones. In the Lower Clastic Succession, rocks that contain biotite assemblages are found mainly between ~L10500N and ~L12000N where they are bordered by zones of anthophyllite/gedrite alteration to the east and by granite to the west. Biotite is rare in mafic lava flows, and alteration zones are not definable on 1:5000 scale map (Plate 1).

In the field, rocks within biotite zones are typically well-foliated and dark brown. Biotite is pervasive in the rocks or, as in felsic volcanic or volcaniclastic rocks, is concentrated in brickwork style veins or in the matrix to pseudofragments.

In well-layered rocks biotite frequently dominates the dark layers and is modally subordinate in the lighter layers.

Rocks within biotite alteration zones are dominated by quartz and biotite (Figure 25) in modal abundances that vary depending largely on protolith (Appendix I). Major associated minerals include opaques, plagioclase, muscovite, chlorite, epidote, garnet, cordierite, staurolite, K-feldspar, hornblende, and tremolite/actinolite in widely ranging modes. Plagioclase phenocrysts or crystal clasts are preserved locally.

Thomas (1991) provides a limited amount of compositional data from biotite zone assemblages within the FWF, MMF, and QFF units (Table 6). The data indicate that biotites are dominantly Mg-rich and locally phlogopitic; chlorite analyses are similarly Mg-rich. In contrast, microprobe analyses of biotites, chlorite, garnet, and spinel grains from the PCC unit consistently indicate Fe-rich compositions (Table 6).

Sillimanite Zone

Sillimanite alteration zones occur within volcaniclastic, felsic lava flows (QFP, QFF), pyroclastic (CLR), and volcaniclastic-sediment (PCC) units (Plate 1) and make up approximately 10% of the stratigraphic succession. No sillimanite zones have been recognized within mafic lava flows; this probably reflects the primary Fe- and Mg-rich nature of these rocks. By definition the sillimanite zones contain sillimanite-bearing mineral assemblages with no associated staurolite (Table 5).

Figure 23. Hornblende-rich, brickwork-style alteration veins within felsic tuffs immediately east of Cleaver Lake.

Figure 24. Photomicrograph of biotite alteration within altered main QFP. Crossed polars, field of view is approximately 2 x 1.5mm.

In outcrop, rocks within sillimanite zones are grey to dark grey where biotite is abundant and bright white where sillimanite ± muscovite is abundant.

Sillimanite-bearing rocks at the base of the stratigraphy are found primarily in a 5-50m wide zone near the top of the Lower Clastic Succession (LCS) between ~L10700N and L11500N (Plate 1). The sillimanite zone is in relatively sharp contact with overlying tremolite/actinolite or least altered zones and with an underlying anthophyllite/gedrite zone.

A major zone of sillimanite assemblages occurs within QFP in the QFP-Loon lakes area (Plate 1) and in down dip subsurface extensions. Similar rocks are found in isolated zones near the top of the QFP near North Cleaver Lake. The sillimanite zones are surrounded gradationally by biotite and least altered zones, suggesting that the sillimanite zones represent progressively more intense alteration than the biotite zones. Locally, however, the sillimanite zones are in relatively sharp contact with anthophyllite/gedrite alteration zones. The sharp contact relationships and radically different composition suggests temporally distinct formation of the adjacent zones.

Quartz, biotite, and sillimanite dominate rocks within the sillimanite zones (Figure 26)(Appendix I); volcaniclastic and pyroclastic protoliths always contain muscovite and chlorite. Associated minerals, in widely ranging amounts, include plagioclase, epidote, garnet, cordierite, pinite, and rare andalusite. No plagioclase phenocrysts are preserved in these rocks. The rocks are thoroughly recrystallized and are slightly coarser in grain size than those within least altered and biotite zones. Sillimanite occurs as bundles or knots of very fine thready grains and if present in

only minor amounts is difficult to recognize in hand sample. Garnet is highly variable in appearance from fine to coarse grained, idioblastic to subidioblastic, inclusion-rich porphyroblasts. Cordierite is partially retrograded to pinite, and biotite is retrograded to chlorite.

Sillimanite-Staurolite Zones

Sillimanite-staurolite alteration zones are present in approximately 5% of the rocks of the Winston Lake Sequence and generally occur in close association with sillimanite zones. The sillimanite-staurolite alteration zones are defined as rocks that contain coexisting sillimanite and staurolite-bearing mineral assemblages (Table 5). In the Lower Clastic Succession such rocks occur as a zone extending from ~L11500N to ~L11700N northward of a sillimanite zone and as an isolated zone surrounded by a biotite zone near the granite contact west of Fish Lake (Plate 1).

Within the felsic volcanic units (QFP and QFF) sillimanite-staurolite alteration occurs as an isolated zone north of QFP Lake surrounded by a sillimanite zone, as a narrow (≤50m) zone within biotite alteration south of Fish Lake, and as a zone near the top of the QFP between ~L10100N and L10700N. Isolated occurrences of sillimanite-staurolite- bearing QFF are present near L10100N and between L10600N and L10700N (Plate 1). In outcrop and drill core sillimanite-staurolite-bearing rocks generally look similar to rocks within sillimanite alteration zones, because staurolite is frequently not recognizable in hand sample.

Mineralogically, rocks within sillimanite-staurolite zones are similar to those within sillimanite zones except muscovite is somewhat less pervasive in sillimanite-staurolite-bearing volcaniclastic and pyroclastic units than in the sillimanite-bearing rocks of the same units (Appendix I). As in rocks containing sillimanite assemblages, no plagioclase phenocrysts are preserved and grain size is coarser than in least altered and biotite zone rocks. Microprobe analyses (Table 6) of Fe-Mg-bearing minerals within the sillimanite/staurolite-altered PCC shows that biotite, garnet, and staurolite are all Fe-rich.

Anthophyllite/Gedrite Zones

Zones of rock that contain anthophyllite/gedrite-bearing assemblages (Table 5) compose approximately 15% of the stratigraphy and occur in several lithologic units at the surface (Plate 1) and at depth. Near the base of the stratigraphy, within the Lower Clastic Succession, such rocks are found in a 50-200m wide subconformable zone south of the Fish Lake area. Within the QFP unit, anthophyllite/gedrite is rare and is found in an isolated zone near North Cleaver Lake. Anthophyllite/gedrite alteration is best developed in mafic rocks of the LF unit where it is relatively pervasive between ~L10000N and L12400N. The QFF unit contains anthophyllite/ gedrite-bearing assemblages mainly between L10000N and L10400N. There occur as irregular zones bounded sharply by biotite or sillimanite-staurolite zones. MMF and CLR units contain anthophyllite/gedrite assemblages only in the vicinity of Selim Creek near L9900N. In the Rain Mountain-Gesic area,

anthophyllite zones are extensive within the volcaniclastic sediment unit (RGSIV) but are localized in mafic lava flows.

Although contacts with other alteration zones appear to be subconformable, they are relatively sharp, which suggests they overprint adjacent alteration zones. Development of anthophyllite/gedrite alteration zones therefore, at least in part, post-dates development of other alteration zones.

On outcrop and in thin section anthophyllite/gedrite varies widely in appearance. Fine to medium grained, dark green, bladed crystals are abundant in the CCLR and are concentrated in alternating layers and are difficult to distinguish from tremolite/actinolite in hand sample. Very coarse grained anthophyllite/gedrite is present in the PCC and occurs as ≤ 1.5cm rosettes or sheaf-like masses (Figure 26). In altered mafic lava flows anthophyllite/gedrite occurs as very coarse grained, long (≤3cm) bladed crystals or bow-ties (≤2cm) with associated cordierite and/or garnet. In felsic lava flows (QFP, QFF) anthophyllite/gedrite is found as fine to coarse grained (≤7mm) bows or bladed crystals that give the rock a dark grey to greyish brown color.

Anthophyllite/gedrite is developed in all rock categories within anthophyllite/gedrite alteration zones. It is associated with opaques in altered mafic lava flows, quartz and opaques in volcaniclastic rocks and felsic lavas, and chlorite in felsic pyroclastic rocks (Appendix I). Other minerals that may be present in the rocks include plagioclase, biotite, chlorite, epidote, garnet, cordierite, staurolite, and pinite. In the CLR pyroclastic rocks, variation in modal abundance of

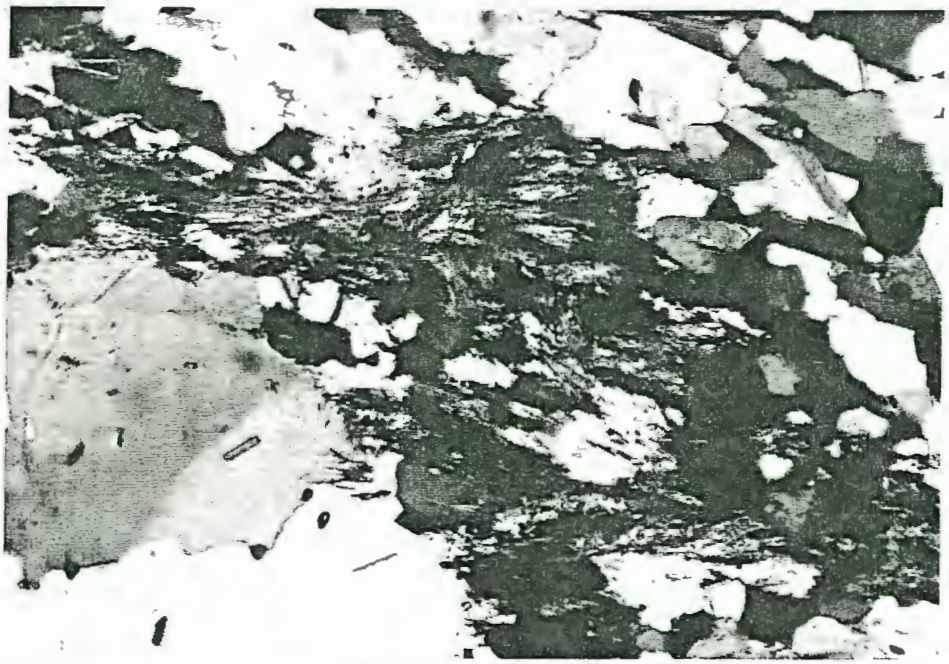

Figure 25. Photomicrograph of sillimanite alteration within altered QFP. Crossed polars, field of view approximately 2 x 1.5mm.

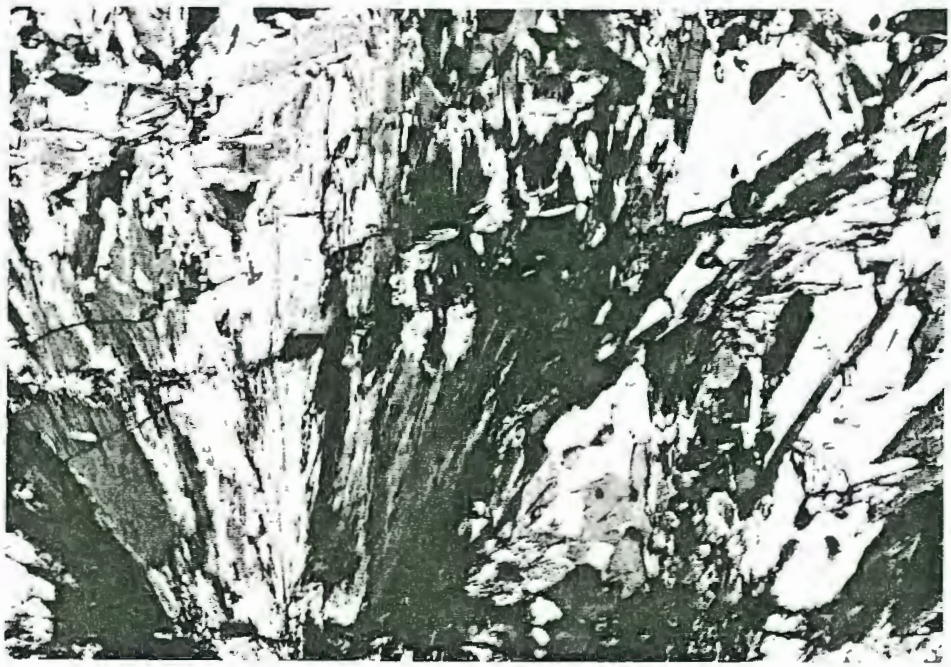

Figure 26. Photomicrograph of coarse grained sheaf-like anthophyllite/gedrite within altered PCC volcaniclastic-sediments. Cross polars, field of view approximately 2 x 1.5mm.

anthophyllite/gedrite in parallel layers may reflect alteration along primary bedding planes.

Microprobe data (Table 6) from Thomas (1991) of biotite, anthophyllite/gedrite, and chlorite indicate dominantly Mg-rich compositions as Mg-biotite to phlogopite, Mg-anthophyllite (with only minor gedritic compositions), and mostly Mg-rich chlorite (ripidolite) in altered units in the upper portions of the stratigraphy. In contrast, data from PCC and CCLR units near the base of the stratigraphy indicate distinctly Fe-rich compositions as ferrogedrite, almandine garnet, Fe-cordierite, staurolite, Fe-biotite, and Fe-ripidolite. No significant chemical differences are present between textural variations of gedrite or garnet in the CCLR and PCC units.

Chlorite Zone

Approximately 30% of the Winston Lake massive sulfide deposit is stratigraphically underlain by an alteration zone consisting of massive chlorite-rich rocks (Morrison and Sim, 1989). The chloritic rocks do not occur on surface; they comprise only 1% of the stratigraphy. Balint and Severin (1989) concluded that chloritic alteration left the rocks with a relatively low silica content. Because of the low silica content, chlorite was stabilized during metamorphism even to amphibolite grade.

The chlorite alteration zone is restricted to the Winston Lake Horizon-Footwall Flow (WLH-FWF) unit and ranges in thickness from 0-10m. It is in

relatively sharp contact with adjacent biotite or anthophyllite alteration zones. In drill core chlorite zone rocks appear massive and coarse grained and contain greenish chlorite ± anthophyllite, biotite/phlogopite, cordierite, and garnet as major constituents.

Chlorite dominates the rocks and along with the other major constituents, pinite (0-4%), and gahnite (0-15%) are evident in thin section (Appendix I). Chlorite occurs as poorly foliated, coarse grained, plate-like aggregates enclosing bladed anthophyllite or subhedral cordierite and spinel crystals. Garnet occurs as subhedral porphyroblasts or aggregates of porphyroblasts up to 3cm across.

Quartz Zone ("Silicified" Rocks)

Quartz is locally conspicuously abundant in the most intensely altered rocks within previously described anthophyllite/gedrite and sillimanite ± staurolite zones and represents an apparent silicification of the rocks. Silicification is best developed between L10700N and L12000N near the top of the LCS, and is associated with mineralization at the Ciglen occurrence and Anderson showing. Elsewhere it occurs as isolated zones near the top of the LCS in the QFP Lake area and near L12000N adjacent to the granite contact. The silicified rocks are distinct in outcrop due to conspicuous quartz and have been termed "diseased rocks" in mine terminology.

Quartz is typically light grey and occurs in ≤ 1cm veinlets or ridges or in net-like webs (Figure 27) and is most conspicuous in garnet and/or anthophyllite/gedrite-rich rocks. Garnet is ubiquitous in the quartz-rich rocks, is distinctly red, and may

Figure 27. Photograph of light grey silicified rock with a rough, uneven outcrop surface created by weathering of quartz.

occur as isolated single inclusion-rich subidioblastic crystals, or ≤ 5mm inclusion-poor idioblastic crystals. Silica forms 5mm to 2cm halos or rims around individual garnet crystals or aggregates of crystals and separates them from adjacent garnet(s). The garnet and silica weather positively and give the rock a very rough outcrop surface. Anthophyllite appears as coarse grained blades and sillimanite as thread-like or fibrous bundles embedded within quartz. Mineral modes are difficult to estimate due to the very coarse grain size of the rocks and the limitations imposed by thin section size. Qualitative estimates are of 10-20% quartz, with 5-20% garnet and 5-20% anthophyllite/ gedrite; biotite, sillimanite, and rare plagioclase make up the remainder of the rock.

The geochemical nature of the quartz-rich rocks, and their genetic relationship to anthophyllite/gedrite and sillimanite/staurolite development is discussed in succeeding sections.

V.5 Structural Transposition of Alteration Zones

Structural studies of metamorphosed VMS deposits (Walford and Franklin, 1982) indicate that associated substratiform alteration zones reflect post-hydrothermal, tectonic transposition of original high angle alteration zones. Detailed mapping in the Winston Lake footwall stratigraphy indicates transposition had only a minor control on the present position of alteration zones. Two factors suggest this including: (1) the integrity of the stratigraphy is well preserved, and (2) excellent preservation of primary volcanic and sedimentologic structures. In spite of these factors slight transposition may have occurred along conjugate shears. Such shears were not identified during field mapping, however as noted previously, sinistral kineamatic indicators have been noted near the base of the stratigraphy within altered PCC, and the North Cleaver Fault is approximately centered within subconformable alteration between the LF and QFF units north of ~L10000N (Plate 1). No dextral kineamatic indicators have been recognized along the North Cleaver fault, but they may exist adjacent to the unexposed fault zone. Sinistral shear near the base of the altered stratigraphy, coupled with dextral shear towards the altered upper portions of the stratigraphy would effectively elongate and exaggerate the substratiform alteration zones.

VI. WHOLE ROCK AND TRACE ELEMENT GEOCHEMISTRY

VI.1 Introduction

Mineralogical variation that reflects premetamorphic hydrothermal alteration has been described in the previous chapter as recognized through field and petrographic study. In this chapter variations in the whole rock and trace element geochemical data are examined. These variations form patterns across the property that are more definitive than variations in mineralogy.

VI.1.1 Review of Previous Studies

Several geochemical studies of the Winston Lake area have been undertaken by previous workers and include those by Mattinen (1978), Severin (1979), and Balint and Severin (1984). These studies were directly associated with reconnaissance and detailed exploration of the mine property and were based on a limited suite of analyzed components. Areas of Na_2O depletion and MgO and Zn enrichment were delineated in volcanic rocks through multi-element ratio studies. Zoning within the altered areas was not distinguished, and most alteration within volcaniclastic-sediment units was not recognized.

Thomas (1991) studied whole rock and mineral chemistry data from the upper portion of the Winston Lake Sequence and attempted to geochemically discriminate alteration facies as a function of proximity to the orebody. The study used a geochemical approach assuming no *a priori* knowledge of systematic compositional zoning within the altered volume of rocks. The database consisted of major oxide

and trace element analyses of drill core samples collected along strike from the down-section projection of the Winston Lake deposit. Evaluation of the data included examination of raw chemical analyses, multielement variation studies (ratios), and mass balance studies. Thomas (1991) concluded that FeO, MgO, Na_2O, CaO, and Zn were significantly mobile during alteration; however, apart from distinction of altered from unaltered rocks, only rare, poorly defined systematic trends in distribution of these components were recognized.

VI.1.2 Methods

Two hundred and forty-seven samples were collected and analyzed for major oxides and trace elements. The analyses were done by the Geological Survey of Canada's Analytical Laboratory Section. The results, along with analytical methods used, are tabulated in Appendix 2. Sample locations are shown on Plates 1,2, and 3 .

Samples were selected for analyses based on petrographic and field studies. Specifically, the samples are representative of alteration mineralogies and styles at given outcrop locations. Care was taken to collect samples large enough to normalize the effects of inhomogeneity due to coarse grain size.

The analytical data collected during this study have been evaluated through several means. Raw data were statistically summarized for each alteration zone within each lithology. Balint and Severins' (1984) classification of least altered lithologies was confirmed using standard petrochemical diagrams. Standard variation

diagrams and the isocon method of Grant (1986) have been used to evaluate mobility of elements, primary petrochemical variation, correlations of stratigraphy between the Winston Footwall and Rain Mountain-Gesic Blocks, and metasomatism.

Isocon Method

Element mobility during metasomatism of the Winston Lake Sequence was evaluated through graphical comparisons of geochemical data using the isocon method of Grant (1986). The method has been widely applied in the study of protoliths and metasomatically altered equivalents. The method can also be used to recognize primary chemical relationships among rocks, to chemically correlate rocks, and to compare analytical data. In comparisons of geochemical data, differences in overall rock mass and individual component concentrations can be directly evaluated through isocon analyses. Furthermore, the method allows the chemical comparison of a single rock to several others on a single diagram.

To apply the isocon method, chemical analyses of an altered rock are plotted against chemical analyses of an unaltered or less altered equivalent on an XY graph (Figure 28). A series of data points that correspond to chemical components is generated on the graph. For convenience in plotting and clarity in interpretation, data points can be mathematically scaled; Grant (1986) illustrates in detail the mathematical validity of such scaling. A reference line connecting points of equal geochemical concentration ("isocon") is generated through the graph origin. The isocon line is selected on the basis of a best-fit of data, chemical immobility of

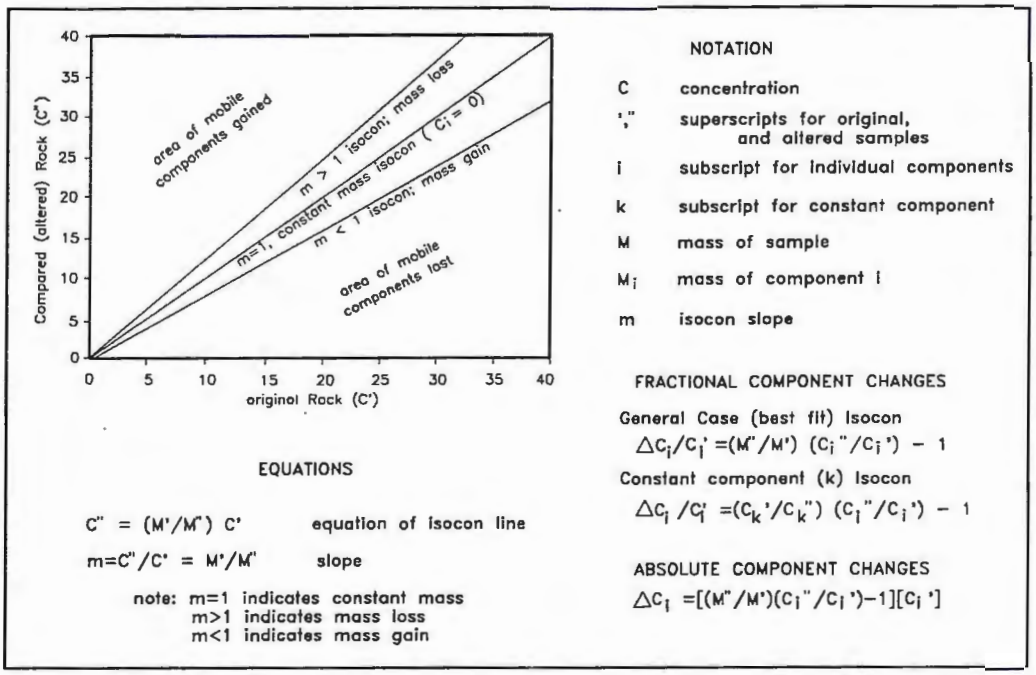

Figure 28. An illustration of isocon systematics and mathematical relationships (after Grant, 1986).

particular species such as high field strength elements, or on the basis of assumed constant mass or volume. The slope of the isocon line yields mass change information. The most immobile components fall nearest the isocon line, and the relative abundance of components in the compared sample analyses can be evaluated by their data point positions relative to the isocon or by simple calculation. Components that plot above the isocon have been gained by the altered rock, and those that plot below the isocon have been lost. Compositionally similar rocks will contain data points concentrated along the isocon line with slope = 1. Figure 28

summarizes the geometry and method of calculation of mass and component changes on isocon diagrams.

Similar principles are applied when analyses of two fresh rocks are compared on an isocon diagram. Linear alignment of analyzed components along an isocon line indicates similar rock chemical compositions. If rocks of distinct compositions are compared, points situated above the isocon represent components enriched, and points below represent components depleted in the compared rock relative to the original rock.

VI.2 Primary Chemistry

VI.2.1 Classification

Balint and Severin (1984) distinguished least altered volcanic rocks of the Big Duck Sequence from the Winston Lake Sequence by classification on Jensen (1976) cation plots. The Winston volcanic rocks form a well-defined calc-alkaline suite of basalts to rhyolites, whereas the Big Duck volcanic rocks plot in the field of iron-rich tholeiites (Balint and Severin, 1984). Analyses of least altered volcanic rocks of the Winston Lake Sequence collected during this study, when plotted on an AFM diagram of Irvine and Baragar (1971), confirms the calc-alkaline classification (Figure 29). The Winston volcanic rocks are strongly peraluminous to metaluminous and subalkaline according to classifications of Minor and Peccoli (1975) and Irvine and Baragar (1971, figure 3), respectively. Such characteristics are consistent with the plagioclase-rich, K-feldspar-poor mineralogy of the rocks.

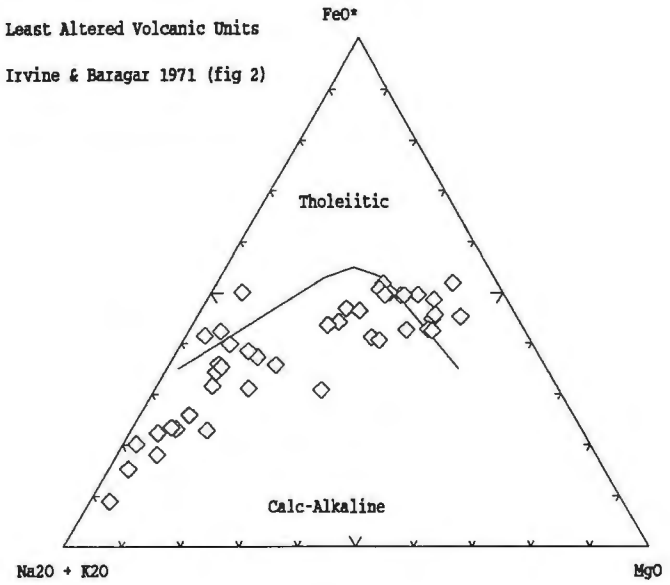

Figure 29. Ternary plot of Na_2O+K_2O - FeO* - MgO of least altered Winston Lake volcanic rocks illustrating calc-alkaline affinity.

VI.2.2 Characterization of Least Altered Lithologies

Table 7 is a compilation of average analyses and standard deviation statistical calculations on a unit by unit basis for the concentrations of major oxide and selected trace elements for 51 least altered analyses. An inspection of the data indicates standard deviations range widely among components. In general, the standard deviations for most components increase progressively from lava flows, to felsic pyroclastic rocks, to volcaniclastic-sedimentary rocks. This reflects the clastic origin of the latter two rock types.

Table 7.
Average and Standard Deviations of Major Oxides (%) and ZR (ppm) for Least Altered Units

N	STATS	UNIT	SiO_2	TiO_2	Al_2O_3	FE-T*	MNO	MGO	CAO	Na_2O	K_2O	H_2OT	CO_2T	P_2O_5	S%	ZR
N=2	AVG:	QFP	78.10	0.16	11.10	2.80	0.01	1.01	0.58	4.90	0.67	0.70	0.20	0.02	0.02	355
	STD:	QFP	0.50	0.02	0.00	0.60	0.00	0.10	0.18	0.10	0.03	0.10	0.00	0.00	0.02	15
N=3	AVG:	QFF	78.37	0.14	11.53	1.37	0.01	0.27	0.75	4.57	1.65	0.47	0.33	0.03	0.00	387
	STD:	QFF	0.50	0.01	0.42	0.45	0.00	0.07	0.34	0.58	0.97	0.12	0.05	0.00	0.00	12
N=3	AVG:	CCLR	72.3	0.43	12.6	3.9	0.04	1.60	3.19	4.8	0.13	0.5	0.2	0.12	0.00	600
	STD:	CCLR	2.5	0.03	1.1	0.7	0.01	0.08	0.53	0.5	0.05	0.0	0.1	0.02	0.00	50
N=11	AVG:	CLR	74.01	0.40	12.30	3.59	0.04	0.91	2.03	5.38	0.33	0.67	0.21	0.06	0.04	455
	STD:	CLR	2.38	0.10	0.55	1.64	0.02	0.85	0.65	0.42	0.26	0.30	0.10	0.04	0.06	139
N=6	AVG:	LF'S(FSP)	49.58	0.58	18.90	9.28	0.20	6.60	9.81	2.12	1.17	2.08	0.18	0.07	0.09	42
	STD:	LF'S(FSP)	1.52	0.11	1.37	0.69	0.04	1.91	0.94	0.49	0.64	0.61	0.16	0.01	0.10	13
N=2	AVG:	LF'S(APH)	51.30	0.74	15.45	11.30	0.23	7.44	10.20	2.25	0.20	1.45	0.25	0.09	0.01	49
	STD:	LF'S(APH)	1.20	0.00	0.05	0.60	0.05	0.93	0.70	0.85	0.04	0.05	0.05	0.00	0.01	5
N=2	AVG:	MMF	54.10	0.79	15.45	10.25	0.13	5.87	8.64	2.95	0.47	1.55	0.40	0.11	0.02	55
	STD:	MMF	0.10	0.03	0.15	0.15	0.04	0.32	0.96	0.35	0.27	0.35	0.00	0.00	0.02	2
N=4	AVG:	WLH-MA	51.55	0.98	15.78	10.63	0.08	5.91	8.11	3.80	1.45	1.85	0.20	0.23	0.12	69
	STD:	WLH-MA	0.50	0.01	0.23	0.90	0.02	0.56	0.79	0.25	0.49	0.18	0.10	0.01	0.07	5
N=8	AVG:	PCC	66.86	0.67	12.03	10.99	0.24	1.68	3.86	2.63	0.44	0.95	0.35	0.17	0.14	450
	STD:	PCC	2.37	0.06	0.70	1.56	0.10	0.60	0.66	0.63	0.43	0.27	0.32	0.03	0.15	39
N=10	AVG:	SIV/RGSIV	64.79	0.67	12.80	8.97	0.16	2.37	4.52	3.71	0.85	1.25	0.23	0.16	0.14	252
	STD:	SIV/RGSIV	7.04	0.21	2.65	3.38	0.11	2.03	2.82	1.08	0.29	0.40	0.21	0.10	0.22	226

N = number of samples
LF'S(FSP) = average of least altered feldspar phyric LF and RGLF units
LF'S(APH) = average of least altered aphyric LF and RGLF units
SIV/RGSIV = average of least altered SIV and RGSIV units
see Table 2 for rockunit codes
FE-T = FE_2O_3T

The data were examined for evidence of primary petrochemical variation within map units. Recognition of the presence or absence of variation is necessary to establish the accuracy of averaging data for comparison purposes. Furthermore, primary variation must be considered when establishing isocons upon which comparisons of least altered rocks to altered equivalents are based.

Thomas (1991) examined the QFF and LF units for evidence of fractionation by comparing analyses collected at closely spaced intervals through the units. He concluded that fractionation was negligible except for a slight increase in Na_2O towards the center of the QFF and a slight decrease of MgO and FeO up-section in the LF. However, Thomas' (1991) sampling apparently did not include aphyric lava flows, so he did not address their chemical distinctiveness.

To further test for fractionation within volcanic units in this study, individual least altered analyses were compared to the average composition for each lithology on isocon graphs. Where fractionation was minimal or absent, data points of all components plot near the slope = 1 isocon. Such comparisons in the QFF support the conclusions of Thomas (1991). Evaluation of the QFP and MMF units similarly indicates primary fractionation was negligible; however, significant chemical variability was noted within the LF, RGLF, and MMF mafic lava flow units, and within felsic pyroclastic units (CLR, CCLR). Because the lava flows were not necessarily sheet-like in primary distribution, it is not possible to identify consistent relationships of chemistry to stratigraphic position within the map units. This factor is important when evaluating chemical variability in altered portions of these units.

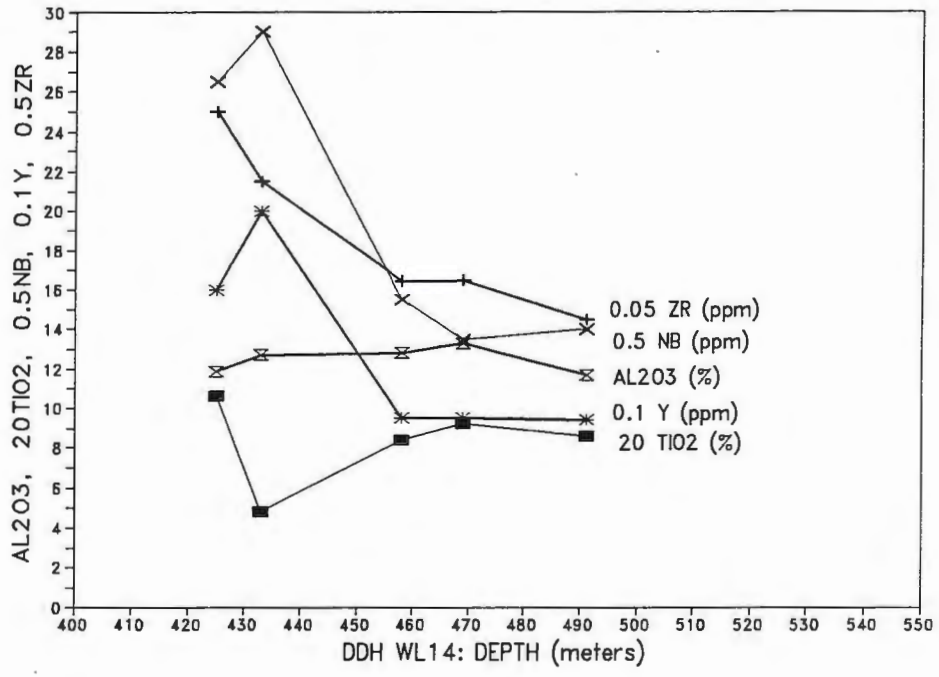

Figure 30. Plot of selected components versus depth through the Clotted Rhyolite (CLR) unit.

Isocon comparisons of individual analyses to average analyses in the CLR and CCLR units indicates primary variation in the concentration of certain high field strength components, especially Zr. In addition, comparisons of analyses of high field strength components in five closely spaced samples through a section of least altered CLR in DDH WL-14 shows systematic variation of TiO_2, Nb, Y, and Zr concentrations across section; in contrast, Al_2O_3 and the other major oxides are relatively constant (Figure 30). This is consistent with chemical zoning of trace elements in pyroclastic flows as recognized in other studies (Morton et al., 1991; Fisher, 1982).

VI.2.3 Comparisons Between Similar Lithologies

Isocon comparisons were made between average analyses of least altered units of similar composition and origin. Such comparisons support stratigraphic correlations based on mapping and volcanologic study.

Felsic Lava Flows (QFP, QFF)

Isocon comparisons were made between QFP and QFF felsic lava flow units. Significant distinctions were noted including elevated K_2O and decreased MgO and Fe_2O_3T in the QFF relative to the QFP. These distinctions are consistent with classification of the QFF and QFP as rhyolites and rhyodacites, respectively. They are also consistent with formation by eruption from similar, perhaps related, sources as indicated previously through volcanological analyses.

Felsic Pyroclastic Units (CLR, RMCLR, CCLR)

Although pyroclastic rocks are chemically more variable than lava flow units, isocon comparisons were made between averages of least altered CCLR and CLR units. The chemical similarity in average analyses (Figure 31) supports the interpreted cogenetic relationship of these units based on similar facies distribution and lithologic character as indicated by stratigraphic studies. Only K_2O differs markedly between the units and is increased within the CLR relative to the CCLR. This may reflect primary fractionation.

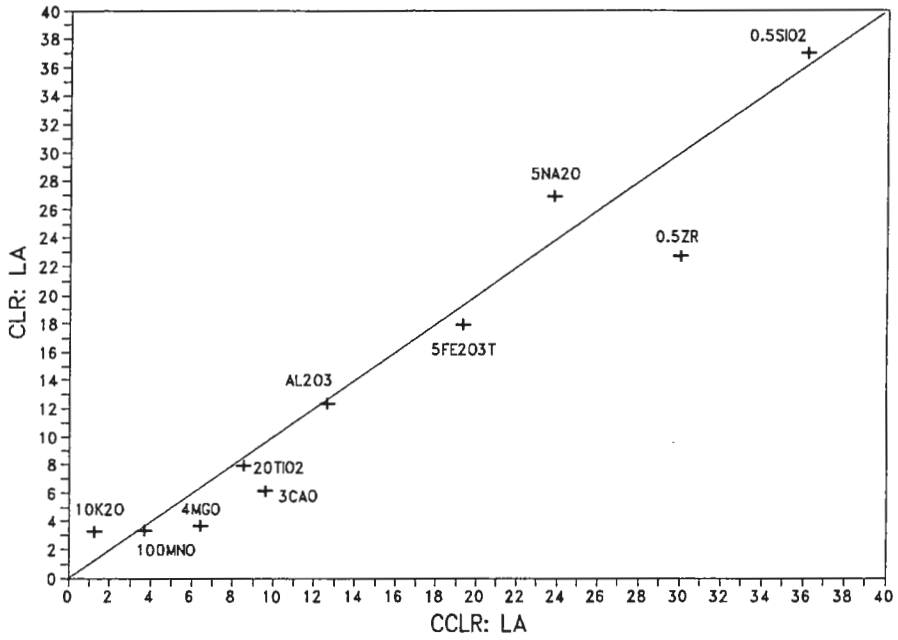

Figure 31. Isocon diagram comparing least altered (LA) Ciglen Clotted Rhyolite (CCLR) and Clotted Rhyolite (CLR) units.

Isocon comparisons of the felsic lava flow units (QFP and QFF) average analyses to average CLR shows wide scatter of several major oxides and trace elements. The distinct chemistries of the lavas and pyroclastics is consistent with the interpretation of distinct sources based on volcanologic studies.

Mafic Lava Flows (LF/RGLF, MMF, WLH-MA)

Analyses of aphyric and feldspar phyric least altered LF were compared to analyses of similar least altered rocks of the RGLF unit on the isocon diagrams of Figure 32. All major components fall within ±10% of a line of unit slope. This

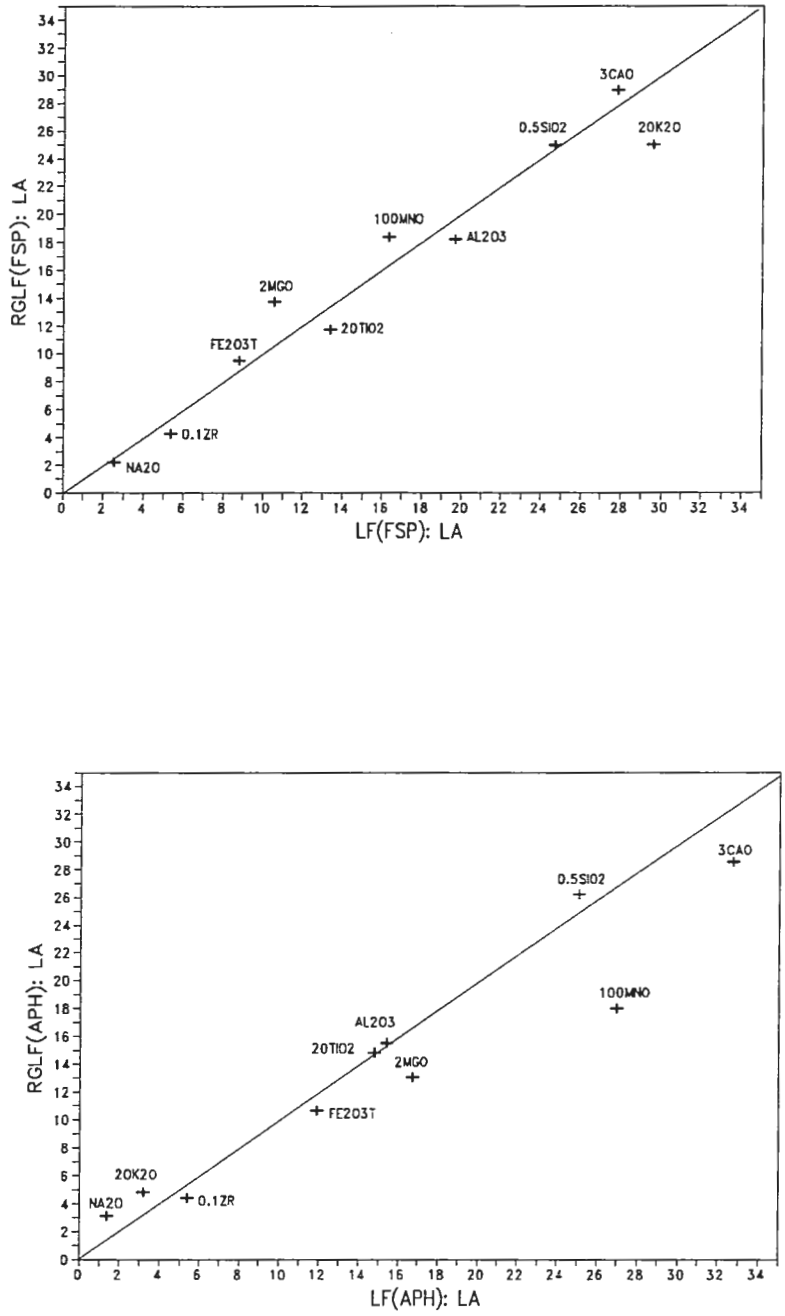

Figure 32. Isocon diagrams comparing least altered (LA) feldspar-phyric (FSP) (top) and aphyric (APH) (bottom) Ladder Flow (LF) and Rain Mountain-Gesic Ladder Flow (RGLF) units.

supports the stratigraphic correlation of these rocks as established through volcanological analyses. Comparisons between aphyric and feldspar-phyric compositions indicate the most notable distinction is in decreased K_2O in the aphyric compositions relative to the feldspar-phyric compositions (Figure 33).

Chemical comparisons of aphyric RGLF lava flows of the Rain Mountain area to aphyric lava flows from the Gesic area (Figure 34) indicate distinctions including increased K_2O and Zr and decreased CaO in the units.

These distinctions are similar to, but less pronounced than, those between aphyric LF and MMF units. The comparisons suggest the Gesic area aphyric lava flows are chemically more closely related and therefore more likely correlable to MMF rocks than to LF rocks.

Volcaniclastic-Sediment Lithologies (PCC, SIV/RGSIV)

As noted previously and illustrated on Table 7, moderate range in standard deviations of analyzed chemical components of volcaniclastic-sediment units are due to a clastic origin. Nevertheless, comparisons were made between clastic units to support stratigraphic correlations. Figure 35 is an isocon graph comparing SIV and RGSIV average analyses. The distribution of the oxides and trace elements in a relatively tight envelope around the 45° isocon indicates compositional similarity of the units. This similarity supports correlation of the SIV and RGSIV units and is consistent with stratigraphic interpretations. Comparisons were also made of the PCC to the SIV and RGSIV analyses; data points in these comparisons are widely scattered, indicating chemical distinction of the units.

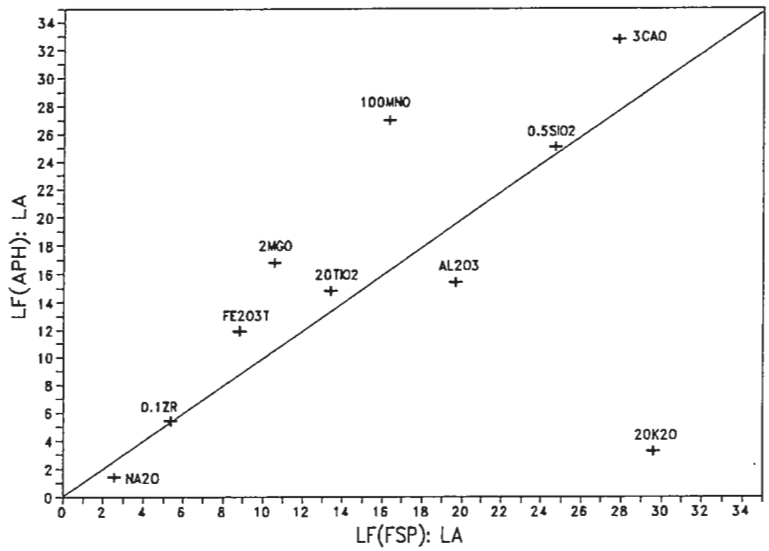

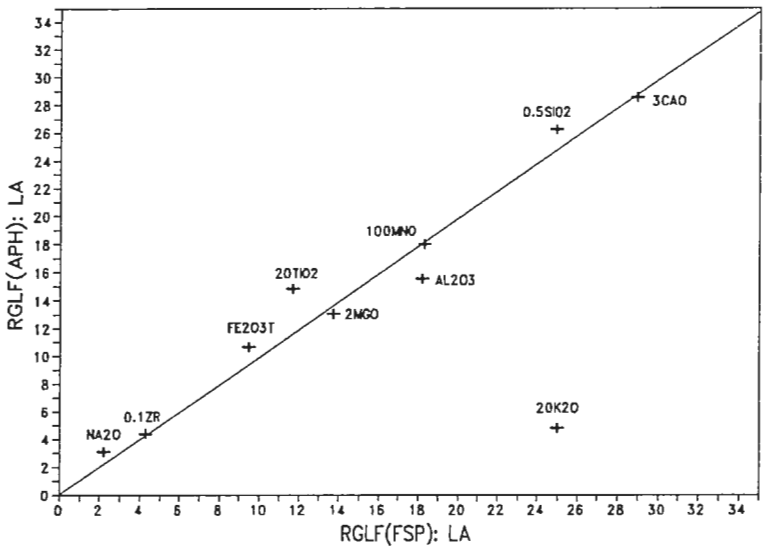

Figure 33. Isocon diagrams comparing least altered (LA) feldspar-phyric (FSP) to aphyric (APH) Ladder Flow (top) and Rain Mountain-Gesic Ladder Flow (RGLF) (bottom).

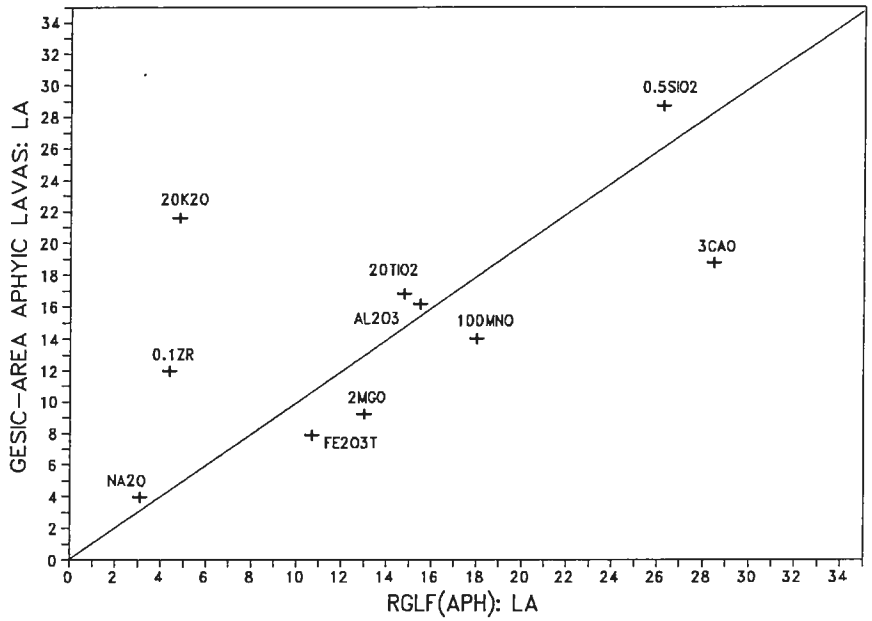

Figure 34. Isocon diagram comparing least altered (LA) aphyric (APH) Rain Mountain-Gesic Ladder Flow (RGLF) to average least altered Gesic area aphyric mafic lava flow.

VI.3 Geochemistry of Altered Rocks

VI.3.1 Inspection of Data

Appendix II (Tables 21-24) summarizes the analytical data for each alteration zone on a unit-by-unit basis. Units correlated between the Winston Footwall and Rain Mountain-Gesic Blocks are treated together as they are considered to be lithologic and stratigraphic equivalents. An inspection of the statistical data indicates average values of several analyzed components in alteration zones differ significantly from the values in the least altered zones. Na_2O and CaO variations are most

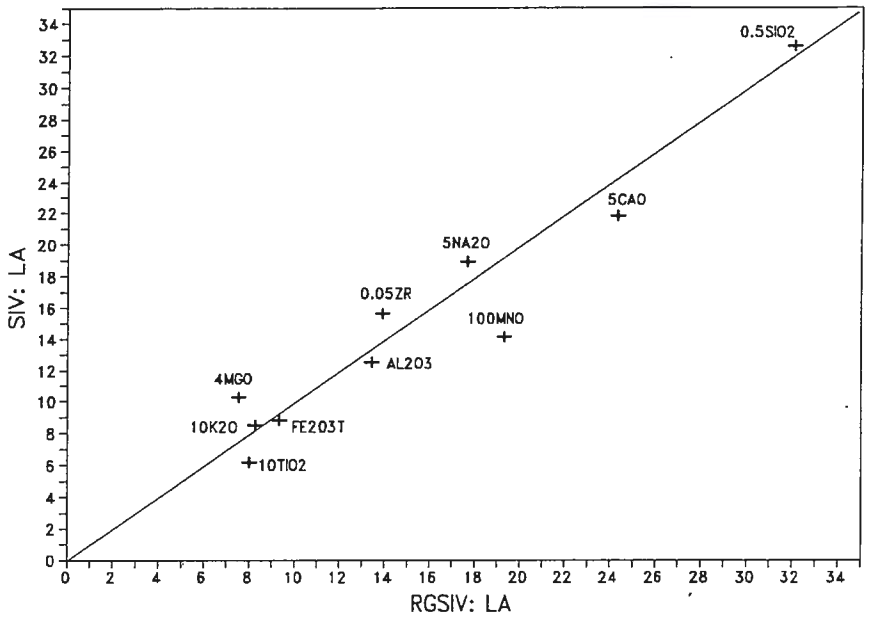

Figure 35. Isocon diagram comparing least altered (LA) RGSIV and SIV Volcaniclastic-sediment units.

noticeable and the concentrations of these components are nearly always highest in least altered analyses.

The relative abundance of components in alteration zones is generally consistent with the abundance predicted based on petrographic analyses. For example, biotitic rocks characteristically exhibit higher K_2O values relative to other alteration types. Similarly, MgO values are highest in anthophyllite/gedrite-bearing rocks. Fe_2O_3T and CaO concentrations show the most variation. Fe_2O_3T is typically higher in staurolite-bearing rocks than in others, and CaO depletion in altered rocks correlates with modal decrease of plagioclase, hornblende, or tremolite/actinolite. SiO_2, TiO_2, and Al_2O_3 concentrations are less variable and are relatively consistent in analyses from various alteration zones.

Chemical trends within volcaniclastic-sediment units (PCC, SIV/RGSIV) are comparable to those in volcanic units. These trends, along with mineralogical zoning and garnet compositional data (from microprobe analysis) verify the alteration of the rocks.

VI.3.2 Immobile Elements

Recognition of elements that were immobile during alteration and metamorphism represents an important step in evaluation of chemical alteration of rocks. Immobile elements represent vestiges of the parent rock, and the absolute abundances of such elements are relatively unaffected by metasomatism. Finlow-Bates (1981), Larson (1986), Costa et al. (1983), Franklin et al. (1981), and numerous other workers have found that, in massive sulfide systems, elements with high field strengths such as Ti, Al, and Zr are typically immobile during metasomatism. Because of their immobility, such elements can be used to monitor the behavior of mobile elements. Within a suite of rocks that were derived through alteration of chemically equivalent protoliths, the concentrations of the immobile elements varies only as a result of the gain or loss of mobile elements. Finlow-Bates and Stumpfl (1981) illustrated that on Cartesian graphs, points representing immobile elements in a suite of variably altered rocks are distributed along a line that projects through the graph origin. This indicates the ratios of the immobile elements remain constant. Through such studies of the LF, QFF, MMF, and WLH-FWF units Thomas (1991) concluded TiO_2 and Zr were relatively immobile. Analyses of the felsic lava flows

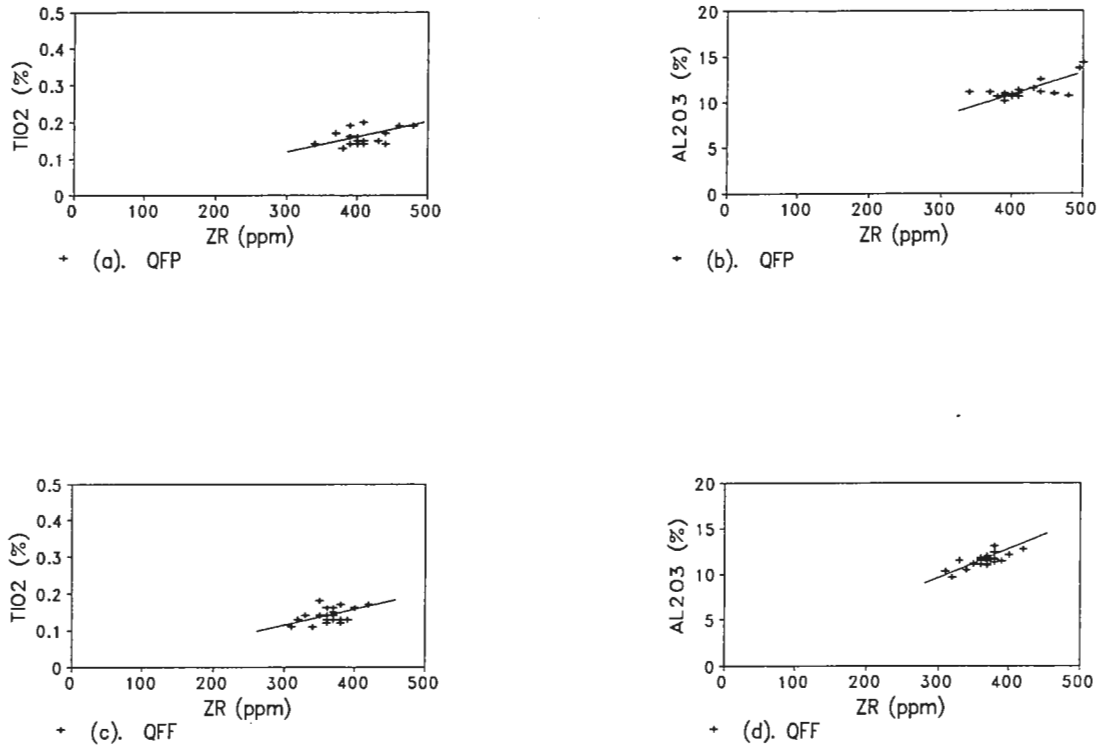

Figure 36. Cartesian graphs of TiO2(%) vs. Zr(ppm) and Al2O3(%) vs. Zr(ppm) for variably altered QFP (a,b) and QFF (c,d) felsic lava flows.

(QFP, QFF) in this study generally support this interpretation and further indicate that Al_2O_3 was relatively immobile during alteration and metamorphism (Figure 36). However, in contrast to Thomas'(1991) conclusions, Cartesian plots involving Al_2O_3, TiO_2, and Zr for the LF, RGLF, and WLH-MA units show linear distribution, but

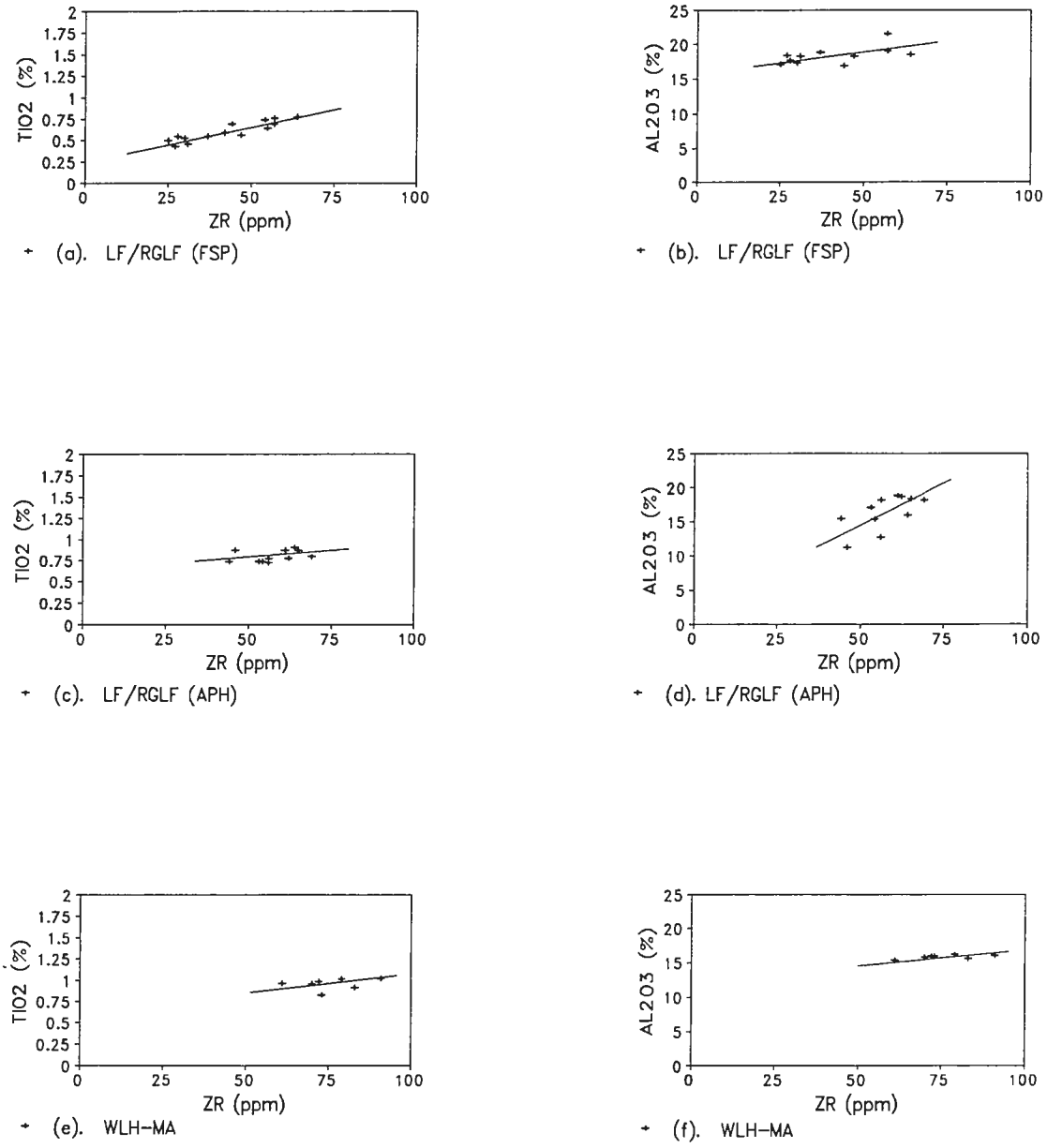

Figure 37. Cartesian graphs of TiO2(%) vs. Zr(ppm) and Al2O3(%) vs. Zr(ppm) for variably altered feldspar-phyric (FSP) and aphyric (APH) Ladder Flow (LF), and Winston Lake Horizon mafic lava flows (WLH-MA).

not through the graph origin (Figure 37). Whitford et al. (1989) found similar relationships in volcanic rocks of the Que River area of Tasmania and concluded the trends represent variation due to primary fractionation. Considering the clearly demonstrated immobility of these components in other volcanic units, it is likely that they were immobile in the mafic rocks as well and that the distribution on the variation diagrams reflects primary variation in the rocks.

VI.3.3 Alteration Zones

In order to determine relative gains and losses of chemical constituents during alteration, average analyses from alteration zones within individual units were compared through isocon analyses. Comparisons were made between average analyses from alteration zones and from least altered zones thought to most closely approximate the premetamorphic primary chemistry of the rocks.

For most units, the reference isocon was chosen as the best fit line through the points representing TiO_2, Al_2O_3, and Zr data. For felsic pyroclastic rocks and mafic lava flows, which show variability of most high field strength elements, constant Al_2O_3 was selected for defining reference isocons. For SIV/RGSIV units, the best fit line was drawn through the points representing TiO_2 and Al_2O_3.

Chemical changes induced during alteration of the Winston Lake stratigraphy are discussed separately for felsic lava flows, felsic pyroclastic rocks, mafic lava flows, and volcaniclastic-sediments. Appendix II (Tables 21-24) includes average chemical analyses on a unit by unit basis and includes chemical changes and mass changes

based on isocon calculations. Table 8 is a summary of the major oxides gains and losses for each unit and alteration type.

Felsic Lava Flows (QFP, QFF)

Isocon diagrams are presented in Figure 38 for alteration types defined within QFP and QFF lava flow units. Average analyses as listed in Appendix II (Table 22) are plotted with the exception of least altered QFF, which is represented by the individual analyses WLO-123. WLO-123 was chosen as it contains notably higher Na_2O and CaO than the average least altered QFF analyses. As previously noted, Na_2O and CaO contents are typically progressively depleted through alteration. Calculated component changes and mass changes are summarized on Table 8.

Calculated mass change for TiO_2, Al_2O_3, and Zr are mostly between -5% to +5%; this supports the interpretation of relative immobility of these components during alteration. In the QFP, overall mass changes range from -1% to -3%; in contrast, the QFF shows mass changes of -1% to +6% (Table 8).

Relative to least altered compositions, each alteration type except biotite shows consistent gains of concentration in Fe_2O_3T, MgO, and K_2O; consistent losses are evident in Na_2O, and CaO except within the biotite zone of the QFF. CaO was gained only in the later case and is not understood at present. MnO is strongly enriched in alteration zones within the QFP, but remained relatively constant in the QFF. SiO_2 concentrations remained relatively constant during alteration of the QFP and QFF. Gains in MgO relative to Fe_2O_3T are notably smaller in the QFP than in

Table 8.

Summary of Major Oxide Component and Mass Changes*

UNIT	COMPARISON	MASS%	SiO_2	TiO_2	Al_2O_3	FE-T	MNO	MGO	CAO	Na_2O	K_2O	H_2O	CO_2T
QFP	BIO-LA	-3	=	=	=	G	G	G	L	L	G	G	G
QFP	SIL-LA	-1	=	=	=	G	G	G	L	L	G	G	=
QFP	SIL-ST - LA	-3	=	=	=	G	G	G	L	L	G	G	L
QFF	BIO-LA	+6	=	=	=	G	L	G	G	L	L	G	L
QFF	SIL-LA	+2	=	=	=	G	G	G	L	L	G	G	L
QFF	SIL-ST-LA	+3	=	=	=	G	L	G	L	L	=	G	L
QFF	AN/GD-LA	-1	=	=	=	G	G	G	L	L	L	G	L
CCLR	BIO-LA	+14	G		=	G	=	G	L	L	G	G	G
CCLR cg	AN/GD-LA	+10	=		=	G	G	G	L	L	G	G	L
CCLR fg	AN/GD-LA	+7.5	=		=	G	G	=	G	G	=	L	L
CLR	BIO-LA	-1	L		=	L	L	G	L	L	G	G	G
CLR	SIL-LA	-10	L		=	L	L	G	L	L	G	G	L
CLR	SIL-ST-LA	0	=		=	=	L	G	L	L	G	G	L
CLR	T/A-LA	+7	=		=	L	ND	G	G	=/G	L	=	G
CLR	AN/GD-LA	-24	L		=	G	G	G	L	L	G	G	L
LFS(FSP)	BIO-LA	+3	=		=	=	L	G	=	=	G	G	G
LFS(FSP)	T/A-LA	+6	=		=	G	G	G	L	L	=	G	L
LFS(FSP)	AN/GD-LA	+9	=		=	=	G	G	L	L	L	G	G
LFS(APH)	BIO-LA	-6	=/L	=/L	=	G	G	L	L	L	G	G	G
LFS(APH)	T/A-LA	-9	=	=	=	=	=	G	L	L	G	G	L
LFS(APH)	AN/GD-LA	-8	=	=	=	=	L	G	L	L	G	G	L
MMF	T/A-LA	-4	=	=	=	=	=	G	L	L	L	=	L
MMF	AN/GD-LA	-15	L	L	=	=	L	G	L	L	G	G	L
WLH-FWF	AN/GD-LA	-1	L/=	=	=	=	L	G	L	L	=	G	L
PCC	BIO-LA	-1	=	=	=	L	L	G	L	=?	G	G	G
PCC	SIL-ST-LA	-5	=	=	=	G	L	L	=	L	G	G	L
PCC	T/A-LA	-6	=	=	=	=	=	G	L	G?	L	L	L
PCC	AN/GD-LA	-9	L?	=	=	G	L	G	L	L	G	G	L
SIVS	BIO-LA	+3	=	L	G	G	G	G	L	L	G	G	=
SIVS	T/A-LA	-1	=	L	G	G	G	G	L	L	G	G	=
SIVS	AN/GD-LA	-2	=	L	G	G	G	G	L	L	G	G	L

* "=" = approximate constancy (± 10%) G = >10% component gain
L = >10% component loss; fg = fine grained; cg = coarse grained.

-blank spaces represent components affected by primary fractionation and therefore not considered here

BIO = biotite; SIL = sillimanite; ST = staurolite; T/A = tremolite/actinolite;
AN/GD = anthophyllite/gedrite

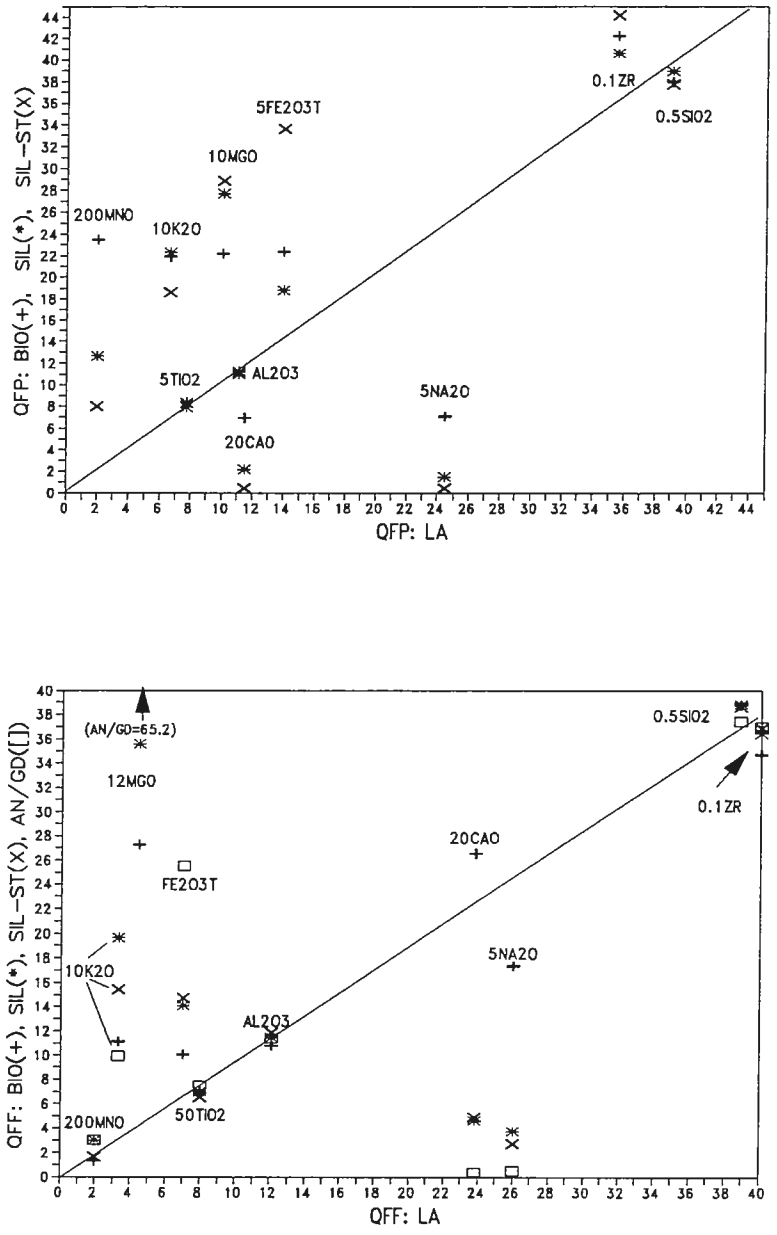

Figure 38. Isocon diagrams for QFP (top) and QFF (bottom) units comparing biotite (BIO = +), sillimanite (SIL = *), sillimanite-staurolite (SIL-ST = X), and anthophyllite/gedrite (AN/GD = []) to least altered (LA) compositions.

the QFF implying alteration of the QFP was relatively Fe-rich.

In the QFP and QFF, gains in Fe_2O_3T are evident mineralogically by the presence of biotite and staurolite. K_2O gains are directly associated with biotite development. MgO gains also reflect biotite development along with anthophyllite in the QFF. Losses of CaO and Na_2O directly coincide with the modal decrease of plagioclase. MnO gains generally correlate with widespread development of garnet in the altered rocks.

Felsic Pyroclastic Rocks (CCLR, CLR)

Figure 39 shows isocon diagrams for comparisons of various alteration zones with least altered equivalents in the CCLR and CLR units. Average analytical data of alteration zones, and component and mass change calculations based on constant Al_2O_3 are listed in Appendix II (Table 23) and summarized in Table 8.

Calculated mass changes range from +7.5% to +14% in the CCLR and from -24% to +7% in the CLR.

As in felsic lava flows, the most dramatic changes resulting from alteration are associated with development of anthophyllite/gedrite zones in the CLR; biotite, tremolite/actinolite, and sillimanite-bearing alteration zones illustrate less dramatic chemical changes. In the CCLR, dramatic chemical changes are evident in both biotite zones and coarse grained portions of anthophyllite/gedrite zones. Fine grained portions of anthophyllite/gedrite alteration zones show less extreme chemical changes and are therefore considered to have been less intensely altered than coarse

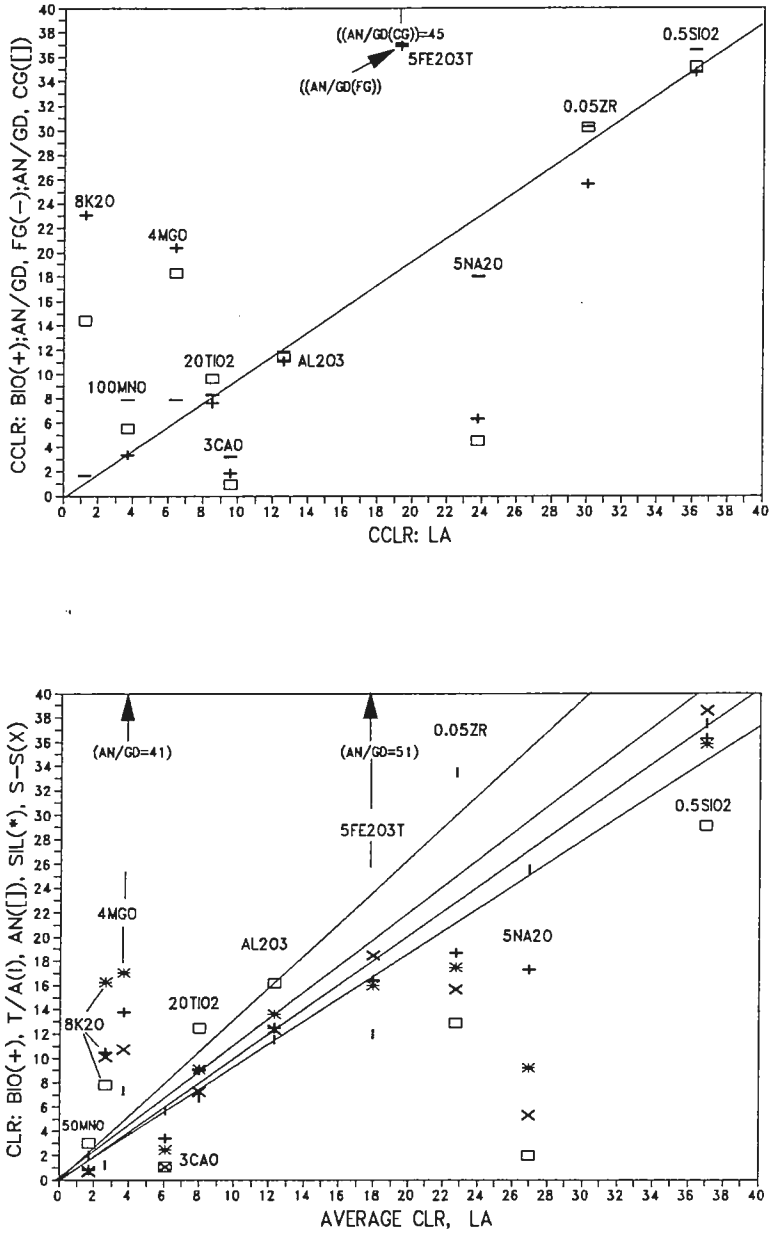

Figure 39. Isocon diagrams for the CCLR (top) and CLR (bottom) units comparing altered to least altered (LA) compositions. fg = fine grained, cg = coarse grained.

grained portions.

In the CLR and CCLR, gains in MgO and K_2O and losses of CaO and Na_2O are evident in most alteration zones. Exceptions include approximately constant MgO and K_2O in fine grained portions of the anthophyllite/gedrite alteration zone in the CCLR. This exception reflects the relatively biotite-poor character of the fine grained relative to coarse grained anthophyllite/gedrite-bearing rocks.

SiO_2 is constant in most comparisons for the CLR and CCLR units. Constant SiO_2 is typical of most isocon comparisons for other units. Variation of SiO_2 is most evident in the CLR and may reflect slight primary fractionation.

Fe_2O_3T is constant or gained in the CCLR but is lost in most comparisons in the CLR. This correlates well with relatively high Fe:Mg ratios in ferromagnesian minerals in the CCLR and lower Fe:Mg ratios in the CLR as noted in microprobe data (Table 6). MnO gains may reflect garnet development in altered CCLR, but MnO losses in the CLR are not understood at present.

Gains in K_2O correlate with widespread development of biotite in altered rocks.

Mafic Lava Flows (RGLF/LF, MMF, WLH-MA)

RGLF/LF

As indicated previously, feldspar phyric and aphyric rocks in the LF and RGLF units have distinctive primary chemistries. Unfortunately, the primary porphyritic character is not visually distinguishable where the rocks are extensively

altered. To assess the likely parentage of pervasively altered LF/RGLF rocks, individual altered samples were compared to least altered feldspar-phyric and aphyric rocks on isocon diagrams. Three groups of graphs resulted as defined by the distribution of TiO_2, Al_2O_3, Zr. Considering the relative chemical immobility of these components during alteration, wide divergence from the best fit isocon must reflect primary variability in their abundance. Six altered samples were found to have fair to well-defined TiO_2-Al_2O_3-Zr isocons when compared to least altered feldspar-phyric equivalents, whereas ten correlated well with aphyric equivalents; five samples showed poor correlation with feldspar-phyric and aphyric equivalents and protolith affinity was not confidently distinguished. The latter group of samples may represent rocks of a mixed feldspar-phyric to aphyric parentage.

Biotite, tremolite/actinolite, and anthophyllite/gedrite alteration is developed within both aphyric and feldspar-phyric varieties of the RGLF and LF units. Isocon diagrams comparing these alteration types to least altered rocks are presented in Figure 40. Appendix II (Table 24) includes average analyses and mass balance calculations for these comparisons, and Table 8 summarizes the trends.

Based on the slope of the isocons, overall rock mass changes are calculated at +9% to -9% for the mafic lava flows. Component changes are generally similar among alteration zones, as well as between feldspar-phyric and aphyric protoliths. However, as in felsic units, the magnitude of chemical changes varies considerably.

The isocons and calculations illustrate that SiO_2 was approximately constant or lost in all comparisons in both aphyric and feldspar-phyric rocks. SiO_2 changes

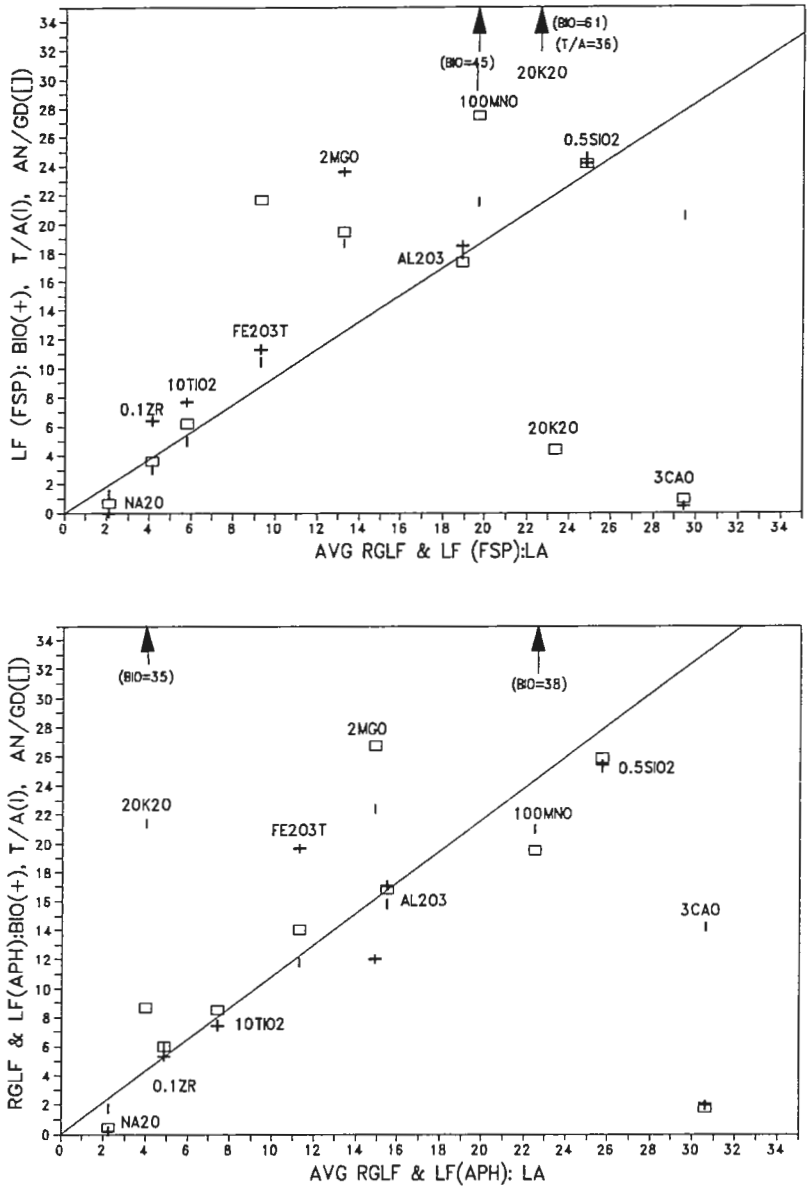

Figure 40. Isocon diagrams comparing averaged Ladder Flow (LF) and Rain Mountain-Gesic Ladder Flow (RGLF) altered compositions to least altered (LA) feldspar-phyric (FSP) and aphyric (APH) compositions.

were accompanied by major losses of CaO and Na_2O in all alteration zones. This reflects the breakdown of primary plagioclase during metasomatism. Fe_2O_3T was approximately constant or gained in all comparisons; MgO was similarly gained in all zones except biotite alteration of aphyric protoliths. The Fe_2O_3T and MgO enrichment reflects development of ferromagnesium silicates during alteration. K_2O was gained in all zones except anthophyllite/gedrite in feldspar-phyric rocks. The K_2O gains correlate best with biotite distribution in altered rocks. K_2O loss in anthophyllite/gedrite-bearing feldspar-phyric rocks may reflect the relatively high K_2O content of least altered protoliths that contain sericitized plagioclase phenocrysts, and the total destruction of such phenocrysts in the altered rocks. Furthermore, the anthophyllite/gedrite-bearing rocks are typically biotite-poor. MnO is variable in abundance among alteration zones and may be related to garnet distribution.

MMF

Figure 41 is an isocon diagram comparing tremolite/ actinolite and anthophyllite alteration to average least altered MMF analyses. Appendix II (Table 24) includes average analyses and mass balance calculations; the mass balance data is summarized in Table 8.

Calculated mass changes range from -4 to -15% based on constant Al_2O_3. Overall component changes are similar to those in the RGLF/LF alteration zones. MgO and Fe_2O_3T are gained and approximately constant, respectively, in both

alterations and primarily reflect development of tremolite/actinolite or anthophyllite. K_2O is lost in tremolite/actinolite alteration, but gained in anthophyllite zones. This may reflect the coexistence of biotite with anthophyllite but not with tremolite/actinolite. As in other units, the loss of CaO and Na_2O are largely offset by gains in other components. MnO and SiO_2 are approximately constant to slightly lost in both alteration zones.

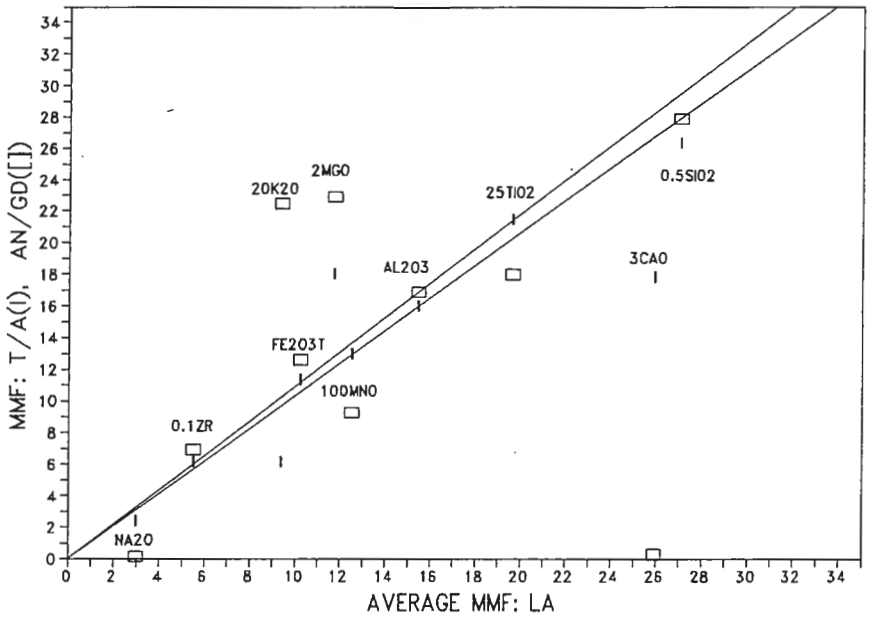

Figure 41. Isocon diagram comparing least altered (LA) to tremolite/actinolite (T/A=▌) and anthophyllite/gedrite (AN/GD=[]) altered Middle Mafic Flow (MMF) unit.

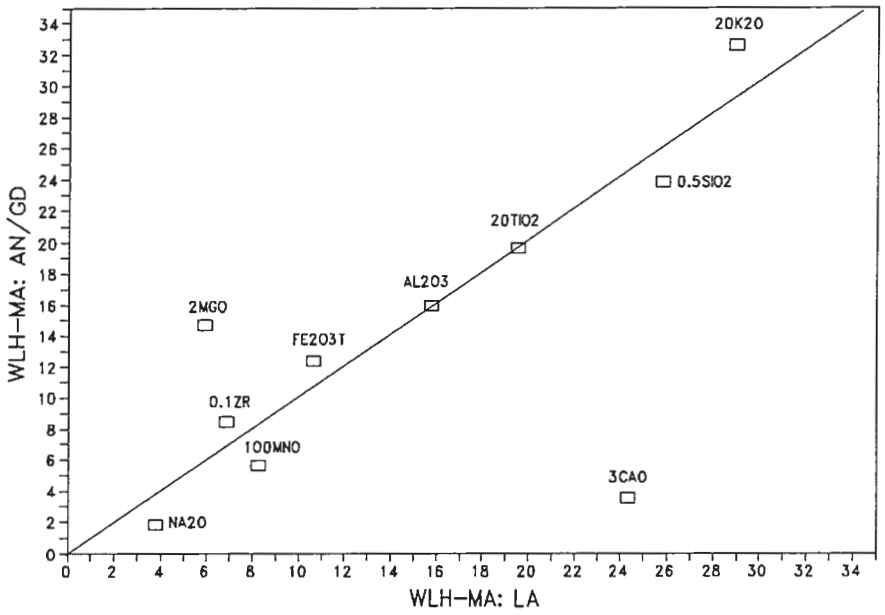

Figure 42. Isocon diagram comparing least altered (LA) to anthophyllite/ gedrite (AN/GD=[]) alteration in mafic lava flows of the Winston Lake Horizon (WLH-MA).

WLH-MA

Eight samples of the WLH-MA were collected; five represent least altered and three represent anthophyllite/gedrite zones. No rocks representative of chlorite or tremolite/actinolite alteration zones were analyzed. Figure 42 is an isocon comparison of anthophyllite/gedrite to least altered rocks. Average analyses and mass balance calculations are included in Appendix II (Table 24) and are summarized on Table 8. Based on the constant Al_2O_3 isocon, development of

anthophyllite/gedrite alteration is principally characterized by gains in MgO, and loss of CaO and Na_2O; other components remained relatively constant.

Volcaniclastic-Sedimentary Rocks (PCC, SIV/RGSIV)

Considering the relatively uniform original composition of the volcaniclastic units, average analyses of various alteration zones were compared to average least altered zones as was done with the volcanic units. Such chemical studies along with field and petrographic work indicate that alteration of the volcaniclastic-sediment units was similar to that in the volcanic units except for the development of an apparent "silicified" zone in the PCC.

Average analyses of the alteration types and mass balance calculations are listed in Appendix II (Table 25). The calculations are based on a well defined TiO_2-Al_2O_3-Zr isocon for the PCC comparisons and a best fit TiO_2-Al_2O_3 isocon for the SIV/RGSIV comparison. Table 8 is a summary of the calculations. Overall mass changes range from -5% to -9% in the PCC, and -2 to +3% in the SIV/RGSIV units. Isocon diagrams of Figure 43 illustrate overall rock mass change and individual component changes.

Relative to average least altered compositions, in general, each alteration type exhibits constant, to concentration gains in Fe_2O_3T, MgO, and K_2O; CaO and Na_2O are generally lost. Exceptions within the PCC include losses of Fe_2O_3T in biotite, and K_2O in tremolite/actinolite alteration zones, and constant to increased Na_2O in tremolite/actinolite and biotite zones, respectively. Several components illustrate

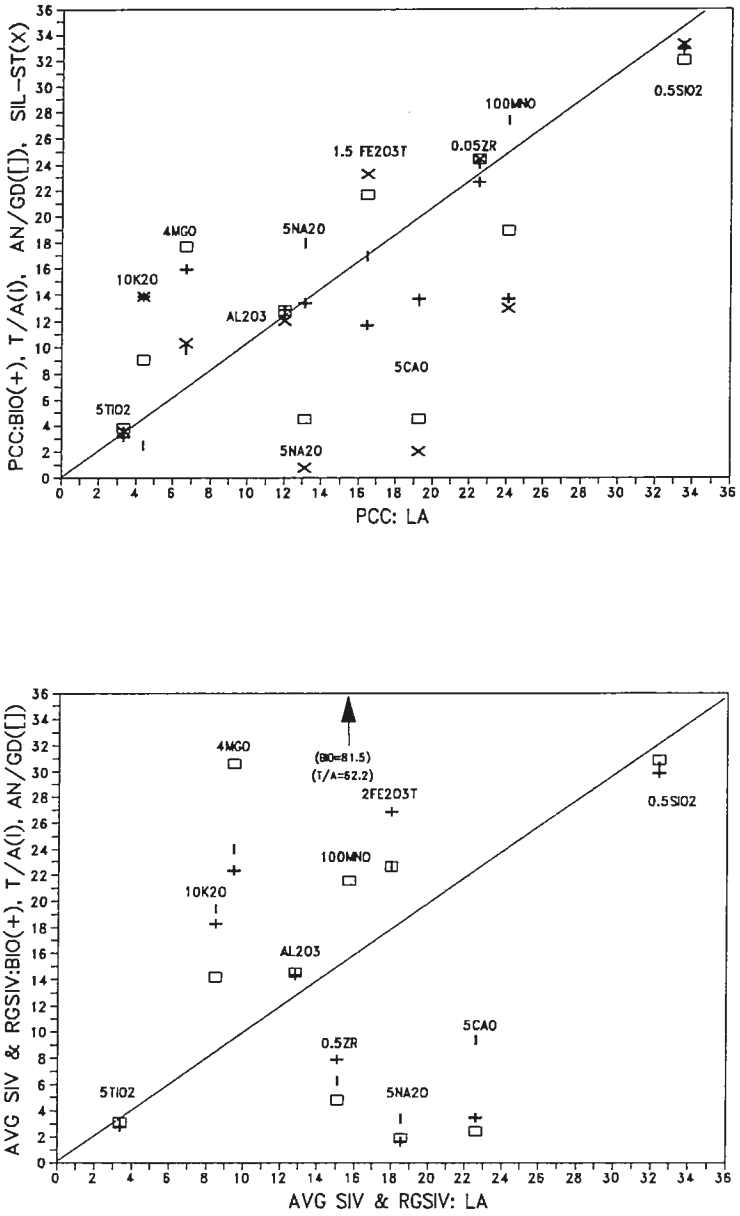

Figure 43. Isocon diagram comparing Pick-Ciglen Clastic (PCC) (top) and averaged SIV and RGSIV volcaniclastic-sediment (bottom) altered to least altered (LA) compositions.

inconsistent behavior relative to least altered compositions. MnO shows losses in altered PCC in contrast to consistent gains in altered SIV/RGSIV. Major losses of Zr in alteration of the SIV/RGSIV units are evident and enigmatic as Zr is typically relatively immobile in other units. SiO_2 was relatively immobile except for slight average losses in anthophyllite/gedrite-alteration of the PCC in spite of apparent quartz-rich character that is evident on outcrop. The development of the silicification is discussed in the following section. Mineralogical changes that reflect chemical variability in the altered volcaniclastic rocks are similar to those in altered volcanic rocks.

Although no silicates from the SIV/RGSIV units were analyzed by microprobe, generally greater gains in MgO relative to Fe_2O_3T gains in altered rocks suggests the silicates are relatively Mg-rich and Fe-poor. This contrasts with the ferromagnesium silicates in the PCC volcaniclastic unit.

Development of Apparent "Silicification"

As noted previously, apparent "silicification" is most conspicuous in intensely altered garnet-bearing anthophyllite/ gedrite or in sillimanite-staurolite-altered PCC. Where anthophyllite/gedrite or sillimanite-staurolite are minor, silicification is generally not as well-developed.

Mass balance calculations and isocons (Figure 43) indicate that both overall rock mass and SiO_2 content decreased slightly during alteration. Silica dumping or

enrichment through cation leaching therefore does not account for the local quartz-rich nature of the PCC.

Based on the mass balance calculations along with petrographic data the apparent "silicification" of the rocks likely represents a redistribution of SiO_2 into coexisting relatively SiO_2-poor minerals (e.g. gedrite, garnet, staurolite, biotite, chlorite) and quartz. Mottl (1983) reached similar conclusions based on experimental study of quartz-chlorite ± albite-epidote altered basalts.

VI.3.4 Summary

It is evident from previous discussion that there was significant mobility of all major oxides with the exception of TiO_2 and Al_2O_3 during metasomatism of the Winston Lake Sequence. Component changes are similar in each alteration type except for variation in the magnitude of change. The magnitude of change generally increases in the order tremolite/actinolite ≤ biotite < sillimanite ± staurolite ≤ anthophyllite/gedrite.

Overall rock mass changes are variable. Losses are evident in rocks at the base of the stratigraphy in the PCC. These losses reflect overall net-total leaching of the rocks during metasomatic processes. In contrast, mass changes vary from gains to losses in the upper portion of the stratigraphy.

Component and mass changes associated with development of various alteration types are summarized in Table 9.

Table 9.
Summary of general trends in mass balance analysis based on comparison with least altered equivalents.

ALTERATION ZONE	% MASS CHANGE	GAINED COMPONENTS	LOST COMPONENTS	IMMOBILE COMPONENTS	INCONSISTENT COMPONENTS
BIOTITE (BIO)	-6to +14	**K_2O, FE_2O_3T, MGO**, H_2O, CO_2	**NA_2O,CAO**	AL_2O_3, TIO_2, ZR	SIO_2, MNO
SILLIMANITE (SIL)	-10to +2	**K_2O, MGO**, H_2O	**NA_2O,CAO**, CO_2	AL_2O_3, TIO_2, ZR	SIO_2, MNO, FE_2O_3T
SILLIMANITE-STAUROLITE (SIL-ST)	-5to +3	**K_2O, FE_2O_3T, MGO**[1], H_2O	**NA_2O,CAO**, CO_2	AL_2O_3, TIO_2, ZR	SIO_2, MNO
TREMOLITE/ ACTINOLITE (T/A)	-9to +7%	**MGO**, MNO[2], H_2O	**CAO**[4]	SIO_2, AL_2O_3[2]	TIO_2, K_2O, FE_2O_3T, NA_2O, CO_2
ANTHOPHYLLITE/GEDRITE (AN/GD)	+9 to -24%	K_2O[6,9], FE_2O_3T, **MGO**[7], H_2O	**NA_2O**[6], **CAO**[6], CO_2[8]	SIO_2[10], TIO_2[3], AL_2O_3[2]	MNO[5]

exceptions

[1]loss in PCC; [2]gain in SIV/RGSIV; [3]loss in SIV/RGSIV; [4]gain in CLR; [5]loss in CLR; [6]gain in CCLR(fg AN/GD); [7]loss in CCLR(fg AN/GD); [8]gain in LF(FSP); [9]loss in LF(FSP); [10]loss in LF(aph),MMF

*components in bold type generally show maximum enrichment or depletion relative to others.

Microprobe analysis of ferromagnesium silicates in altered rocks indicates Mg/Fe ratios are distinctly lower near the base of the stratigraphy than in alteration zones high in the section (Table 6).

Mineralogically, the concentration of K_2O correlates well with modal abundance of biotite. Similarly, MgO and Fe_2O_3T correlate with the presence of garnet, biotite, anthophyllite/ gedrite, cordierite, and tremolite/actinolite; staurolite and spinel are also present in Fe_2O_3T-enriched rocks. CaO and Na_2O concentrations decrease with increased alteration.

The chemical gains and losses demonstrated in altered rocks at Winston Lake are not unlike those of many other Cu-Zn VMS deposits (Franklin et al., 1981). Detailed studies (Riverin and Hodgson, 1980; Gibson et al., 1983; Roberts and Reardon, 1978; Osterberg et al., 1987; Hudak, 1989) on greenschist metamorphosed massive sulfide deposits generally interpret K_2O gains to be associated with extensive sericitization peripheral to MgO ± FeO enriched chloritic alteration domains. CaO and Na_2O losses correlate closely with plagioclase destruction through sericitization or chloritization.

At Winston Lake, amphibolite grade metamorphism prevents the direct recognition of the original silicate mineralogy produced by metasomatism. However, numerous authors (Morton et al., 1982; Walford and Franklin, 1982; Speakman et al., 1982; Bristol and Froese, 1989; Skirrow, 1987) have suggested that cordierite-anthophyllite/gedrite-bearing rocks likely represent quartz-chlorite rich rocks that were metamorphosed to amphibolite grade. Similarly, biotite may represent reaction

of sericite and chlorite during metamorphism, and sillimanite-bearing assemblages reflect relatively Al_2O_3-enriched phases that formed by metamorphism of hydrothermal andalusite, pyrophyllite, or kaolinite-rich assemblages.

VII. ALTERATION MODEL

VII.1 Introduction

Zones of metamorphosed hydrothermally altered rocks at Winston Lake are relatively widespread and are mineralogically distinct as indicated by anomalous modal abundance of biotite, chlorite, anthophyllite/gedrite, tremolite/actinolite, cordierite, garnet, sillimanite, andalusite, staurolite, and spinel. The mineralogical variation in the rocks is reflected chemically by enrichment of MgO, Fe_2O_3T, and K_2O, and depletion of Na_2O and CaO. As such, the alteration is mineralogically and chemically similar to that in numerous metamorphosed volcanogenic massive sulfide (VMS) deposits (Franklin et al., 1981). However, the alteration at Winston Lake is somewhat unusual for Archean Cu-Zn massive sulfide deposits in that its distribution is not pipe-like but instead varies from subconcordant, to conformable, to locally cross-cutting.

Hydrothermal alteration associated with VMS deposits is attributed to the interaction of hydrothermal fluids and rocks in a geothermal system that developed contemporaneously with volcanism. Franklin et al. (1981) summarize the essential features of metalliferous geothermal systems to include a fluid phase(s), permeable rocks, and a heat source at depth. Experimental studies (Seyfried and Mottl, 1982; Seyfried and Bischoff, 1977; Mottl, 1983), observation of natural geothermal systems (Franklin, 1986), and alteration studies of ancient deposits (Morton et al., 1991; Gibson et al., 1981; Roberts and Reardon, 1978; Osterberg et al., 1987; Large, 1992)

indicate that metasomatism in VMS systems is multi-staged and that hydrothermal fluids vary widely in physiochemical character.

Permeability in the hydrothermal systems is thought to be inherited from the primary rock type or enhanced through fracture or faulting of impermeable rocks. Synvolcanic pluton(s) are generally believed to represent the heat source that drives convective circulation of hydrothermal fluids through the permeable rocks (Franklin and Thorpe, 1982; Mottl, 1983; Campbell et al., 1981). The plutons may also contribute metalliferous fluids to the geothermal system (Urabe and Sato, 1978; Sawkins and Kowalik, 1981; Urabe and Marumo, 1991; Stanton, 1990). Synvolcanic plutons have been recognized in several ancient VMS districts (Franklin and Thorpe, 1982; Campbell et al., 1981; Gibson, 1989).

At Winston Lake several of the features characteristic of metalliferous geothermal systems are recognized from stratigraphic, petrographic, and chemical studies. The distribution of alteration is believed to reflect original rock permeability and synvolcanic structures and is thereby related to the physical volcanologic environment; post volcanic structural transposition may have redistributed the alteration to its present location. Chemical and mineralogical variability of the alteration zones, coupled with the relationship of the zones to the stratigraphy, indicate the Winston Lake geothermal system developed in stages and involved multiple hydrothermal fluids. A synvolcanic plutonic heat source has not been recognized at Winston Lake, but it may have been displaced or digested by post-volcanic granite.

VII.2 Nature of Hydrothermal Fluids at Winston Lake

Mass balance studies indicate alteration in the Winston Lake stratigraphy is dominantly characterized by variable MgO, Fe_2O_3T and K_2O enrichment, and CaO and Na_2O depletion. Figure 44 summarizes these trends in approximate order of stratigraphic height as absolute component changes that are based on mass balance calculations. The figure, and isocon graphs illustrate that the chemical trends generally occur regardless of alteration type, and that alteration is relatively Fe-rich (vs. Mg) towards the base compared to the upper portion of the section. However, experimental studies and direct sea floor observations indicate that it is unlikely MgO and Fe_2O_3T were contemporaneously enriched from a single hydrothermal fluid through a single hydrothermal process. Furthermore, field studies at Winston Lake locally show cross-cutting relationships between rocks and alteration zones, and mineral chemistry studies show wide variation in Mg/Fe content of various alteration silicates. As such both chemistry and mapping imply that chemically distinct fluids were present at various stages during development of the Winston Lake geothermal system. Enrichment of both Mg and Fe, which is evident from isocon diagrams and mass balance calculations, reflects the integrated effects of the multiple stages of interaction of various hydrothermal fluids with the strata at Winston Lake. Based on experimental geochemical studies, direct seafloor observations, and other studies of ancient VMS deposits, such hydrothermal fluids can generally be categorized as seawater-based, and various chemically-evolved fluids that differ in metal content. In fact, evidence is recognized that at least three such fluids reacted with the Winston

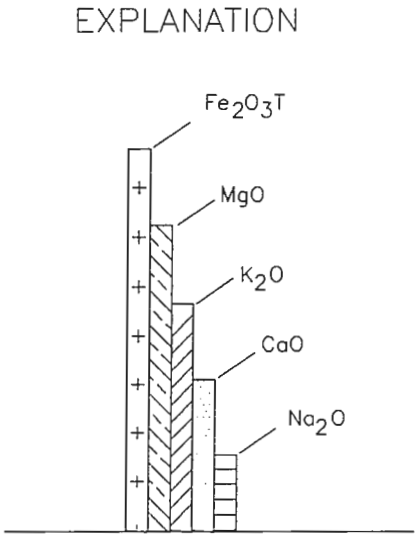

Figure 44. (following page) Bar graphs of calculated absolute weight percent changes in Fe_2O_3, MgO, K_2O, CaO, and Na_2O for various alteration zones at Winston lake. Graphs for various units are arranged in general order of increasing stratigraphic height.

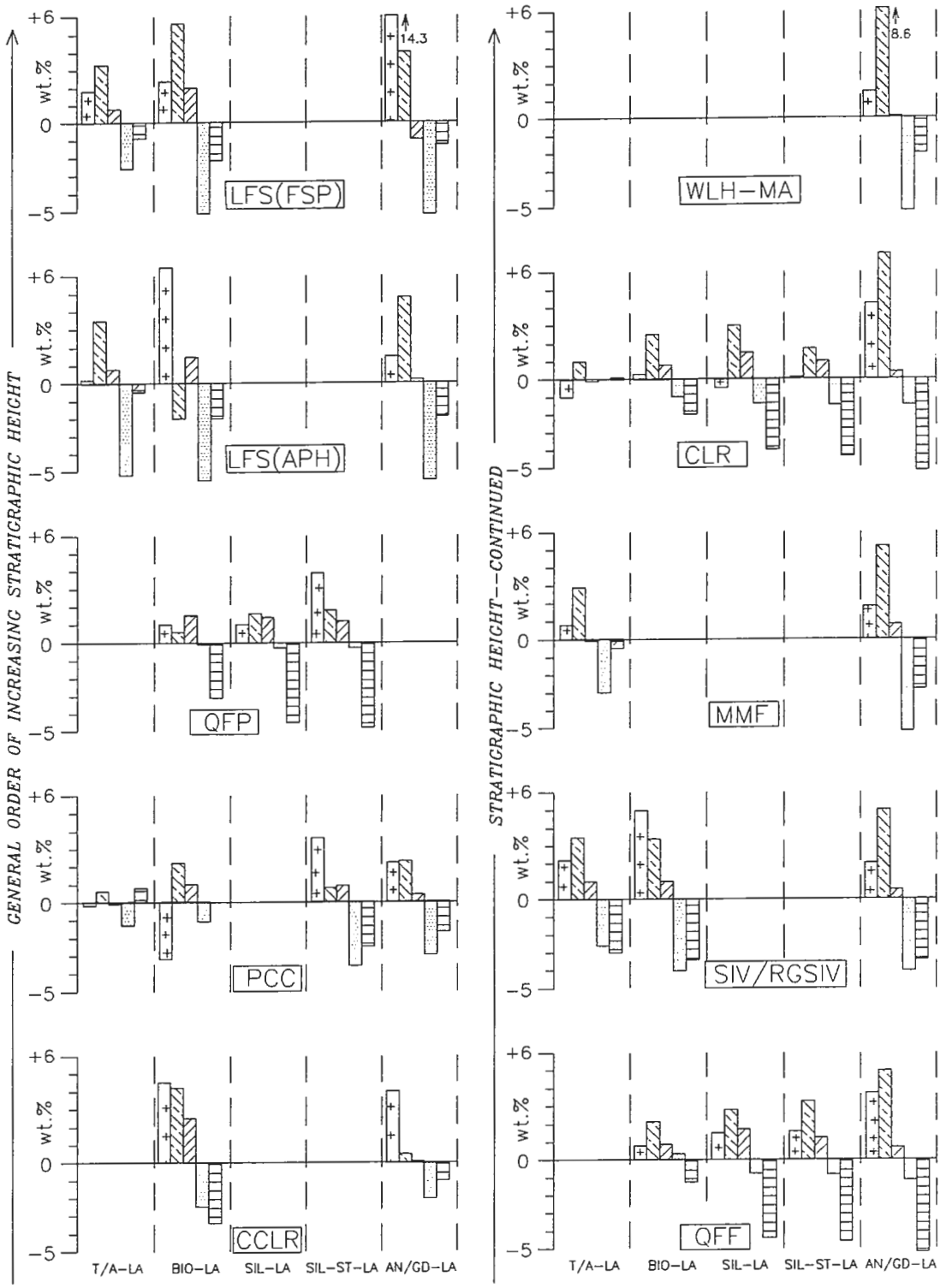

Figure 44. (caption on previous page).

Lake rocks.

Seyfried and Mottl (1982), and Mottl (1983) experimentally demonstrated that strong Mg enrichment of basaltic rocks results from chemical exchange between heated seawater (T=150-350°) and rocks at high seawater/rock (>10-40:1) ratios. To balance Mg lost from solution and fixed as Mg(OH) components of clays and chlorite, Ca and Na along with minor Fe, Mn, K, and Si are leached from the rock through dissolution of primary feldspars and ferromagnesium silicates. Fluid pH becomes acidic through the chemical exchange process. The experimental studies indicate the process of Mg-fixation in rocks is relatively efficient (especially at high temperatures) regardless of the absolute Mg content of the primary seawater-based fluid (Seyfried, pers. comm.). In fact Mg enrichment of rocks can even occur through interaction with heated relatively Mg-poor fluids provided large fluid volumes are available and the temperature is high enough.

At Winston Lake, Mg enrichment and Ca- and Na- depletion is present in altered mafic and felsic volcanic and volcaniclastic rocks as illustrated by the isocons and Figure 44. Although Archean seawater at Winston Lake may have differed significantly in Mg content from modern seawater compositions used in experimental studies, seawater-based fluid-rock alteration processes were nevertheless likely responsible for the Mg enrichment, and the Ca and Na depletion, in altered rocks as water/rock ratios were likely very high. Mineralogically the alteration likely occurred as widespread Mg chloritization.

In submarine hydrothermal systems, chemically-evolved fluids may develop at depth by further modification of seawater at fluid/rock ratios less than 10:1 or by direct magmatic exsolution. Analysis of moderate to high temperature hydrothermal vent fluids (Mottl, 1983; Franklin, 1986; Von Damm, 1990) and experimental studies (Seyfried and Bischoff, 1977; Seyfried and Mottl, 1982) on mafic rocks indicate that the chemically-evolved fluids develop with increased temperature (150-375°C) and pressure (350-400 bars) through Ca ± Na fixation in the rocks (in the absence of dissolved Mg) and Fe, Mn, K, and Si ± Na enrichment in solution. Acidic pH develops with increased temperatures as Ca-rich plagioclase and clinozoisite form and primary ferromagnesium minerals are dissolved.

At Winston Lake there is no evidence for extensive Ca enriched alteration. In contrast, widespread Fe-enriched, Na and Ca-depleted rocks are present. This suggests that chemically-evolved fluids lost their Ca ± Na content outside of the study area prior to interaction with the Winston Lake stratigraphy. The resulting chemically-evolved, relatively Ca- ± Na- deficient fluids reacted with the Winston Lake rocks causing Fe enrichment of previously Mg-enriched, Ca and Na-depleted rocks. The distribution of Fe-enriched sillimanite-staurolite, anthophyllite/gedrite, and biotite alteration zones at Winston Lake indicates widespread interaction of such fluids with the stratigraphy.

The occurrence of widespread K_2O enrichment at Winston Lake is not clearly understood at present. Based on the mass balance and mapping studies, no clear association is recognized between Mg-, and/or Fe- and K-enrichment. Unfortunately,

K behavior during metasomatism of intermediate to felsic rocks is not well understood. Most experimental studies to-date have involved mafic rock compositions, in which K is a relatively minor component.

Nevertheless, it is possible that in felsic-bearing systems, such as Winston Lake, the charge balance for Mg addition during seawater alteration may involve primarily Na- and K-leaching in the absence of abundant Ca in the protoliths. K may then be re-precipitated in the host rocks via higher temperature, chemically-evolved fluid-rock reactions, perhaps accompanying Fe addition. If such a process occurred, K-enrichment of altered rocks at Winston Lake reflects variable leaching vs. addition during distinct alteration events. This would provide further evidence that multistage alteration processes occurred.

Deposition of the Pick Lake and Winston Lake massive sulfide deposits, and other base metal occurrences indicates that metalliferous fluids were also present within the Winston Lake geothermal system. Experimental studies (Mottl, 1983; Seyfried and Mottl, 1982; Seyfried and Bischoff, 1977) and sea floor observations (Davis et al., 1987; Koski et al, 1988; Franklin, 1986) indicate base metals in VMS systems are transported as chloride complexes in hydrothermal fluids. Such fluids likely originated at or near the upper margin of a synvolcanic magma chamber through direct fluid exsolution from the magma or through high temperature ($\geq$385-400°C), high pressure (450-750 bars) (Bischoff and Rosenbauer, 1984; Mottl, 1983; Franklin, 1986) fluid-rock reaction. Seyfried et al. (1988) demonstrated that such reactions can develop in mafic rocks by continued (progressive) modification of

chemically-evolved, Mg-deficient, Ca- ± Na- rich fluids. Epidosites develop in fluid-rock reaction zones as Ca and ferric Fe are fixed as epidote-quartz ± Fe-chlorite assemblages. As pH remains acidic, base metals are leached and become soluble as chloride complexes wherein they can be transported to a site of deposition. Sodium and Fe contents remain relatively high in this "metalliferous fluid."

The absence of epidosite alteration zones and the lack of metal depletion indicates such reaction zones are not preserved within the Winston Lake stratigraphy. They may have been present at depth but, if so, have since been displaced by the granitic intrusives that border the stratigraphy.

Apart from metal content, the metalliferous fluids at Winston Lake were likely similar to the previously described, non-metalliferous, chemically-evolved fluids. This is indicated by the lack of any recognized mineralogical record of their interaction with the stratigraphy. The substratiform rather than high angle cross-cutting distribution of the alteration zones suggests the metalliferous fluids did not rapidly transect the stratigraphy from depth. Therefore, either the metalliferous fluids were in relative chemical equilibrium with previously altered host rocks or their signature has been obscured by later alteration events. In regard to the former, Cathles (1991) indicates that large volumes of hydrothermal fluid can pass relatively unchanged through host rocks if the fluids move rapidly and/or are confined within vein selvedges in which the fluids are in chemical equilibrium. Such selvedges could have been present within the altered rocks at Winston Lake but have been obscured by other alteration minerals and metamorphism.

VII.3 Reconstruction of the Winston Lake Geothermal System

Mass balance studies indicate alteration in the CCLR (Figure 39) and PCC (Figure 43) clastic units is characterized by widespread MgO, Fe_2O_3T, and K_2O enrichment and CaO and Na_2O depletion (Figure 44). This, coupled with the presence of the Pick Lake massive sulfide deposit and Ciglen Zn occurrence, suggest that seawater-based, chemically-evolved, and metalliferous fluids reacted with the clastic rocks at various times. MgO and Fe_2O_3T enrichment in the hangingwall rocks to the Zn occurrences indicates that seawater-based and chemically-evolved alteration also occurred after metal deposition.

Stratigraphically widespread stratiform MgO enrichment and CaO and Na_2O depletion likely developed as large volumes of seawater-based fluids were flushed through and reacted with permeable clastic rocks (Figure 45a). Alteration was likely manifested as stratiform chloritization. During the process of chloritization, silica remained relatively immobile, but formation of relatively low silica-bearing silicates locally redistributed some SiO_2 as quartz resulting in a stratiform apparent "silicification".

Exhalative zinc mineralization at the Ciglen occurrence and Pick Lake Deposit implies high-temperature metalliferous fluids locally transected the stratigraphy (Figure 45a). Formation of the deposit near the south end of the preserved clastic stratigraphy at Winston Lake suggests metal deposition was situated near the rift axis in a zone of high heat flow related to cooling of a synvolcanic magma chamber beneath the developing rift. Chemically-defined compositional lineaments within the

Pick Lake deposit suggest that metalliferous fluids were focussed and directed to the sea floor environment along synvolcanic faults.

Approximately contemporaneous with deposition of the Pick Lake deposit, metalliferous fluids vented approximately 2 km northward at the Ciglen occurrence (Figure 45a). Synvolcanic movement along the Ciglen Fault apparently focussed cross-stratal flow of hydrothermal fluids to the sea floor. Interaction of these fluids and host rocks resulted in intense Fe enrichment and Ca- and Na-depletion of the rocks; iron-aluminous alteration mineral assemblages developed in the rocks and minor zinc sulfides and chert were deposited upon the sea floor.

Clastic sedimentation in the upper portions of the PCC continued during and after metal deposition at the Ciglen and Pick Lake occurrences. Widespread, unfocussed seawater-based hydrothermal activity must have continued for a period during clastic deposition as noted by stratiform MgO enrichment in the hangingwall to the metal occurrences. Eventually the Pick Lake Deposit, Ciglen occurrence, and stratiform MgO enriched alteration zones were buried (Figure 45b).

Iron enrichment of stratiform biotite and anthophyllite/gedrite alteration zones was likely distinct from and unrelated to metasomatism associated with metalliferous fluids at the Pick Lake and Ciglen occurrences. The absence of zinc enrichment in the stratiform zones suggests metalliferous fluids were not involved in the alteration. Therefore stratiform Fe enrichment of the rocks was likely related to later alteration involving chemically-evolved fluids that overprinted Mg-enriched alteration.

Sedimentation ended with eruption and deposition of the QFP. Continued subsidence centered in the axial rift region effectively changed the hydrologic regime for hydrothermal fluid movement (Figure 45c). Shallow circulation of sea-water-based fluids into the clastic rocks was prevented as the QFP physically restricted shallow downward fluid circulation. However, seawater-based fluids apparently circulated locally through the QFP rocks in the axial rift region during QFP eruption and resulted in local Mg enrichment. Subsidence centered in the rift axis created a south-facing paleoslope in the clastic rocks beneath the QFP between the Pick Lake deposit and Ciglen occurrence (Figure 45c).

Fluid-rock interactions at depth resulted in development of acidic, Fe-, and possibly K-enriched, Na-, Ca-, and Mg-depleted, chemically-evolved fluids. The hot hydrothermal fluids buoyantly migrated up-section where they became effectively channeled northward through the south-facing paleoslope in the clastic rocks (Figure 45c). Interaction of the acidic chemically-evolved fluids and host rocks resulted in stratiform Fe and possible K addition to the rocks through continued leaching of Na and Ca; alteration zones became iron-enriched, and following metamorphism, Fe-rich biotite, gedrite, staurolite, sillimanite, and andalusite-bearing assemblages developed. The chemically-evolved fluids were likely not significantly metal-enriched as interaction with host rocks that resulted in Fe-enrichment would also likely have caused precipitation of metals had they been present in solution.

Similar chemically-evolved hydrothermal fluids were also directed, perhaps along synvolcanic faults in the rift axis, into the base of the QFP as noted by

extensive iron-enriched alteration in the Cabin-QFP Lake- and Rain Mountain- areas (Figure 45c; Plate 1). Zinc enrichment in the altered QFP suggests a component of metalliferous fluids was also present. Within the QFP, fluids likely permeated along synvolcanic fractures and zones of hyaloclastite. Based on the distribution of alteration, the fluids breached through the QFP in the Rain Mountain area but not elsewhere.

High-temperature metasomatism in the QFP near the rift axis ceased prior to volcanic eruption of the LF in the rift axis. This is indicated by least altered mafic volcanic feeder material intruded into altered QFP in the Cabin area, and by altered QFP overlain by least altered mafic lava (RGLF) at Rain Mountain (Figure 45d; Plate 1). However, Mg-enriched biotite, chlorite, and anthophyllite, and localized base-metal-poor exhalative mineralization at the Trail showing within the LF indicates seawater-based metasomatism occurred during and after mafic volcanism while the rocks were readily accessable to circulating seawater. The seawater-based hydrothermal fluids flowed through porous pillowed, lobed, brecciated, or hyaloclastite zones and, as indicated by mass balance studies (Figures 40,44), deposited Mg in the rocks while leaching Ca and Na; base metals were not extensively mobilized by these fluids.

Eruption of felsic (QFF) and mafic (MMF) lava flows terminated seawater-based alteration and exhalative deposition associated with the LF (Figure 45e). Seawater-based metasomatism likely continued within the QFF and MMF during and immediately after eruption as indicated by Mg enrichment (Figures 38,41,44), but no

exhalites were deposited. Stratigraphic development continued with basinal volcaniclastic (SIV/RGSIV) and pyroclastic (CLR/RMCLR) deposition and mafic volcanism (WLH-FWF,-MA). The general absence of alteration within the CLR and WLH (except in the L10000N area) indicates that the CLR acted as a relatively impermeable barrier to circulation of seawater-based hydrothermal fluids through the upper portions of the stratigraphy. At the Rain Mountain and Gesic areas where the correlative RMCLR is thin and/or absent, Mg-dominated alteration (Figures 43,44)(anthophyllite-biotite-cordierite) in the RGSIV (Figure 45e) indicates seawater circulated through and reacted with the permeable clastic rocks. Minor associated exhalative activity resulted in development of the Rain Mountain and Gesic showings. Zinc enrichment at Gesic suggests a component of metalliferous fluid from depth was also discharged to the sea floor.

The distribution of Fe-enriched alteration in the QFF-LF-QFP vicinity between Fish Lake and the L10000N area (Plate 1) indicates moderate to high temperature chemically evolved hydrothermal fluids interacted with the rocks sometime following QFF eruption (Figure 45f). A lack of associated exhalative mineralization suggests the metasomatism occurred at depth. Iron enrichment evident from mass balance studies (Figures 38,44) was apparently temporally and genetically distinct from the seawater-based Mg metasomatism that previously affected the rocks. The chemically-evolved fluids were likely similar to those that produced stratiform, Fe-enriched alteration as iron-aluminous mineral assemblages in clastic rocks at the base of the stratigraphy.

The CLR-unit apparently acted as an impermeable cap-rock and sealed the hot, buoyant fluids within and beneath the QFF and prevented their upward cross-stratal escape (Figure 45f); there was limited mixing and dilution by seawater. The evolved hydrothermal fluids were chemically reactive with the QFF, QFP, LF, and MMF as they migrated through primary permeable zones or along secondary fractures.

The chemically-evolved fluids originated at depth and migrated buoyantly northward through the clastic rocks at the base of the stratigraphy to the Ciglen-Fish Lake area, or originated directly down-section of the Ciglen area in an unknown source (Plate 1; Figure 45f). Regardless of their position of origin, the buoyant fluids migrated primarily south from the Fish Lake area through the upper portions of the stratigraphy as indicated by the distribution of Fe-rich sillimanite-bearing alteration in the QFF and in the upper portions of the QFP, and Fe-enrichment of the LF. Southward migration suggests that subsidence had not yet levelled the primary north-facing paleoslope of the lava flows north of the L10000N area.

The southernmost limit of alteration in the QFP(top)-LF-QFF vicinity indicates that the L10000N area (Plate 1) was the furthest extent of southward migration of the chemically-evolved fluids (Figure 45f). Subsidence centered in the rift axis may have reversed the paleoslope of the QFF and LF units from north- to south-facing in the L10000N area. As such, further southward migration of the buoyant fluids would have been restricted by the aquifer morphology.

The presence of the Winston Lake deposit indicates that metalliferous fluids must have passed through the footwall stratigraphy to the sea floor environment sometime following WLH deposition. The lack of a mineralogical or chemical fingerprint from metalliferous fluid-rock interaction suggests the fluids were in relative chemical equilibrium with previous Fe-enriched altered rocks, or that the fingerprint was obscured by later alteration. However, the overall distribution of alteration indicates the metalliferous fluids must have traveled southward somewhere within the vicinity of the alteration zones defined in the QFP(top)-LF-QFF units (Plate 1; Figure 45g).

The distribution of alteration minerals in the CLR in the L10000N area immediately down-section of the Winston deposit clearly indicates that hydrothermal fluids were eventually discharged across the CLR and WLH. Detailed mapping of the WLH indicates the L10000N area was the site of at least small-scale high-angle synvolcanic faulting. Such faults likely breached the WLH and CLR cap-rock and allowed flow of metalliferous hydrothermal fluids to the sea floor (Figure 45h). Faulting was likely induced by stresses related to continued subsidence centered near the rift axis.

Experimental studies (Mottl, 1983; Seyfried et al., 1988) and direct sea floor (Franklin, 1986) observations indicate that metalliferous fluids are expelled episodically and rapidly across stratigraphy from high pressure, high temperature reservoirs. At Winston Lake the QFP(top)-LF-QFF vicinity may have acted as such a reservoir and transport of the metalliferous fluids to the sea floor would have

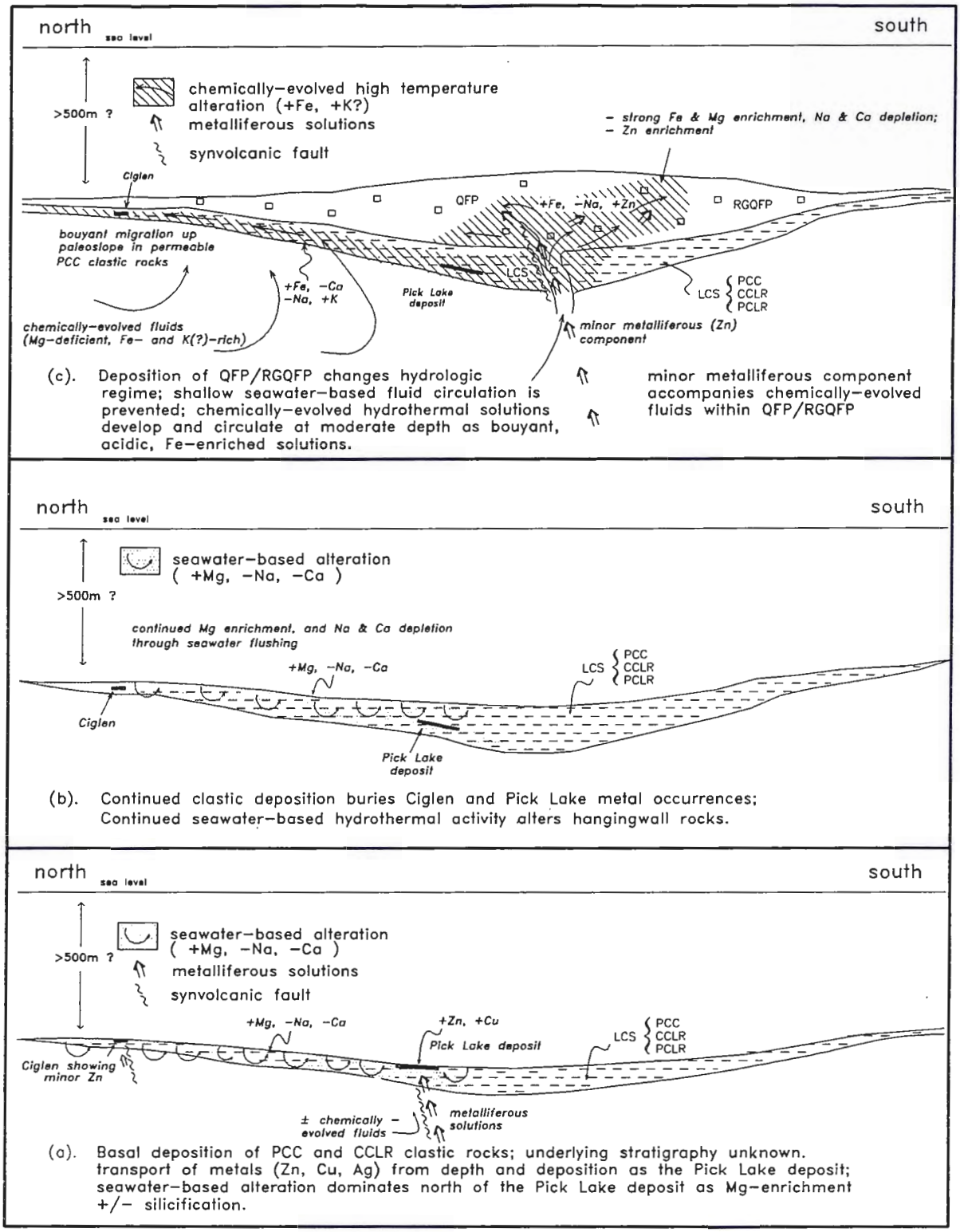

Figure 45. Schematic model illustrating progressive development of the Winston Lake geothermal system and metal occurrences.

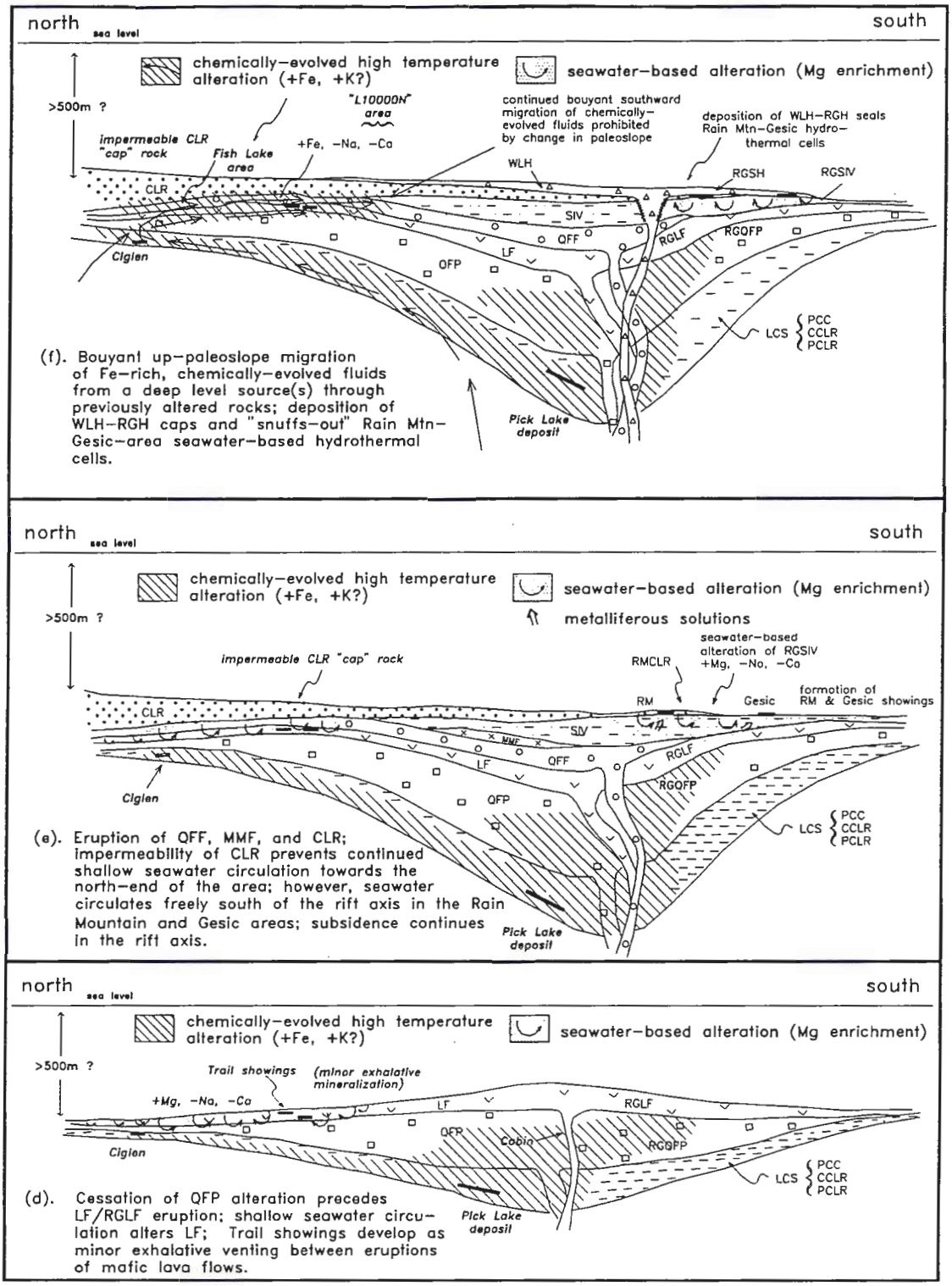

Figure 45. (continued).

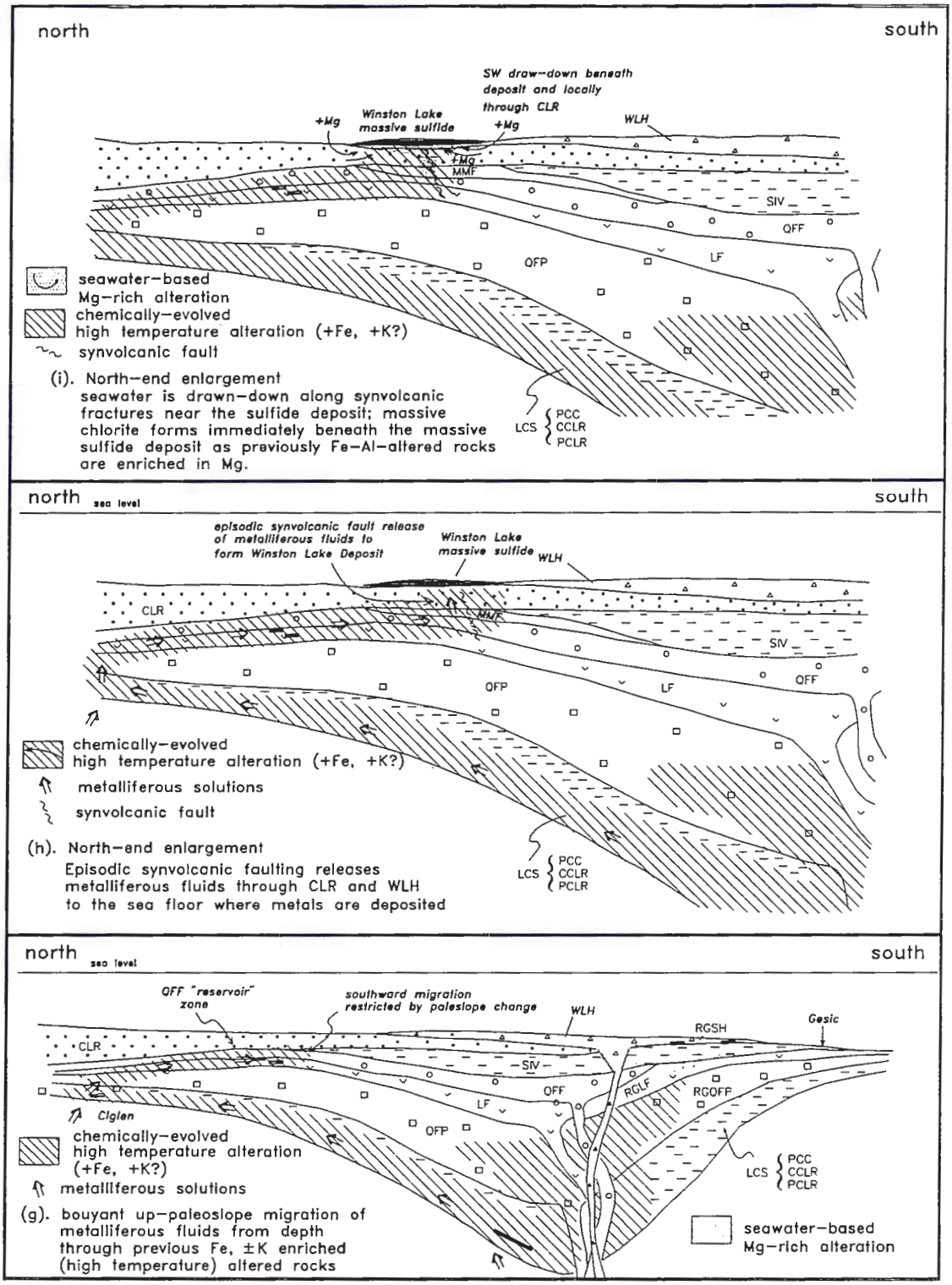

Figure 45. (continued).

occurred across the upper 200 m(±) of stratigraphy during repeated synvolcanic faulting (Figure 45h). During ascent of the fluids, decreased temperature and pressure, and increased pH initiated precipitation of Cu from solution immediately beneath the sea floor in water-saturated ash as represented by disseminated mineralization at the Creek showing (Plate 1). Massive Zn sulfide deposition in the near sea floor environment resulted from interaction of metalliferous fluids with cool seawater.

Intense chlorite alteration in the WLH-FWF and strong Mg-enriched alteration zones in the WLH-FWF, CLR, and MMF (Figures 39,41,42,44) beneath the Winston Lake deposit indicate intense seawater-based alteration occurred in proximity to the massive sulfide deposit (Figure 45i). Franklin (1986) notes that such alteration near hydrothermal vents reflects massive draw-down and flushing of seawater-based hydrothermal fluids through rocks. Based on active sea floor systems, it is believed that the vertical extent of such draw-down is a function of permeability and the exit velocity of the hydrothermal fluids. At Winston Lake, the impermeable CLR largely restricted initial drawdown to the WLH-FWF unit and adjacent CLR and MMF units immediately beneath the massive sulfide deposit.

VIII. SUMMARY AND CONCLUSIONS

VIII.1 Introduction

The Winston Lake Zn-Cu-Ag massive sulfide deposit is situated at the top of the Winston Lake Sequence (WLS), which consists of calc-alkaline, amphibolite-grade metamorphosed volcanic and volcaniclastic rocks (Figures 4 and 5). The stratigraphy strikes north-northwest and dips east to northeast at 45-60°; stratigraphic top is to the east-northeast. The sequence of volcanic and volcaniclastic rocks is intruded by variably differentiated mafic sills and granite; the granite borders the WLS to the west and south. Post-volcanic block faulting displaced the original stratigraphy into its present position (Figure 5).

A detailed geologic reconstruction of the WLS has been completed to aid in assessing the volcanic and hydrothermal evolution of the stratigraphy. Specifically the spatial, genetic, and temporal relationships among volcanology, hydrothermal alteration, and sulfide mineralization have been evaluated with regard to volcanic deposit types, environment of deposition, lithologic diversity, and metasomatism.

VIII.2 Stratigraphy and Volcanology

Based on detailed mapping, drill core examination, and petrographic studies, the Winston Lake Sequence has been subdivided here into two geographically distinct domains known as the Winston Footwall Block (WFB) and the Rain Mountain-Gesic Block (RGB) (Figure 5). The blocks consist of alternating successions of lava flows

and volcaniclastic rocks and represent an originally continuous section of stratigraphy that was dextrally displaced along the strike-slip Pond Fault.

The lowermost stratigraphic units in the WFB consist of metamorphosed interlayered volcaniclastic-sedimentary and felsic pyroclastic rocks (Table 4). No correlative rocks are present within the RGB, but such rocks may have been displaced or digested by emplacement of granite intrusions. The volcaniclastic-sedimentary rocks are of intermediate composition, massive to laminated, and contain rare pebble to cobble-sized felsic volcanic, quartz- and feldspar-crystal clasts. They are interlayered over their entire strike length with massive to laminated felsic pyroclastic rocks or turbiditic equivalents. Facies analysis of the pyroclastic rocks indicates two sources. The dominant source was in a northward and up-dip direction; the subordinate source was in the southward, down-dip direction. Toward the south the pyroclastic rocks form marker horizons. Volcaniclastic-sedimentary rocks between the marker horizons thicken in a southward direction.

Hydrothermal activity occurred contemporaneously with the clastic sedimentation. Exhalative deposition of chert and sulfides at the Ciglen occurrence, Pick Lake deposit, and Anderson showing was accompanied by laterally widespread, variably intense, hydrothermal alteration of the rocks.

Clastic sedimentation ceased in the Winston Lake area as a thick, laterally extensive succession of alternating felsic and mafic lava flows were deposited upon the clastic deposits (Figure 5, Table 4). These flows dominate the footwall stratigraphy (70%) and are present in both the WFB and RGB. In the WFB,

individual units thicken southward; whereas in the RGB, correlative units thicken westward (Figure 17).

Massive quartz-feldspar porphyry (QFP) forms the base of the flow succession; chemical and lithological homogeneity indicates the QFP may have been emplaced endogenously in part. In the WFB, the QFP is overlain by a lithologically and chemically similar but texturally distinct felsic lava flow unit. The upper felsic unit is locally flow banded and has a length:thickness ratio on the order of 50:1 indicating a highly fluid character during eruption and deposition. The upper felsic flow was north-directed; southward flow into the RGB was prohibited by north facing growth fault(s) in the vent area (Figure 18).

Aphyric to feldspar phyric, massive to pillowed and tubed mafic lava flows were erupted and deposited between and after the felsic volcanic events and separate the felsic units. During relatively brief pauses in mafic volcanism between felsic events clastic and exhalative sediment accumulated between individual lava flows in the Winston Trail area. Local alteration of the sediments and associated flows indicates hydrothermal activity occurred during these pauses in volcanism.

Following deposition of the mafic and felsic lava flow successions, volcaniclastic-sediments, up to 200m thick, accumulated conformably on the lava flows. Massive to bedded and locally graded intermediate volcaniclastic-sediments with rare volcanic clasts accumulated as a basinal succession (Figures 17 and 19). Volumetrically minor felsic pyroclastic material was erupted simultaneously from a source within the basin and became interlayered with the volcaniclastic-sediments.

Felsic pyroclastic rocks or their turbiditic equivalents cap the volcaniclastic-sediments and extend the length of the WFB and into the western end of the RGB (Figure 19). Facies analyses indicate that the pyroclastic material was erupted from a northward source.

The Winston Lake Horizon (WLH) and Rain Mountain-Gesic Sulfide Horizon (RGSH) were deposited during a final cycle of volcanism. The WLH and RGSH cap the footwall stratigraphy as 0-100m thick successions of alternating mafic lava flows and volcaniclastic deposits with local chert and massive sulfides. Up to six thin (typically <10m), laterally extensive (≥ 2km), highly fluid lava flows were erupted northward and southward into the WFB and RGB from a centrally located feeder source.

The individual lava flows are typically separated by 3-5m of massive to well-laminated volcaniclastic-sediment. The volcaniclastic material appears lithologically and chemically similar to the rocks immediately underlying the WLH and RGSH and represents settling of clastic detritus from the water column during temporary pauses in mafic volcanism.

Synvolcanic faulting near L10000N initiated minor soft-sediment deformation of the clastic rocks of the WLH. The faulting resulted in discontinuity in the northward distribution of lava flows.

Hydrothermal activity during a pause in mafic volcanism eventually led to hydrothermal venting and alteration of the stratigraphy beneath the Winston Lake deposit and the stratigraphically correlative Rain Mountain and Gesic showings.

Volcanic feeder structures and dikes lithologically similar to overlying lava flows cross-cut the Winston Lake stratigraphy. The structures and dikes are located at various stratigraphic levels and are laterally positioned between the WFB and RGB in the vicinity of the Pond Fault. Such dikes and structures represent volcanic vent sources.

Unit thickness variation, basinal clastic deposits, facies relationships within lava flows, and localization of volcanic feeder dikes and feeder structures indicates the footwall stratigraphy formed through cyclic clastic sedimentation and volcanism in a rift environment. The rift was centered between the WFB and RGB in the present vicinity of the Pond Fault (Figure 17). The abundance of pillowed lava flows as passive eruption products, the paucity of hyaloclastite and amygdules, the absence of hyalotuffs, and the unusually fluid felsic lava flows suggest that the volcanic rocks were erupted and deposited in relatively deep water below the volatile fragmentation depth (VFD) at high water/magma ratios and high hydrostatic confining pressures.

The basinal thickness variation of clastic deposits that alternate with volcanic successions indicates subsidence occurred during sedimentation and volcanism. Because of subsidence no major subaqueous volcanic edifices were formed at Winston Lake; instead, a relatively broad, gently-sloping, platform-like morphology was present. Synvolcanic structures developed within and on the flanks of the rift axis in response to stratigraphic stresses induced by subsidence.

The post-volcanic Rain Mountain Gabbro (RM-GB) intruded the rift axis stratigraphy as a feeder keel to the Zenith Sills of the Winston Lake hangingwall

stratigraphy. Intrusion was focussed through the axial rift zone containing pre-existing synvolcanic structural weaknesses (Figure 19i). Late stage structural stresses reactivated synvolcanic faults in the rift-axis and Ciglen areas as the Pond and Ciglen Faults.

VIII.3 Alteration

Approximately 50% of the footwall rocks exposed at Winston Lake have been variably altered by hydrothermal solutions in subconcordant zones and subsequently metamorphosed to amphibolite facies. The original porosity and permeability of the rocks and synvolcanic faults were important controls on the distribution of alteration. Alteration is extensive in volcaniclastic-sedimentary rocks and pillowed or brecciated mafic lava flows; such rocks had high original permeabilities. Felsic pyroclastic rocks are less pervasively altered indicating they had relatively low permeability. Synvolcanic faulting at the Ciglen occurrence and near L10000N created cross-stratal permeable zones that focussed fluid movement.

Detailed field mapping, supplemented by petrographic study, has resulted in subdivision of the rocks into eight alteration zones (Plate 1) that developed in response to metamorphism of variably hydrothermally altered rocks. The zones are characterized as follows:

(1). Least Altered Zone

-comprising ~50% of the footwall stratigraphy including portions of all volcanic and volcaniclastic units.

-found in gradational contact with other alteration zones.

-distinguished by the presence of hornblende in mafic and intermediate rocks, and preserved relict plagioclase phenocrysts in mafic and felsic volcanic rocks.

(2). Tremolite/Actinolite Zone

-comprising ~3% of the footwall stratigraphy as rare domains restricted to volcaniclastic-sedimentary rocks and mafic lava flows.

-found in gradational contact with least altered and anthophyllite/gedrite zones.

-distinguished by the presence of tremolite/actinolite in modal amounts greater than hornblende or anthophyllite/gedrite.

(3). Biotite Zone

-comprising ~16% of the footwall stratigraphy primarily as alteration within felsic lava flows and volcaniclastic rocks.

-found gradationally situated between least altered and other alteration zones.

-includes rocks containing biotite in modal amounts greater than hornblende or tremolite/actinolite and containing no anthophyllite/gedrite or sillimanite.

(4). Sillimanite Zone

-comprising ~10% of the footwall stratigraphy, developed within felsic lava flows, pyroclastic rocks, and volcaniclastic-sedimentary rocks.

-typically found in sharp contact with tremolite/actinolite or anthophyllite/gedrite zones, and in gradational contact with biotite or sillimanite-staurolite zones.

-distinguished as domains of rock containing sillimanite in the absence of staurolite.

(5). Sillimanite-Staurolite Zone

-comprising ~5% of the footwall stratigraphy where developed within volcaniclastic rocks and felsic lava flows. -typically in gradational contact with biotite and sillimanite zones.

-distinguished by the presence of sillimanite with coexisting staurolite.

(6). Anthophyllite/Gedrite Zone

~comprising 15% of the footwall stratigraphy dominantly developed in mafic lava flows and volcaniclastic-sedimentary rocks and locally present in felsic lava flows and pyroclastic rocks.

-typically in gradational contact with tremolite/actinolite, and in sharp contact with other zones.

-includes all rocks with distinguishable anthophyllite/gedrite.

(7). Chlorite Zone

-confined to ~1% of the footwall stratigraphy within mafic lava flow (WLH-FWF) immediately beneath the Winston Lake massive sulfide deposit.

-found in relatively sharp contact with adjacent biotite and anthophyllite/gedrite zones.

-distinguished by the presence of massive chlorite with variable associated anthophyllite/gedrite, biotite, cordierite, and garnet.

(8). Quartz-rich Zone

-developed within volcaniclastic-sedimentary rocks at the base of the stratigraphy.

-associated with anthophyllite/gedrite and sillimanite-bearing alteration zones.

-recognized as quartz-rich (10-20%), garnetiferous rocks with associated anthophyllite/gedrite or sillimanite ± staurolite.

Microprobe analyses of ferromagnesium silicates in altered rocks indicates Mg/Fe ratios are distinctly lower near the base than in the upper portions of the stratigraphy (Table 6), regardless of alteration type.

In general, hydrothermal alteration has greatly changed the primary geochemistry of the rocks. All major oxides, with the exception of TiO_2 and Al_2O_3 show significant mobility. Using the isocon method of Grant (1986), mass balance comparisons were made between various lithologies in altered zones and least altered zones. Mineralogic variation in the rocks is reflected chemically by variable enrichment of MgO, Fe_2O_3T, and K_2O and depletion of CaO and Na_2O. Component changes (Tables 8 and 9) are similar in each alteration type except for the magnitude of change, which generally increases in the order Tremolite/Actinolite ≤ Biotite < Sillimanite ± Staurolite ≤ Anthophyllite/Gedrite. In general, Fe-enrichment dominates over Mg-enrichment towards the base of the stratigraphy, whereas the reverse is true in units higher in the section.

Mineralogically the concentration of K_2O correlates well with modal abundance of biotite, and MgO and Fe_2O_3T correlate with garnet, biotite, anthophyllite/gedrite, cordierite, and tremolite/ actinolite. Staurolite and spinel are also present in Fe_2O_3T-enriched rocks. CaO and Na_2O concentrations decrease with increasing alteration. Mass changes vary from +14% to -24%. Losses are concentrated in volcaniclastic-sediments and felsic units at the base of the stratigraphy reflecting metasomatic leaching of the rocks. Both gains and losses are found in the upper portions of the stratigraphy (Table 9).

The mineralogical and chemical variability of alteration zones, the relationship of the zones to the stratigraphy, the distribution of metal occurrences, and the results of recent experimental studies of hydrothermal fluids indicate that the geothermal activity at Winston Lake was multistaged and developed contemporaneously with the stratigraphy. In fact, the presence of at least three distinct hydrothermal fluids is inferred. These include: (1) seawater-based fluids that were primarily responsible for Mg-enrichment, (2) chemically-evolved fluids that reacted with the rocks to produce stratiform zones of variable iron-aluminous mineral assemblages, and (3) metalliferous fluids that were base metal-rich and probably otherwise similar to chemically-evolved fluids. No metal-depleted reaction zones or associated synvolcanic plutons have been recognized at Winston Lake.

Hydrothermal Model

Based on the general characteristics of ore-forming geothermal systems and on the characteristics of the stratigraphy and alteration, the following multistaged model is proposed to explain development of the Winston Lake system.

A pluton centered beneath a developing rift initiated shallow convective circulation of seawater through porous and permeable volcaniclastic-sediments (Figure 45a). Interaction of seawater and sediments occurred at high water/rock ratios (≥ 10-40:1) and resulted in widespread Mg addition and Ca- and Na-depletion through stratiform Mg-chloritization. Hot (≥385-400°C) metalliferous fluids that originated at depth crossed through the clastic deposits along synvolcanic faults near the rift axis at the Pick Lake deposit and distal to the rift axis at the Ciglen occurrence (Figure 45a). Metals were deposited as the fluids were expelled to the sea floor.

Continued volcaniclastic sedimentation ultimately buried the metal deposits, and continued seawater flushing altered much of the upper portion of the clastic succession (Figure 45b).

Sedimentation and convective seawater alteration of the clastics ended as eruption and intrusion of quartz-feldspar porphyry (QFP/RGQFP) from the rift axis buried the clastic deposits; accompanying subsidence centered in the rift axis created a north-facing paleoslope in the clastic deposits underlying the QFP and effectively changed the hydrologic paleoslope. Minor seawater circulated through the QFP in the rift axis zone and resulted in local Mg enrichment (Figure 45c). Hot (> 150-

375°C) acidic, Fe-, and possibly K-rich, and Na- and Ca-depleted fluids evolved at depth and migrated buoyantly up-paleoslope in the clastic deposits where they reacted to produce stratiform alteration zones comprised of iron-aluminous ± potassic mineral assemblages. Similar chemically-evolved fluids, with an additional metalliferous fluid component, were redirected into the QFP/RGQFP in the axial rift zone whereupon similar alteration developed with accompanying zinc enrichment; such fluids apparently breached the sea floor only in the Rain Mountain area (Figure 45c).

High temperature alteration of the QFP/RGQFP ceased as erupting mafic lava flows (LF/RGLF) capped the QFP/RGQFP. In the feeder zones to the lava flows, mafic magma intruded previously iron-potassic(?)-enriched altered QFP/RGQFP. Pauses in mafic volcanism were marked by convective seawater circulation through porous portions of the LF lava flows. This resulted in stratiform Mg enrichment and local interflow base metal-deficient exhalative activity at the Trail and Cabin showings (Figure 45d).

Felsic and mafic volcanism resumed with eruption and deposition of the felsic (QFF) and mafic (MMF) lava flows which terminated exhalative activity associated with the LF. Seawater likely circulated through porous zones in the QFF and MMF after eruption, but no exhalites developed.

Volcanism ceased for a period, whereupon basinal volcaniclastic-sediments (SIV/RGSIV) were deposited in the rift axis. Felsic tuffs (CLR) were then deposited primarily north of the rift axis where they capped the volcanic-volcaniclastic

stratigraphy. The tuffs were relatively impermeable and prevented seawater circulation north of the rift axis. However, seawater circulated relatively freely through the volcaniclastic-sediments in the Rain Mountain-Gesic area, and minor associated exhalative activity occurred contemporaneously. At Gesic a component of metalliferous fluid from depth accompanied seawater-based fluids and resulted in minor zinc deposition (Figure 45e).

Meanwhile, high-temperature, chemically-evolved fluids developed at depth in the Winston Lake area and migrated primarily up the paleoslope. Eventually they progressed southward through the QFP(top)-LF-QFF vicinity to the L10000N area while sealed beneath the impermeable CLR unit. The chemically-evolved fluids extensively leached the rocks of Na and Ca while enriching them in Fe and possibly K (Figure 45f).

Metalliferous fluids eventually migrated up the paleoslope through the altered QFP(top)-LF-QFF vicinity to the L10000N area where they were trapped and pressurized beneath the impermeable CLR cap-rock (Figure 45g). The fluids were in relative equilibrium with the previously Fe-K(?) enriched rocks.

Synvolcanic faults developed in the L10000N area in response to subsidence of the rift axis and episodically released the metalliferous fluids from their pressurized reservoir to the sea floor. Copper was precipitated at the Creek showing as temperature and pressure decreased, and pH increased in the fluid during ascent towards the sea floor. In the sea floor environment massive Zn-rich sulfides were precipitated from solution. Fluid rock reactions sealed the fault channels until

repeated pressurization and faulting re-initiated the exhalative processes. Ultimately the Winston Lake deposit accumulated (Figure 45h).

As metalliferous fluids were expelled to the sea floor, massive seawater draw-down developed in proximity to the hydrothermal vents (Figure 45i). Initially draw-down was focussed in the mafic flows (WLH-FWF) immediately beneath the Winston Lake deposit where massive Mg-chloritization occurred. Eventually seawater-circulation occurred at greater depths in the fault vicinity, and the CLR, and MMF became Mg enriched.

VIII.4 Metamorphism and Deformation

Following volcanism, hydrothermal activity, and post-volcanic intrusion, the Winston Lake area underwent amphibolite-grade metamorphism that converted chlorite-rich assemblages to cordierite-anthophyllite/gedrite, sericite-chlorite to biotite, and alumino-silicates (kaolinite, pyrophyllite) to sillimanite-andalusite-rich assemblages.

Progressive, multistaged deformation accompanied metamorphism. Development of foliation, lineation, and minor folds was coincident with regional folding and rotation of the stratigraphy. Subsequent stresses initiated faulting of previously deformed stratigraphy and locally reactivated synvolcanic structures. Movement of ≥ 1 km along the Pond Fault cut the stratigraphy in the vicinity of the paleorift-axis and dextrally displaced the Winston Footwall and Rain Mountain-Gesic Blocks into their present relationship. Development of joints may have accompanied

faulting. Following intrusion of late stage diabase dikes, faults were locally reactivated.

VIII.5 Conclusions

A geologic reconstruction of the rift-related footwall stratigraphy to the Winston Lake Zn-Cu-Ag massive sulfide deposit indicates that the physical character of the rocks controlled the development of the hydrothermal system and the localization of mineralization. Hydrothermal fluids were focussed and passed through primary permeable stratigraphic zones. The paleoslope of the zones was controlled by variable subsidence of the stratigraphy. Cross-stratal permeable synvolcanic fault zones developed in response to subsidence-related stresses. Mineralization was concentrated along favorable stratigraphic breaks marked by pauses in volcanic deposition, and by the position of the synvolcanic faults through which fluids transported metals to the sea floor environment where they were deposited. Interaction of hydrothermal fluids with the stratigraphy, and subsequent amphibolite-grade metamorphism, changed the primary mineralogy of the rocks into that of pseudopelites.

REFERENCES

Allen, C.C., 1980a, Volcano-ice interactions on Earth and Mars. Advances in Planetary Geology (NASA TM-81979), 161-164.

Allen, C.C., Jercinovic, J., and Allen, J.S.B., 1982, Subglacial volcanism in north-central British Columbia and Iceland. J. Geol., 90, 699-715.

Balint, F.B., 1984, Geologic Map, Winston-Zenmac Project, Corporation Falconbridge Copper, 1:5000 Scale.

Balint, pers. comm.

Balint, F., and Severin, P.W.A., 1984, Winston Lake Project--NTS 42-D-14, Exploration 1978 to 1983. Unpublished internal Corporation Falconbridge Copper report, July, 1984.

Bartley, N.W., 1942, Geology of the Big Duck-Aguasabon Lakes Area, in Forty-Ninth Annual Report of the Ontario Department of Mines, Vol. XLIX, part VII, p.1-11.

Bischoff, J.L,, and Rosenbauer, R.J., 1987, Phase separation in seafloor geothermal systems: an experimental study of the effects on metal transport, Am. J. Sci., 287, #10, 953-978.

Branney, M.J. and Suthren, R.J., 1988, High-level peperititic sills in the English Lake District; distinction from block lavas and implications for Borrowdale Volcanic Group stratigraphy, Geol. Journ., 23, #2, 171-187.

Bristol, C.C., and Froese, E., 1989, Highly metamorphosed altered rocks associated with the Osborne Lake volcanogenic massive sulfide deposit, Snow Lake area, Manitoba, Canadian Mineralogist, 27, 593-600.

Buchan, R., 1983, Mineralogic examination of 10 samples from Winston Lake Project, Ontario; Falconbridge Metallurgical Laboratories Report, February 3, 1983.

Busby-Spera, C.J., and White, J.D.L., 1987, Variation in peperite textures associated with differing host-sediment properties: Bull. Volcanology, V. 49., p.765-775.

Campbell, J.H., Franklin, J.M., Gorton, M.P., Hart, T.R., and Scott, S.D., 1981. The role of subvolcanic sills in the generation of massive sulfide deposits. Econ. Geol., 76, pp. 2248-2253.

Cas, R.A.F., 1979, Mass-flow arenites from a Paleozoic inter-arc basin, New South Wales, Australia: mode and environment of emplacement. Jour. Sed. Petrol., 49, pp. 29-44.

Cas, R.A.F., and Wright, J.V., 1987, Volcanic Successions: Modern and Ancient. Allen and Unwin, London.

Cathles, L.M., 1991, The importance of vein selvedging in controlling the intensity and character of subsurface alteration in hydrothermal systems, Econ. Geol., 86, p. 461.

Collins, W.H., 1909, Report on the region lying north of Lake Superior between the Pic and Nipigon Rivers, Ontario; Geol. Survey Canada, Publication No. 1081.

Costa, U.R., Barnett, R.L., and Kerrich, R., 1983, The Matta-gami Lake mine Archean Zn-Cu sulfide deposit, Quebec: Hydrothermal coprecipitation of talc and sulfides in a sea-floor brine pool--evidence from geochemistry, $^{18}O/^{16}O$, and mineral chemistry, Econ. Geol., 78, p1184-1203.

Davis, E.E., Goodfellow, W.D., Bornhold, B.D., Adshead, J.,Blaise, B., Villinger, H., and LeCheminant, G.M., 1987, Massive sulfides in a sedimented rift valley, northern Juan de Fuca Ridge, Earth Planet. Sci. Lett. 82, 49-61.

Deer, W.A., Howie, R.A., and Zussman, J., 1966, An Introduction to the Rock Forming Minerals, Longman Group Ltd., London, 528p.

Dixon, R.J., 1990, The Moel-y-Golfa Andesite; an Ordovician (Caroduc) intrusion into unconsolidated conglomeratic sediments, Breidden Hills Inlier, Welsh Borderland: Geol. Journ., 25(1), 35-41.

Finlow-Bates, T., and Stumpfl,E.F., 1981, The behavior of so-called immobile elements in hydrothermally altered rocks associated with volcanogenic submarine exhalative altered rocks associated with volcanogenic submarine-exhalative ore deposits. Mineralium Deposita, 16, 319-328.

Fischer, R.V., 1982, Pyroclastic Surges. In Ayres, L.D.,(eds), Pyroclastic Volcanism and deposits of Cenozoic intermediate to felsic volcanic islands with iimplications for Precambrian greenstone belt volcanoes, pp. 71-110.

Fischer, R.V., and Schminke, H.V., 1984, Pyroclastic Rocks. Springer-Verlag, New York, New York, 472 p.

Franklin, J.M., 1986, Volcanic-associated massive sulphide deposits- an update. pp. 49-69, in C.J. Andrews, R.W.A. Crowe, S. Finlay, W.M. Pennell, and J.F. Pyne, eds. Geology and Genesis of Mineral Deposits in Ireland. Irish Association for Economic Geologists.

Franklin, J.M., Sangster, D.M., and Lydon, J.W., 1981, Volcanic-associated massive sulfide deposits, in Skinner, B.J., ed., Econ. Geol. 75th Anniversary Volume. Economic Publishing Co., 964 p.

Franklin, J.M. and Thorpe, R.I., 1982, Comparative metallogeny of the Superior, Slave, and Churchill Provinces. in Precambrina Sulphide Deposits, edited by R.W. Hutchinson, L.D. Spence, and J.M. Franklin. Geol. Assoc. of Can. Special Paper 25.

Franklin, J.M., Goodfellow, W.D., Blaise, B, Anglin, C.D., Harvey-Kelly, F.E.L., MacDonald, R., and Kappel, E., 1987, Geological map and distribution of sulfide deposits in Middle Valley, northern Juan de Fuca Ridge [abst.]; in AGU 1987 fall meeting, EOS, Trans. Amer. Geophys. Union, 68(44), p.1545.

Galley, A., 1991, pers. comm.

Gibson, H.L., Watkinson, D.H., and Comba, C.D.A., 1983, Silicification: Hydrothermal alteration in an Archean geothermal system within the Amulet Rhyolite Formation, Noranda, Quebec, Econ. Geol. 78, 954-971.

Gibson, 1989, The mine sequence of the central Noranda volcanic complex: geology, alteration, massive sulphide deposits and volcanological reconstruction. Ph.D. thesis, Carlton University, Ottawa, Ontario (unpubl.).

Gibson, H.L., Watkinson, D.H., and Comba, C.D.A., 1989, Subaqueous phreatomagmatic explosion breccias at Buttercup Hill, Noranda, Quebec, Can. Jour. Earth Sci., 36: 167-188.

Grant, J.A., 1986, The isocon diagram - a simple solution to Gresan's equation for metasomatic alteration. Econ. Geol., v.81, pp. 1976-1982.

Hawthorne, F.C., 1981, Crystal chemistry of the amphiboles.
pp 1-9 in D.R. Veblen, ed., Amphiboles and other hydrous pyriboles-mineralogy. Reviews in Mineralogy, v.9A. Mineralogical Society of America.

Hopkins, P.E.,1915, Gold at Big Duck Lake; in Statistical Review of the Mineral Industry of Ontario for 1914, Ontario Bureau of Mines (Ont. Dept. Mines), Vol XXIV, pt. 1, pp. 9-13.

Hopkins, P.E., 1922, Schreiber-Duck Lake Area; Ontario Dept. Mines, Vol XXX, 1921, pt. 4, pp. 1-26.

Hudak, G.J., 1989, The Physical Volcanology and Hydrothermal Alteration Associated with the F-Group Archean Volcanogenic Massive Sulfide Deposit, Sturgeon Lake, Northwestern Ontario, unpublished MS. thesis, University of Minnesota-Duluth, Duluth, MN, 172p.

Irvine, T.N., and Baragar, W.R.A., 1971, A guide to the chemical classification of the common volcanic rocks. Can. Jour. Geology, 76: 485-488.

Jones, J.G., 1968, Pillow lava and pahoehoe. Jour. of Geol., 76: 485-488.

Jensen, L.S., 1976, A new cation plot for classifying subalkalic volcanic rocks: Ontario Geol Surv., Miscellaneous Paper 66, 22p.

Kappel, E.S., and Franklin, J.M., 1989, Relationships between geologic development of ridge crests and sulfide deposits in the northeast Pacific Ocean, Econ. Geol., 84:3, p. 485.

Koski, R.A., Shanks, W.C., Bohrson, W.A., and Oscarson, R.L., 1988, The composition of massive sulfide deposits from the sediment-covered floor of Escanaba trough, Gorda Ridge: Implications for depositional processes, Can. Mineral. 26, 655-673.

Larson, P.B., 1984, Geochemistry of the alteration pipe at the Bruce Cu-Zn volcanogenic massive sulfide deposit, Arizona, Econ., Geol., 79, p.1880-1896.

Large, R.R., 1992, Australian volcanic-hosted massive sulfide deposits: features, styles, and genetic models, Econ. Geol., 87: 3, p. 471.

Lydon, J.W., 1988, Ore deposit models #14. Volcanogenic massive sulphide deposits, part 2: genetic models. Geoscience Canada, 15:1, 43-65.

MacGeehan, P.J., 1977, The geochemistry of altered volcanic rocks at Matagami, Quebec: a geothermal model for massive sulphide genesis, Can. Jour. Earth Sci., 15, pp. 551-570.

Mattinen, P.R., 1978, Exploration possibilities in the Zenith Mine (Big Duck Lake) area, Schreiber, Ontario. Unpublished internal Corporation Falconbridge Copper report, April, 1978.

McKenzie, D., Nesbet, E., and Sclater, J.G., 1980, Sedimentary basin development in the Archean, Earth Planet. Sci. Letter, 48(1), 35-41.

Maniar and Piccoli, 1989, Tectonic discrimination of granitoids, Geol. Soc. of Amer. Bull., 101, pp.625-643.

Moore, J.M., 1975, Mechanism of formation of pillow lava. Amer. Jour. Sci., 63, pp 269-277.

Morrison, I.R., and Sim, R.C., 1989, Winston Lake project: exploration to mining, unpublished internal Minnova, Inc. report.

Morrison, I.R., 1991, pers. comm.

Morton, R.L., 1983, Lithology, stratigraphy and hydrothermal alteration in the Winston-Cleaver Lakes areaa, Ontario, A preliminary report, Winston Lake Project--PN 070, unpublished Corporation Falconbridge Copper report, November, 1983, 21p.

Morton, R.L., 1984, Lithology, stratigraphy, and hydrothermal alteration of volcanic rocks in the Winston-Cleaver Lakes area, Ontario; summary of work for Corporation Falconbridge Copper, unpublished company report.

Morton, R.L. and Franklin, J.M., 1987, Two-fold classification of Archean volcanic-associated massive sulfide deposits. Econ. Geol., 82, pp. 1057-1063.

Morton, R.L., Walker, J.S., Hudak, G.S., and Franklin, J.M., 1991, The early development of the Archean Submarine caldera complex with emphasis on the Mattabi ash-flow tuff and its relationship to the Mattabi massive sulfide deposit, Econ. Geol., 86, pp. 1002-1011.

Mottl, M.J., 1983, Metabasalts, axial hot springs, and the structure of hydrothermal systems at mid-ocean ridges, G.S.A. Bull., 94, 161-180.

Osterberg S.A., Morton, R.L., and Franklin, J.M., 1987, Hydrothermal alteration and physical volcanology of Archean rocks in the vicinity of the Headway-Coulee massive sulfide occurrence, Onaman area, Northwestern Ontario. Econ. Geol., 82, pp. 1505-1520.

Parry, S., and Hutchinson, R.W., 1981, Origin of a complex alteration assemblage, Four Corners Cu-Zn prospect, Quebec, Canada, Econ. Geol., 76, pp.1186-1201.

Pye, E.G., 1964, Mineral deposits of the Big Duck Lake area. Ontario Dept. Mines, Geological report number 27. Accompanied by map 2023 (colored), scale 1 inch to 1/4 mile, 47p.

Riverin, G., 1991, pers. comm.

Riverin, G., and Hodgson, C.J., 1980, Wall-rock alteration at the Millenbach Cu-Zn mine, Noranda, Quebec, Econ. Geol. 75, 424-444.

Roberts, R.G., and Reardon, E.J., 1978, Alteration and ore-forming processes at Mattagami Lake Mine, Quebec: Can. Jour. Earth Sci., 15, pp.1-21.

Sawkins, F.J., and Kowlik, J., 1981, The source of ore metals at Buchans: magmatic versas leaching models, in Swanson, E.A., Stropng, D.F., and Thurlow, J.G., eds., The Buchans Orebodies: Fifty years of Geology and Mining: Geol. Assoc. Can, Special Paper 22, p.255-267.

Schandl, E.S., and Gorton, M.P., 1991, Post ore mobilization of rare earth elements at Kidd Creek and other Archean massive sulfide deposits, Econ. Geol., 86, #7, pp.1546-1553.

Severin, P.W.A., 1979, Proposed exploration- Big Duck Lake area-Schreiber, Ontario, unpublished Corporation Falconbridge Copper report, February, 1979.

Severin, P.W.A., and Balint, F., 1985, Geological Setting of the Winston Lake Massive Sulphide Deposit, in McMillan, R.H. and Robinson, D.J., 1985, eds, Gold and copper-zinc metallogeny within metamorphosed greenstone terrain, Hemlo-Manitouwadge-Winston Lake Ontario, Canada, a joint publication of the Mineeral Deposits Division, Geological Association of Canada, and Geology Division, The Canadian Institute of Mining and Metallurgy.

Seyfried, W.E., Jr., 1984, Experimental basalt-solution interaction: alteration, heavy metal mobility and implications for the chemistry of ridge crest hydrothermal fluid. in Volcanic Rocks, Hydrothermal alteration, and associated massive sulfide and gold deposits. ed. by R.L. Morton and D.A. Groves. Short Course notes, Univ. of Minnesota-Duluth, 74-91.

Seyfried, W.E., 1987, Experimental and theoretical constraints on hydrothermal alteration processes at mid-ocean ridges: Ann. Rev. Earth Planet. Sci., 15, p.317-335.

Seyfried, W., and Bischoff, J.L., 1977, Hydrothermal transport of heavy metals by seawater: The role of seawater/basalt ratio, Earth Planet. Sci. Lett., 34, 71-77.

Seyfried and Mottl, 1982, Hydrothermal alteration of basalt by seawater under seawater-dominated conditions, Geochim. Cosmochim. Acta, 46, 985-1002.

Seyfried, W.E., Berndt, M.E., and Seewald, J.S., 1988, Hydrothermal alteration processes at mid-ocean ridges: Constraints from diabase alteration experiments, hot spring fluids and composition of the oceanic crust, Can. Mineral. 26, 787-804.

Sheridan, M.F., and Wohletz, R.H., 1981, Hydrovolcanic explosions: the systematics of water-pyroclast equilibration. Science, 212, pp.1387-1389.

Sim, R., 1991, pers. comm.

Sim, R., Balint, F., and Morrison, I.R., pers. comm.

Skirrow, R.G., 1987, Silicification in a semiconformable alteration zone below the Chisel Lake massive sulphide deposit, Manitoba, unpublished MSc. thesis, Carlton Univ., Ottawa, Ont.

Speakman, D.S., Chornoby, P.J., Haystead, B.C.W., and Holmes, G.F., 1982, Geology of the Ruttan Deposit, Northern Manitoba, in Precambrian Sulphide Deposits, H.S. Robinson Memorial Volume, eds. R.W. Hutchinson, C.D. Spence, and J.M. Franklin, G.A.C. Special Paper 25, 481-523.

Stanton, R.L., 1990, Magmatic evolution and the ore type; lava type affiliations of volcanic exhalative ores: in Geology of the mineral deposits of Australia and Papua New Guinea, ed. F.E. Hughes, Monograph series-Australasian Institute of Mining and Metallurgy, 14, pp.101-107.

Synder, G.L., and Fraser, G.D., 1963, Pillow lavas, I: intrusive layered lava pods and pillowed lavas, Unalaska Island, Alaska. A review of selected recent literature. In Shorter Contributions to General Geology, U.S.G.S. Professional Paper 454-B, 23p.

Thomas, D.A., 1991, The application of mineralogy, whole rock chemistry, and mineral chemistry to volcanogenic massive sulphide exploration at the Winston Lake Zn-Cu deposit, northwestern Ontario, unpublished MSc. thesis, Queen's Univ., Kingston, Ontario, 329p.

The Canadian Mining Review: various articles 1899; 1903; 1905.

Urabe, T., and Marumo, K., 1991, A new model for Kuroko-type deposits of Japan, Episodes, 14, #3, p.246.

Urabe, T., and Sato, T., 1978, Kuroko deposits of the Cosaka Mine, Northeast Honshy, Japan--Products of submarine hot springs in Miocene sea floor. Econ. Geol, 73, pp.161-179.

Von Damm, K.L., 1988, (Oak Ridge Natl. Lab., Environ. Sci. Div., Oak Ridge, TN, United States), Chemistry of submarine hydrothermal solutions from sediment covered ridge crests [abstr.] in Third chemical congress of North America, Abstracts of Paper, 3, GEOG 51, 1988. Meeting: June 5-10, 1988, Toronto, Ont., Canada.

Walford, P.C., and Franklin, J.M., 1982, The Anderson Lake Mine. Snow Lake, Manitoba. pp.481-523. in R.W. Hutchinson, C.D. Spence, and J.M. Franklin, editors, Precambrian Sulphide Deposits, H.S. Robinson Memorial Volume, Geol. Assoc. Can., Special Paper 25, 791p.

Whitford, D.J., 1989, McPherson, W.P.A., and Wallace, D.B., 1989, Geochemistry of the host rocks of the volcanogenic massive sulphide deposit at Que River, Tasmania, Econ. Geol., 84:1, p.1.

Winkler, H.G.F., 1979, Petrogenesis of Metamorphic Rocks, 5th edition, Springer-Verlag, New York, 348p.

Yardley, B.W.D., 1989, An Introduction to Metamorphic Petrology, John Wiley and Sons, Inc., New York, 248pp.

APPENDIX I.
MODAL MINERALOGY OF ROCK AND DRILL CORE SAMPLES

Table 10: Modal mineral estimates of rock and drill core samples.

Tables 11-16: Modal mineral ranges grouped by similar rocktypes, and alteration types.

Abbreviations

Mineral codes
QP=quartz phenocrysts, PP=plagioclase phenocrysts, QTZ=quartz, PL=plagioclase, KSP=potassium feldspar, HBL=hornblende, T/A=tremolite/actinolite, MUSC=muscovite/sericite, BIO=biotite, CHL=chlorite, EPI=epidote, GNT=garnet, AN/GD=anthophyllite/gedrite, CDT=cordierite, AND=andalusite, SIL=sillimanite, ST=staurolite, SP=spinel, OPA=opaques

Lithologic codes
-as listed on Tables 2 and 3 of text.

Rock categories	Lithologic Units
Mafic Rocks	LF, RGLF, MMF, WLH-FWF, WLH-MA
Volcaniclastic-sediments	PCC, SIV, RGSIV, CT
Felsic Lava Flows	QFP, QFF
Felsic Pyroclastic Units	CCLR, PCLR, CLR, RMCLR, SIV-FT

others

MW-XX	rock samples collected by Morton, 1983
WLO-XX	rock samples collected in this study
n	number of samples

Note
-blank spaces in Tables indicate no presence
-in Appendix I, entries of "0" indicate trace amounts
-all modal percents are visual estimates

Table 10.
Modal Mineral Estimates of Rock and Drill Core Samples

TYPE	SAMPLE	LOCATION	LITHUNIT	QP	PP	QTZ	PL	HBL	T/A	MUSC	BIO	CHL	EPI	GNT	AN/GD	CDT	SIL	ST	OPA	SPHE	APA	ZIR	PIN	OTHER
GO01	G1-232.2	440E, 430N	WLH-CRT			30	38					15	0						2					KSP: 15
GO01	G1-287.5	440E, 430N	RGLF(GES)			30	22			1	35	0		10					2			0		KSP: tr
GO01	G1-308	440E, 430N	LF		20		30	35				3	7						5					
GO01	G1-319.8	440E, 430N	LF		30	0	23	40				2	4						1					
GO01	G1-383	440E, 430N	QFP	10		30				13	15	0		10		20			2			1		
GO01	G1-420	440E, 430N	QFP	10	8	40	22			8	10			0					2			0		semiOPA: 2
GO01	G1-433	440E, 430N	QFP	12	13	30	22			0	10	10							3			0		CB: 0
GO01	G1-464	440E, 430N	QFP	7	2	28				15	20			7		20						1		CB: 0
GO01	G1-531	440E, 430N	FQP	1	9	30	30	10			15								1	4	0			
GO01	G1-531.5	440E, 430N	QFP	5		40				25	0	8		5				15	1					UNKNOWN:2 with fibrous habit
WL02	WL2-114	10300N, 9560E	LF			10					3	5			57	20			0				4	MONAZITE?: 1
WL02	WL2-169	10300N, 9560E	QFP			57	17					3		0		0	8	15	0			0	0	
WL06	8-253.5	7880N, 10210E	WLH-CRT			30	30		16		1	2		8	8				5		0			QTZ-PL difficult to distinguish
WL06	8-294.4	7880N, 10210E	WLH-CRT			35	37				21		1						3					FSP sericitized
WL06	8-393	7880N, 10210E	SIV-FT	10	5	30	31	10			8		3						2		1			
WL07	WL7-426.5	11260N, 9800E	QFF	7		45	5			2	12	0				5	7	0	0			0	17	
WL07	WL7-533	11260N, 9800E	QFP			50	2				20	3		2		16	0	5	1			1		
WL07	WL7-540	11260N, 9800E	QFP			44					25	0		5		14	5	5	0			1	1	
WL07	WL7-574	11260N, 9800E	LCS			35	0				14	0			30	15		0	2			0	4	
WL07	WL7-588	11260N, 9800E	LCS			30				0	10	3		32		10	2	6	3		0	1	3	
WL08	8-170	7750N, 10060E	WLH-CRT			30	35		5		22	3	3						2		0			
WL08	8-199	7750N, 10060E	WLH-CRT			32	35	15			15	1	0						2		0			
WL08	8-252	7750N, 10060E	CLR	3	0	47	40	5		0	4	0	0						2	1	0	1		HBL clots 5%
WL08	8-287.7	7750N, 10060E	SIV-FT	1		35	25	7			1		1						3	0	0			KSP: 25
WL08	8-348	7750N, 10060E	SIV-FT	4	1	34	32	5			20		1	6					2		0			some PL is poss. KSP
WL08	8-423	7750N, 10060E	SIV-FT	3	1	35	25	3					5						3	0				KSP: 24
WL08	8-506	7750N, 10060E	RGLF		20	0	20		20			28	15						2					
WL08	8-632	7750N, 10060E	RGQFP	10	2	30	28			12	5	7							3			0		CB:0; PL poss. partly CDT
WL08	8-671	7750N, 10060E	RGQFP	18	2	23	17			17	17	5		0					1			0		
WL10	WL10-233	9680N, 8660E	QFP			25	8			0	7	1			30	25		1	3		0	0	0	
WL10	WL10-252	9680N, 8660E	PCC			25	20		28	0	5	2	0	8					12					
WL10	WL10-263	9680N, 8660E	PCC			30	12			0	20	4		12	3	15		1	3					
WL10	WL10-293	9680N, 8660E	PCC			35	15	20		0	0	1	1	25					3		0			
WL10	WL10-349	9680N, 8660E	LCS			35	13			0	28	4				7	10	2	1				8	
WL10	WL10-380	9680N, 8660E	CCLR			35	25			0	20	2		5		7		1	2			0	3	
WL10	WL10-418	9680N, 8660E	CCLR			35				0	45	4				3			0			1	12	
WL10	WL10-436	9680N, 8660E	PCC			40	10			0	3				37	8		0	2				0	
WL10	WL10-509	9680N, 8660E	PCC			30	20		24	0	5	6	2	10					3					
WL14	14-563	11750N, 9940E	QFF	0		64				8	15	2				5	5		0			0	1	CB: 0
WL14	14-837	11750N, 9940E	QFP			40				4	17	2				23	8	2	0			0	4	
WL14	14-661.2	11750N, 9940E	LCS			4	0				12	3		55	10	8			3		0	1	4	
WL15	15-456	7900N, 10560E	WLH-CRT			27	32	20		5	5	4	5						2					UNKNOWN: 0, vfg, fibrous
WL15	15-483	7900N, 10560E	WLH-CRT			30	29			8	23	3	5						2		0	0		
WL15	15-548.2	7900N, 10560E	WLH-CRT			35	27	3		2	17	4	5						2	0	0			
WL15	15-577	7900N, 10560E	SIV-FT		1	39	39	4			6		2						1		0			HBL clots: 5%
WL15	15-651	7900N, 10560E	RGSIV	1	5	29	23	20		0	15								1	1		0		
WL15	15-741	7900N, 10560E	QFF	5	3	35	25			2	2								3			0		KSP: 25
WL15	15-768	7900N, 10560E	RGLF		25	4	30	35			2		3						1					

Table 10. (continued)

Modal Mineral Estimates of Rock and Drill Core Samples

TYPE	SAMPLE	LOCATION	LITHUNIT	QP	PP	QTZ	PL	HBL	T/A	MUSC	BIO	CHL	EPI	GNT	AN/GD	CDT	SIL	ST	OPA	SPHE	APA	ZIR	PIN	COMMENTS
WL15	15-786	7900N, 10560E	RGLF/CT?		5	5	34	50		0	2		4											CB 0
WL15	15-859	7900N, 10560E	RGQFP	8	7	36	25			2	5								2			0		KSP: 15; CB: 0
WL15	15-964	7900N, 10560E	RGQFP			45				15	17			13				10	0			0		
WL15	15-1024	7900N, 10560E	QFP	7		30				20	15	0		3		22			2			0		semiOPA: 1; CDT?, poss. is PL
WL16	WL18-318	9280N, 8400E	QFP	25		30	20			6	10	4					7		0		0	1	2	
WL18	WL16-344.5	9280N, 8400E	PCLR*			32	38	32		1	0		5	7					5					
WL16	WL16-423	9280N, 8400E	PCC			45				0	12	1		7			0	5	0			0	30	
WL18	WL18-459	9280N, 8400E	PCLR*			40	28			0	5	3		0	20				6					
WL18	WL18-518	9280N, 8400E	LCS			27				0	20	3		15		15	20	0	0			0		
WL16	WL16-568.5	9280N, 8400E	PCLR			30	29			3	30	4	2						2		0			
WL18	WL18-583.3	9280N, 8400E	PCLR			40	32	8		4	10	3	1						2		0			
WL17	WL17-570	12230N, 9850E	QFF			55	5			14	7	2				5	10		0			0	2	
WL17	WL17-58	12230N, 9850E	WLH-PERV			10	15		25		8	2			15	20			5		0	0	2	
WL17	WL17-583.5	12230N, 9850E	QFP	8		35	13			2	10	5				3	5		0			0	12	
WL17	WL17-618	12230N, 9850E	QFP	5		45	5			2	15	0				13	10		0			0	5	
WL17	WL17-845	12230N, 9850E	QFP			50	15			2	10	10	0			0			0			0	13	
WL17	WL17-881.5	12230N, 9850E	LCS			40	32			0	20	5	0						1					MONAZITE: 1; CB: 1
WL18	WL18-188.4	9160N, 8490E	QFP	5		40	25			0	15	0		5		0	4	1	0			0		
WL18	WL18-486	9160N, 8490E	PCC			28	20		20	3	0	7	0	20					2					
WL18	WL18-544	9160N, 8490E	PCLR*			40	18		25	0	10	5							3		0	1		
WL18	WL18-562	9160N, 8490E	PCC			30	14			0	6	9		30			0	0	1			0	12	
WL18	WL18-812	9160N, 8490E	PCC			35	30	2		1	15	7	0	7					3			0		
WL18	WL18-634.4	9160N, 8490E	PCC			30	20			0	6	1		32		4	4	1	2			0		
WL18	WL18-661	9160N, 8490E	PCC			25	13				13	1			35	5			2			0	6	
WL18	WL18-698	9160N, 8490E	PCLR			27	25			2	25	10	0						2			1		CB: 1
WL20	20-599	7750N, 10790E	RGCRT			30	35	26		1		0	1						7	0	0			CB: 0
WL20	20-619	7750N, 10790E	RGSH*			35	35	1			12								2		0			15% clot fragments: QTZ 15, BIO 45, HBL 40
WL20	20-628	7750N, 10790E	RGSH*			33	30	5		3	25	1	1						2		0			
WL21	21-108	7500N, 8840E	QFP			40	17			10	18	4				0	15		0			1		
WL21	21-425	7500N, 8840E	PCC			40	5			0	25	2		0		4	7	14					3	
WL21	21-492	7500N, 8840E	PCC			28	20			0	5	20	0	25		2			2			0		
WL21	21-560	7500N, 8840E	LCS			40	5			1	17	1				18	10	5	2			0	1	
WL21	21-567	7500N, 8840E	PCC			40	25		14	3		0		15					3		0	0		
WL21	21-619	7500N, 8840E	PCC			35	10			0	2	5		8	28	5			2				5	
WL21	21-650	7500N, 8840E	PCLR			15	15			1	48	15			0	0			3		0	2		CB: 1
WL25	25-1018	8900N, 9000E	PCC			29	0			0	8	5		10	40	0			3			0	5	
WL25	25-1055	8900N, 9000E	PCC			35	0			0	30	4			12	11		1	1			0	6	
WL25	25-1120	8900N, 9000E	PCLR*			27	32		8	2	25	2	0						4		0	0		
WL25	25-1133	8900N, 9000E	PCLR			27	25			2	17	5		3	14	0			5		0	0		CB: 2
WL25	25-152	8900N, 9000E	QFP	8		36	7			25	10	5		5					3			1		
WL25	25-286	8900N, 9000E	QFP	7		30	10			12	22	1		1		3	10		0			0		
WL25	25-809	8900N, 9000E	PCLR			20	19	25	5	1	8	0	0	8					4		0			
WL25	25-888	8900N, 9000E	PCC			26	25	2	5	2	30	0		8					2		0	0		
WL25	25-916	8900N, 9000E	PCLR	5		35	25	6		2	25	0	0						2					0
WL25	25-982	8900N, 9000E	PCC			50	3			5	6	3					28	1	4					
WL26	26-1084	8700N, 9120E	PCC			35	5			0	12	6			37	0			5		0	0		
WL26	26-1148.7	8700N, 9120E	PCC			32	30			1	23	1	0	10					3		0	0		
WL26	26-1250	8700N, 9120E	PCC			25	25				2	22		22	0				2		0	0		
WL26	26-1278	8700N, 9120E	PCC			30	10			0	7	4			25	20		2	2			0		
WL37	37-302	10800N, 10000E	CLR			40	23		20	0	13	0	0						4			1		
WL37	37-380	10800N, 10000E	QFF			50					10	3				17	7	5	5				2	MONAZITE/ZIR? 1

*protolith uncertain

Table 10. (continued)

Modal Mineral Estimates of Rock and Drill Core Samples

TYPE	SAMPLE	LOCATION	LITHUNIT	QP	PP	QTZ	PL	HBL	T/A	MUSC	BIO	CHL	EPI	GNT	AN/GD	CDT	SIL	ST	OPA	SPHE	APA	ZIR	PIN	COMMENTS
WL37	37-458	10800N, 10000E	QFF	5		50				8	20	0				8	6	3	0			0	2	
WL37	37-506.7	10800N, 10000E	QFF	5		40	13				20	0				15	0		0			1	5	AND: 1
WL36	38-546.2	10800N, 10300E	CLR*			10					15	3			34	33		3	1				1	MONAZITE 0
WL38	38-587	10800N, 10300E	QFF*			57					15	3				14	0	7	2			1	1	
WL38	38-604	10800N, 10300E	QFF*			70					8	0					8	0	2		0	0	7	
WL38	38-708.8	10800N, 10300E	QFF	5		35	30				24	1				2			0			0	3	
WL41	WL41-210	10800N, 9770E	CLR			50	25			10	7	0				0	8		0					
WL41	WL41-333	10800N, 9770E	QFF	5		45				7	15					8	20		0			0	0	
WL41	WL41-387	10800N, 9770E	QFP	8		58				5	15	2					12		0			0		
WL41	WL41-529	10800N, 9770E	PCC			35	25		27	0	2	0	0	8					3		0			
WL41	WL41-555	10800N, 9770E	PCC			35					13	1		20	5	15		5	4			1	1	
WL41	WL41-589	10800N, 9770E	CCLR*			30	21				7	5			25	10			1		0	0	1	
WL44	44-544.2	12800N, 9940E	CLR			50	8			0	7	7				7			1			0	22	
WL44	44-555.4	12800N, 9940E	QFF			65				25	0	7		3			0		3			0		
WL44	44-580	12800N, 9940E	QFF	5		55	10			3	15	7				0	4		0			0	1	
WL47	47-135	9300N, 8630E	QFP			38				35	0	22					0		1			0		
WL47	47-422	9300N, 8630E	PCC			30	25		25	2		4	2	10					2		0			
WL47	47-457	9300N, 8630E	PCC			30	5			0	20	10		5	12	3			2			0	13	
WL47	47-503.5	9300N, 8630E	PCC			40	26			0	13	2		15		1			3		0	0		
WL47	47-566	9300N, 8630E	LCS			25	5			0	8	0			30	25		2	1			0	6	
WL47	47-598.2	9300N, 8630E	PCLR*			36	30			0	8	0		20	3	0			5		0	0		
WL47	47-818	9300N, 8630E	PCC			25	20			0	5	15			24	5		1	2			0	3	
WL47	47-651	9300N, 8630E	PCLR			35	12			0	10	0			30	10		1	2			0		
WL47	47-684	9300N, 8630E	PCLR			25	30			2	15	5			8				15		0	0		AN/GD??
WL48	46-140	9340N, 8600E	QFP			45	5			3	22	4				7	10		0			1	3	
WL48	48-333	9340N, 8600E	QFP	10		30	27			7	20	5							0			1		
WL48	48-362	9340N, 8600E	PCLR*			35	25	27		0	1		0	10					2		0			
WL48	48-433	9340N, 8600E	PCLR/PCC*			28	20			0	10	2	0	25	15				2		0	0		
WL48	48-451	9340N, 8600E	PCC			45				0	15	4		17		7	8	2	1			0	3	
WL48	48-484	9340N, 8600E	PCC			40	25			0	3	14	0	15	0				2		1			
WL48	48-577	9340N, 8600E	PCLR			35	35			0	20	5	0						5		0	1		
WL50	50-344	10400N, 10070E	CLR			35	5				20	5				30		3	2			0		
WL50	50-363	10400N, 10070E	CLR			26	5					60		3	0				1					MONAZITE? :5
WL50	50-378	10400N, 10070E	CLR	5		50	20			5	8	0				0	12	0	0		0	0		
WL50	50-467	10400N, 10070E	QFF			60	7				10					10	10	0	0			0	3	
WL50	50-517	10400N, 10070E	QFP/CT*			65					15			0			7	10	0			0		
WL50	50-570	10400N, 10070E	QFP	0		7					10	10		12	10	40		5	0			1	5	
WL50	50-588	10400N, 10070E	QFP	5		52				0	24	0				7	10	2	0			1	4	
WL50	50-731	10400N, 10070E	PCC			25	24	25	7	2	8	0	0	8					3		0			
WL50	50-778.4	10400N, 10070E	PCC			32	25			1	8	5	1	25					5			0		
WL50	50-803.9	10400N, 10070E	CCLR			60					24	5				6			1		0	0	4	
WL50	50-886	10400N, 10070E	PCC			27	35		7	0	15		0	5					6		0	0		
WL51	51-320	10600N, 9990E	CLR	5		40	10				13	5				10	5	0	2			0	10	
WL51	51-431	10600N, 9990E	QFF	5		40	9			7	20	2				8	7	0	0			0	4	
WL51	51-494	10600N, 9990E	QFP	8		43	0			8	20						20		0			1		
WL52	52-502.6	10800N, 10190E	CLR			25	20		26	0	25	1	0						3			0		
WL52	52-661	10600N, 10190E	LF			2						3			37	45		2	4				4	PHLOGOPITE?: 3
WL52	52-685	10600N, 10190E	QFP	8		50	25			0	17	0	0						0			0		
WL54	54-560	11400N, 10100E	CLR			45	0		20	8	0	1	2			20			2		0	0	2	
WL54	54-570.2	11400N, 10100E	CLR			49	0				15	5				4	8	10	4			1	6	

*protolith uncertain

Table 10. (continued)

Modal Mineral Estimates of Rock and Drill Core Samples

TYPE	SAMPLE	LOCATION	LITHUNIT	QP	PP	QTZ	PL	HBL	T/A	MUSC	BIO	CHL	EPI	GNT	AN/GD	CDT	SIL	ST	OPA	SPHE	APA	ZIR	PIN	COMMENTS
WL54	54-671	11400N, 10100E	QFF			50	8			7	0	13				0	2		0			0	20	
WL54	54-721	11400N, 10100E	QFP	5		45				5	18	1				5	20		0			2	1	
WL55	55-668	11700N, 10140E	CLR			50					18	2				2	5	0	5			0	18	CB: 0
WL55	55-712	11700N, 10140E	QFF*	5		60	0			8	12	3				4	5		0			0	5	
WL55	55-806	11700N, 10140E	QFP	7		40				0	20	0				18	10	0	0			1	8	
WL55	55-815	11700N, 10140E	PCC			37	0				8	5		0	25	15		5	3		0	0	2	
WL55	55-857	11700N, 10140E	LCS			40					10	5			18	10		1	2		0	0	1	
WL55	55-877	11700N, 10140E	LCS			44	5			10	8	2		7	5	7		2	2		0	0	8	CB: 0
WL55	55-889	11700N, 10140E	LCS			30	18			0	30	3			5	7		0	3		0			MONAZITE: 4
WL57	57-1004	12700N, 10220E	QFP	5		35	40			2		12	1	0					2			0		CB: 3
WL57	57-1064	12700N, 10220E	PCC			35	28			2	20	8	0			2			0				1	MONAZITE: 1; CB: 5
WL57	57-905	12700N, 10220E	QFF			50				0	30	5			5	0			0		0	0	10	PIN OR SER???
WL57	57-923	12700N, 10220E	QFF			50	8				12	5				18	2		0			0	5	
WL57	57-982	12700N, 10220E	QFF			38	30			2	20	4	0			5			0				0	MONAZITE?: 1
WL57	57-989	12700N, 10220E	QFP			50				2	20	0				11	13	1	0		0	0	3	
WL59	59-371	9250N, 8770E	LCS			35					20	3		8	10	7		1	3				13	
WL59	59-391	9250N, 8770E	PCLR*			40	37		0	1	10	2	0	7					2		1	0		
WL59	59-398	9250N, 8770E	PCC			27	27		20	0	8	2	0	15					3			0		
WL59	59-422	9250N, 8770E	LCS			30	25			0	34	4	0	8					1			0		
WL59	59-439.5	9250N, 8770E	LCS-ALTD			50					15	2		10		5	5	3	2			1	7	
WL59	59-468	9250N, 8770E	PCC			50				7	24	2				8	8	0	0			1		
WL59	59-502	9250N, 8770E	PCC			27	27			0	8	3		0	25	1		0	2			0	4	CB: 0
WL59	59-612	9250N, 8770E	PCLR			20	59			1	12	3	1						3					CB:1
ZO25A	25A-444.2	10100N, 10170E	WLH-FWF			0					5	5			35	40			4				8	MONAZITE: 5
ZO25A	25A-451	10100N, 10170E	WLH-FWF									66			8	10			5				2	PHLOG: 4, MONAZITE: 5
ZO25A	25A-456	10100N, 10170E	CLR	5		35	35			0	20	5				0			0			0	0	
ZO36A	36A-1037	9950N, 10300E	CCLR			50	35		8	0	5								2			0		some AMPH poss. AN/GD??
ZO36A	36A-506	9950N, 10300E	WLH-FWF			0						35			30	8			2				1	MONAZITE? 2; PHLOG: 22
ZO36A	36A-548	9950N, 10300E	MMF*			8					8	8			35	30		0	4				5	MONAZITE: 2; PHLOG/BIO ??
ZO36A	36A-576	9950N, 10300E	QFF			30					20	8			12	15		0	3			2	10	
ZO36A	36A-587	9950N, 10300E	QFF	8		53				5	15	2				10	5		0			0	2	
ZO36A	36A-944.5	9950N, 10300E	PCC			28	24	25	15	0	0		0	7					1					
ZO36A	36A-957	9950N, 10300E	LCS			35	30	0		2	20	2	0	8					2		0	0		CB: 2
ZO36A	36A-971	9950N, 10300E	PCC			30	12		13	0	18	8	0	20	2				1			1		
ZO36A	36A-988	9950N, 10300E	LCS			35	25		1	8	5	8	0	15					3		0	0		
ZO36A	36A-999	9950N, 10300E	LCS			35	8				20	2				25		4	0			1	3	
ZO01	1-198.55	9900N, 10000E	WLH-CRT			10	40	30				10	8						3	1				
ZO01	1-202.8	9900N, 10000E	WLH-MA				45	13			45								3	4	0			
ZO01	1-218.55	9900N, 10000E	CLR			35	45				10	8	1						3					
ZO01	1-240.75	9900N, 10000E	CLR			5	8				40	20			5	0			2				20	
ZO01	1-244.8	9900N, 10000E	CLR			5	10				77	5	1		0				2		0			retrograded AN/GD??
ZO01	1-257.7	9900N, 10000E	CLR			43					20	8			8	0		7	3					AND: 8
ZO01	1-272.7	9900N, 10000E	CLR			52	10			5	9	0					13	8	2			0	1	
ZO01	1-284.5	9900N, 10000E	MMF			5	29	50		0	10								8		0			
ZO01	1-290.5	9900N, 10000E	QFF	7		47	40			0	8		0						0					
ZO02	2-100.8	9710N, 9840E	WLH-CRT			31	31	8			15	5	5						2	3				
ZO02	2-104.5	9710N, 9840E	WLH-MA				37	40			2	8	8						5		0			CB: tr
ZO02	2-105.5	9710N, 9840E	WLH-CRT			34	35	15				4							2	5	0			
ZO02	2-110.65	9710N, 9840E	WLH-MA				30	31				5	3						2	4				
ZO02	2-149.9	9710N, 9840E	CLR			34	39	7			8	8	1						3	2				CB: 1
ZO03	3-183.5	9970N, 9980E	WLH-CRT			7	50	10				8	23						3	1				CB: tr

*protolith uncertain

Table 10. (continued)

Modal Mineral Estimates of Rock and Drill Core Samples

TYPE	SAMPLE	LOCATION	LITHUNIT	QP	PP	QTZ	PL	HBL	T/A	MUSC	BIO	CHL	EPI	GNT	AN/GD	CDT	SIL	ST	OPA	SPHE	APA	ZIR	PIN	COMMENTS
ZO03	3-184.2	9970N, 9980E	WLH-CRT*			5	85	5			0	15	8						3	1				
ZO03	3-188.9	9970N, 9980E	WLH-CRT			0	56	20				4	0						4		1			
ZO03	3-188.35	9970N, 9980E	WLH-MA				40	41			10	3	2						4					
ZO03	3-192.9	9970N, 9980E	WLH-MA			7	40	40				5	1							6	1			
ZO03	3-207.3	9970N, 9980E	CLR	0		32	25				22	4				4			4		0	2		
ZO04	4-273	9850N, 10000E	CLR			40	15			5	7	24	2						7			0		
ZO04	4-283	9850N, 10000E	CLR			55	5			1	15	0				13	4		0			0	7	
ZO04	4-294.7	9850N, 10000E	CLR/QFF*			0					33	33				10			3			1	3	SP: 15; SPH: 2
ZO04	4-335	9850N, 10000E	QFF	7		60	18			3	7						5		0			0		
ZO07	7-411	9810N, 10170E	WLH-PERV									8			58	0			4				30	
ZO07	7-428.5	9810N, 10170E	CLR			2					5	73				0			4			1	15	possibly retrograded AN/GD??
ZO07	7-440	9810N, 10170E	CLR	7		35	25			2	25	5							1			0		
ZO07	7-475	9810N, 10170E	QFF			18					4	60				3			0			0	12	CHL serpentine/amph??
ZO09	9-563	9900N, 10320E	WLH-MA			0						8			60	15			2			0	5	PHLOG: 15
ZO09	9-570	9900N, 10320E	CLR	5	2	40	40			2	10	0	0						1			0		CB: 0
ZO09	9-574.7	9900N, 10320E	CLR*			3					35	35			6	15			1		0	0	5	
ZO09	9-591	9900N, 10320E	CLR*			5					12	10			30	36			2		0	0	5	ZIR/MONAZITE? 0
ZO09	9-628.2	9900N, 10320E	QFF			30					10	22			20	15		0	2			1		ZIR/MONAZITE 1
ZO15	Z15-706	10150N, 10460E	CLR								15	10			20	46			4			0	5	
ZO15	Z15-738	10150N, 10460E	CLR/QFF*			50	25					2				5	13	0	0			0	5	AND: tr
ZO15	Z15-783	10150N, 10460E	QFF			40					20	10			12	13		0	3			0	2	
ZO18	18-751	10400N, 10530E	CLR*			35	30			0	23	10					0		0			1		SPH:1; CB: 1; SIL ??
ZO16	18-800	10400N, 10530E	QFF			20					9	30			25	10			1			2	3	
ZO16	18-805	10400N, 10530E	QFF*	5		34	20			0	10	1				10	10	5	0			0	5	
ZO17	17-681	10000N, 10430E	WLH-FWF									51			15	20			2			0	4	PHLOG: 8
ZO17	17-708.3	10000N, 10430E	CLR			5					2				45	45			3			0		
ZO17	17-724	10000N, 10430E	CLR*			17					2	0			40	35			3		0		3	
ZO17	17-743.8	10000N, 10430E	MMF*			8					4	48			6	30			2			1	4	SPH: 0
ZO17	17-754	10000N, 10430E	QFF			54				10	15						15		0			1		
ZO18	18-645	10150N, 10460E	WLH-FWF									43			20	5			15					SP: 15; MONAZITE: 2
ZO18	18-862	10150N, 10460E	CLR	5		50	17			0	25	3							0			0		
ZO18	18-879	10150N, 10460E	QFF*			60					10	5				18	5		0			0	2	
ZO18	18-697	10150N, 10460E	QFF*			33	5			4	20	15				20			0			0	3	
ZO18	18-704	10150N, 10460E	QFF*			65	20			3	0					5	7		0			0		
ZO18	18-784.7	10150N, 10460E	QFF	4		60	10			5	13					0	8		0			0		
ZO19	19-884.1	10400N, 10530E	MMF*			5	7			8	52	10	2		2			5	6		1			MON:2; PL/CDT ??; SER/PIN ??
ZO19	19-702.4	10400N, 10530E	QFF			55					23	5				15	0		0			0	2	
ZO23	23-393	10000N, 10170E	WLH-CRT			30	20			5	21	9	2						1			1		partially retro'd AN/GD-T/A??
ZO23	23-412	10000N, 10170E	CLR			50	42			1	7	0	0						0			0		SPH: 0 ??
ZO23	23-421	10000N, 10170E	CLR*			5	53			5	30	0	0						3					MONAZITE: 4; PIN ??
ZO23	23-425	10000N, 10170E	MMF*			10					7	5			30	46		0	2			0	2	
ZO23	23-454	10000N, 10170E	QFF			45	7			0	15	2				25			0			0	3	
ZO23	23-465	10000N, 10170E	QFF			45					5	35			7	8			0			0	0	CB: 0; SPH: 0
ZO27	27-658	10400N, 10490E	CLR			34	30		15	0	20		0						1			0		
ZO27	27-682	10400N, 10490E	MMF*			0					35	7				45			3				6	MONAZITE: 4
ZO27	27-735	10400N, 10490E	QFF*			35	25			0	15	20	0			5			0			0	0	
ZO32	32-469	10400N, 10260E	CLR	5		50	12			0	8	2			13	7		0	2			0	1	
ZO32	32-514	10400N, 10260E	MMF			2					24	5			20	40		3	4				1	BIO OR PHLOG?
ZO32	32-543.3	10400N, 10260E	QFF			52				2	15					20	8		1		0	0	3	SPH??: 0
ZO34	34-925	9860N, 10700E	CLR	8	7	39	30	1		2	4	3	2						4			0		

*protolith uncertain

Table 10. (continued)

Modal Mineral Estimates of Rock and Drill Core Samples

TYPE	SAMPLE	LOCATION	LITHUNIT	QP	PP	QTZ	PL	HBL	T/A	MUSC	BIO	CHL	EPI	GNT	AN/GD	CDT	SIL	ST	OPA	SPHE	APA	ZIR	PIN	COMMENTS
ZO34	34-939	9860N, 10700E	SIV-VC			40	32	10		0	15		0						3	0	0			SP: tr
ZO34	34-975	9860N, 10700E	QFF			41	10			0	35	1				1			0			0	12	
ZO34	34-984.2	9860N, 10700E	QFF			35					25			7		0	0	30	3			0		
ZO41	41-474.2	'9700N, 10130E	WLH-CRT				60	14			17	0							8	2	1			CB: tr
ZO41	41-498.6	'9700N, 10130E	WLH-MA				48	45			5		0						0	4				
ZO41	41-500.8	'9700N, 10130E	CLR	2	3	36	37	5			13	1							2	1				
ZO41	41-511	'9700N, 10130E	CLR		5	35	40	7			10		1						2	0				
ZO41	41-511	'9700N, 10130E	CLR	3	0	35	37	8			10		3						4		0	0		
ZO58	58-481.6	8200N, 10530E	WLH-CRT			36	36	25											2		0			
ZO58	58-512	8200N, 10530E	WLH-CRT*			25	28	25				3	15						4		0			
ZO58	58-612	8200N, 10530E	SIV-VC	8		32	15	25			20		0						0		0			
ZO56	58-645.4	8200N, 10530E	SIV-VC*	2		30				5	20		0	30					1		0	0		
ZO61	61-457.5	8500N, 10300E	WLH-CRT			30	30	32		0		0							7		1			CB: 0
ZO61	61-458.2	8500N, 10300E	WLH-CRT			50	24	20		0		0	1						5		0			CB: 0
ZO61	61-476.2	8500N, 10300E	WLH-CRT			35	30	24		0		5	0						8	0	0			
ZO61	61-480.9	8500N, 10300E	WLH-MA			7	41	40				4	5						3	0				
ZO61	61-465	8500N, 10300E	WLH-CRT			35	35	20			4	3	0						3		0			
ZO61	61-467.8	8500N, 10300E	WLH-CRT			47	40	0				4	4						4		0			
ZO61	61-499	8500N, 10300E	WLH-CRT			35	41	7				5	8						4	0				
ZO61	61-499.5	8500N, 10300E	WLH-CRT			30	28	20				5	15						2					
ZO61	61-518	8500N, 10300E	CLR*	2	3	45	35	8			6								1		0			
ZO61	61-562.2	8500N, 10300E	SIV-VC	6	3	40	25				25											0		1% CLOTS of BIO 80%; QTZ 20%
ZO61	61-675	8500N, 10300E	QFF	6	5	40	40	2			5								2			0		
ZO61	61-812.8	8500N, 10300E	LF		50	5	20	21					3						0	1				
ZO61	61-819	8500N, 10300E	LF		5		38	45		2			9						0	1				
ZO66	66-464.45	9100N, 10270E	WLH-CRT			7	55	25				2	7						2	2	0			CB: tr
ZO68	66-467.95	9100N, 10270E	WLH-CRT			20	48	25					5						1	3	0			CB: tr
ZO66	66-473.7	9100N, 10270E	WLH-MA				52	40					0						2	8	0			
ZO66	66-479.5	9100N, 10270E	WLH-CRT			38	37	15				0	4						6	1	0			
ZO68	66-480.8	9100N, 10270E	WLH-CRT				55	40				0							5		0			
ZO66	66-485.1	9100N, 10270E	WLH-MA				50	44				1							1	4				CB: tr
ZO68	66-571.9	9100N, 10270E	MMF			1	49	43				1							1	5				
ZO66	66-571.9	9100N, 10270E	MMF				45	45											0	5				
ZO67	67-747.1	9100N, 10670E	WLH-CRT			30	44	7				5	10						3	1	0			
ZO67	67-751.45	9100N, 10670E	WLH-MA*				43	40					5						5	2	0			CDT: tr?
ZO67	67-753.55	9100N, 10670E	WLH-CRT			38	38	15					4						3	2	0			
ZO67	67-760.25	9100N, 10670E	WLH-MA			5	47	45		0			0						3	0				
ZO67	67-807.7	9100N, 10670E	CLR/SIV*	10	15	27	28	10	10		10								2		0			UNKNOWN AMPH
ZO67	67-865.15	9100N, 10670E	MMF			5	31	50											4	0				
MW-	1	10175N, 9650E	QFF	10		54				2	12	2			5	15			0			0		
MW-	2	10170N, 9470E	LF		5	2	30			5		5	8						2		0	0		rel fresh except T/A=45% after HBL
MW-	3	10160N, 9475E	LF			32					0			5	40	20		0	3				0	
MW-	4	10200N, 9390E	QFP	10		46				0	25	0				7	10	1	0			1		CDT??
MW-	5	10150N, 9310E	QFP	8	7	37	30			2	12	3	1						0			0		
MW-	6	10150N, 9240E	QFP	15	13	25	24			5	15	1	1						0			1		
MW-	7	10250N, 8900E	QFP	20	10	29	28			2	7	5	0						0			0		CB: 1
MW-	8	10200N, 8910E	QFP	8	7	35	30				15	5	0						0			1		
MW-	9	10250N, 8900E	PCC			30	28		25	2	3	1	0	8					3		0	0		
MW-	10	10020N, 9250E	QFP	15	10	32	32			1	8	0	0						1			1		
MW-	11	9750N, 9030E	QFP	5		45				13	17	5				5	10		0		0	0		

*protolith uncertain

Table 10. (continued)

Modal Mineral Estimates of Rock and Drill Core Samples

TYPE	SAMPLE	LOCATION	LITHUNIT	QP	PP	QTZ	PL	HBL	T/A	MUSC	BIO	CHL	EPI	GNT	AN/GD	CDT	SIL	ST	OPA	SPHE	APA	ZIR	PIN	COMMENTS
MW-	12	9720N, 9030E	CT	7		35	35			8	12	3							0			0		
MW-	13	9580N, 9100E	QFP	10		40				15	12	5					18		0			0		UNKNOWN: 0-ZIR?
MW-	14	9580N, 9120E	QFP	12	8	34	30			4	10	1	0						0			1		
MW-	15	9940N, 9625E	QFF	1		60				3	18	0				13			0			0		
MW-	16	9950N, 9660E	QFF	15		40				12	7	8				15	7		0		0	0		
MW-	17	10050N, 9475E	QFP	10	4	35	24			3	22	1							0			1		
MW-	18	10050N, 9465E	LF		0	0	0	0		0		0	0						0	0	0			qtz-amygdules:2
MW-	19	10075N, 9440E	QFP	10		29	25			1	20	8	2						2			0		
MW-	20	10050N, 9475E	QFP	10	5	30	25			5	20	2	2						0			1		abun. GNT on otc
MW-	23	10000N, 9525E	LF			2	40		48										20					
MW-	24	10120N, 9480E	QFP	10	5	28	25			4	15	4	4						0			0		
MW-	26	9470N, 8680E	QFP	15		41	5			15	10	8				0	7		0			1		
MW-	28	9480N, 8640E	QFP	15		44				20	12					0	8		0			1		
MW-	29	9350N, 8660E	QFP	5		38	28			15	17	0		3		0			0		0	0		1% UNKNOWN: equant, high relief, clear
MW-	31	9200N, 8750E	QFP	10		40	0			7	15	5		8		5	10		0			0		
MW-	32	9150N, 8790E	QFP	15		30	20			10	3	18	3	0					1					
MW-	33	9400N, 8900E	QFP	15		28				7	15	4				8	5	15	0		0	0		CDT partially retrograded??
MW-	34	9600N, 9550E	LF		5	3	39	34		5	2	1	5						4		1			rel fresh MA fsp
MW-	35	9800N, 9610E	QFF	10	0	35	30			5	20								0			0		
MW-	36	9700N, 9600E	QFF	5	12	30	30			2	20	0	0						1			0		
MW-	38	9000N, 9166E	QFP	5		38	30			5	10	0				1	10		1					PL, CDT ID uncertain
MW-	39	9400N, 8600E	QFP	0	0	0	0				8	0	0						0					
MW-	41	9700N, 8960E	QFP	15		37				8	20	5				0	13		0			2		
MW-	43	9700N, 8940E	QFP	10	5	34	30			2	10	2	1	4					2			0		
MW-	44	9670N, 8800E	QFP	15	0	30	30			2	12	5	0	5					1			0		
MW-	45	9250N, 8810E	QFP	10		30	17			15	12	4		5			7		0			0		tr. UNKNOWN: clear, blocky, low biref
MW-	46	9120N, 8960E	QFP	10		38				15	20					5	12		0			0		CDT ID uncertain
MW-	47	8750N, 8960E	QFP	10	1	31	30			15	13	0	0						0			0		
MW-	48	8870N, 9060E	QFP	10		25	23			26	5	3	1	5					0					CB: 2
MW-	49	8900N, 9170E	QFP	15	5	30	29			5	7	3		3					2			1		
MW-	50	10130N, 9660E	QFF			60				5	12	5	0			16	1		1			0		
MW-	52	10110N, 9480E	LF			10	7			2	4	7			35	31			4					
MW-	53	10100N, 9470E	LF			8		38		7		10	30						3		0			CB: 8
MW-	54	10100N, 9470E	LF		5	5	18	25	40	0			5						2		0			
MW-	55	10100N, 9470E	LF		5	5	44	45		0			0						1		0			
MW-	56	10050N, 9545E	LF			2	0			3	10	15			25	30			3		2	0		
MW-	57	10050N, 9545E	LF			5	5	40	33	10		0	2						5					
MW-	58	10120N, 9460E	QFP	10		35	15			4	9	2				7	12	8	0			0		
MW-	59	10120N, 9460E	QFP			60	12			2	7	1		8				3	8			1		QTZ/PL % uncertain
MW-	60	10120N, 9460E	QFP	7		25	25			4	25	5	1	3		3		1	0			1		
MW-	61	10120N, 9460E	CT	10		29				6	10	30		1		5	8	1	0			0		
MW-	62	10120N, 9340E	QFP	8	7	30	28			5	1	20	1						0			0		
MW-	63	10300N, 9360E	QFP	8		32	15			10	10	3	0	1		5	15		0			0		
MW-	64	10270N, 9360E	QFP	5		35				8	16	5				5	12	12	0			2		some gnt on otc
MW-	65	10300N, 9360E	QFP	8		45				0	25	0		5			13	3	1			0		
MW-	66	10275N, 9475E	LF			7	12	40	15	3		7	8						8		0			
MW-	67	10275N, 9475E	LF			1				5	15	5			53	15		4	2			0		
MW-	68	10280N, 9460E	LF		40	7	18	20		3		3	5						4		0	0		
MW-	69	10320N, 9445E	QFF			40				10	5	7			15	14		8	1			0		protolith uncertain
MW-	70	10245N, 9620E	QFF	5		35	7			7	15	8				10	15	0	0			0		

*protolith uncertain

Table 10. (continued)

Modal Mineral Estimates of Rock and Drill Core Samples

TYPE	SAMPLE	LOCATION	LITHUNIT	QP	PP	QTZ	PL	HBL	T/A	MUSC	BIO	CHL	EPI	GNT	AN/GD	CDT	SIL	ST	OPA	SPHE	APA	ZIR	PIN	COMMENTS
MW-	71	10330N, 9720E	CLR	5	1	45	15	5			20	6							2			1		
MW-	72	10400N, 9720E	CLR	0		0	0	0											0					FRESH CLR
MW-	73	10350N, 9525E	LF							2	5	7			40	41			5					some gnt on otc
MW-	74	10320N, 9525E	LF			7				0	2	3		35	35	10		4	4					
MW-	75	10330N, 9435E	LF			8	2				2	6		7	58	12		0	5					
MW-	76	10330N, 9435E	CT			50	7					3		5	30			3	2					PROB NOT MAFIC
MW-	77	10450N, 8850E	LCS	20		26	27			1	20	5	0						1					
MW-	78	10420N, 9410E	QFP	7		13				13	20	2		5		3	10		1			1		
MW-	79	10420N, 9430E	CT	10		45				5	12	2		7		1	10	8	0			0		
MW-	80	10420N, 9450E	CT			23	5			5		2		30	25	2		8	2					
MW-	81	10410N, 9450E	MA SILL		10	3	15	7	55	2		1	5						2		0			poss. HBL
MW-	82	10400N, 9720E	CLR			0	0	0		0									0					QP-QTZ-PL-HBL-
MW-	83	10520N, 8450E	QFF	5		20				2	13	7			2	45		5	0			1		
MW-	85	10425N, 9460E	MA			7				2	5	1			40	43			2		0			
MW-	87	10600N, 9460E	QFF	5		50				2	15	10			7	10			0		0	1		
MW-	88	10525N, 9515E	QFF	10		46	0			3	10	8			6	10		6	1			0		
MW-	89	10600N, 9370E	QFP	5		44	5			5	15	3		8		2	10	6	1			1		
MW-	90	10520N, 8950E	QFP			52				1	20	1		5		0	5	15	0			1		
MW-	91	10530N, 9340E	QFP	15	5	35	30			1	3	10							1			0		
MW-	92	10530N, 9000E	PCC			35	22	10	25		6								3					
MW-	94	10600N, 8970E	LCS			34	25			2		2	1	5					3					3% UNKNOWN: chl-like mineral in veinlets
MW-	95	10610N, 9410E	LF			10				2	0	5		8	42	30			3					
MW-	97	10670N, 9420E	LF			5				1	3	6		5	40	38		0	2		0			
MW-	98	10670N, 9430E	LF			5				2	0	5		7	45	34		0	2		0			
MW-	99	10620N, 9470E	CLR			25				2	10	5			16	40			2			0		
MW-	100	10720N, 9400E	QFP			50				0					34	15			1					
MW-	101	10720N, 9407E	LF			24				0	5	4			25	30		8	3		0			
MW-	102	10775N, 9450E	QFF	3		55	9			0	8	0				15	10	0	0		0	0		
MW-	103	10720N, 9280E	QFP	7	8	34	34			2	15	0							0			0		
MW-	105	10710N, 9050E	QFP	10	1	34	30			0	18	2		5					0		0	0		
MW-	107	10800N, 9060E	QFP	10		35	15			5	12	7				5		8	0		0	0		UNKNOWN: 3; retrograde of CDT
MW-	108	10800N, 9425E	LF			35				2	0	2		5	34	7		4	2		0	0		
MW-	110	10800N, 9510E	QFP/CT/QFF?	6		40	26			7	10	3					6		0			0		
MW-	111	10920N, 9560E	CLR	5		35	13			10	15	10				10			2			0		
MW-	112	10950N, 9420E	QFF	8		35				2	15	1				36	2		1			0		
MW-	113	10930N, 9280E	QFP	8	5	34	34			8	4	6	1						0					
MW-	114	10920N, 9360E	QFP*			30				6	20	5		6		27		5	1			0		
MW-	115	10950N, 9385E	LF*			5				0	3	7			52	30			3		0			
MW-	118	10950N, 9390E	LF							2	25	3			63			4	3		0	0		
MW-	120	11150N, 9560E	CLR			42	41	1		1	0	2	5						1			0		7% FRAGS: PL:65, HBL: 25, QTZ:2, EPI:5, CHL: 3
MW-	121	11125N, 9450E	QFF	7		40				15	13	5				10	10		0			0		
MW-	122	11250N, 9340E	QFP	15		40	33			8	9	2				6	7		0			0		
MW-	123	11220N, 9350E	LF							3	10	4			68	10		2	3					
MW-	124	11320N, 9350E	LF*			3	15			3	4		5		66				3		1			
MW-	125	11400N, 9330E	QFP	7		50	16			2	15	10	0						0			0		
MW-	126	11400N, 9350E	LF			10				3	4	4			55	20			4		0			
MW-	127	11430N, 9340E	QFF			47				15	15	15				5	2		0			1		SIL?, CDT?
MW-	128	11530N, 9490E	CLR			34	34	15		0	2	2	2						1		0	0		10% FRAGS: QTZ:34, PL:50, HBL:36, SER:tr, BIO
MW-	129	11600N, 9000E	LCS*	7		39	30			5		10	3						1			0		CB: 0
MW-	130	11600N, 89703	LCS	1		32	30			0	4	3		15	15				4		0	0		

*protolith uncertain

Table 10. (continued)

Modal Mineral Estimates of Rock and Drill Core Samples

TYPE	SAMPLE	LOCATION	LITHUNIT	QP	PP	QTZ	PL	HBL	T/A	MUSC	BIO	CHL	EPI	GNT	AN/GD	CDT	SIL	ST	OPA	SPHE	APA	ZIR	PIN	COMMENTS
MW-	131	10550N, 8980E	LCS	1		50				20		25		2					2		0	0		
MW-	132	11600N, 9050E	LCS			25				5	11	1		27		18	4	7	2		0	0		
MW-	134	11500N, 9375E	QFP	5		30				4	25	5				12	7	12	0			0		
MW-	135	11600N, 9335E	LF*			7		43	10	20			15						5					
MW-	136	11600N, 9335E	LF			5				1	0				55	30		5	4					
MW-	138	11610N, 9290E	QFF/QFP*	5		60	10			1	15					0	8		1			0		
MW-	139	11740N, 9430E	CLR			40	40	9		0	0	1	3						2		0	0		5% FRAGS: PL:50, QTZ:20, HBL:20, OPA:5, EPI: 5
MW-	141	10075N, 8660E	QFP	15		31	30			2	12	8	1						1			0		
MW-	142	10075N, 8830E	QFP	15		32	30			2	2	15	1						3		0	0		CB: 0
MW-	143	10100N, 8510E	PCC	0		35	25	5	22	3	0	1		7					2					
MW-	144	10275N, 9620E	QFF	3		51	30			1	12	2				0			0			1		
MW-	145	10210N, 9530E	QFF*	2		50	13			3	20			2		5	4	1	0			0		
MW-	146	10280N, 9525E	QFF	8		50	12			2	10	5			2	10			0			0		
MW-	147	10300N, 9530E	LF		5	0	20			5		0	3						2					T/A: 65
MW-	148	10290N, 9690E	CLR	5	2	40	21	8		1	12	1	3						2					FRAGS: 5 HBL,PL
MW-	149	10320N, 9650E	QFF			35				2	13	3			16	30		1	2		0	0		
MW-	150	9850N, 9635E	QFF	5		54				7	8	1				10	15	0	0			0		st?
MW-	151	9915N, 9725E	QFF	7		38	35			2	10	5	2						0			1		
MW-	152	9915N, 9725E	QFF			50	12			17	8	12				0			1			0		CDT: ??
MW-	153	9915N, 9725E	QFF*			8	2			32	7	40				8			2			1		
MW-	154	9940N, 9750E	CLR	10		37	37			0	15	0							1			0		
MW-	156	9940N, 9750E	CLR	7	2	45	18	7		1	0		5						4		0	0		FRAGS: 5, CLOTS
MW-	157	9940N, 9750E	CLR	5	2	40	32				4	6	2						4	3				KSP: 2
MW-	158	10150N, 9700E	CLR/QFF?			21	1			1	20	0		15	5	25		5	3			0		SP: 5
MW-	159	10320N, 9660E	QFF*			40				1	15	3			19	22								
MW-	161	10320N, 9700E	QFF*			45	13			2	20	2				22	13		2		0	1		
MW-	163	9750N, 9700E	QFF	4	0	40	5			30	0	15	5						1		0	0		
MW-	171	8130N, 9700E	CLR/SIV?	1		40	34	0		0	15	0	0						2			0		CLOT FRAGS: 3
MW-	175	8650N, 9650E	QFF	7	5	30	28			1	20	5	2						2					
MW-	176	8650N, 9650E	SIV	7	3	45	43			0	20		0						2			0		
MW-	178	9650N, 9660E	CLR	5	4	40	38			2	8	0	1						2			0		
MW-	180	9900N, 9650E	QFF			65	10			4	8	1				5	6		0			0		
MW-	181	9900N, 9650E	QFF	7		52				5	15	3				5	8		0		0	0		
MW-	182	9900N, 9650E	QFF	0		0				0	0					0	0		0		0	0		
MW-	183	9900N, 9650E	QFF	0		0				0	0	0				0	0		0		0	0		
MW-	184	10250N, 9540E	QFF*			21				3	15	8			22	25		3	1			2		
MW-	200	10100N, 9690E	CLR	2		25	5			1	25	2				25	12	3	0			0		
MW-	201	10100N, 9700E	MMF			5				2	17	5			30	38			3		0	0		
MW-	202	10200N, 9700E	QFF*			43				0	8	7		5	7	10		17	3			0		
MW-	203	10100N, 9680E	QFF			15				0	1	1		10	62	10		0	3			0		
MW-	204	10200N, 9720E	QFF*			20				5	17	5		28		8		15	2			0		
MW-	205	10270N, 9720E	QFF	2		35	34			2	15	5				6			1			0		
MW-	206	10350N, 9750E	CLR	3		40	8			1	20	1				25			2			0		
MW-	207	10350N, 9660E	GB?			10	41	41		1		1	4						2		0			
MW-	208	10280N, 9710E	CLR*	5		38	35	7		0	3	2	3						2		0	0		FRAGS: 5
MW-	209	10450N, 9670E	CLR			35	34	10		0	17	2	0						2		0	0		
MW-	210	10450N, 9650E	GB SILL																					QTZ-PL-HBL...
MW-	211	10450N, 9690E	QFF*	5		30	25	0		5	5	25	4						1			0		
MW-	212	10480N, 9680E	QFF			39	30			0	30	0	0						1			0		
MW-	213	10400N, 9710E	CLR*	5		39	35	8		0	3	5	3						3			0		

*protolith uncertain

Table 10. (continued)

Modal Mineral Estimates of Rock and Drill Core Samples

TYPE	SAMPLE	LOCATION	LITHUNIT	QP	PP	QTZ	PL	HBL	T/A	MUSC	BIO	CHL	EPI	GNT	AN/GD	CDT	SIL	ST	OPA	SPHE	APA	ZIR	PIN	COMMENTS
MW-	214	10525N, 9640E	QFF			39	30			3	25	2	0						1		0	0		
MW-	215	10530N, 9660E	GB SILL						90															QTZ-PL-HBL
MW-	216	10325N, 9625E	GB?			0	25		54			10	3						8					
MW-	217	10525N, 9550E	QFF	10		39	35			2	8	5	0						1			0		
MW-	218	10650N, 9650E	QFF	15		30	30			5	20	0	0						0			0		
MW-	219	10650N, 9575E	QFF			38	35			0	28						0		0			1		
MW-	220	10650N, 9580E	QFF	8		37	30			15	0		0						2			0		
MW-	221	10660N, 9615E	CLR			35	34			0	20	6	3						2		0	0		
MW-	222	10720N, 9550E	QFF*			25				0	25	3				23	2	20	2			0		
MW-	223	10730N, 9600E	QFF			40				30	15	10						3	2			0		
MW-	224	10730N, 9650E	GB?		8	5	49	30		0		0	5						3					
MW-	225	10800N, 9550E	QFF	2		40	35			3	13	4							1			0		
MW-	226	10800N, 9570E	QFF*			10				3	25	8			27	25			2		0	0		
MW-	228	10800N, 9325E	QFP	10		35	35			1	10	7	1						1			0		
MW-	229	10900N, 9580E	QFF*	5		40	30			5	7	5				6			2			0		
MW-	230	10900N, 9580E	QFF			50	13			2	10	3				12	8		2		0	0		
MW-	231	11000N, 9525E	QFF*			40	32			2	20	5	0			0			1			0		
MW-	232	11025N, 9560E	CLR			41	40	12		0	0	1	2						4		0	0		
MW-	233	11025N, 9575E	CLR			38	38	20		0	3	0	0						5		0	0		
MW-	234	11025N, 9450E	QFF			63				12	16					1	8							
MW-	235	11020N, 9275E	QFP			50					17	10				5		3	0			0	15	
MW-	236	12025N, 9420E	QFF*	5		52	15			10	10	4				3			1			0		
MW-	237	12025N, 9420E	GB			5	15	75		1									4		0			
MW-	238	11200N, 9550E	CLR			37	30	3		0		2	1						2	1	0			25% FRAGS: HBL,PL,EPI,QTZ,OPA
MW-	239	11200N, 9550E	CLR			35	35	20		0			2						6	2	0			
MW-	243	11400N, 9370E	QFF	10		40	32			1	15	2							0			0		
MW-	244	11400N, 9520E	CLR			38	36	17		0	1	1	2						3		0	0		
MW-	245	11500N, 9495E	CLR			37	37	20		0	0	3	0						3		0	0		
MW-	246	11500N, 9520E	CLR			35	34	15		0	2	2	3						4		0	0		
MW-	247	11500N, 9435E	QFF			35	9			0	25	7				10			1		0	0	10	
MW-	248	11500N, 9320E	QFP	20		55	18			5	0	20							2			0		
MW-	249	11500N, 9325E	QFP	6		45	12			20	3	10	0						2			0		
MW-	250	11500N, 9375E	QFF			35	5			25	20	5					10		0			0		
MW-	251	11600N, 9420E	QFF			40	34			3	10	12							1			0		
MW-	252	11600N, 9470E	CLR	5	0	43	30	10		0		3	5						0		0	0		
MW-	253	11600N, 9310E	QFP	15		34	20			1	8	15	3						1			0		
MW-	254	11600N, 9200E	QFP	5		45	15			15	8	10				2			0		0	0		
MW-	255	11700N, 9225E	QFP	7		35	5			7	15	7		3		13	0	13	0			0		
MW-	257	11700N, 9430E	CLR			45	35	8		0		3	4						1	4	0	0		
MW-	258	11700N, 9375E	CLR	3		37	20			1	25	5				8			1		0	0		
MW-	259	11700N, 9385E	QFF	12		35	20			13	4	7				0	8		1					
MW-	260	11815N, 9455E	CLR	5		40	39	7		1	0	3	3						3	0	0	0		
MW-	261	111815N, 9440E	CLR			40	46					7	3						3			1		
MW-	262	11805N, 9155E	QFP			50				15	15	6		3		3	3	4	0			1		
MW-	104A	10720N, 9100E	QFP			62									30	7			1		0			
MW-	1A	10175N, 9650E	QFF/CLR?	6	3	35	35	5		2	5	2	2						1	4	0	0		KSP: 2
MW-	7A	10250N, 8900E	LCS	10		33	30			1	15	5				5			0			1		
MW-	57A	10050N, 9480E	LF		5	7	8		75	1									4					
MW-	161A	9900N, 9750E	MMF*			8	7		35	40	4	3							3		0			
MW-	232A	11025N, 9560E	CLR			38	37	15		0	0	0	4						4	2				

*protolith uncertain

Table 10. (continued)

Modal Mineral Estimates of Rock and Drill Core Samples

TYPE	SAMPLE	LOCATION	LITHUNIT	QP	PP	QTZ	PL	HBL	T/A	MUSC	BIO	CHL	EPI	GNT	AN/GD	CDT	SIL	ST	OPA	SPHE	APA	ZIR	PIN	COMMENTS
MW-	261A	11810N, 9290E	QFP	20		50	12			0	13	4				1			0		0	0		
WLO-	2	9000N, 9640E	SIV-VC			30	35	20		3		5	5						2		0			UNKNOWN tr
WLO-	6	9250N, 6775E	WLH-CRT				80	18				1	0						3	0	0			
WLO-	7	9250N, 6775E	WLH-CRT				75	18			4	0							1	2				
WLO-	8	9250N, 6775E	WLH-CRT				83	15				0								2	0			
WLO-	10	8950N,9575E	MMF				50	43			0	7							0	0				
WLO-	15	9180N, 9675E	CLR*	5		45	22	5					1						2	5				KSP: 15
WLO-	16	9198N, 9603E	MMF				50	44				0							1		0			poss. amygdules
WLO-	17	9219N, 9700E	WLH-MA			0	34	50				8	1						7	0	0			
WLO-	18	9219N, 9700E	WLH-CRT			30	40	15			7	1							5	2	0			
WLO-	19	9219N, 9700E	WLH-CRT			8	48	35				3							1	5	0			
WLO-	20	9219N, 9700E	WLH-MA*				42	45			5		2						3	2	1			
WLO-	26	L9600-9700N	CLR			30	34	5					25								3			
WLO-	28	9682N, 9302E	WLH-MA				50	41			3								1	5	0			
WLO-	35	9181N, 9690E	WLH-CRT			5	78	9				5	0						2	1	0			
WLO-	36	9181N, 9690E	WLH-CRT			7	67	20				3							3	0	0			KSP: tr
WLO-	37	9703N, 9155E	GB			1	39	52					5						3					
WLO-	38	9703N, 9155E	WLH-CRT*			0	35	40				15	2						3	5				
WLO-	39	9703N, 9155E	WLH-MA*			1	45	45			3	1	1						3	1	0			
WLO-	40	9703N, 9155E	WLH-CRT			45	44	0				6							4		1			
WLO-	41	9703N, 9155E	WLH-CRT				67	30											0	3	0			
WLO-	42	9703N, 9155E	WLH-CRT			25	32	30				6							3	3	1			
WLO-	43	9154N, 9683E	WLH-CRT			30	45	12			4	2	1						2	1	0			KSP: 3
WLO-	44	9140N, 9695E	WLH-MA*				42	42			1	5	1						1	7	1			
WLO-	46	9651N, 9786E	GB				43	50					4						3					
WLO-	47	9651N, 9766E	WLH-CRT			5	50	55				6							1	2				FIBROUS MIN: 1
WLO-	48	9651N, 9766E	WLH-MA*				42	40					3						4	3	0			
WLO-	50	9651N, 9766E	WLH-CRT				43	40				8	10						3	6				
WLO-	51	9651N, 9766E	WLH-CRT			38	40	12					5						2	3				
WLO-	57	9650N, 9740E	WLH-MA				42	40			2	10	1						1	4				
WLO-	58	9630N, 9715E	CLR	7		45	42	3				1	1	3						5				
WLO-	60	9800N, 9765E	CLR	5	1	47	37				7	1							2					
WLO-	61	9910N, 9770E	WLH-MA				40	40			9	2	1						3	5				
WLO-	62	9800N, 9765E	WLH-CRT			28	45	15			7	0	1						0	4				
WLO-	63	9800N, 9785E	WLH-CRT			50	37	2				6	0						4	1	0			
WLO-	64	9930N, 9770E	WLH-MA				48	42			0	1	0						1	6	0			
WLO-	65	9930N, 9770E	WLH-CRT				59	35				2							1	3				
WLO-	66	9930N, 9770E	WLH-MA				41	44				1	1						2	9	2			
WLO-	67	9930N, 9770E	WLH-CRT			1	54	35				4	0						3	2				NEEDLY GRS. 1%
WLO-	68	9930N, 9770E	WLH-CRT				89	12				3	1						4	6	3			
WLO-	69	9930N, 9770E	GB			2	45	50				1							2					
WLO-	70	9910N, 9725E	MMF			15	40	34	4			4	0						3	0	0			
WLO-	72	9910N, 9725E	MMF			10	39		45										6					
WLO-	73	9910N, 9725E	MMF			15	15		28			2	10			15			5				10	CDT,PL % ??
WLO-	76	9950N, 9730E	CLR			28	25			8	25	1	0			5		7	3		0	0		
WLO-	77	9950N, 9750E	CLR			30	20	8			0	24	5						2	3				
WLO-	79	9975N, 9715E	ALT CLR			20	28				25	3			6			7	2	1				ST??
WLO-	99	10250N, 9730E	CLR	5		35	45		7		3	0	2						2		1			
WLO-	100	10260N, 9740E	WLH-MA				40	45				7	2						2	4				

*protolith uncertain

Table 10. (continued)

Modal Mineral Estimates of Rock and Drill Core Samples

TYPE	SAMPLE	LOCATION	LITHUNIT	QP	PP	QTZ	PL	HBL	T/A	MUSC	BIO	CHL	EPI	GNT	AN/GD	CDT	SIL	ST	OPA	SPHE	APA	ZIR	PIN	COMMENTS
WLO-	103	10340N, 9722E	WLH-CRT			40	40	15				1	0						2	2	0			
WLO-	104	10340N, 9725E	WLH-CRT				65	31				1	1						0	2	0			
WLO-	105	10340N, 9726E	WLH-CRT			35	35	16				3	5						8					
WLO-	106	10300N,9728E	GB		2		46	47					0						3	2	0			PP glomerocrysts
WLO-	108	10280N, 9730E	WLH-CRT			39	39	12				3	2						5	0	0			
WLO-	109	10280N, 9730E	WLH-CRT*				30	50				7	8						5					
WLO-	111	10480N, 9680E	QFF/CLR?			30	33	15			20								2					
WLO-	114	11250N,9500E	CLR			40	43	8				5							2	2	2			CLOT FRAG: hbl:37, pl:48, qtz:5, epi:5, sphe:3, opa:2
WLO-	115	11500N, 9600E	CLR	2	23	21	37	0				1	1						1		0			
WLO-	116	11510N, 9463E	CLR			39	55	3				2	0						1		0			CLOT FRAG: hbl:50, pl:35, opa:5, epi:4, qtz:5, chl:1
WLO-	118	11565N, 9470E	CLR			30	54	3			5	1	0						8		0			
WLO-	119	11570N, 9475E	CLR			40	45	7			2	1	1						3		0			CB tr
WLO-	120	11570N, 9475E	CLR			25	57	5			4		0						4	5	0			
WLO-	122	8700N, 9625E	MMF																					abun. EPI-CHL grunge: poss. hyaloclastite??
WLO-	123	8600N, 9550E	QFF	15	15	39	27			1	3		0						0					
WLO-	129	9800N, 9542E	LF*				5		83			30							2					
WLO-	132	9740N, 9542E	QFF	4	1	45	37				15		3						0					
WLO-	136	9980N, 9630E	QFF*			60				13	17					2	7		1					
WLO-	140	10040N, 9660E	QFF*	3		20		40		5	15		5			10			5			0		some CDT could be PL; QTZ-EP-CDT
WLO-	145	10050N, 9760E	CLR			38	32			4	25	0	0						1	0				
WLO-	147	10100N, 9730E	CLR			45	38				15	0							2	0		0		
WLO-	148	10050N, 9760E	CLR			43	39				15	2	0						1	0		0		
WLO-	151	10210N, 9710E	QFF/CLR*			58				0					40	0		0	2			0		
WLO-	154	10040N, 9560E	LF				0		80			19							1					
WLO-	155	10040N, 9500E	LF				10		79		7		2						2					
WLO-	156	10045N, 9550E	QFF			55					17		0			10	10		0		0		8	
WLO-	157	10096N, 9467E	LF		0	20	20	56					0						2					QTZ/PL % very uncertain
WLO-	158	10097N, 9467E	LF				35		53	0	8		1						3			0		ZIR very uncertain
WLO-	159	10097N, 9467E	LF				7				7				41	40			5					PL % uncertain
WLO-	165	10108N, 9488E	LF			5	5	85					3						2					
WLO-	167	10198N, 9493E	LF		0	6	7	70		0			15						2					
WLO-	168	10198N, 9493E	LF			7						2			53	35		0	3					
WLO-	171	10234N, 9500E	LF		30	0	10	58											2					
WLO-	176	10293N, 9516E	LF									2			45	51			2					
WLO-	177	10305N, 9501E	CT?			20					5	3		13	50	5			4			0		
WLO-	179	10312N, 9491E	LF			29				3		7		25	28			4	4			0		
WLO-	180	10335N, 9483E	LF		5	6			54		6	2	25						2					
WLO-	181	10348N, 9478E	LF		15	5	17	15	30				15						3					
WLO-	188	10600N, 9600E	CLR			35	30			5	25	3	0						2		0	0		
WLO-	189	11035N, 9565E	CLR			46	50	2			0	0	1						1		0			CLOT FRAG: qtz:35, pl:50, hbl:5, chl:4, epi:2, opa:1
WLO-	190	10960N, 9550E	CLR			35	25			5	20	3	0			10			2					
WLO-	191	10800N, 9580E	QFF*			7	10			0	20	3	0		43	15			2			0		
WLO-	196	10415N, 9705E	CLR	3		42	50	2				1	0						2	0	0			CLOT FRAGS: pl:30, hbl:50, epi:10, opa:5, chl:3, qtz:
WLO-	199	10525N, 9520E	QFF			42				15	25	4				3	10		1			0		
WLO-	200	10575N, 9575E	QFF	5	1	33	33			15	10		0				3		0		0	0		
WLO-	202	10800N, 9530E	QFF			29	5			17	22	5	0			10	11		1					
WLO-	204	10270N, 9680E	QFF	3		64	0			5	10					10	7		1		0	0		
WLO-	205	10270N, 9680E	QFF	5		66					9	1		3	2	3		8	2			1		perhaps 40% of 66% QTZ is CDT
WLO-	216	9905N, 9510E	LF			6	15	75					2						2					
WLO-	218	9900N, 9525E	LF								5	15			30	47			3					

*protolith uncertain

Table 10. (continued)

Modal Mineral Estimates of Rock and Drill Core Samples

TYPE	SAMPLE	LOCATION	LITHUNIT	QP	PP	QTZ	PL	HBL	T/A	MUSC	BIO	CHL	EPI	GNT	AN/GD	CDT	SIL	ST	OPA	SPHE	APA	ZIR	PIN	COMMENTS
WLO-	222	8800N, 9225E	LF		20	5	35	58			1	0							1					
WLO-	226	11550N, 9425E	CLR			5	58	30			1	1	4						1					MA/GB FRAGMENT IN CLR
WLO-	227	11555N, 9455E	CLR			49	47	2											1		1			(1) fragment present: qtz:10, plag:45, hbl:35, opa:5, e
WLO-	234	10254N, 9496E	LF			7	10	60	5	3			10						5					
WLO-	235	10255N, 9396E	LF							10		10			27	40			3				10	
WLO-	239	10102N, 9493E	LF			12	5					10	88						5					spilitized? otc
WLO-	243	10060N, 9770E	CLR			20					12	2			5	54		2	3			0	2	protolith uncertain
WLO-	244	10050N, 9700E	CLR			45	5				30	2	2			5	7		1		1		0	
WLO-	247	10050N, 9760E	WLH-MA*			5	35				30	5			9				4	1			11	
WLO-	248	310E, 250N	GR	2	5	33	33	6			12	3	1						1	2	0			KSP: 2
WLO-	250	310E, 1070N	RGLF			5	50	40			0		2						3					
WLO-	259	235E, 1600N	RGSIV			10			25	4	15	11	4			25			4			0	2	
WLO-	264	305E, 2008N	RGSIV			25						20		40					2			0	13	
WLO-	265	250E, 2020N	RGSIV			20					7	45		10		8			2				10	
WLO-	267	2055E, 2035N	RGSH			25					5	38		5	3				15			0		SP: 11
WLO-	270	1850E, 9650N	SIV-VC	5		37	30	8			7		1	10					2		0			
WLO-	273	8075N, 9710E	SIV-VC	7		55	20	2			15					0			1			0		
WLO-	276	8060N, 9680E	SIV-VC	2		42	45	0			10	2	0			0			1		0	0		5% FRAGS: HBL 40, QTZ 60
WLO-	282	8120N, 9805E	CLR	3	0	40	49	2		0	1	1	3						1					
WLO-	284	8100N, 9830E	WLH-MA			7	44	44					3						1	1	0			
WLO-	287	8080N, 9830E	WLH-CRT			42	42	6			1	5								0				
WLO-	288	8090N, 9840E	WLH-MA			3	45	45					1						4	0				
WLO-	304	7980N, 9880E	WLH-CRT			30	37					25	2						4			0		2% UNKNOWN: clear, high relief v. low birefringence
WLO-	308	8000N, 9930E	WLH-CRT			35	25	25				0	0						15					tr. UNKNOWN: clear, high relief, v. low birefringence
WLO-	314	7870N, 9830E	WLH-CRT			40	32				13	12	0						3					
WLO-	321	7900N, 9740E	WLH-MA			0	40	46		5		1	2						1	5				
WLO-	328	7865N, 9700E	WLH-MA			10	44	35			7	1	3							0	0			
WLO-	335	7800N, 9670E	WLH-CRT			33	33				20	3	0						4		0			
WLO-	345	7790N, 9780E	WLH-CRT			45	35				3	12	2						3	0				
WLO-	366	430E, 060N	RGLF(GES)			6	50	40			3		2						1					
WLO-	373	410E, 1060N	RGSIV			28					22	5		35		3		0	2			0	10	SP: tr
WLO-	376	390E, 1080N	RGSIV			25			22	25			10	15					3					
WLO-	377	375E, 1085N	RGSIV			25					15	8		20		7		7	6			0	8	SP: 6
WLO-	385	602E, 1800N	RGSIV/FD?		1	43	42	12					0						2					
WLO-	391	1320S, 0095W	RGSIV			5					28				30	35			4					FIBROUS MIN: 0
WLO-	396	1365S, 1160W	RGSIV			20	29	40				0	3						8	0				
WLO-	409	1430S, 1140W	RGSIV			5			20	7	18	8		25		12						0	7	SP: 5
WLO-	413	1520S, 1130W	RGLF			13					22			35		20		3	2				5	SP: tr
WLO-	417	1610S, 1000W	RGLF			5					15	1			40	35		0	2				2	
WLO-	421	1550S, 1130W	RGLF			10	10		30	5	22	5	5						2					CB: 1
WLO-	422	1575S, 1400W	RGSIV*	8	2	35	33			0	12	1	0	7					2			0		
WLO-	424	1650S, 0050W	RGLF			5			15		17	3		25	25	25			5					
WLO-	429	1690S, 1080W	RGSIV/LF?			5					15	10	3		20	35			2				10	
WLO-	439	1750S, 1025W	RGLF			5	5	72				1	10						8					
WLO-	442	1975S, 980W	RGQFP			40		3	28	5	10			8					3					
WLO-	443	2000S, 1000W	RGLF		25			57		15	0								3					
WLO-	449	'1820S, 935W	RGQFP			8				0	20	2		8	5			15	1	0		0		
WLO-	452	1565S, 995W	RGLF			3	45	50		0									2					
WLO-	453	1400S, 1100W	RGLF			27	14		25		7	3				14			5				5	
WLO-	455	1330S, 1060W	RGSIV			7				5	12	5	8		28	30			5					

*protolith uncertain

Table 10. (continued)

Modal Mineral Estimates of Rock and Drill Core Samples

TYPE	SAMPLE	LOCATION	LITHUNIT	QP	PP	QTZ	PL	HBL	T/A	MUSC	BIO	CHL	EPI	GNT	AN/GD	CDT	SIL	ST	OPA	SPHE	APA	ZIR	PIN	COMMENTS
WLO-	456	1300S, 1040W	RGLF		2	17	18	40			0		3						2					
WLO-	463	1309S, 1130W	RGSIV			20					15	13			25	25			5			0	7	
WLO-	468	1310S, 1105W	RMCLR	4	3	22	26			2	17	1	0								0	0		KSP: 25
WLO-	476	1700S, 2160W	RMGB			2	45		52	0			0						1					
WLO-	478	8020N, 9280E	RMGB			0	47		50	1			2						0					
WLO-	479	8080N, 9200E	RMGB				45		47	3			4						1					
WLO-	481	9950N, 8510E	QFP*			37					10	5			35	10			3					
WLO-	482	9950N, 8490E	LCS			32				0	10	1		13	17	23		1	3					
WLO-	484	9950N, 8455E	PCC			33	32	15		2	3	2	3	5					5		0			
WLO-	485	9950N, 8412E	CCLR			35	30			0	8	2	0	12	10				3		0	0		
WLO-	488	9950N, 8360E	CCLR			36	35			0	3	2		12	10				2		0			
WLO-	489	9950N, 8290E	CCLR			32	31				5	4	0	6	15	2		0	2			0	3	
WLO-	501	9950N, 8180E	CCLR			30	10			0	15	2		5	1	22		2	3		0	0	4	2% altn of CDT??
WLO-	502	10010N, 8130E	LCS			25	2	25		8		0	7	20					15					
WLO-	504	9960N, 8130E	LCS			34	33		7	3	15	0	3						5		0	0		
WLO-	510	10300N, 8510E	LCS			35	35			2	25	0	2						0			1		
WLO-	513	10300N, 8580E	CCLR			32	20			0	5	3			10	25		1	3		0	0	1	
WLO-	514	10300N, 8550E	CCLR			25	3			0	15	5			15	22		0	1		0	0	4	
WLO-	516	10300N, 8640E	LCS			31	5			0	12	2		3	10	31		2	1		0	0	3	tr altn of CDT??
WLO-	517	10300N, 8645E	LCS			62	7			0	5	3	0	8	13				2		0	0		
WLO-	518	10300N, 8655E	LCS			33	2				15	3		2	0	25		10	2		0	0	5	8% UNKNOWN altn of CDT??
WLO-	520	10300N, 8790E	LCS			40	3			0	17	4		8	8	15			0	0	0		3	2% UNKNOWN altn of CDT??
WLO-	521	10300N, 8865E	PCC			40	34		13	0			0	10					3		0			AMPHIBOLE: 13
WLO-	523	10300N, 8930E	PCC			30	30		4	1		3	3	13					3		0			
WLO-	524	10300N, 8980E	QFP	8	5	35	35			1	15								1					
WLO-	527	10900N, 8770E	CCLR			42	42			0	15	0	0	0					1		0	0		tr UNKNOWN altn of CDT??
WLO-	529	10900N, 8820E	LCS			34	34			1	2	4	0		15	5		0	2		1		2	1% UNKNOWN altn of CDT??
WLO-	532	10900N, 8990E	LCS			45				5	14	4		10			12	8	2		0	0		UNKNOWN: 0
WLO-	533	10900N, 9033E	PCC			33	32	12	12	0	3	0	0	5					2		0			
WLO-	535	11600N, 8800E	LCS			25	27				30	3		5		2		2	1		0	0	5	
WLO-	536	11600N, 8830E	PCC	0		30	30	7		3	18	0	0	6					6		0			
WLO-	538	11600N, 8860E	LCS			39	39			0	10		0		10				2			0		
WLO-	539	11600N, 8960E	LCS	2		35				20	7	3		7		19	7		0			0		
WLO-	540	11600N, 8950E	LCS			28	10	3	25	20	7	2							3					
WLO-	542	11600N, 9000E	LCS			58				6	5	5		12					4				16	GNT-SILICA *deceased rock*
WLO-	543	11600N, 9070E	LCS			29	5			0	15	3		25		2	1	8	3		0	0	9	
WLO-	545	11600N, 9100E	PCC			35	35	12	1	1	2	1	2	7					4		0			
WLO-	547	12000N, 8850E	LCS			29	15				15	2	0	20		5	1	3	2		0	0	2	
WLO-	558	12900N, 9030E	LCS			10	40	40			4	3	1						4	2	0			
WLO-	562	12900N, 9050E	CCLR			45	45	8				0							2		0	0		10% CLOT FRAGS: stretched, HBL 80, QTZ 5, PL 5,
WLO-	565	12900N, 9090E	PCC			27		25		27		2	10	7					2		0	0		
WLO-	567	12600N, 9100E	CCLR	0		35	29	21		6		0	2						3		0			
WLO-	568	12600N, 9030E	LCS			35	35			1	10	6	3	4					6					
WLO-	571	12200N, 8995E	CCLR			45	45	7	1										2			0		
WLO-	572	12150N, 8985E	LCS			41	41			0	15	0	0						2		0	1		
WLO-	574	12150N, 8985E	CCLR			42	40	9		0	5	1							2		0	0		CLOT FRAGMENT
WLO-	575	12200N, 9020E	PCC			42	41				10	3			1				3		0	0		
WLO-	578	12100N, 8965E	LCS	1		37	36			1	15	8	0						2		0	0		tr UNKNOWN: AMPH??
WLO-	579	12100N, 8965E	LCS			40					4	4		44		5			3		0	0		
WLO-	581	12100N, 8965E	CCLR			37	37			1	5	3			15				2		0	0		

*protolith uncertain

Table 10. (continued)

Modal Mineral Estimates of Rock and Drill Core Samples

TYPE	SAMPLE	LOCATION	LITHUNIT	QP	PP	QTZ	PL	HBL	T/A	MUSC BIO	CHL	EPI	GNT	AN/GD	CDT	SIL	ST	OPA	SPHE	APA	ZIR	PIN	COMMENTS
WLO-	583	8200N, 9245E	LF		25	2	8	35			10	20						2					
WLO-	597	8450N, 9000E	RGLF		30	2	10	53				3						2					
WLO-	609	9260N, 9600E	CLR	2	2	43	42	0		5								3					3% clot frags
WLO-	610	9260N, 9600E	CLR			10	10	75				0						5					HBL altn veinlets--brickwork
WLO-	611	9260N, 9600E	SIV-VC			36	35	6		20								3					
WLO-	612	9260N, 9600E	CLR	3	2	40	35	10		6		0						4		0	0		
WLO-	613	8280N, 9590E	QFF	3	3	40	25			1 7		0						0		0			KSP: 21
WLO-	615	8040N, 9590E	SIV-VC			6	45	40		7		0						0	0				
WLO-	617	8080N, 9580E	SIV-VC			5	5	65				5						3			4		PYX? :13
WLO-	621	8080N, 9610E	SIV-VC	5		40	30			20		0	5						0				poss. relic lithic frags.
WLO-	641	8700N, 8625E	MMF			9	23	22				6						0	1	0			extensive sericitization of PL
WLO-	642	8700N, 8625E	SIV-VC	7	7	31	30	20		0	0	1						3		1			CB tr
WLO-	644	8760N, 9675E	CLR	5	0	35	49	0		7		1						2					1% lithic frags: bio-hbl
WLO-	646	8900N, 9625E	SIV-VC	7	4	24	25			17		0						3		0			
WLO-	650	8900N, 9625E	SIV-VC			21	30	40		8	2	0						1		0			
WLO-	655	300E, 145N	RGSIV	2		30				25	6		4	7	8		9	4			0	7	
WLO-	656	302E, 187N	RGSIV			35			10	25	5		7		8		0	2				6	SP: 2
WLO-	657	300E, 170N	RGSIV		7	30	20	25		3 10								5		0	0		
WLO-	661	300E, 180S	GESSILL		6	5	41	35		0 7	1	0						3					
WLO-	664	315E, 220S	RGSIV			33				4 20	20		25					2					
WLO-	668	350E, 162N	RGSIV			25				15	5		25		10		20	3			0	7	
WLO-	671	395E, 192N	FD			50	35			2 1	4							2		0			KSP: 5; PYX:? 1
WLO-	676	1340S, 1170W	RMCLR			30	40	12	3	0		7	7						1				lenses (frags?) of HBL, QTZ, FSP
WLO-	677	1340S, 1170W	RMCLRclot			28	34	21				4						0	0	0			CLOT FRAGS: HBL:13%, PL:1, QTZ 1
WLO-	678	1420S, 1160W	RMCLR	2	1	39	38			4 5	2	2	1					5	1				
WLO-	692	8714N, 8772E	CT	10		56				0 10	0		7			6	7	1				0	SP: 3
WLO-	693	8730N, 8767E	MA		2	8	35	35		4 5	3	3						5		0			
WLO-	694	8750N, 8758E	GB			5	35	47		3	1	7						2	0				
WLO-	695	8708N, 8745E	LF			8	45		40	1 0	0	3						3		0			
WLO-	696	8895N, 8735E	LF			12				12	36	1						2		0			35% CHL retrograded AN/GD?
WLO-	698	8700N, 8705E	MA		35	7	20	35		28	0	27						3		0			PP AND PL sauseritized
WLO-	699	8727N, 8692E	CT			40			25	3 0	7		12					13		0	0		SP: 12
WLO-	700	8720N, 8715E	MA			20	0			8	8		9	16	18			8				5	SP: 10
WLO-	701	8810N, 8777E	MA			5	42	42		5 0	0	5						1	0				
WLO-	702	8820N, 8760E	RGLF		0	3	8		40	15 6	10	15						3	0				
WLO-	703	8800N, 8755E	QFP	7		35	23			10 10	2	2	8					2			1		
WLO-	705	8785N, 8723E	GR			43	40			1 10	2	1						2	1	0	1		
WLO-	706	8797N, 8702E	MA			5	35	44		5 3	0	7						1	0				
WLO-	712	8875N, 8705E	QFP	5		40	30			12 10	5		7					1			0		
WLO-	713	8656N, 8800E	CAB-MA			5	38	2	40	5 5	0	5						1					
WLO-	716	8745N, 8693E	CT			30	5	10	20	0 1		1	15					12					
WLO-	717	8720N, 8802E	CT			25	10			0 7	5			40	10			3					
WLO-	718	8672N, 8820E	CT			20	5			0 20	15			30	8			2		0	0		
WLO-	719	8625N, 8824E	CT			20	0			14	15		10	15	15			3				8	SP: tr
WLO-	720	8625N, 8818E	CT			25				5	12			30	15			3				10	
WLO-	721	8604N, 8830E	LF		5	7	21	7	30	7 6	5	2						10	0				
WLO-	722	8680N, 8900E	MA			12	8	55		15 2	2	3						3					
WLO-	728	8736N, 8625E	CAB-MA			5	5			5 15	25			25	15			5			0		
WLO-	729	8150N, 9200E	GB			2	25	65			0	0						1	2				SAUSSERITE: 5
WLO-	731	8130N, 9270E	LF		25	5	5	54		25	0	7						1	0				

*protolith uncertain

Table 10. (continued)

Modal Mineral Estimates of Rock and Drill Core Samples

TYPE	SAMPLE	LOCATION	LITHUNIT	QP	PP	QTZ	PL	HBL	T/A	MUSC	BIO	CHL	EPI	GNT	AN/GD	CDT	SIL	ST	OPA	SPHE	APA	ZIR	PIN	COMMENTS
WLO-	733	8135N, 8175E	LF- MA APH			8	4	60		15		6	5						1	1				
WLO-	736	8112N, 9310E	QFFdike	9	6	45	37			0	2								1			0		KSP: tr
WLO-	742	8150N, 9340E	LF/MA			30	15	30		5	4	8	5						1	2	0	0		
WLO-	744	8150N, 9340E	QFF-dike	10	4	34	30			5	7	8	1						1					
WLO-	745	8150N, 9340E	LF/MA?			30	20	30		10		5	3						2	0	0			
WLO-	755	12300N, 9190E	CT			40	17				15	10		2	10	0			1			0	5	
WLO-	757	12300N, 9220E	LF			4					0	50	0		3	7			2	0	0		34	
WLO-	758	12300N, 9240E	QFF	5		50	5			5	30					0	3		1			1		CDT: ??
WLO-	784	10600N, 8650E	LCS			40	35	20		0		0	2						3		0			
WLO-	785	10600N, 8650E	LCS			35	25	15		0	10	5	1						3	5	1			
WLO-	786	10600N, 8750E	CCLR			45	25			0	3	3			20	10		0	2		0		2	
WLO-	787	10600N, 8650E	LCS			45	33			1	12	5						8	3			1		
WLO-	788	10600N, 8825N	CCLR			25	25				5	5		7	30	0			3	0		0	0	
WLO-	789	10600N, 8875E	LCS			31	25			0	5	2		5					2				0	
WLO-	790	10600N, 8925E	LCS			30				0	6	4		45	7	2		0	3		0	1	1	
WLO-	791	10600N, 8960E	PCC			35	30	21		2	5	1	1	5					5		0			
WLO-	792	10600N, 9000E	LCS			35	18		25	1	1	1	2	15					4		0			
WLO-	793	10600N, 9075E	QFP	10	5	39	20			2	15	1		5					3			0		
WLO-	794	10600N, 9100E	QFP	7		39	15			3	15	2		8		2	6	0	1		1	1		
WLO-	795	10600N, 9250E	QFP	10	10	40	25			10	3	0	0						1			1		
WLO-	796	10600N, 9270E	QFP			46				2	20	2		20			10		0			0		
WLO-	798	10025N, 8160E	LCS			38	35			1	30		0						4		2	0		
WLO-	799	10035N, 8160E	LCS			35	25			5	28	1	0						7		1	0		
WLO-	800	10040N, 8150E	LCS			25	20				7	25		5		5			7				1	SP: 5
WLO-	801	10035N, 8140E	LCS			22	15				5	0		10	20	15		0	8			0	0	SP: 5; probable AN/GD
WLO-	802	10030N, 8130E	LCS			25	10			0	5	15		40					5					
WLO-	803	10000N, 8110E	QFP			30	12				15	10		12	7	0			4				7	SP: 3
WLO-	804	9960N, 8060	LCS			20	2				20	3		4	10	20			9			1	8	SP: 5; AN/GD uncertain
WLO-	805	8910N, 8980E	QFP	10		38	10			5	2					10	8		0			1		
WLO-	807	8930N, 8920E	QFP	7		50				20	10					5	7		0			1	0	
WLO-	811	9300N, 9060E	QFP	7	13	30	20			6	22								0			0		
WLO-	822	9750N, 8400E	QFP	8		40	30			5	17								0			0		
WLO-	824	9750N, 8310E	LCS			30	25	35	4	1	0								5		0			
WLO-	831	11200N, 8960E	LCS			45	5			0	3				30	13		1	3		0			
WLO-	832	11200N, 8990E	LCS			42					7	0		40		0	6	3	2			0		
WLO-	834	10900N, 9425E	QFF			45					15	0			20	20		0	0					
WLO-	837	11750N, 9000E	LCS			35					7	4		35	1	12		1	1			0	4	
WLO-	841	11700N, 9097E	LCS			47					1	2		5	20	20		1	2				2	
WLO-	844	10370N, 9430E	LF/CT?			5	36	45	10	0			0						4		0			
WLO-	847	10040N, 9580E	QFF	8		50	10			5	15	0				5	8	0	0			0		
WLO-	849	8700N, 9335E	LF *			47	5	35	10										3		0			re-entrant selvedge
WLO-	850	8700N, 9335E	LF		30	8	10	65		8			7						2	0				
WLO-	852	11750N, 9170E	QFP	10		50				2	15	0				10	8	0	0			0	5	
WLO-	853	11200N, 9060E	QFP			50	5				15	0		10		7	8	5	0			0	0	
WLO-	858	12000N, 9030E	LCS			12					15	0			40	30		0	2				1	
WLO-	862	11710N, 9350E	CLR			45	14			8	7	25							1					
WLO-	801B	8700N, 9075E	LF			20	5				5	3			40	20			4				3	
WLO-	803B	8600N, 9030E	QFP	5	2	30	20			20	20	0	0						2			1		

*protolith uncertain

Table 11.

Mineral Modal Ranges of Least Altered Rocks

Rock Category	MINERAL MODAL RANGES																	
	QP	PP	QTZ	PL	KSP	HBL	T/A	MUSC	BIO	CHL	EPI	GNT	AN/GD	CDT	SIL	ST	SP	OPA
Mafic Rocks: n=32	0	0-50	0-30?	4-50	0	7-85	0-15	0-28[1]	0-10?	0-10	0-27	0	0	0	0	0	0	tr-5
Volcaniclastics: n=32	0-10	0-15	5-47	2-45	0-25	5-50	0-7	0-27	0-20	0-5	0-10	0-25	0	0	0	0	0	0-15
Felsic Lava Flows: n=42	1-20	tr-15	23-45	5-40	0-25	0-5	0	0-30	0-22	0-20	0-5	0-7	0	0	0	0	0	0-3
Felsic Pyroclastics: n=67	0-10	0-23	10-49	10-58	0-25	tr-32	0-10	0-4	0-25	0-24	0-25	0-10	0	0	0	0	0	0-6

n = number samples

Defining Criteria:
0< hornblende > tremolite/actinolite, > biotite
- plagioclase phenocrysts >0 for Felsic Lava Flows

[1]mostly <2% as altered plagioclase

Table 12.

Mineral Modal Ranges of Tremolite/Actinolite Zone Alteration

Rock Category	MINERAL MODAL RANGES																	
	QP	PP	QTZ	PL	KSP	HBL	T/A	MUSC	BIO	CHL	EPI	GNT	AN/GD	CDT	SIL	ST	SP	OPA
Mafic Rocks: n=19	0	0-20	0-27	tr-45	0	0-15	20-80	0-10[2]	0-22	0-30	0-25	0[3]	0	0-15	0	0	0	1-20
Volcaniclastics: n=23	0-10	0-15	5-40	0-34	0	0-12	1-27	0-25	0-25	0-11	0-10	0-25	0	0-25	0	0	0-5	0-12
Felsic Lava Flows: n=0																		
Felsic Pyroclastics: n=9	0-15	0-15	20-50	tr-45	0	0	tr-26	0-8	tr-25	0-5	0-2	0-7	0	0-20	0	0	0	1-4

Defining Criteria:
0< tremolite/actinolite > hornblende; anthophyllite/gedrite = 0

n = number samples
[1]includes retrograded cordierite as pinite?
[2]altered plagioclase
[3]rare garnet observed on outcrop

Table 13.

Mineral Modal Ranges of Biotite Zone Alteration

Rock Category	MINERAL MODAL RANGES																
	QP	PP	QTZ	PL	KSP	HBL	T/A	MUSC	BIO	CHL	EPI	GNT	AN/GD	CDT	SIL	ST	SP	OPA
[2]Mafic Rocks: n=6	0	0	tr-30	0-20	0	0	0	0-5	12-35	0-38	0-2	0-60	0	0-63	0	0-3	0-tr	tr-5
[3]Volcaniclastics: n=16	0-20	0-4	13-58	0-45	0	0-2	0-7	0-5	5-45	0-45	0-3	0-40	0	0-25	0	0-20	0-6	0-7
[3]Felsic Lava Flows: n=92	0-20	0-13	23-60	0-50	0-15	0	0	0-32	5-35	0-40	0-3	0-28	0	0-27	0	0-15	0	0-3
[3]Felsic Pyroclastics: n=31	0-10	0-7	tr-50	0-49	0-25	0-tr	0-tr	0-8	tr-33	tr-73	0-3	0-7	0	0-30	0	0-7	0	tr-7

n = number samples

Defining Criteria:
[2]0< biotite > hornblende, > tremolite/actinolite; anthophyllite = sillimanite = 0

[3]5≤ biotite > hornblende, > tremolite/actinolite; anthophyllite = sillimanite = 0

[1]includes retrograded cordierite as pinite

Table 14.

Mineral Modal Ranges of Sillimanite Zone Alteration

Rock Category	MINERAL MODAL RANGES																
	QP	PP	QTZ	PL	KSP	HBL	T/A	MUSC	BIO	CHL	EPI	GNT	AN/GD	CDT	SIL	ST	SP	OPA
Mafic Rocks: n=0																		
Volcaniclastics: n=2	2-8	0	35-40	0-26	0	0	0-7	7-20	5-45	3	0	0-7	0	0-19	6-7	0	0	tr
Felsic Lava Flows: n=68	0-25	0	13-65	0-35	0	0	0	0-35	tr-28	0-22	0-2	0-20	0	0-36	tr-20[2]	0	0	0-3
Felsic Pyroclastic: n=3	0	0	33-55	5-30	0	0	0	tr-10	7-23	tr-10	0	0	0	0-13	tr-8	0	0	tr

n = number samples

Defining Criteria:
sillimanite > 0; staurolite > 0

[1]includes retrograded cordierite as pinite
[2]includes andalusite

Table 15.

Mineral Modal Ranges of Sillimanite-Staurolite Zone Alteration

Rock Category	MINERAL MODAL RANGES																
	QP	PP	QTZ	PL	KSP	HBL	T/A	MUSC	BIO	CHL	EPI	GNT	AN/GD	CDT	SIL	ST	SP	OPA
Mafic Rocks: n=0																		
Volcaniclastics: n=18	0-5	0	25-50	0-20	0	0	0	0-7	7-28	tr-9	0	0-40	0	0-30	tr-28	tr-14	0	0-4
Felsic Lava Flows: n=42	0-15	0	25-70	0-25	0	0	0	0-15	0-25	0-30[2]	0	0-10	0	tr-25	tr-15	tr-30	0	tr-3
Felsic Pyroclastics: n=6	0-5	0	40-52	0-25	0	0	0	tr-10	0-18	tr-15	0	0	0	0-18	5-13	tr-10	0	0

n = number samples

Defining Criteria
sillimanite > 0; staurolite > 0

[1]includes retrograded cordierite as pinite
[2]mostly ≤3%

Table 16.

Mineral Modal Ranges of Anthophyllite/Gedrite Zone Alteration

Rock Category	MINERAL MODAL RANGES																	
	QP	PP	QTZ	PL	KSP	HBL	T/A	MUSC	BIO	CHL	EPI	GNT	AN/GD	CDT	SIL	ST	SP	OPA
Mafic Rocks: n=25	0	0	0-20	0-15	0	0	0	0	0-25	0-66	0	0-35	2-68	0-46	0	0-8	0-15	tr-15
Volcaniclastics: n=65	0-5	0	4-62	0-20	0	0	0-15	0	0-30	0-22	0-8	0-55	tr-50	0-35	0	0-10	0	1-9
Felsic Lava Flows: n=31	0-10	0	7-66	0-12	0	0	0	0	0-30	0-22	0-tr	0-15	2-62	0-54	0	0-17	0-5	tr-3
Felsic Pyroclastics: n=24	0-5	0	3-50	0-37	0	0	0	0	0-77	tr-60	0-1	0-25	tr-40	0-46	0	0-7	0-5	1-15

n = number samples

Defining Criteria:
anthophyllite > 0%

[1]includes retrograded cordierite as pinite

APPENDIX II.
WHOLE ROCK AND TRACE ELEMENT ANALYTICAL DATA, AND MASS BALANCE CALCULATIONS

Table 17.

Whole Rock and Trace Element Analytical Methods.

The following is a compilation of the major and trace element analytical methods and analyses as determined by the Geological Survey of Canada, Mineral Resources Division, Analytical Chemistry Section, Ottawa, Ontario.

All analyses were completed by XRF and/or ICP except FeO, H_2OT, CO_2T, and S by chemical methods. Fe_2O_3 is calculated using $Fe_2O_3 = Fe_2O_3T$ (ICP) - 1.11134*FeO (volumetric). ICP major oxide data are obtained on 0.5g of sample fused with lithium metaborate, dissolved in 5% HNO_3 and diluted to 250ml. ICP trace element data are obtained on 1.0g of sample (acid + fusion of residue) dissolved in 10% HCL and diluted to 100ml.

As an analytical check pulps from 11 samples were analyzed as a group distinct from the original suite. Analyses of these "reruns" is included at the end of the data tables.

Spaces labelled "0" represent values below detection limits.

Table 18.

Estimates of Accuracy of Analytical Data

The accuracy of the analytical data is as follows as reported by the Geological Survey of Canada, Mineral Resources Division, Analytical Chemistry Section:

Element	±	Estimate of Error (Absolute + Relative)
SiO_2	±	(0.4 + 1% of concentration)
TiO_2		(0.02 + ")
Al_2O_3		(0.4 + ")
$Fe_2O_3(t)$		(0.1 + ")
MnO		(0.01 + 2 ")
MgO		(0.1 + 1 ")
CaO		(0.1 + 1 ")
Na_2O		(0.5 + 1 ")
K_2O		(0.05 + 1 ")
FeO		(0.2 + 5 ")
$H_2O(t)$		(0.1 + 5 ")
$CO_2(t)$		(0.1 + 3 ")
P_2O_5		(0.02 + 1 ")
S(t)		(0.04 + 5 ")

Ba	±	(20 PPM + 10% of concentration)
Be		(0.5PPM + 5% ")
Co		(5 PPM + 5% ")
Cr		(10 PPM + 5% ")
Cu		(10 PPM + 5% ")
La		(10 PPM + 5% ")
Nb		(30 PPM + 10% ")
Ni		(10 PPM + 5% ")
Pb		(20 PPM + 10% ")
Rb		(20 PPM + 2% ")
Sc		(0.5PPM + 5% ")
Sr		(20 PPM + 10% ")
V		(5 PPM + 5% ")
Y		(5 PPM + 5% ")
Yb		(0.5PPM + 5% ")
Zn		(5 PPM + 5% ")
Zr		(20 PPM + 10% ")

Table 19.
Whole Rock and Trace Element Analytical Data

TYPE	SAMPLE	LOCATION (ddh collar)	LITHUNIT	ALTN ZONE	SIO2	TIO2	AL2O3	FE2O3t	FE2O3	FEO	MNO	MGO	CAO	NA2O	K2O	H2O+	CO2t	P2O5	S	BA	AG	BE	CO	CR	CU	LA	NB	NI	PB	RB	SC	SR	V	Y	YB	ZN	ZR
GO01	G1-287.5	440E, 430N	RGLF(GES)	BIO	50.8	0.77	15.5	11.1	2	8.2	0.17	8.76	7.44	1.9	1.31	3	0	0.12	0	380	0	1.5	35	190	1	4	15	56	4	40	25	160	150	17	1.6	190	100
WL02	WL2-189	10300N, 9560E	QFP	SIL-ST	77.5	0.14	10.7	6.5	1.3	4.7	0.03	2	0.02	0	1.62	1.8	0.1	0.02	0.02	670	0	1.8	3	130	5	31	51	0	3	30	0.9	4	0	170	22	75	390
WL07	WL7-540	11280N, 9800E	QFP	SIL-ST	66.6	0.19	13.7	9.8	1.1	7.8	0.05	4.9	0.03	0.1	2.73	2.1	0.1	0.03	0.28	650	0	1.7	5	61	49	3	62	0	9	43	1.4	7	0	190	20	62	510
WL07	WL7-426.5	11280N, 9800E	QFF	SIL-ST	77.3	0.13	11.6	1.3	0.1	1.1	0	3.91	0.34	1	1.45	2.2	0	0.02	0	210	0	1.9	6	88	1	4	63	3	4	30	1.7	53	0	160	22	0	380
WL07	WL7-574	11260N, 9800E	LCS	AN/GD	64.3	0.78	12.4	12.8	1.5	10.2	0.26	8.94	0.34	0.7	1.27	1.9	0	0.21	0.02	130	0	1.5	6	54	3	25	31	2	5	51	23	3	0	96	10	200	460
WL07	WL7-588	11260N, 9800E	LCS	SIL-ST	67.2	0.73	11.4	15.4	2	12.1	0.18	2.69	0.45	0.3	1	1.4	0.1	0.2	0.94	270	0	1.4	9	150	180	21	25	8	5	30	19	5	0	91	10	300	390
WL08	8-252	7750N, 10060E	CLR	LA	74.7	0.29	11.6	4.9	1.2	3.3	0.06	0.34	1.43	4.9	0.92	0.6	0.1	0.04	0.03	290	0	4.2	2	210	19	66	50	4	5	15	3.8	84	0	240	28	280	630
WL10	WL10-360	9680N, 8660E	LCS	BIO	73.9	0.39	13	3.6	0.2	3.1	0.05	1.73	2.28	3.1	1.06	1	0.1	0.07	0	230	0	3.4	5	160	0	31	27	3	3	24	5.8	100	10	89	10	13	380
WL10	WL10-418	9680N, 8660E	CCLR	BIO	62.4	0.49	12.9	8.7	1.3	6.7	0.03	8.71	0.29	0.4	3.45	3.4	0.1	0.1	0	820	1	2.5	7	61	1	34	47	0	10	86	7.8	9	3	160	17	17	550
WL10	WL10-436	9680N, 8660E	CCLR	AN/GD	71.6	0.55	12.2	8.6	0.7	7.1	0.06	2.52	0.63	3.7	0.12	0.6	0	0.14	0	50	2	2.4	7	170	8	39	38	3	8	7	10	24	0	150	17	16	580
WL10	WL10-252	9680N, 8660E	PCC	T/A	64.2	0.74	12.3	13.4	4.7	7.8	0.3	2.12	3.07	3.3	0.32	0.8	0.2	0.2	0.02	60	1	1.9	5	160	10	20	28	2	4	11	21	110	0	97	11	200	460
WL10	WL10-293	9680N, 8660E	PCC	LA	66	0.72	13.3	12.1	0.9	10.1	0.25	1.35	4.35	2.4	0.1	0.6	0.1	0.19	0.2	110	0	2.3	5	200	17	24	27	1	4	3	16	75	0	120	13	130	450
WL10	WL10-349	9680N, 8660E	LCS	SIL-ST	70.8	0.58	11.3	8.2	1.1	6.4	0.04	3.29	0.27	0.3	3.01	2.6	0	0.2	0.01	890	0	3.5	7	200	2	34	33	0	2	79	11	8	0	130	14	24	560
WL14	14-637	11750N, 9940E	QFP	SIL-ST	77.2	0.19	10.7	5.4	0.5	4.4	0.03	3.12	0	0.1	1.61	1.6	0	0.02	0	620	1	2.9	4	72	4	37	52	0	7	33	1.6	0	0	170	19	26	480
WL14	14-661.2	11750N, 9940E	LCS	AN/GD	42.9	1.32	18.7	25.3	6.2	17.2	0.27	7.33	1.99	0.4	1.23	2	0	0.74	0.02	140	2	8.8	9	66	8	36	40	10	11	39	48	5	0	420	40	63	720
WL14	14-491	11750N, 9940E	CLR	LA	69.9	0.43	11.7	4.3	0.9	3.1	0.05	3.63	2.7	4.6	0.56	1.4	0.3	0.06	0.03	140	1	1.6	15	67	55	12	28	14	7	22	8	150	19	94	11	19	290
WL14	14-433	11750N, 9940E	CLR	LA	75.1	0.24	12.7	2.3	0.4	1.7	0.01	0.58	1.61	6	0.13	0.7	0.3	0.01	0.06	40	0	5.4	3	57	10	14	58	8	5	5	4.5	140	8	200	20	0	430
WL14	14-425	11750N, 9940E	CLR	LA	72.7	0.53	11.9	7	2.6	4	0.06	0.66	1.74	5.4	0.24	0.6	0.1	0.11	0.24	70	1	3	27	41	43	160	53	0	5	7	12	120	0	160	17	20	500
WL14	14-469	11750N, 9940E	CLR	LA	71.7	0.46	13.3	5.1	0.4	4.2	0.03	0.96	1.67	5.2	0.72	1	0.3	0.06	0	190	2	2.3	15	62	3	38	27	2	9	16	7.4	130	14	95	9.2	11	330
WL14	14-458	11750N, 9940E	CLR	LA	73.6	0.42	12.8	2.4	0.5	1.7	0.03	0.7	3.02	5.3	0.15	0.5	0.4	0.1	0.03	40	1	2	6	67	20	8	31	15	9	7	5.8	170	13	95	11	8	330
WL15	WL15-651	7900N, 10560E	RGSIV	LA	71	0.81	10.6	8.2	1.4	6.1	0.16	0.86	3.89	3.1	0.84	0.8	0.1	0.2	0.04	180	1	2.5	5	150	5	31	30	10	4	25	15	130	0	130	14	400	560
WL17	WL17-570	12230N, 9850E	QFF	SIL	77.2	0.12	11.8	1.9	0.3	1.4	0.01	2.69	0.22	0.7	2.53	2.2	0.1	0.01	0	700	0	2.7	7	68	3	17	67	0	5	36	2.2	17	0	240	32	0	360
WL17	WL17-681.5	12230N, 9850E	LCS	BIO	62	0.77	13.1	7.2	0.8	5.8	0.07	6.76	3.38	2.6	1.39	2.1	0.8	0.17	0.02	300	0	2.7	19	180	3	40	35	65	4	42	14	150	57	130	15	47	510
WL17	WL17-618	12230N, 9850E	QFP	SIL	77.3	0.15	11	3.4	0.5	2.6	0.02	3.13	0.04	0.1	2.05	2.3	0	0.02	0	660	0	3.1	2	57	2	58	57	0	2	49	0.8	15	0	220	25	18	410
WL17	WL17-545	12230N, 9850E	QFP	BIO	74	0.19	10.9	6.3	0.9	4.9	0.03	4.01	0.06	0.3	1.76	3.2	0.1	0.02	0.01	360	0	2.5	4	130	2	44	52	0	3	41	1.2	5	0	190	21	26	460
WL25	25-1133	8900N, 9000E	PCLR	AN/GD	65.7	0.72	12.8	8.3	0	7.6	0.04	4.46	2.06	2.4	1.84	1.8	0.1	0.2	0.6	200	1	2.1	13	100	43	29	21	3	3	48	16	79	0	100	11	31	460
WL25	25-916	8900N, 9000E	PCLR	AN/GD	74.2	0.31	12.5	4.6	0.4	3.8	0.03	1.19	2.86	3.1	1.03	0.8	0.1	0.05	0.01	200	0	3.9	4	150	2	46	42	4	10	28	3.1	100	0	180	17	370	650
WL25	25-809	8900N, 9000E	PCLR	AN/GD	65.9	0.74	12.9	11	1.7	8.4	0.46	1.45	3.98	2.9	0.39	0.7	0.1	0.19	0.04	70	0	2	5	160	12	26	33	3	8	6	23	59	0	120	13	190	490
WL41	WL41-529	10800N, 9770E	PCC	T/A	65.2	0.74	12.1	12.4	1.8	9.5	0.2	2.79	2.7	3.7	0.12	0.4	0	0.2	0.44	70	0	2.2	5	37	12	22	23	1	6	3	25	70	0	99	11	180	460
WL41	WL41-210	10800N, 9770E	CLR	SIL	71.6	0.46	14	1.2	0	1.1	0	3.99	1.33	3.4	2.04	1.3	0	0.06	0	350	2	2	18	130	2	150	25	9	4	47	8.4	130	13	170	15	0	350
WL50	50-570	10400N, 10070E	QFP/CT*?	AN/GD	62.6	0.17	14.3	12.7	1.4	10.2	0.11	7.32	0.06	0.1	1.16	3	0	0.03	0.02	190	0	2.7	3	49	6	26	62	2	1	22	1.2	0	0	230	26	410	560
WL50	50-588	10400N, 10070E	QFP	SIL-ST	76.7	0.15	10.8	5.4	0.5	4.4	0.04	3.53	0.02	0.1	2.07	1.6	0	0.02	0.01	240	1	1.8	3	77	3	73	54	1	5	38	0.8	7	0	240	26	90	400
WL50	50-467	10400N, 10070E	QFF	SIL-ST	78.5	0.13	12.4	2.7	0.4	2.1	0.01	3.46	0.14	0.3	1.43	1.1	0	0.02	0	470	0	2.4	4	87	2	6	59	0	4	20	2	50	0	270	35	14	380
WL50	50-803.9	10400N, 10070E	CCLR	BIO	74.2	0.35	9.3	7.1	0.5	5.9	0.05	4.96	0.16	0.1	1.77	2.6	0.1	0.06	0	290	1	1	6	190	3	38	32	20	6	190	6.6	0	11	90	9.3	130	370
WL50	50-378	10400N, 10070E	CLR	SIL-ST	78.9	0.13	12.6	0.9	0	0.6	0	2.32	0.55	2.7	1	0.9	0	0.02	0	260	1	1.4	3	110	2	5	83	1	6	16	1.7	74	0	160	20	0	380
WL55	55-857	11700N, 10140E	LCS	AN/GD	61.9	0.86	14	17.4	2.6	13.3	0.39	4.26	0.5	0.1	0.56	1	0.2	0.27	0	240	0	1.1	5	87	2	31	32	0	2	6	26	4	0	100	11	410	490
WL55	55-712	11700N, 10140E	QFF*?	SIL	79	0.14	11.5	1	0	1	0	2.2	1.02	3.4	0.81	1.1	0.1	0.02	0	380	1	2.3	3	140	2	9	56	2	4	20	2.3	96	0	140	20	0	330
WL59	59-371	9250N, 8770E	LCS	AN/GD	62.2	0.81	12.8	12.2	1.2	9.9	0.23	5.46	0.4	0.2	2.7	3.6	0.1	0.23	0.2	160	1	2.2	5	110	21	25	34	1	2	87	22	10	0	100	11	490	460
ZO07	7-440	9810N, 10170E	CLR	BIO	72.3	0.32	10.6	5	0.8	3.8	0.02	4.72	1.16	2.5	1.32	2.5	0.2	0.04	0.02	160	1	1	18	200	18	12	36	9	3	35	4.4	92	15	62	9.1	100	510
ZO09	9-563	9900N, 10320E	WLH-MA	AN/GD	49	1.02	16.1	12.3	1.3	9.9	0.05	16.7	0.41	0.7	0.57	3.6	0	0.21	0.01	60	1	0.9	10	200	3	39	18	99	6	35	29	17	200	39	2.5	280	91
ZO1	ZO1-240.75	9900N, 10000E	CLR	AN/GD	44.8	0.7	17.9	11.4	1.7	8.7	0.06	16.3	0.26	0.2	1.24	7.9	0	0.14	0	80	1	0.6	35	150	4	9	14	57	6	35	25	4	170	26	1.9	630	77
ZO1	ZO1-272.7	9900N, 10000E	CLR	SIL-ST	80.5	0.45	11.5	4.5	0.7	3.4	0.02	1.49	0.05	0.1	1.02	0.9	0	0.04	0.06	220	2	0.8	5	190	23	35	28	10	3	18	8.5	6	27	66	7.8	830	260
ZO15	Z15-706	10150N, 10460E	CLR	AN/GD	45.9	0.74	20.1	13.2	1.6	10.4	0.06	13.3	0.36	1	1.2	4.9	0.1	0.06	0.09	110	1	0.3	8	100	58	130	18	34	3	30	10	32	53	110	5.5	440	120
ZO17	17-754	10000N, 10430E	QFF	SIL	77.7	0.14	12	3.5	0.3	2.9	0.02	2.17	0.26	0.8	2.08	1.1	0.2	0.02	0.07	440	0	1.8	5	120	35	120	64	0	5	46	3	28	0	230	28	72	370
ZO17	17-708.3	10000N, 10430E	CLR	AN/GD	50.1	0.79	21	12.9	1.8	10	0.15	14	0.34	0.2	0.1	1.7	0	0.15	0.01	60	0	1.3	22	190	0	15	20	44	0	5	33	0	150	27	1.9	250	85
ZO18	18-784.7	10150N, 10460E	QFF	SIL	78.2	0.13	11.7	1.5	0.2	1.2	0	3.32	0.26	1	1.54	1.5	0.1	0.02	0	440	1	1.7	3	130	3	5	58	0	6	36	2.1	27	0	180	21	0	380
ZO23	23-393	10000N, 10170E	WLH-CRT	T/A	60.8	0.59	13	7.4	1.4	5.4	0.03	8.29	1.4	1.9	3.28	2.9	0.2	0.06	0.07	210	1	1.8	8	80	16	54	35	7	6	73	14	100	0	130	14	140	530
ZO23	23-425	10000N, 10170E	MMF*	AN/GD	65.1	0.56	14.6	9.6	1	7.9	0.04	8.34	0.05	0.2	0.7	1.5	0	0.05	0	180	1	0.6	12	150	2	63	16	36	3	19	25	0	140	33	2.2	110	62
ZO27	27-682	10400N, 10490E	MMF*	BIO	40.7	0.78	21.1	11.9	1.8	9.1	0.04	14.2	0.17	1.1	5.21	4.5	0.1	0.18	0	510	1	4	14	160	6	480	15	41	4	130	24	28	150	230	15	410	110
ZO27	27-735	10400N, 10490E	QFF*?	BIO	67.7	0.27	10.5	5.4	0.6	4.3	0.02	9.38	0.6	0.9	1.09	4	0.2	0.04	0	110	1	0.5	19	140	3	9	43	19	2	33	5.8	38	3	210	24	67	530
ZO32	32-469	10400N, 10260E	CLR	AN/GD	72.3	0.54	10.8	9	0.7	7.5	0.04	4.96	0.36	0.7	0.94	1.2	0.2	0.06	0.07	190	1	1.4	12	95	70	47	50	5	3	29	14	31	0	170	19	350	890
ZO32	32-514	10400N, 10260E	MMF	AN/GD	47.5	0.89	16.3	15.7	1.4	12.9	0.07	14.5	0.02	0.2	1.7	2.1	0.1	0.11	0.19	280	1	0.4	19	110	110	280	16	36	4	25	27	0	240	47	2.2	520	73
ZO36A	36A-944.5	9950N, 10300E	PCC	LA	62.8	0.73	11.7	14.1	1.3	11.5	0.43	3.09	3.19	3.2	0.24	0.9	0	0.2	0.09	80	2	2.1	3	130	9	20	29	3	15	7	23	84	0	95	10	780	440
ZO36A	36A-506	9950N, 10300E	WLH-FWF	AN/GD	42.4	0.92	15.7	17.5	2.1	13.9	0.09	15.6	0.29	1	2.95	4.3	0.1	0.16	0	270	1	0.4	9	180	4	420	18	83	20	76	30	19	220	260	12	600	83
ZO36A	36A-971	9950N, 10300E	PCC	T/A	69	0.54	12.4	10	1.1	8	0.22	2.36	1.57	3.6	0.5	0.7	0	0.1	0.02	200	0	2.3	3	96	5	30	34	0	4	18	14	79	0	130	14	500	460
ZO36A	36A-957	9950N, 10300E	LCS	BIO	61.2	0.72	12.5	12.5	1.1	10.3	0.29	3.46	2.55	2.3	1.71	2.2	1.2	0.19	0.02	300	1	2.8	4	120	3	35	29	2	5	280	22	66	0	110	12	200	470

*Intensely altered, protolith uncertain; **LF/RGLF: FSP vs. APH protolith uncertain

Table 19.(continued)
Whole Rock and Trace Element Analytical Data

TYPE	SAMPLE	LOCATION	LITHUNIT	ALTN ZONE	SIO2	TIO2	AL2O3	FE2O3t	FE2O3	FEO	MNO	MGO	CAO	NA2O	K2O	H2O+	CO2t	P2O5	S	BA	AG	BE	CO	CR	CU	LA	NB	NI	PB	RB	SC	SR	V	Y	YB	ZN	ZR
MW-	1	10175N, 9650E	QFF	AN/GD	77	0.16	11.4	2.6	0	2.4	0.01	5.73	0.04	0.1	1	1.6	0.3	0.02	0	80	0	0.8	1	190	6	130	55	2	12	23	3.3	6	0	200	22	39	370
MW-	9	10250N, 8900E	PCC	T/A	64.4	0.64	13.1	11.1	1.1	9	0.4	2.96	2.84	3.9	0.34	0.8	0.2	0.22	0.01	110	0	3.5	4	110	6	25	16	2	9	15	25	120	0	100	11	190	510
MW-	11	9750N, 9030E	QFP	SIL	74.5	0.17	12.5	4	0.8	2.9	0.04	4.07	0.02	0.2	2.9	1.5	0.2	0.02	0.01	250	0	4.8	1	130	7	45	45	0	11	51	0.8	5	0	200	25	190	440
MW-	12	9720N, 9030E	CT	BIO	70	0.52	13.1	2.5	0.3	2	0.01	5.04	1.31	3.6	2.13	1.4	0.6	0.08	0.01	170	0	2.6	9	140	2	48	18	7	10	52	7.1	150	32	88	9.3	13	310
MW-	31	9200N, 8750E	QFP	SIL	76.6	0.16	10.6	6.8	0.7	5.5	0.14	2.06	0.02	0	2.2	2	0.2	0.02	0.02	380	0	1.9	2	190	25	48	33	1	11	46	0.9	6	0	240	29	160	400
MW-	35	9800N, 9610E	QFF	BIO	76.6	0.16	11.1	1.5	0.3	1.1	0	2.97	1.18	3.5	1.52	0.7	0.1	0.02	0	90	0	3.8	5	150	4	20	41	5	17	37	1.8	130	0	86	12	0	380
MW-	61	10120N, 9460E	CT	SIL-ST	75.1	0.48	13	2.3	0.1	2	0.02	4.54	0.32	1	1.47	1.6	0.3	0.08	0.01	290	0	1.5	10	110	3	31	5	10	12	36	7.9	43	23	88	9.3	85	320
MW-	65	10300N, 9360E	QFP	SIL-ST	77.7	0.16	10.1	6.5	0.6	5.1	0.05	2.03	0	0	1.72	1.7	0.5	0.02	0.02	420	0	1.3	6	280	140	1	33	3	10	26	0.7	10	0	120	20	110	390
MW-	69	10320N, 9445E	QFF	AN/GD	72.1	0.13	9.7	9.1	1.4	6.9	0.02	4.77	0	0.1	1.12	3.6	0.2	0.02	0.06	110	0	0.8	7	40	22	4	48	4	10	22	1.9	6	0	84	14	66	320
MW-	73	10350N, 9525E	LF(APH)	AN/GD	50.1	0.87	18.4	14.1	1.4	11.4	0.22	14.9	0.27	0.2	0.1	2	0.1	0.1	0.01	20	0	1.3	38	120	4	4	3	38	9	6	34	4	180	22	2	260	65
MW-	79	10420N, 9430E	CT	SIL-ST	74.3	0.37	7.8	13.1	0.9	11	0.06	3.12	0.26	0.5	0.09	1.3	0.1	0.11	0.07	50	0	0.3	12	380	68	180	0	53	6	4	10	10	86	180	6	74	48
MW-	88	10525N, 9515E	QFF	AN/GD	72.7	0.17	12.7	6.2	0.2	5.4	0.02	5.84	0.02	0.1	1	1.6	0.2	0.05	0	200	0	0.8	13	180	420	30	44	20	36	18	4.4	9	0	180	20	330	420
MW-	92	10530N, 9000E	PCC	T/A	65.3	0.74	12.3	11.5	0.9	9.5	0.21	2.85	2.94	3.8	0.12	0.6	0.2	0.18	0	100	0	2	8	140	8	4	14	4	8	7	22	97	0	82	10	210	460
MW-	99	10620N, 9470E	CLR	AN/GD	64.1	0.49	15	7.2	0.5	6	0.03	9.21	0.02	0.1	0.99	2.5	0.2	0.06	0	130	0	0.9	17	250	6	190	4	73	6	16	11	6	66	120	6.2	380	90
MW-	101	10720N, 9407E	LF(APH)	AN/GD	56.7	0.77	18.2	15.4	2.2	11.9	0.07	7.76	0.16	0.3	0.09	1.5	0.2	0.07	0.04	150	0	0.6	23	160	27	22	0	33	8	7	26	14	130	20	0.9	350	56
MW-	102	10775N, 9450E	QFF	SIL-ST	80.3	0.14	11.1	3.1	0	3	0.01	3.13	0	0.1	0.9	1.1	0.2	0.02	0	170	0	4.5	5	560	7	13	49	6	7	15	1.9	8	0	160	24	62	360
MW-	111	10920N, 9560E	CLR	BIO	75	0.47	12.1	1.7	0.4	1.2	0.01	2.44	1.08	3.9	1.1	1.1	0.8	0.06	0	310	0	0.9	8	47	19	33	16	1	8	24	6.1	110	28	74	7.7	0	270
MW-	122	11250N, 9340E	QFP	SIL	80.4	0.13	10.6	2.2	0	2	0.01	2.11	0.33	1	1.31	1.7	0.3	0.02	0	580	0	3	3	270	4	10	43	1	9	24	0.5	36	0	110	16	0	380
MW-	130	11600N, 89703	LCS	AN/GD	70.9	0.69	11.9	9.4	1.1	7.5	0.13	2.14	2.51	2.2	0.23	0.7	0.2	0.19	0.01	60	0	3.1	6	320	10	18	27	3	10	7	16	86	0	96	11	130	450
MW-	132	11600N, 9050E	LCS	SIL-ST	64.3	0.66	13	17.3	2.9	13	0.15	2.74	0.46	0.1	1.19	1.6	0.2	0.11	0	420	0	1.7	9	370	9	28	24	0	10	32	18	0	0	120	13	220	510
MW-	143	10100N, 8510E	PCC	T/A	66.7	0.72	12.7	10.7	1.1	8.6	0.31	2.39	2.48	3.7	0.41	0.9	0.1	0.19	0.01	220	0	2.1	9	160	11	26	24	1	11	15	19	150	0	110	12	210	490
MW-	145	10210N, 9530E	QFF	SIL-ST	74.4	0.14	11.2	5.3	0.5	4.3	0.01	2.88	0.95	1.7	1.44	1.9	0.1	0.01	0	160	0	4.8	2	100	4	16	47	0	10	27	2.1	150	0	170	23	130	350
MW	146	10280N, 9525E	QFF	AN/GD	77.5	0.14	11.8	2.5	0.1	2.2	0.01	5.56	0.01	0.1	0.83	1.4	0.1	0.02	0	40	0	1.3	1	180	6	92	56	1	8	14	2.1	6	0	210	24	34	370
MW-	149	10320N, 9650E	QFF*?	AN/GD	74.3	0.41	10.2	7.9	0.5	6.7	0.04	4.32	0.02	0.2	1	1.6	0.2	0.04	0	260	0	1.1	8	190	7	34	0	2	8	15	5.3	10	7	75	7.8	140	260
MW-	150	9580N, 9635E	QFF	SIL-ST	77	0.12	11.7	2.7	0.5	2	0.01	3.92	0.02	0.1	2.22	1.8	0.2	0.02	0.01	200	0	8.6	1	150	4	39	57	0	10	58	2.2	13	0	180	26	68	360
MW-	178	9650N, 9660E	CLR	BIO	79.1	0.37	10.6	2.1	0	1.9	0.01	0.8	1.52	3.8	0.48	0.7	0.4	0.07	0.02	80	0	2.4	9	290	150	1	9	1	7	18	4.6	150	3	55	6.1	19	280
MW-	180	9900N, 9650E	QFF	SIL	78.8	0.18	11.1	1	0	1.1	0	2.98	0.61	1.8	1.3	1.3	0.2	0.02	0	140	0	3.7	3	190	3	9	30	1	10	31	1.6	83	0	140	17	1	350
MW-	200	10100N, 9690E	CLR	SIL-ST	71.9	0.51	12.9	5.7	0.1	5	0.03	4.2	0.43	0.4	1.77	1.6	0.2	0.07	0	300	0	1.5	7	250	6	23	0	2	8	32	6.8	65	10	81	8.8	110	320
MW-	201	10100N, 9700E	MMF	AN/GD	54.8	0.71	17.8	12.4	1.1	10.2	0.17	11.5	0.22	0.1	0.97	2.2	0.1	0.13	0.01	250	0	1.2	31	230	2	5	0	43	8	12	30	4	160	16	1.4	620	74
MW-	203	10100N, 9680E	QFF/CLR?	AN/GD	64.5	0.63	10	15.8	1.6	13.7	0.12	7.07	0.1	0.5	0.06	1.6	0.1	0.08	0	50	0	0.3	14	150	6	46	30	2	10	8	19	4	0	130	13	520	650
MW-	209	10450N, 9670E	CLR	BIO	68.6	0.46	12.8	5.4	1.6	3.4	0.02	3.55	1.6	4.2	1.28	1.5	0.3	0.04	0.18	150	0	1	19	70	680	23	16	4	7	37	7.5	120	17	77	8.6	7	330
MW-	221	10660N, 9615E	CLR	BIO	69	0.53	14.2	2	0.3	1.5	0.01	4.64	1.36	4.5	1.43	1.6	0.2	0.08	0.01	100	0	3.9	8	53	2	42	23	38	10	41	7.7	160	26	110	11	8	340
MW-	222	10720N, 9550E	QFF*?	SIL-ST	70.9	0.53	13.7	8.5	1.7	6.1	0.03	3.31	0.05	0.1	1.84	1.5	0.2	0.09	0.04	400	0	2.2	16	260	29	120	5	54	8	27	12	6	74	90	4	37	110
MW-	234	11025N, 9450E	QFF	SIL	77.7	0.14	11.5	4.5	0.5	3.6	0.03	2.1	0	0.1	2.43	1.6	0.2	0.02	0.01	660	0	2.3	5	180	5	1	46	0	9	29	2.5	9	0	110	21	20	370
MW-	243	11400N, 9370E	QFF	BIO	76.6	0.15	11	2.9	0.1	2.5	0.02	2.12	1.9	2.8	1	1.2	0.3	0.02	0	200	0	2.9	8	260	13	4	39	4	9	21	2.7	180	3	130	16	2	370
MW-	250	11500N, 9375E	QFF	SIL	77.3	0.17	11.3	3.5	0.4	2.8	0.01	2.13	0.31	1.1	1.77	1.8	0.2	0.02	0	400	0	4	5	100	4	86	42	0	8	47	2.1	36	0	230	26	0	380
MW-	258	11700N, 9375E	CLR	BIO	72	0.49	13.6	2.4	0.1	2.1	0.01	3.57	1.13	3.8	1.37	1.4	0.4	0.06	0	150	0	2.4	9	190	2	31	24	9	9	27	7.1	99	21	87	9.3	0	330
WLO-	2	9000N, 9640E	SIV-VC	LA	83.4	0.64	14.7	7.3	1.1	5.6	0.05	2.89	2.7	5.1	0.84	2.2	0.3	0.13	0.14	160	0	1.1	26	110	81	18	0	60	6	31	12	230	70	29	2.4	41	150
WLO-	7	9250N, 6775E	WLH-CRT	LA	60.8	0.74	16.6	5.5	0.9	4.1	0.06	3.07	4.84	7	0.25	0.9	0.4	0.2	0	80	0	1.3	23	180	21	1	0	73	5	8	14	220	110	17	1.5	16	110
WLO-	8	9250N, 6775E	WLH-CRT	LA	66.8	0.56	15.9	3.3	0.3	2.7	0.03	1.63	2.54	7.5	0.14	1	0.5	0.13	0	70	0	1.2	20	180	21	0	0	55	7	9	11	170	70	6	0.8	0	100
WLO-	16	9196N, 9603E	MMF	LA	54	0.82	15.6	10.1	2.2	7.1	0.09	5.55	9.6	3.3	0.2	1.2	0.4	0.11	0	80	1	0.5	26	130	6	3	0	27	10	4	32	250	200	13	1.1	17	57
WLO-	26	L9600-9700N	CLR	LA	75.7	0.33	12.4	1.6	0	1.4	0.03	0.53	3.01	5.7	0.1	0.2	0.2	0.04	0	40	0	5.4	7	110	12	69	48	7	10	5	3.2	130	0	190	21	12	560
WLO-	35	9181N, 9690E	WLH-CRT	LA	66.2	0.61	17.6	2.6	0.3	2.1	0.03	1.29	2.93	7.4	0.38	0.8	0.2	0.15	0.01	80	0	1.1	9	130	8	0	2	18	5	16	7.2	250	36	7	0.7	3	100
WLO-	41	9703N, 9155E	WLH-CRT	LA	62.5	0.58	15.8	5.6	1	4.1	0.06	2.72	4.95	6.7	0.39	8.5	0.2	0.18	0	80	0	1.2	23	100	4	0	4	46	5	9	7.7	170	43	10	0.8	14	98
WLO-	44	9140N, 9695E	WLH-MA*?	LA	51.8	1.83	12.8	13.9	2.7	10.1	0.11	5.01	7.22	5.1	0.35	1.6	0.2	0.31	0	50	0	1.1	40	48	0	12	0	21	6	5	32	150	150	44	4.3	26	160
WLO-	57	9650N, 9740E	WLH-MA	LA	51.6	0.96	15.8	11	2.9	7.3	0.07	5.25	7.65	3.8	2.18	1.8	0.3	0.23	0.16	200	0	1.5	48	230	27	0	4	56	7	65	29	260	200	48	4.6	40	70
WLO-	58	9630N, 9715E	CLR	LA	77.9	0.39	12.2	1.2	0.4	0.7	0.02	0.23	1.87	5.3	0.29	0.4	0.2	0.02	0.02	70	0	3.6	4	110	65	4	22	5	6	10	1.7	130	0	110	17	0	740
WLO-	61	9910N, 9770E	WLH-MA	LA	52.3	0.97	15.4	9.1	2	6.4	0.07	6.8	7.83	3.9	1.31	1.9	0.3	0.23	0.2	150	0	1.4	32	220	100	0	0	57	7	40	28	270	200	20	1.8	22	51
WLO-	68	9930N, 9770E	WLH-CRT	LA	56.1	2.66	17.5	6	0	0	0.05	1.24	4.76	7.3	1.02	0	0.2	0.54	1.48	130	1	1.8	80	65	310	3	6	860	17	36	14	280	57	46	4.4	16	100
WLO-	70	9910N, 9725E	MMF	LA	54.2	0.75	15.3	10.4	2.6	7	0.16	6.19	7.67	2.6	0.74	1.9	0.4	0.11	0.03	100	1	0.8	33	160	41	0	0	26	7	18	30	210	180	14	1.3	91	53
WLO-	72	9910N, 9725E	MMF	T/A	52.7	0.86	16	11.4	0.8	9.5	0.13	9.02	5.94	2.4	0.31	1.5	0.1	0.11	0.06	40	1	0.6	30	98	28	1	0	24	8	9	33	210	170	14	1.3	190	62
WLO-	75	9950N, 9730E	CLR	BIO	61.1	0.7	17.8	6	1.2	4.3	0.07	4.16	1.32	3.1	2.45	2.7	0.2	0.06	0.43	530	1	1.7	21	230	100	6	0	29	8	62	29	130	130	13	1.1	2200	64
WLO-	77	9950N, 9750E	CLR	BIO	66.2	0.7	14.1	5.7	1.3	4	0.02	2.55	1.82	4.7	0.78	2.4	0.4	0.14	0.05	120	1	3.4	27	120	660	16	18	9	10	18	14	150	0	110	15	23	620
WLO-	99	10250N, 9730E	CLR	T/A	74.9	0.34	11.5	2.4	0.5	1.7	0.02	1.84	1.9	5.1	0.15	0.6	0.3	0.09	0.08	40	1	1.8	8	67	940	29	24	41	10	7	3.6	65	4	190	23	21	670
WLO-	100	10260N, 9740E	WLH-MA	LA	51.4	0.99	15.9	11	2.3	7.6	0.08	5.8	7.48	4.1	1.49	2.1	0.1	0.24	0.11	180	0	1.6	30	210	210	2	0	65	9	56	28	240	210	24	2.2	37	72
WLO-	104	10340N, 9725E	WLH-CRT	LA	58.5	0.99	15.9	8.2	2.1	5.5	0.08	2.84	6.71	5.6	0.45	0.8	0.3	0.23	0	90	0	0.9	23	55	24	6	0	21	21	4	15	320	120	28	2.5	30	160

*intensely altered, protolith uncertain; **LF/RGLF: FSP vs APH protolith uncertain

Table 19.(continued)
Whole Rock and Trace Element Analytical Data

TYPE	SAMPLE	LOCATION	LITHUNIT	ALTN ZONE	SIO2	TIO2	AL2O3	FE2O3t	FE2O3	FEO	MNO	MGO	CAO	NA2O	K2O	H2Ot	CO2t	P2O5	S	BA	AG	BE	CO	CR	CU	LA	NB	NI	PB	RB	SC	SR	V	Y	YB	ZN	ZR
WLO-	106	10280N, 9730E	WLH-CRT	LA	57.2	0.45	14.6	4.3	0.9	3.1	0.03	1.86	2.94	6	0.25	1	0.5	0.14	0.46	80	0	1.1	30	91	1400	0	0	59	15	8	8.3	180	44	6	0.8	41	130
WLO-	114	11250N,9500E	CLR	LA	72.4	0.48	12.5	4.2	0.8	3.1	0.02	0.89	2.15	5.8	0.11	0.6	0.2	0.1	0.01	60	1	2	25	250	44	56	9	23	9	5	8.1	100	31	140	14	4	300
WLO-	115	11500N, 9600E	CLR	LA	71.8	0.47	13	4	0.7	3	0.03	0.92	2.65	5.9	0.12	0.5	0.1	0.1	0.01	50	0	2.2	16	62	7	13	19	28	8	3	7	73	21	220	21	7	320
WLO-	120	11570N, 9475E	CLR	LA	74.5	0.51	11.8	4.1	1.3	2.5	0.03	0.95	1.71	5.6	0.15	0.6	0.1	0.02	0.04	230	0	1.9	10	180	23	5	29	15	11	5	10	550	15	140	14	8	510
WLO-	123	8600N, 9550E	QFF	LA	77.7	0.18	12.1	1.4	0	1.7	0.01	0.37	1.19	5.2	0.33	0.6	0.3	0.02	0	90	0	4.5	5	110	8	38	53	3	7	10	2	150	0	120	19	22	400
WLO-	132	9740N, 9542E	QFF	BIO	79.5	0.11	10.3	1.6	0.2	1.3	0	1.73	0.9	4.1	0.81	0.6	0.2	0.02	0	100	0	5.2	6	120	4	140	54	3	8	25	1.9	100	0	140	16	0	310
WLO-	145	10050N, 9760E	CLR	BIO	71.1	0.29	11.3	3.9	0.7	2.9	0.01	5.31	1.06	2.8	2.3	1.7	0.1	0.05	0.06	200	0	2.9	18	200	110	68	36	4	11	52	3.5	110	0	180	20	29	620
WLO-	147	10100N, 9730E	CLR	BIO	61.2	0.25	8.8	1.9	0	1.8	0.01	1.62	0.85	3	0.94	0.6	0.5	0.05	0	170	0	0.9	7	280	22	35	36	5	6	22	5.9	110	0	130	15	16	490
WLO-	148	10050N, 9760E	CLR	BIO	83.3	0.26	8.3	1.4	0.2	1.1	0	1.46	0.59	2.9	0.84	0.8	0.2	0.04	0	100	0	0.8	6	45	15	32	37	2	10	20	5.8	83	0	110	15	16	410
WLO-	151	10210N, 9710E	QFF/CLR?	AN/GD	66.5	0.6	9.8	16.1	2.5	12.2	0.13	6.3	0.11	0.5	0.04	1.3	0.1	0.07	0	30	0	0.3	13	40	4	43	21	4	15	4	16	8	0	140	16	510	830
WLO-	154	10040N, 9560E	LF*	T/A	46.5	0.65	9	13.8	2.8	9.9	0.2	18.3	8.12	0.5	0.03	3.6	0.1	0.08	0.01	30	0	0.4	76	1400	67	0	0	610	6	0	24	7	130	14	1.2	72	55
WLO-	155	10040N, 9500E	LF(APH)	T/A	50.5	0.73	12.8	13.6	1.4	11	0.16	13.8	4.92	1.1	1.12	2.1	0.2	0.06	0	130	0	0.4	58	760	7	2	6	310	6	39	29	96	200	29	2.7	68	56
WLO-	156	10045N, 9550E	QFF	SIL	77.4	0.11	10.5	2.4	0.4	1.8	0.02	5.38	0.18	0.4	1.76	1.6	0.1	0.01	0	150	0	5.1	4	72	4	83	57	7	9	43	2.2	47	0	160	22	25	340
WLO-	158	10097N, 9487E	LF*	T/A	51.6	0.94	13	11.8	0.9	9.8	0.27	13.6	5.05	1.5	0.96	1.5	0.1	0.33	0	110	1	0.8	45	620	2	35	10	330	20	32	21	180	110	22	1.4	490	120
WLO-	159	10097N, 9487E	LF(APH)	AN/GD	51.5	0.87	11.2	14.3	1.1	11.9	0.31	17.4	1.12	0.9	0.86	2.7	0.2	0.03	0	80	0	1.5	43	240	0	0	13	74	14	36	51	55	180	28	3	610	46
WLO-	165	10108N, 9488E	LF(FSP)	LA	48.2	0.55	18.9	9.3	2.2	6.4	0.23	6.01	11.6	1.5	0.98	3	0.5	0.07	0.16	130	1	0.9	38	340	110	0	6	89	15	27	30	170	130	13	1.1	190	37
WLO-	168	10198N, 9493E	LF(FSP)	AN/GD	47.7	0.69	17	20.1	1.7	16.6	0.35	11.7	0.22	0.6	0.22	3.1	0.5	0.07	0.11	60	0	0.4	33	280	54	0	11	89	15	6	41	0	190	19	1.3	1600	44
WLO-	171	10234N, 9500E	LF(FSP)	LA	49.7	0.43	18.4	10.1	1.7	7.6	0.2	9.12	9.7	1.7	0.23	1.2	0.1	0.05	0.01	20	0	0.4	37	330	5	0	9	99	13	12	27	160	110	8	0.6	210	27
WLO-	176	10293N, 9516E	LF(APH)	AN/GD	50.5	0.87	18.9	13.2	1.2	10.8	0.21	13.4	1.07	0.5	0.26	1.8	0.1	0.1	0	80	1	1.5	35	96	2	0	0	36	5	4	31	53	200	19	1.6	260	61
WLO-	179	10312N, 9491E	LF(FSP)	AN/GD	48.8	0.55	17.7	23.3	4.2	17.2	0.2	7.75	0.39	0.7	0.22	1.9	0.1	0.07	0.2	90	1	0.4	24	320	70	19	0	72	6	6	34	13	150	34	1.8	640	28
WLO-	180	10335N, 9483E	LF(FSP)	T/A	50.3	0.53	17.4	11.1	0.9	9.2	0.24	8.95	7.1	0.8	1.49	2.7	0.2	0.07	0	220	0	0.8	32	270	4	0	0	74	7	41	34	200	140	11	0.9	250	30
WLO-	188	10600N, 9600E	CLR	BIO	70.5	0.48	13.9	3.7	0.4	3	0.02	6.07	0.45	1.4	1.82	1.7	0.2	0.06	0	110	0	2.3	8	67	3	21	20	11	8	53	8	37	17	77	8.7	19	350
WLO-	190	10960N, 9550E	CLR	BIO	74.8	0.46	12.1	2.2	0	2	0.01	2.95	1.17	3.7	1.25	1.2	0.4	0.07	0.01	240	1	0.7	9	130	12	42	19	13	3	31	6.8	110	23	89	9.4	8	300
WLO-	199	10525N, 9520E	QFF	SIL	76.9	0.13	11.5	4.2	0.8	3.1	0.03	2.96	0	0.1	2.31	2.5	0.5	0.01	0	530	1	1.7	3	37	8	0	49	0	3	32	2.2	7	0	110	16	71	360
WLO-	216	9905N, 9510E	LF(APH)	LA	50.1	0.74	15.4	11.9	2.8	8.2	0.27	8.37	10.9	1.4	0.16	1.5	0.2	0.09	0	40	0	1.3	37	240	0	0	7	52	13	3	41	110	200	18	1.8	140	54
WLO-	218	9900N, 9525E	LF(APH)	AN/GD	50.4	0.91	16	12.7	1.3	10.3	0.17	15.1	0.71	0.5	0.39	3.8	0.2	0.1	0	60	0	0.5	42	170	4	1	11	38	9	39	45	33	190	23	2.1	240	64
WLO-	243	10060N, 9770E	CLR	AN/GD	71.6	0.48	12.1	7.8	1.8	5.4	0.04	4.3	0.82	0.2	1.37	1.5	0.1	0.07	0	330	0	0.6	9	80	3	21	26	5	6	27	7	59	21	72	7.7	92	280
WLO-	244	10050N, 9700E	CLR	SIL	71.6	0.45	13.2	5.2	0.5	4.2	0.02	4.54	0.3	0.3	2.02	2.2	0.1	0.07	0	270	0	0.6	6	110	1	24	21	4	9	31	7.7	43	11	110	12	110	350
WLO-	247	10050N, 9760E	WLH-MA	AN/GD	51.9	1.01	16.2	7.4	0.6	6.1	0.03	11.9	2.84	3.7	1.36	3.4	0.4	0.27	0.01	110	0	0.9	32	190	6	22	5	61	10	32	27	240	180	18	1.3	92	79
WLO-	250	310E, 1070N	RGLF(GES)	LA	56.7	0.84	16.3	7.7	1.5	5.6	0.14	5.4	6.6	3.6	0.93	1.6	0.1	0.14	0	140	0	0.8	28	80	9	10	0	49	14	29	26	290	160	18	1.8	59	99
WLO-	259	235E, 1600N	RGSIV	T/A	58.1	0.74	15	10.6	1.2	8.5	0.62	8.4	2.86	0.6	2.67	3.2	0.1	0.12	0	500	0	0.7	27	130	0	8	7	40	10	44	27	100	150	14	1.5	1100	88
WLO-	265	250E, 2020N	RGSIV	BIO	65.5	0.5	12.2	10.7	1.3	8.5	0.17	6.22	0.19	0.1	1.16	4	0.2	0.1	0	330	0	1	24	180	8	5	8	130	11	30	10	13	55	8	0.7	300	120
WLO-	270	1850E, 9650N	SIV-VC	LA	72.9	0.52	10.9	7.7	2.8	4.4	0.29	0.57	2.44	3.8	0.32	0.7	0.1	0.09	0	80	0	3.6	5	51	5	46	32	5	12	5	13	89	0	180	18	120	590
WLO-	273	8075N, 9710E	SIV-VC	LA	74.5	0.26	11.5	5.8	1	4.3	0.06	0.51	1.01	4.3	0.61	1.1	0.3	0.03	0	110	0	4.5	2	35	2	33	43	18	8	20	3	64	0	190	23	42	600
WLO-	282	8120N, 9805E	CLR	LA	78.1	0.23	11.7	2	0.2	1.6	0.01	0.58	0.82	4.9	0.42	0.9	0.2	0.03	0.01	40	0	4.4	6	83	18	45	53	2	12	6	2.3	110	0	84	12	0	520
WLO-	284	8100N, 9830E	WLH-MA	LA	50.9	0.99	16	11.4	2.1	8.4	0.11	5.79	9.46	3.4	0.81	1.6	0.1	0.21	0	80	0	0.8	27	200	19	0	7	67	10	17	29	330	200	15	1.2	78	72
WLO-	328	7865N, 9700E	WLH-MA	LA	51.7	0.83	16	11.6	2	8.6	0.3	6.3	8.17	3.1	1.17	1.8	0.1	0.2	0	410	0	0.7	28	180	7	6	3	57	10	47	28	290	180	14	0.9	170	73
WLO-	366	430E, 060N	RGLF(GES)	LA	58.1	0.84	16	8.1	2.1	5.4	0.14	3.88	5.88	4.3	1.23	1.7	0.1	0.21	0.02	190	0	0.7	20	100	15	9	6	56	13	34	15	290	110	14	1.2	73	140
WLO-	373	410E, 1060N	RGSIV	BIO	58.3	0.54	14.6	17.2	7.1	9.1	1.35	4.2	0.84	0.1	1.76	2.1	0.2	0.11	0.11	550	0	1.2	18	150	47	12	5	30	14	42	17	4	67	49	4.7	970	150
WLO-	376	390E, 1080N	RGSIV	T/A	65.2	0.56	14.4	6.6	1.3	4.8	0.65	3.47	3.26	1.2	2.19	2.2	0.2	0.11	0.2	440	0	1	18	150	54	13	0	39	25	57	17	120	65	32	3.6	950	180
WLO-	377	375E, 1085N	RGSIV	BIO	54.4	0.62	16.3	16.8	5.2	10.4	0.25	5.38	0.35	0.3	2.15	2.9	0.3	0.12	0.72	410	0	1.6	21	190	170	16	11	56	19	36	16	31	110	21	2.2	5800	210
WLO-	391	1320S, 0095W	RGSIV	AN/GD	56.8	0.79	15.7	12.1	1.2	9.8	0.25	11.7	0.33	0.3	0.82	2.1	0.2	0.16	0	150	0	1.2	30	250	3	9	12	82	14	14	27	0	150	13	1.3	250	95
WLO-	396	1365S, 1160W	RGSIV	LA	61.1	0.66	14.2	11.7	4.7	6.3	0.29	1.76	4.73	3.9	1.02	1.4	0.2	0.15	0.05	190	0	2.4	23	340	40	7	4	120	22	20	14	290	91	14	0.9	430	94
WLO-	409	1430S, 1140W	RGSIV	T/A	51.1	0.73	15.1	19.9	5.8	12.7	1.14	8.84	1.09	0.3	1.15	2.2	0.2	0.12	0	250	0	1.1	32	330	13	4	15	68	13	16	32	21	150	25	2.2	2200	90
WLO-	413	1520S, 1130W	RGLF(APH)	BIO	50.9	0.74	17.1	19.7	8.4	10.2	0.59	6.01	0.65	0.2	1.88	3	0.4	0.09	0.02	460	0	0.8	26	110	10	1	8	28	14	39	31	17	160	20	1.7	1000	53
WLO-	417	1510S, 1000W	RGLF(APH)	AN/GD	51.5	0.8	18.2	14.5	1.7	11.5	0.19	11.7	0.2	0.3	0.9	2.6	0.2	0.1	0	70	0	0.8	23	110	1	1	11	37	12	20	33	6	180	19	1.9	330	69
WLO-	421	1550S, 1130W	RGLF(APH)	T/A	50.3	0.78	18.7	10	1.1	8	0.26	8.6	4.53	2.4	1.02	4	0.2	0.08	0	140	0	0.4	34	91	10	0	8	33	15	20	31	180	160	12	1.3	420	62
WLO-	424	1650S, 0050W	RGLF**?	AN/GD	44.3	0.63	18.4	22.1	8	12.7	0.25	10.7	0.59	0.1	1.87	2.9	0.2	0.07	0	170	0	0.9	20	120	2	1	6	39	14	39	24	10	120	27	2.6	89	47
WLO-	429	1690S, 1080W	RGLF**?	AN/GD	49.2	0.59	19.9	12.3	1.4	9.8	0.18	10.1	2.55	0.8	2	3.7	0.1	0.07	0	320	0	0.8	35	170	2	0	7	84	15	55	26	120	120	12	1	150	42
WLO-	439	1750S, 1025W	RGLF**?	LA	44.3	3.14	13	20.4	7.1	12	0.45	6.56	7.27	0.9	0.59	3.2	0.1	0.86	0.24	190	0	0.8	45	72	92	0	13	95	17	16	34	79	260	26	1.8	130	190
WLO-	443	2000S, 1000W	RGLF(FSP)	LA	48.6	0.5	17.1	9.8	2.1	6.9	0.26	8.64	9.7	1.9	1.36	2.3	0.1	0.06	0	280	0	0.5	43	300	10	0	0	97	16	45	33	180	140	9	0.9	160	25
WLO-	452	1565S, 995W	RGLF(APH)	LA	52.5	0.74	15.5	10.7	2.3	7.6	0.18	6.51	9.5	3.1	0.24	1.4	0.3	0.09	0.01	90	0	0.8	36	270	36	0	0	57	15	3	42	190	200	14	1.4	160	44
WLO-	453	1400S, 1100W	RGLF**?	T/A	57.1	0.79	15	13.8	1.5	11.1	0.21	10.2	0.42	0.2	0.65	2.7	0.2	0.14	0	170	0	0.8	34	240	23	8	13	92	14	18	26	4	160	14	1.5	260	110
WLO-	456	1300S, 1040W	RGLF(FSP)	LA	52.6	0.69	19.1	9.4	2.5	6.2	0.15	4.66	9.15	2.6	0.58	1.4	0.2	0.08	0.1	100	0	0.6	30	120	94	3	8	28	18	13	28	180	170	15	1.7	110	57
WLO-	463	1309S, 1130W	RGSIV	AN/GD	64.4	0.53	13.9	9.7	1.3	7.6	0.13	6	0.86	0.5	1.66	2.7	0.2	0.11	0.05	410	0	1.8	23	150	15	6	0	62	15	28	13	95	79	9	0.6	260	90
WLO-	468	1310S, 1105W	RMCLR	BIO	76.6	0.14	11.8	2	0.4	1.4	0.06	1.76	1.02	3.1	3	0.8	0.4	0.02	0	490	0	6.3	5	39	11	56	56	3	31	46	1.8	57	0	120	17	160	340

*intensely altered, protolith uncertain; **LF/RGLF: FSP vs APH protolith uncertain

Table 19.(continued)
Whole Rock and Trace Element Analytical Data

TYPE	SAMPLE	LOCATION	LITHUNIT	ALTN ZONE	SIO2	TIO2	AL2O3	FE2O3t	FE2O3	FEO	MNO	MGO	CAO	NA2O	K2O	H2Ot	CO2t	P2O5	S	BA	AG	BE	CO	CR	CU	LA	NB	NI	PB	RB	SC	SR	V	Y	YB	ZN	ZR
WLO-	482	9950N, 8490E	LCS	AN/GD	63	0.83	13.5	14.9	3.5	10.3	0.36	5.27	0.44	0.5	0.46	1.9	0.4	0.25	0.05	130	0	2.1	11	90	20	26	26	8	16	9	25	3	0	110	13	530	520
WLO-	484	9950N, 8455E	PCC	LA	68.9	0.59	11.9	8.9	2.9	5.4	0.21	1.59	4.22	2.8	0.14	0.8	1	0.13	0.01	70	0	2.6	6	230	13	13	30	7	17	6	16	89	0	110	13	260	530
WLO-	485	9950N, 8412E	CCLR	AN/GD	72.9	0.3	11.8	7.5	1.8	5.1	0.1	1.57	1.19	3.5	0.32	0.9	0.3	0.05	0	120	0	2.8	6	110	8	49	36	6	15	8	3.9	35	0	180	21	46	640
WLO-	486	9950N, 8360E	CCLR	AN/GD	73.1	0.4	11.6	7.6	1.6	5.4	0.12	1.76	1.67	3.2	0.11	1	0.1	0.1	0.01	90	0	2.7	6	180	2	46	36	5	16	2	5.9	54	0	160	19	81	650
WLO-	489	9950N, 8290E	CCLR	AN/GD	73	0.42	11.6	7.4	2.3	4.6	0.1	1.68	0.91	3.7	0.28	1.2	0.2	0.09	0.01	120	0	2.1	6	92	5	45	34	2	20	14	6.2	43	0	160	18	31	670
WLO-	501	9950N, 8180E	CCLR	AN/GD	68.6	0.53	11.7	11.1	3.3	7	0.07	3.41	0.33	1.2	1.83	1.9	0.1	0.18	0.01	190	0	2.7	8	130	9	19	35	2	18	60	8	15	0	110	13	55	590
WLO-	513	10300N, 8560E	CCLR	AN/GD	73.4	0.42	11.5	8.1	2.5	5	0.04	1.67	0.43	3.5	0.12	1.1	0.4	0.11	0.06	50	0	1.9	5	220	18	62	27	4	21	9	6.1	28	0	160	17	8	620
WLO-	514	10300N, 8550E	CCLR	AN/GD	72.2	0.43	11.4	7	0.7	5.7	0.04	5.72	0.27	0.6	1.08	2	0.2	0.12	0	300	0	2.1	7	110	7	43	28	4	19	26	6.9	16	0	180	18	37	620
WLO-	516	10300N, 8640E	LCS	AN/GD	74.6	0.3	11	8.9	0.5	5.8	0.06	3.28	0.15	1.1	1.34	1.6	0.3	0.04	0	550	0	2.8	5	150	2	19	29	0	6	41	4.3	5	0	110	13	41	640
WLO-	520	10300N, 8790E	LCS	AN/GD	70.7	0.35	9.8	12	3.1	8	0.1	4.2	0.22	0.2	1.46	1.7	0.2	0.07	0	370	0	1.3	11	190	3	19	26	30	13	26	7.1	0	20	87	10	66	280
WLO-	521	10300N, 8865E	PCC	T/A	68.8	0.59	12.3	9.2	2.9	5.7	0.15	2.01	2.18	4.4	0.08	0.5	0.3	0.12	0.05	70	0	2.5	5	110	13	25	21	5	12	5	15	82	0	94	12	210	540
WLO-	523	10300N, 8930E	PCC	T/A	65.5	0.75	12.2	12.3	3.6	7.8	0.4	2.15	3.75	2.4	0.12	0.8	0.5	0.19	0.01	80	0	2.3	6	180	9	13	17	7	11	2	25	61	0	100	12	250	470
WLO-	527	10900N, 8770E	CCLR	BIO	71.7	0.3	10.9	8.3	1.4	4.4	0.02	1.59	1.38	3.3	1.7	1.1	1.2	0.12	0.01	470	0	1.8	6	100	11	66	30	0	12	120	6.2	62	0	130	14	35	620
WLO-	532	10900N, 8990E	LCS	SIL-ST	66.3	0.83	13.2	13.7	4.3	8.5	0.11	2.42	0.3	0	1.92	1.9	0.5	0.2	0.01	520	0	5.1	6	180	35	25	28	3	16	300	18	1	0	120	13	300	530
WLO-	533	10900N, 9033E	PCC	LA	65	0.71	12.3	11.9	2.5	8.5	0.3	1.71	3.59	3.6	0.16	0.9	0.7	0.18	0.01	90	0	2	4	180	11	4	22	5	9	3	21	110	0	100	11	160	440
WLO-	536	11600N, 8830E	PCC	LA	67.4	0.67	12.1	10.6	3.7	6.2	0.11	1.7	3.29	1.9	1.43	1.2	0.4	0.17	0	260	0	3	6	170	8	16	16	2	10	51	16	69	0	110	12	200	430
WLO-	543	11600N, 9070E	LCS	SIL-ST	65.5	0.74	11.9	17.8	9.6	7.4	0.13	2.46	0.58	0.2	0.78	1.2	0.2	0.23	0	230	0	1.1	7	95	9	26	27	1	6	15	25	12	0	110	12	97	470
WLO-	545	11600N, 9100E	PCC	LA	70.9	0.59	10.6	9.5	3.5	5.4	0.11	1.1	3.19	2.4	0.34	1	0.2	0.16	0.45	80	0	2.9	8	210	93	7	22	5	10	13	20	120	0	94	10	100	380
WLO-	562	12900N, 9050E	CCLR	LA	68.8	0.45	14.1	4.8	1	3.4	0.05	1.65	3.92	5.4	0.16	0.5	0.1	0.11	0.01	60	0	4.8	5	67	68	10	24	20	10	9	6.1	160	0	140	17	69	670
WLO-	565	12900N, 9090E	PCC	LA	65.6	0.73	12.1	10.7	2.3	7.6	0.28	1.84	5.21	1.6	0.85	1.5	0.2	0.19	0.09	120	0	2.9	5	82	47	19	19	4	8	45	24	130	0	100	12	190	470
WLO-	571	12200N, 8995E	CCLR	LA	73.5	0.45	12.2	3.2	0.8	2.2	0.03	1.49	2.65	4.8	0.16	0.4	0.3	0.14	0	60	0	4.1	4	42	11	78	34	4	4	6	6.8	110	0	180	20	5	560
WLO-	574	12150N, 8985E	CCLR	LA	74.6	0.38	11.6	3.6	0.6	2.7	0.03	1.66	3.01	4.1	0.08	0.5	0.3	0.1	0	50	0	3.6	5	200	10	34	33	13	6	6	5.2	99	0	160	19	18	570
WLO-	581	12100N, 8965E	CCLR	AN/GD	74	0.56	12.2	4.8	0	4.1	0.08	2.31	2.49	4.1	0.1	0.6	0.1	0.16	0.01	60	0	4.2	5	260	13	34	34	11	6	6	9.4	110	0	110	13	25	570
WLO-	597	8450N, 9000E	RGLF(FSP)	LA	48.3	0.56	18.3	9.2	2.2	6.3	0.14	7.22	10.1	2.1	1.81	2.4	0.2	0.07	0.01	340	0	0.6	40	180	6	0	0	150	15	59	25	160	160	12	1.2	130	47
WLO-	611	9260N, 9600E	SIV-VC	LA	64.2	0.52	15	7.7	1.6	5.6	0.02	2.01	3.07	4.4	1.44	1.4	0.2	0.12	0.54	230	0	1.6	39	210	280	9	9	65	9	52	11	280	67	28	2.5	23	110
WLO-	613	8280N, 9590E	QFF	LA	78.5	0.13	11.1	1.9	0.3	1.4	0.01	0.19	0.69	3.8	2.61	0.5	0.4	0.03	0	350	0	5.4	2	83	8	40	63	0	8	48	2	38	0	170	24	6	370
WLO-	617	8080N, 9580E	SIV-VC	LA	50	0.98	7.6	18.2	3.6	13.1	0.37	7.79	11.8	0.9	0.97	1.5	0.1	0.12	0.59	300	0	1.8	74	1200	190	0	6	640	21	17	23	71	150	14	0.8	730	69
WLO-	642	8700N, 8625E	SIV-VC	LA	69.8	0.88	11.5	7.8	1.8	5.4	0.13	1.23	3.83	3.5	0.71	1	0.1	0.22	0	130	0	2.2	11	49	41	32	28	10	13	17	16	220	5	130	15	31	590
WLO-	650	8900N, 9625E	SIV-VC	LA	60.6	0.53	16.5	7.2	1.3	5.3	0.07	3.01	5.76	4.5	1.1	1.2	0.1	0.13	0	210	0	0.9	20	89	8	0	4	34	0	34	13	360	94	10	1	14	81
WLO-	655	300E, 145N	RGSIV	AN/GD	63.8	0.54	14	12.2	2	9.2	0.26	5.23	0.28	0.3	1.78	2.4	0.1	0.11	0.1	540	0	1.1	18	180	25	17	4	34	2	33	16	10	86	40	4	1900	180
WLO-	656	302E, 187N	RGSIV	T/A	61.9	0.54	13.9	7.7	1.6	5.5	0.4	6.33	1.83	1.2	2.75	2.9	0.6	0.11	0.23	910	0	1.3	17	170	170	9	0	30	12	55	16	100	89	29	3	2600	180
WLO-	657	300E, 170N	RGSIV	LA	60.4	0.93	15.5	8.1	2.9	4.7	0.13	3.04	5.97	3.6	0.62	1.2	0.8	0.42	0	260	0	1	17	210	45	19	0	42	8	12	13	640	86	21	2.1	160	180
WLO-	661	300E, 180S	GESSILL	LA	58.2	1.28	15.8	9.6	3.2	5.8	0.12	3.73	6.3	3.4	0.46	1.3	0.5	0.44	0.03	150	0	0.9	21	96	80	12	4	44	11	8	16	420	130	22	2.1	94	170
WLO-	664	315E, 220S	RGSIV	BIO	60.5	0.56	14.3	9.1	2.9	5.6	1.49	6.51	1.59	0.8	2.25	3.1	0.2	0.11	0.04	610	0	1.1	16	130	32	11	8	35	6	50	20	52	97	46	4.1	790	150
WLO-	668	350E, 162N	RGSIV	T/A	69.4	0.44	13	11.9	4	7.1	0.3	2.93	0.32	0.1	0.95	1.2	0.1	0.11	0.01	920	0	1	12	210	7	7	6	44	8	16	10	7	48	17	1.4	610	110
WLO-	676	1340S, 1170W	RMCLR	LA	69.3	0.53	13.6	4	1	2.7	0.64	1.14	4.71	3.9	0.71	1.1	0.1	0.1	0	120	0	3	6	230	2	7	20	71	8	16	13	190	58	40	3.7	670	120
WLO-	677	1340S, 1170W	RMCLRclot	LA	60.5	0.54	16.2	7.7	2	5.1	0.43	1.96	7.29	3.5	0.92	1.1	0.1	0.17	0	190	0	1.1	19	160	0	9	8	70	14	15	14	380	97	12	0.9	690	90
WLO-	678	1420S, 1160W	RMCLR	LA	73.2	0.4	13.2	4.7	1.8	2.6	0.16	0.55	2.19	4.4	0.79	1.2	0.1	0.06	0	170	0	2.1	7	56	5	30	22	10	11	26	5.6	250	12	82	8.9	450	300
WLO-	692	8714N, 8772E	CT	SIL-ST	79	0.26	9.7	6	2.1	3.5	0.3	1.8	0.06	0.1	1.28	1	0.3	0.02	0	370	0	1.6	4	140	18	1	57	2	4	28	1.2	8	3	150	26	2900	450
WLO-	693	8730N, 8767E	MA	LA	58.6	1	16.3	9.2	2.8	5.8	0.13	3.11	6.9	2.8	0.69	1.4	0.3	0.24	0.03	170	0	0.9	23	130	30	5	14	31	7	16	16	270	130	24	2.4	160	160
WLO-	695	8708N, 8745E	LF*	T/A	58.5	0.87	16	8.9	0.3	7.7	0.4	6.1	6.32	2.6	0.19	0.7	0.2	0.16	0	50	0	0.7	18	56	9	5	13	33	7	4	24	210	130	17	1.8	780	110
WLO-	696	8695N, 8735E	LF*	BIO	48.4	0.77	18.5	11.3	1.6	8.7	0.45	11.8	0.15	0	3.08	6.6	0.1	0.08	0	240	0	1.1	26	81	0	0	17	26	3	120	26	6	140	13	1.1	940	64
WLO-	698	8700N, 8705E	MA(FSP)	LA	49.2	0.58	17.4	10.8	2.1	7.8	0.27	7.76	9.8	0.8	1.68	2.5	0.1	0.07	0.02	230	0	0.5	37	220	7	0	12	110	9	55	27	130	180	11	0.9	480	45
WLO-	701	8810N, 8777E	MA(APH)	LA	50.3	0.56	15.9	10.4	2.5	7.1	0.21	8.48	9.8	2.5	0.54	1.9	0.4	0.07	0	50	0	0.4	35	330	6	0	7	69	8	15	36	130	160	10	1.1	140	36
WLO-	702	8820N, 8760E	RGLF(FSP)	T/A	48	0.46	18.3	9.7	1.1	7.7	0.19	9.7	6.58	1.7	2.12	4.3	0.1	0.05	0	270	0	0.4	34	290	0	0	9	93	11	58	28	200	140	7	0.7	320	31
WLO-	706	8797N, 8702E	MA(APH)	LA	48.8	0.52	18.1	9.5	2.2	6.6	0.3	7.62	10.7	1.7	0.87	2.1	0.3	0.06	0	70	0	0.5	31	300	13	0	0	87	6	18	29	130	130	10	0.9	520	26
WLO-	712	8875N, 8705E	QFP	BIO	77.4	0.19	11	3.5	1.1	2.2	0.35	2.01	0.17	0.7	2.31	2.2	0.5	0.02	0.02	230	0	3.3	2	230	43	24	37	4	8	37	1.3	17	0	130	18	90	390
WLO-	717	8720N, 8802E	CT	AN/GD	51.5	0.63	15.5	15.5	1.4	12.7	0.34	15	0.39	0.2	0.52	2.2	0.3	0.07	0	70	0	1.7	32	240	2	1	14	69	2	15	37	10	170	11	1	980	43
WLO-	718	8672N, 8820E	CT	AN/GD	51.4	0.89	17.2	11.7	1.1	9.5	0.2	14	0.98	0.4	1.65	2.9	0.2	0.1	0	180	1	0.5	36	120	1	0	17	34	8	38	36	36	200	15	1.6	510	71
WLO-	719	8625N, 8824E	CT	AN/GD	51.2	0.82	17.5	12.2	2.2	9	0.73	10.2	0.83	0.3	2.13	5.2	0.3	0.09	0.01	390	0	1.9	31	91	0	0	13	30	3	71	32	190	180	16	1.4	1100	59
WLO-	720	8625N, 8818E	CT	AN/GD	53.6	0.9	14.9	15.1	1.4	12.3	0.49	12.3	0.61	0.3	0.62	2.7	0.2	0.12	0.01	120	0	0.8	27	130	2	3	15	36	1	21	36	120	190	17	1.6	1300	64
WLO-	721	8604N, 8830E	LF*	T/A	53	0.74	18.3	10.8	2.9	7.1	0.28	8.24	4.34	4.4	1.1	1.7	0	0.08	0.01	260	0	0.5	29	120	23	1	12	39	3	31	30	250	180	14	1.4	160	54
WLO-	722	8680N, 8900E	MA	LA	56.9	0.75	14.9	8.2	2	5.6	0.17	7.17	7.3	2.4	1.44	1.8	0.2	0.13	0.01	420	0	0.6	25	260	3	3	14	56	3	30	29	200	160	16	1.6	110	88
WLO-	736	8112N, 9310E	QFF	LA	78.9	0.13	11.4	0.8	0.1	0.6	0.01	0.26	0.36	4.7	2.02	0.3	0.3	0.03	0.01	350	0	3.2	1	36	8	51	68	0	26	36	1.6	32	0	97	14	230	390
WLO-	757	12300N, 9220E	LF	BIO(CH	49.3	0.72	14.9	14.6	1.6	11.5	0.07	14	0.18	0	0.24	7.4	0.2	0.09	0	70	0	0.5	17	130	0	22	17	52	2	17	26	0	160	20	1.3	55	98
WLO-	786	10600N, 8750E	CCLR	AN/GD	75.4	0.25	11.5	6.1	0.3	5.2	0.04	2	0.26	4	0.09	1	0.3	0.03	0	40	0	2.2	2	230	2	22	43	2	3	6	2.5	17	0	150	19	7	580

*intensely altered, protolith uncertain; **LF/RGLF: FSP vs. APH protolith uncertain

Table 19.(continued)
Whole Rock and Trace Element Analytical Data

TYPE	SAMPLE	LOCATION	LITHUNIT	ALTN ZONE	SIO2	TIO2	AL2O3	FE2O3t	FE2O3	FEO	MNO	MGO	CAO	NA2O	K2O	H2Ot	CO2t	P2O5	S	BA	AG	BE	CO	CR	CU	LA	NB	NI	PB	RB	SC	SR	V	Y	YB	ZN	ZR
WLO-	788	10600N, 8625N	CCLR	AN/GD	71.2	0.4	11.9	9.4	1.5	7.1	0.09	2.19	1.04	3.1	0.18	1.2	0.3	0.09	0.02	60	0	4.5	4	180	8	45	39	4	0	8	6.8	40	0	170	16	29	540
WLO-	790	10600N, 8925E	LCS	AN/GD	65.9	0.87	12.6	14	4.4	8.6	0.13	3.26	1.48	1.4	0.52	1	0.2	0.29	0	220	0	3.5	7	130	4	31	32	1	0	13	18	24	0	130	14	88	490
WLO-	791	10600N, 8960E	PCC	LA	68.3	0.59	12.2	10.1	4.8	4.8	0.24	1.04	3.83	3.1	0.27	0.7	0.2	0.13	0.29	120	0	2.2	5	73	74	3	32	0	2	9	16	130	0	110	13	130	460
WLO-	793	10600N, 9075E	QFP	LA/BIO	77.6	0.14	11.1	3.4	0.7	2.4	0.01	0.91	0.4	5	0.64	0.8	0.2	0.02	0	210	0	7.6	2	130	4	21	53	1	0	50	0.6	55	0	150	19	6	340
WLO-	795	10600N, 9250E	QFP	LA	78.6	0.17	11.1	2.2	0.3	1.7	0.01	1.11	0.75	4.8	0.7	0.6	0.2	0.02	0.04	150	2	3.2	4	140	130	50	48	2	0	13	0.9	75	0	160	19	5	370
WLO-	801	10035N, 8140E	LCS	AN/GD	59.5	0.75	12.2	21.5	9.6	10.7	0.1	2.89	0.45	1.5	0.12	1.3	0.2	0.17	0.45	80	0	2.9	20	140	430	19	23	0	3	7	19	47	0	91	10	5600	410
WLO-	803B	10000N, 8110E	QFP	BIO	75.4	0.15	11.5	4.1	1	2.8	0.07	1.91	0.38	0.4	3.45	1.9	0.7	0.02	0	500	0	3.4	2	280	8	1	60	0	3	55	0.5	12	0	86	16	180	430
WLO-	805	8910N, 8980E	QFP	SIL	78.1	0.2	10.6	3.8	0.4	3.1	0.1	3.12	0.23	0.4	2.16	1.5	0.1	0.03	0.01	290	0	2.7	2	170	4	12	45	2	2	49	1.4	36	0	160	19	180	410
WLO-	807	8930N, 8920E	QFP	SIL	80.5	0.14	10.6	2.4	0.2	2	0.07	2.15	0	0.1	2.76	1.6	0.3	0.02	0	280	2	3.4	3	320	3	5	47	4	2	42	0.7	4	0	100	14	250	400
WLO-	822	9750N, 8400E	QFP	BIO	76.7	0.14	11.3	4	0.3	3.3	0.02	0.96	0.76	4.3	1.25	0.7	0.3	0.02	0	330	0	3.5	6	180	3	43	52	0	0	30	0.8	60	0	160	19	34	410
WLO-	831	11200N, 8960E	LCS	AN/GD	69.9	0.8	12.8	7.3	0.5	6.1	0.08	3.13	2.66	2.8	0.3	1	0.2	0.29	0	120	0	3.1	7	240	7	23	33	4	2	12	15	65	0	110	12	54	450
WLO-	832	11200N, 8990E	LCS	SIL-ST	64.7	0.75	11.3	20.7	9.5	10.1	0.17	1.92	0.36	0	0.41	0.6	0.2	0.13	0.01	180	0	0.8	9	220	8	26	31	4	2	21	22	0	0	110	13	32	470
WLO-	837	11750N, 9000E	LCS	AN/GD	58.2	0.79	13.3	20.4	5.8	13.1	0.1	4.8	0.28	0.4	1.22	1.8	0.2	0.19	0	210	0	1.1	9	100	3	31	32	2	4	40	24	8	0	120	12	46	500
WLO-	841	11700N, 9097E	LCS	AN/GD	68.1	0.75	11.3	14	2.2	10.6	0.25	4.37	0.25	0.4	0.34	1.3	0.1	0.16	0.01	110	2	1.8	6	190	5	21	30	3	2	19	22	0	0	91	10	140	470
WLO-	844	10370N, 9430E	LF*	LA	44.9	2.21	14.1	16.7	3.9	11.5	0.34	8.97	9.9	1	0.32	2.3	0.2	0.31	0.09	50	2	0.7	52	270	89	0	16	220	8	11	26	68	270	19	1.5	320	100
WLO-	847	10040N, 9580E	QFF	SIL-ST	76.2	0.12	13.1	2.5	0.5	1.8	0.01	4.21	0.02	0.1	1.82	1.8	0.1	0.02	0	170	0	19	2	110	4	77	84	4	2	40	1.6	7	0	250	32	32	380
WLO-	849	8700N, 9335E	LF*-selvedge	LA	62.1	0.2	6.4	14.7	2.6	10.9	0.49	9.27	6.41	0.5	0.1	1.2	0.1	0.09	0.2	30	1	0.7	52	85	110	0	17	39	6	0	11	0	130	18	1.7	150	36
WLO-	850	8700N, 9335E	LF(FSP)	LA	50.1	0.76	21.6	7.9	1.3	5.9	0.2	3.97	8.58	2.9	2.05	2.2	0	0.09	0.27	200	1	2.1	34	120	160	2	8	45	9	75	29	300	120	14	1.4	86	57
WLO-	852	11750N, 9170E	QFP	SIL-ST	77.4	0.14	11.1	4.8	0.5	3.9	0.02	2.62	0.03	0.1	1.73	1.9	0.2	0.02	0	830	0	2.1	4	130	3	14	54	0	5	35	0.8	0	0	160	22	6	440
WLO-	853	11200N, 9060E	QFP	SIL-ST	75.8	0.19	10.7	8.7	1.8	6.2	0.06	2	0.05	0.2	1.51	1.2	0.1	0.03	0.01	350	0	3	3	95	9	32	47	0	4	28	1.6	0	0	200	22	30	490
WLO-	862	11710N, 9350E	CLR	BIO	71.1	0.52	13.9	2.4	0.3	1.9	0.01	3.97	0.92	4	0.93	2.1	0.2	0.09	0	100	0	1.4	9	110	1	7	26	11	8	24	7.2	82	28	93	10	0	310

*intensely altered, protolith uncertain; **LF/RGLF: FSP vs. APH protolith uncertain

ANALYTICAL CHECKS																																					
R-MW-102					80.5	0.1	11	3.1	0	2.9	0.01	3.17	0	0.1	0.9	1.1	0.2	0.02	0	150	2	4.5	4	270	7	12	73	2	6	18	1.9	0	0	160	24	65	360
R-MW-243					77	0.15	11	2.9	0	2.6	0.02	2.16	1.88	2.8	1.01	1	0.2	0.02	0	240	0	2.9	8	240	13	2	51	1	10	24	2.7	180	4	130	16	15	370
R-WLO-104					58.8	0.96	15.9	8.2	1.9	5.7	0.06	2.83	6.75	5.7	0.44	0.8	0.3	0.22	0	80	1	0.9	21	46	24	4	12	19	8	5	16	320	130	27	2.7	26	160
R-WLO-147					81.4	0.24	8.9	1.9	0	1.9	0	1.62	0.85	3	0.94	0.7	0.4	0.05	0.01	180	1	1	8	280	25	35	41	2	8	24	6.1	110	0	140	16	17	440
R-WLO-366					58.1	0.84	16.1	8.1	1.8	5.7	0.14	3.88	5.85	4.3	1.24	1.6	0.1	0.21	0.03	200	1	0.7	22	99	14	6	15	58	8	41	15	290	110	14	1.3	75	140
R-WLO-489					73.3	0.42	11.7	7.3	1.9	4.9	0.1	1.67	0.89	3.8	0.28	1.2	0.2	0.1	0	90	1	2	5	85	5	44	42	0	7	13	6.1	46	0	170	18	26	570
R-WLO-533					65	0.71	12.4	11.9	2.2	8.7	0.31	1.72	3.59	3.6	0.15	0.9	0.7	0.18	0.01	80	2	2	2	180	9	2	29	0	9	6	21	98	0	100	12	160	430
R-WLO-801					59.5	0.73	12.2	21.5	9.4	10.9	0.1	2.9	0.46	1.5	0.12	1.3	0.2	0.17	0.47	70	2	2.9	20	140	430	20	26	1	21	4	19	51	0	92	11	5600	400
R-WL7-540					66.7	0.19	13.7	9.7	1	7.8	0.05	4.68	0.03	0.2	2.72	2	0	0.03	0.27	620	2	1.8	7	86	56	8	67	3	32	42	1.9	3	0	190	21	67	500
R-WL10-436					72.1	0.54	12.1	8.7	0.8	7.1	0.06	2.49	0.62	3.6	0.12	0.9	0.1	0.14	0	60	3	2.3	6	170	8	37	41	0	26	3	9.2	26	0	140	16	18	500

Table 20.

Calculations of Mass Balance Changes and Statistical Data

Calculations

Component gains and losses of various alteration types vs. least altered "equivalents" were calculated according to the method of Grant (1986) as illustrated in Figure 29 on the basis of a best fit Ti-Al-Zr, Ti-Al, or constant Al_2O_3 isocon.

Abbreviations

N = number of analyses statistically calculated

Unit codes as listed on Table 2 in text.
LF's = average of LF and correlative RGLF units

ALTN = alteration zones
LA = least altered; T/A = tremolite/actinolite; BIO = biotite; SIL = sillimanite; SIL-ST = sillimanite-staurolite; AN/GD = anthophyllite/gedrite

Table 21.

Average and Standard Deviation Data and Mass Balance Calculations for Felsic Lava Flows (QFP, QFF)

NUMBER	STATS	UNIT	ALTN	SIO2	TIO2	AL2O3	FE-T	FE2O3	FEO	MNO	MGO	CAO	NA2O	K2O	H2Ot	CO2t	P2O5	S	BA	AG	BE	CO	CR	CU	LA	NB	NI	PB	RB	SC	SR	V	Y	YB	ZN	ZR
N=2	AVG:	QFP	LA	78.10	0.16	11.10	2.80	0.50	2.05	0.01	1.01	0.58	4.90	0.67	0.70	0.20	0.02	0.02	180	1.00	5.40	3.00	135	67.0	35.5	50.5	1.5	0.0	31.5	0.8	65.0	0.0	155	19.00	6	355
	STD:	QFP	LA	0.50	0.02	0.00	0.60	0.20	0.35	0.00	0.10	0.18	0.10	0.03	0.10	0.00	0.00	0.02	30	1.00	2.20	1.00	5	63.0	14.5	2.5	0.5	0.0	18.5	0.2	10.0	0.0	5	0.00	1	15
N=4	AVG:	QFP	BIO	76.50	0.16	11.27	3.67	0.80	2.77	0.15	1.63	0.44	1.80	2.34	1.60	0.50	0.02	0.01	387	0.00	3.40	3.33	230	16.0	22.7	49.7	1.3	3.7	40.7	0.9	29.7	0.0	125	17.67	101	410
	STD:	QFP	BIO	0.83	0.02	0.21	0.26	0.36	0.45	0.15	0.47	0.24	1.77	0.90	0.65	0.16	0.00	0.01	156	0.00	0.06	1.89	41	17.8	17.2	9.5	1.9	3.3	10.5	0.3	21.5	0.0	30	1.25	60	16
N=6	AVG:	QFP	SIL	77.90	0.16	10.96	3.77	0.43	3.02	0.06	2.77	0.11	0.30	2.23	1.77	0.18	0.02	0.01	407	0.33	3.15	2.17	190	7.5	29.3	45.0	1.3	6.2	43.5	0.9	17.0	0.0	172	21.33	133	407
	STD:	QFP	SIL	2.11	0.02	0.69	1.51	0.27	1.19	0.05	0.74	0.13	0.34	0.52	0.29	0.11	0.00	0.01	158	0.75	0.87	0.69	87	8.0	20.9	7.0	1.4	4.2	9.2	0.3	13.9	0.0	53	5.37	92	18
N=7	AVG:	QFP	SIL-ST	75.56	0.17	11.11	6.73	0.93	5.21	0.04	2.89	0.02	0.09	1.66	1.70	0.14	0.02	0.05	540	0.29	2.09	4.00	121	30.4	27.3	50.4	0.6	6.1	33.3	1.1	4.0	0.0	181	21.57	57	441
	STD:	QFP	SIL-ST	3.70	0.02	1.09	1.72	0.48	1.25	0.01	0.99	0.02	0.06	0.39	0.26	0.16	0.00	0.10	193	0.45	0.59	1.07	70	47.3	22.9	8.3	1.0	2.4	5.5	0.4	3.8	0.0	34	2.13	35	46
ISOCON:SLOPE		COMPARISON		FRACTIONAL CHANGES																																	
TI-AL-ZR: 1.03		BIO-LA		-0.05	0.00	-0.01	0.34	0.55	0.31	13.24	0.58	-0.26	-0.84	2.39	1.22	1.43	-0.03	-0.68	1.09	-1.00	-0.39	0.06	0.65	-0.74	-0.38	-0.05	-0.14		0.25	0.12	-0.56		-0.21	-0.10	16.89	0.12
TI-AL-ZR: 1.01		SIL-LA		-0.01	0.01	-0.02	0.33	-0.14	0.46	5.27	1.72	-0.82	-0.94	2.30	1.50	-0.09	0.07	-0.67	1.24	-0.67	-0.42	-0.26	0.39	-0.89	-0.18	-0.12	-0.12		0.37	0.12	-0.74		0.10	0.11	22.94	0.13
TI-AL-ZR: 1.03		SIL-ST-LA		-0.06	0.04	-0.03	1.33	0.80	1.47	2.68	1.77	-0.98	-0.96	1.69	1.38	-0.31	0.11	1.43	1.91	-0.72	-0.63	0.29	-0.13	-0.56	-0.25	-0.03	-0.63		0.03	0.44	-0.94		0.14	0.10	9.06	0.21
		T/A-LA		ABSOLUTE CHANGES																																	
TI-AL-ZR: 1.03		BIO-LA		-3.83	0.00	-0.16	0.95	0.26	0.64	0.13	0.57	-0.15	-3.15	1.60	0.85	0.29	-0.00	-0.01	195	-1.00	-2.10	0.24	68.3	-49.5	-13.5	-2.28	-0.21		7.98	0.09	-36.2		-33.3	-1.85	92.9	43.1
TI-AL-ZR: 1.01		SIL-LA		-0.97	0.00	-0.23	0.93	-0.07	0.94	0.05	1.74	-0.47	-4.60	1.54	1.05	-0.02	0.00	-0.01	223	-0.67	-2.26	-0.85	52.6	-59.6	-6.46	-5.95	-0.18		11.57	0.09	-48.2		15.0	2.12	126	47.6
TI-AL-ZR: 1.03		SIL-ST-LA		-4.74	0.01	-0.31	3.73	0.40	3.01	0.03	1.79	-0.55	-4.62	1.13	0.95	-0.06	0.00	0.03	344	-0.72	-3.38	0.88	-17.8	-37.5	-9.01	-1.54	-0.95		0.82	0.33	-61.1		21.1	1.94	49.8	73.6
		AN/GD-LA																																			
NUMBER	STATS	UNIT	ALTN	SIO2	TIO2	AL2O3	FE-T	FE2O3	FEO	MNO	MGO	CAO	NA2O	K2O	H2Ot	CO2t	P2O5	S	BA	AG	BE	CO	CR	CU	LA	NB	NI	PB	RB	SC	SR	V	Y	YB	ZN	ZR
WLO-123		QFF	LA	77.7	0.16	12.1	1.4	5E-05	1.7	0.01	0.37	1.19	5.2	0.33	0.6	0.3	0.02		90		4.5	5	110	8	38	53	3	7	10	2	150		120	19	22	400
N=3	AVG:	QFF	BIO	77.57	0.14	10.80	2.00	0.20	1.63	0.01	2.27	1.33	3.47	1.11	0.83	0.20	0.02	0.00	130	0.00	4.0	6.67	177	7.0	54.7	44.7	4.0	11.3	27.7	2.1	136.7	1.0	119	14.67	1	347
	STD:	QFF	BIO	1.37	0.02	0.36	0.64	0.06	0.62	0.01	0.52	0.42	0.53	0.30	0.26	0.06	0.00	0.00	50	0.00	0.9	0.94	60	4.2	60.7	6.6	0.8	4.0	6.6	0.4	33.0	1.4	23	1.89	1	26
N=6	AVG:	QFF	SIL	77.85	0.14	11.43	2.61	0.35	2.24	0.02	2.97	0.23	0.75	1.97	1.70	0.20	0.02	0.01	458	0.25	2.9	4.38	112	8.1	40.1	51.6	1.0	6.9	37.5	2.2	31.8	0.0	175	22.88	24	364
	STD:	QFF	SIL	0.57	0.02	0.44	1.21	0.22	0.91	0.01	1.01	0.18	0.53	0.41	0.43	0.12	0.00	0.02	231	0.43	1.2	1.32	50	10.3	45.0	11.5	2.3	2.3	6.5	0.4	23.1	0.0	50	5.11	29	13
N=6	AVG:	QFF	SIL-ST	77.28	0.13	11.65	2.93	0.33	2.38	0.01	3.59	0.25	0.55	1.64	1.65	0.10	0.02	0.00	230	0.00	6.9	3.33	183	3.7	25.8	59.8	2.2	6.2	31.7	1.9	46.8	0.0	198	27.00	51	368
	STD:	QFF	SIL-ST	1.83	0.01	0.70	1.20	0.21	1.02	0.00	0.47	0.34	0.60	0.40	0.41	0.06	0.00	0.00	109	0.00	5.8	1.60	170	1.9	25.6	12.1	2.3	3.1	14.1	0.2	49.9	0.0	45	4.83	43	12
N=4	AVG:	QFF	AN/GD	74.83	0.15	11.40	5.10	0.43	4.23	0.02	5.43	0.02	0.10	0.99	2.05	0.20	0.03	0.02	108	0.00	0.9	5.50	148	113.5	64.0	50.8	6.8	16.5	19.3	2.9	7.3	0.0	164	20.00	117	370
	STD:	QFF	AN/GD	2.44	0.02	1.09	2.75	0.57	2.00	0.01	0.38	0.01	0.00	0.10	0.90	0.07	0.01	0.03	59	0.00	0.2	4.97	62	177.1	49.7	5.0	7.7	11.3	3.6	1.0	1.3	0.0	50	3.74	123	35
ISOCON:SLOPE		COMPARISON		FRACTIONAL CHANGES																																	
TI-AL-ZR: 0.88		BIO-LA*		0.13	-0.01	0.01	0.62		0.09	-0.24	5.98	0.27	-0.24	2.82	0.58	-0.24	0.14		0.64		0.00	0.52	0.83	-0.01	0.63	-0.04	0.52	0.84	2.14	0.21	0.04		0.12	-0.12	-0.97	0.13
TI-AL-ZR: 0.96		SIL-LA*		0.02	-0.11	-0.04	1.05		0.34	0.53	7.18	-0.80	-0.85	5.08	1.89	-0.32	-0.17		4.19		-0.35	-0.11	0.04	0.04	0.08	-0.01	-0.66	0.00	2.83	0.14	-0.78		0.49	0.23	0.10	0.02
TI-AL-ZR: 0.97		SIL-ST-LA*		0.03	-0.16	0.01	1.16		0.45	-0.14	8.99	-0.79	-0.89	3.82	1.84	-0.66	-0.05		1.83		0.57	-0.31	0.71	-0.53	-0.30	0.16	-0.26	-0.09	2.26	-0.01	-0.68		0.70	0.47	1.39	0.03
TI-AL-ZR: 1.01		AN/GD-LA*		-0.05	-0.07	-0.07	2.61		1.46	0.49	13.53	-0.99	-0.96	1.96	2.38	-0.34	0.36		0.18		-0.80	0.09	0.33	13.05	0.67	-0.05	1.23	1.33	0.91	0.45	-0.95		0.35	0.04	4.28	-0.05
ISOCON:SLOPE		COMPARISON		ABSOLUTE CHANGES																																	
		T/A-LA																																			
TI-AL-ZR: 0.88		BIO-LA		10.44	-0.00	0.17	0.87	0.00	0.16	-0.00	2.21	0.32	-1.26	0.93	0.35	-0.07	0.00		57.7		0.01	2.58	90.76	-0.05	24.12	-2.24	1.55	5.88	21.44	0.42	5.30		14.85	-2.33	-21.24	0.00
TI-AL-ZR: 0.96		SIL-LA		1.53	-0.02	-0.44	1.47	0.00	0.58	0.01	2.66	-0.95	-4.43	1.68	1.13	-0.10	-0.00		376.8		-1.57	-0.54	4.41	0.29	2.94	-0.32	-1.96	0.02	26.27	0.26	-1.18		58.57	4.34	2.11	0.00
TI-AL-ZR: 0.97		SIL ST-LA		1.97	-0.03	0.12	1.62	0.00	0.76	-0.00	3.33	-0.94	-4.63	1.26	1.10	-0.20	-0.00		147.1		2.58	-1.56	78.14	-4.22	-11.4	8.68	-0.77	-0.64	22.65	-0.02	-1.02		84.47	8.84	30.58	0.00
TI-AL-ZR: 1.01		AN/GD-LA		-3.62	-0.01	-0.81	3.65	0.00	2.48	0.00	5.01	-1.17	-5.10	0.65	1.43	-0.10	0.01		16.4		-3.58	0.45	36.04	104.4	25.37	-2.75	3.68	9.34	9.06	0.90	-1.43		41.88	0.80	94.09	0.00

*WLO-123 used as Least Altered sample

Table 22.
Average and Standard Deviation Data and Mass Balance Calculations for Felsic Pyroclastic Flow Units (CCLR, CLR)

NUMBER	STATS	UNIT	ALTN	SIO2	TIO2	AL2O3	FE-T	FE2O3	FEO	MNO	MGO	CAO	NA2O	K2O	H2Ot	CO2t	P2O5	S	BA	AG	BE	CO	CR	CU	LA	NB	NI	PB	RB	SC	SR	V	Y	YB	ZN	ZR
N=3	AVG:	CCLR	LA	72.3	0.43	12.6	3.9	0.8	2.8	0.04	1.60	3.19	4.8	0.13	0.5	0.2	0.12	0.00	63	0.0	4.2	4.7	103	29.7	40.7	30.3	12.3	7.3	7.0	6.0	123.0	0.0	160	18.7	30.7	600
	STD:	CCLR	LA	2.5	0.03	1.1	0.7	0.2	0.5	0.01	0.06	0.53	0.5	0.05	0.0	0.1	0.02	0.00	12	0.0	0.5	0.5	69	27.1	28.2	4.5	6.5	2.5	1.4	0.7	26.5	0.0	16	1.2	27.6	50
N=3	AVG:	CCLR	BIO	69.4	0.38	11.0	7.4	1.1	5.7	0.03	5.09	0.61	1.3	2.31	2.4	0.5	0.10	0.00	527	0.7	1.8	6.3	117	5.0	46.0	36.3	6.7	9.3	132.0	6.9	23.7	4.7	127	13.4	60.7	513
	STD:	CCLR	BIO	5.1	0.06	1.5	1.0	0.4	1.0	0.01	2.91	0.55	1.4	0.81	1.0	0.5	0.02	0.00	220	0.5	0.6	0.5	54	4.3	14.2	7.6	9.4	2.5	43.3	0.7	27.4	4.6	29	3.2	49.6	105
N=8	AVG:	CCLR	AN/GD(FG)	73.1	0.41	11.8	7.4	1.3	5.5	0.06	1.96	1.06	3.6	0.17	1.0	0.2	0.10	0.01	74	0.3	2.9	5.1	180	6.0	42.8	36.4	4.6	11.0	7.5	6.4	43.9	0.0	155	17.8	30.4	606
	STD:	CCLR	AN/GD(FG)	1.2	0.10	0.3	1.4	0.9	1.0	0.03	0.33	0.67	0.3	0.06	0.2	0.1	0.04	0.02	30	0.7	0.9	1.5	54	5.1	10.9	4.4	2.7	7.3	3.2	2.3	27.2	0.0	19	2.2	22.6	42
N=2	AVG:	CCLR	AN/GD(CG)	70.4	0.48	11.6	9.1	2.0	6.4	0.06	4.57	0.30	0.9	1.45	2.0	0.2	0.15	0.01	245	0.0	2.4	7.5	120	8.0	31.0	31.5	3.0	18.5	43.0	7.5	15.5	0.0	135	15.5	46.0	605
	STD:	CCLR	AN/GD(CG)	1.8	0.05	0.1	2.1	1.3	0.7	0.02	1.16	0.03	0.3	0.39	0.1	0.1	0.03	0.01	55	0.0	0.3	0.5	10	1.0	12.0	3.5	1.0	0.5	17.0	0.5	0.5	0.0	25	2.5	9.0	15
ISOCON:SLOPE		COMPARISON		FRACTIONAL CHANGES																																
*CNST AL2O3: 0.88		BIO-LA		0.10	0.02	-0.00	1.18	0.53	1.35	0.04	2.64	-0.78	-0.70	19.85	4.81	1.29	-0.02	0.15	8.52		-0.51	0.55	0.30	-0.81	0.30	0.37	-0.38	0.46	20.59	0.30	-0.78		-0.09	-0.18	1.27	-0.02
CNST AL2O3: 0.93		AN/GD(FG)-LA		0.06	0.04	0.00	1.06	0.79	1.11	1.30	0.31	-0.64	-0.19	0.40	1.24	-0.02	-0.12	3.42	0.25		-0.27	0.18	0.88	-0.71	0.13	0.29	-0.60	0.61	0.15	0.13	-0.62		0.04	0.02	0.06	0.08
CNST AL2O3: 0.92		AN/GD(CG)-LA		0.06	0.22	0.00	1.54	1.72	1.49	0.63	2.10	-0.90	-0.79	11.40	3.54	-0.30	0.40	0.63	3.20		-0.37	0.75	0.27	-0.71	-0.17	0.13	-0.74	1.74	5.68	0.34	-0.86		-0.08	-0.10	0.63	0.10
ISOCON:SLOPE		COMPARISON		ABSOLUTE CHANGES																																
		T/A-LA																																		
*CNST AL2O3: 0.88		BIO-LA		7.20	0.01	-0.00	4.57	0.42	3.72	0.00	4.22	-2.49	-3.32	2.51	2.24	0.30	-0.00	0.00	540	0.0	-2.1	2.6	31	-23.9	12.0	11.3	-4.7	3.4	144	1.8	-95.9		-15.0	-3.3	38.8	-12.2
		SIL-LA																																		
		SIL-ST-LA																																		
CNST AL2O3: 0.93		AN/GD(FG)-LA		6.04	0.02	0.00	4.08	0.63	3.08	0.05	0.50	-2.04	-0.91	0.05	0.58	-0.01	-0.01	0.01	16	0.0	-1.1	0.8	90	-21.1	5.2	8.7	-7.4	4.5	1	0.8	-76.0		6.2	0.4	1.9	49.9
CNST AL2O3: 0.92		AN/GD(CG)-LA		4.22	0.10	0.00	5.97	1.37	4.14	0.02	3.36	-2.67	-3.79	1.44	1.65	-0.07	0.05	0.00	203		-1.56	3.49	27.43	-21.0	-6.97	3.91	-9.07	12.78	39.74	2.06	-106		-13.3	-1.82	19.33	57.61

NUMBER	STATS	UNIT	ALTN	SIO2	TIO2	AL2O3	FE-T	FE2O3	FEO	MNO	MGO	CAO	NA2O	K2O	H2Ot	CO2t	P2O5	S	BA	AG	BE	CO	CR	CU	LA	NB	NI	PB	RB	SC	SR	V	Y	YB	ZN	ZR
N=11	AVG:	CLR	LA	74.01	0.40	12.30	3.59	0.78	2.53	0.04	0.91	2.03	5.38	0.33	0.67	0.21	0.06	0.04	105	0.5	3.2	11.3	108	26.6	40.8	35.6	10.3	8.0	8.8	6.2	157.3	10.1	147	16.27	30.6	456
	STD:	CLR	LA	2.38	0.10	0.55	1.64	0.66	1.05	0.02	0.85	0.65	0.42	0.26	0.30	0.10	0.04	0.06	83	0.6	1.3	8.0	65	19.3	42.7	15.4	8.5	2.3	5.6	3.0	121.2	10.0	52	5.26	75.4	139
N=14	AVG:	CLR	BIO	72.52	0.45	12.44	3.27	0.52	2.49	0.02	3.43	1.15	3.45	1.31	1.58	0.32	0.07	0.06	180	0.3	1.8	12.6	145	142.4	26.4	22.6	10.4	7.7	33.1	8.4	110.2	22.0	91	10.43	174.6	373
	STD:	CLR	BIO	5.69	0.14	2.38	1.58	0.50	1.02	0.02	1.49	0.36	0.85	0.54	0.64	0.17	0.03	0.11	114	0.5	1.0	8.4	83	263.5	17.3	10.6	10.3	2.3	13.7	6.2	31.0	31.8	37	4.46	562.3	143
N=2	AVG:	CLR	SIL	71.60	0.46	13.60	3.20	0.25	2.65	0.01	4.27	0.82	1.85	2.03	1.75	0.05	0.08	0.00	310	1.0	1.3	12.0	120	1.5	87.0	23.0	6.5	6.5	39.0	8.1	86.5	12.0	140	13.50	55.0	350
	STD:	CLR	SIL	0.00	0.01	0.40	2.00	0.25	1.55	0.01	0.27	0.52	1.55	0.01	0.45	0.05	0.00	0.00	40	1.0	0.7	6.0	10	0.5	63.0	2.0	2.5	2.5	8.0	0.4	43.5	1.0	30	1.50	55.0	0
N=3	AVG:	CLR	SIL-ST	77.10	0.36	12.33	3.70	0.27	3.07	0.02	2.67	0.34	1.07	1.26	1.13	0.07	0.04	0.03	260	1.0	1.2	5.0	183	10.3	21.0	37.0	4.3	5.7	22.7	5.7	46.3	12.3	109	12.20	313.3	313
	STD:	CLR	SIL-ST	3.73	0.17	0.60	2.04	0.31	1.73	0.01	1.13	0.21	1.16	0.36	0.33	0.09	0.02	0.04	33	0.6	0.3	1.6	57	9.1	12.3	34.5	4.0	2.1	8.6	2.9	30.2	11.1	36	5.53	368.1	41
N=1		CLR	T/A	74.9	0.34	11.5	2.4	0.5	1.7	0.02	1.84	1.9	5.1	0.15	0.6	0.3	0.09	0.06	40	1.0	1.8	8.0	87	940.0	29.0	24.0	41.0	10.0	7.0	3.6	65.0	4.0	190	23	21.0	670
N=6	AVG:	CLR	AN/GD	58.13	0.62	16.15	10.25	1.35	8.00	0.07	10.35	0.36	0.40	0.97	3.28	0.10	0.10	0.03	150	0.5	0.9	17.2	144	23.5	68.7	22.0	36.3	4.0	23.7	16.7	22.0	77.0	88	7.03	357.0	257
	STD:	CLR	AN/GD	11.62	0.12	3.84	2.38	0.54	1.88	0.04	4.55	0.24	0.33	0.42	2.40	0.06	0.03	0.04	90	0.5	0.4	9.3	60	28.9	67.9	14.2	25.2	2.2	10.1	9.2	20.9	62.8	52	5.76	165.2	292
ISOCON:SLOPE		COMPARISON		FRACTIONAL CHANGES																																
*CNST AL2O3: 1.01		BIO-LA		-0.03	0.12	0.00	-0.10	-0.34	-0.02	-0.54	2.72	-0.44	-0.37	2.97	1.34	0.53	0.06	0.41	0.70	-0.43	-0.43	0.10	0.33	4.30	-0.38	-0.37	0.01	-0.05	2.71	0.35	-0.31	1.16	-0.39	-0.37	4.62	-0.19
CNST AL2O3: 1.11		SIL-LA		-0.13	0.03	-0.00	-0.19	-0.71	-0.05	-0.74	3.22	-0.64	-0.69	4.63	1.37	-0.78	0.12	-1.00	1.67	0.81	-0.63	-0.04	0.00	-0.95	0.93	-0.42	-0.43	-0.27	2.99	0.18	-0.50	0.06	-0.14	-0.25	0.62	-0.30
CNST AL2O3: 1.00		SIL-ST-LA		0.04	-0.09	0.00	0.03	-0.66	0.21	-0.53	1.92	-0.83	-0.80	2.87	0.70	-0.68	-0.29	-0.34	1.47	0.99	-0.61	-0.56	0.69	-0.61	-0.49	0.04	-0.56	-0.29	1.56	-0.06	-0.69	0.22	-0.26	-0.25	9.16	-0.31
CNST AL2O3: 0.94		T/A-LA		0.06	-0.09	0.00	-0.29	-0.32	-0.28	-0.39	1.15	0.00	0.01	-0.51	-0.04	0.54	0.58	1.14	-0.59	1.14	-0.39	-0.24	-0.14	36.82	-0.24	-0.28	3.28	0.34	-0.15	-0.37	-0.56	-0.58	0.38	0.51	-0.27	0.58
CNST AL2O3: 1.31		AN/GD-LA		-0.40	0.19	-0.00	1.17	0.31	1.41	0.45	7.83	-0.87	-0.94	1.28	2.75	-0.63	0.21	-0.46	0.09	-0.24	-0.80	0.15	0.01	-0.33	0.28	-0.53	1.70	-0.82	1.04	1.06	-0.89	4.82	-0.55	-0.67	7.84	-0.57
ISOCON:SLOPE		COMPARISON		ABSOLUTE CHANGES																																
CNST AL2O3: 0.94		T/A-LA		6.10	-0.03	0.00	-1.02	-0.25	-0.71	-0.01	1.05	0.00	0.07	-0.17	-0.02	0.11	0.04	0.05	-62	0.6	-1.2	-2.8	-15	979	-9.8	-9.9	33.6	2.7	-1.3	-2.3	-88	-5.8	55.9	8.3	-8.3	282
*CNST AL2O3: 1.01		BIO-LA		-2.21	0.05	0.01	-0.35	-0.27	-0.06	-0.02	2.48	-0.90	-1.97	0.97	0.90	0.11	0.00	0.02	73	-0.2	-1.3	1.1	35	114	-14.7	-13.2	0.1	-0.4	24.0	2.2	-48	11.7	-57.7	-5.9	142.1	-85.6
CNST AL2O3: 1.11		SIL-LA		-9.25	0.01	-0.00	-0.70	-0.56	-0.13	-0.03	2.94	-1.29	-3.71	1.51	0.92	-0.16	0.01	-0.04	175	0.4	-2.0	-0.5	0	-25	37.8	-14.8	-4.4	-2.1	26.4	1.1	-79	0.8	-20.7	-4.1	19.0	-136
CNST AL2O3: 1.00		SIL-ST-LA		2.88	-0.04	0.00	0.10	-0.52	0.53	-0.02	1.75	-1.69	-4.32	0.93	0.46	-0.14	-0.02	-0.01	154	0.5	-1.9	-6.3	75	-16	-19.9	1.3	-5.9	-2.3	13.8	-0.5	-109	2.2	-36.6	-4.1	281.7	-143
CNST AL2O3: 1.31		AN/GD-LA		-29.7	0.06	-0.00	4.21	0.24	3.57	0.02	6.97	-1.76	-5.08	0.42	1.83	-0.13	0.01	-0.02	9	-0.1	-2.5	1.7	2	-9	11.5	-18.8	17.4	-5.0	9.2	6.5	-140	48.6	-80.7	-10.9	241.1	-259

*CNST = constant

Table 23.

Average and Standard Deviation Data and Mass Balance Calculations for Mafic Lava Flows (RGLF/LF, MMF, WLH-MA)

NUMBER	STATS	UNIT	ALTN	SIO2	TIO2	AL2O3	FE-T	FE2O3	FEO	MNO	MGO	CAO	NA2O	K2O	H2Ot	CO2t	P2O5	S	BA	AG	BE	CO	CR	CU	LA	NB	NI	PB	RB	SC	SR	V	Y	YB	ZN	ZR
N=6	AVG:	LF'S(FSP)	LA	49.58	0.58	18.80	9.28	2.00	6.55	0.20	6.60	9.81	2.12	1.17	2.06	0.18	0.07	0.09	178	0.33	0.85	37.00	232	64.2	0.8	5.2	84.7	14.3	38.5	28.7	191.7	138.3	12	1.15	144	42
	STD:	LF'S(FSP)	LA	1.52	0.11	1.37	0.89	0.39	0.56	0.04	1.91	0.94	0.49	0.64	0.61	0.16	0.01	0.10	108	0.47	0.58	4.16	95	60.5	1.2	3.8	39.6	2.8	23.4	2.5	48.1	21.1	3	0.35	49	13
N=1		LF'S(FSP)	BIO	48.4	0.77	18.5	11.3	1.6	8.7	0.45	11.8	0.15	0	3.06	6.6	0.1	0.06	0	240	0	1.1	26	81	0	0	17	26	3	120	26	6	140	13	1.1	940	64
N=2	AVG:	LF'S(FSP)	T/A	49.15	0.50	17.85	10.40	1.00	8.45	0.22	9.33	6.84	1.25	1.81	3.50	0.15	0.06	0.00	245	0.00	0.60	33.00	280	2.0	0.0	4.5	83.5	9.0	49.5	31.0	200.0	140.0	9	0.80	295	31
	STD:	LF'S(FSP)	T/A	1.15	0.04	0.45	0.70	0.10	0.75	0.02	0.38	0.26	0.45	0.32	0.80	0.05	0.01	0.00	25	0.00	0.20	1.00	10	2.0	0.0	4.5	9.5	2.0	8.5	3.0	0.0	0.0	2	0.10	35	1
N=2	AVG:	LF'S(FSP)	AN/GD	48.25	0.62	17.35	21.70	2.95	16.80	0.28	9.73	0.31	0.65	0.22	2.50	0.30	0.07	0.16	75	0.50	0.40	28.50	300	62.0	9.5	5.5	70.5	10.5	6.0	37.5	6.5	165.0	27	1.55	1120	36
	STD:	LF'S(FSP)	AN/GD	0.55	0.07	0.35	1.60	1.25	0.30	0.07	1.97	0.09	0.05	0.00	0.60	0.20	0.00	0.05	15	0.50	0.00	4.50	20	8.0	9.5	5.5	1.5	4.5	0.0	3.5	6.5	15.0	8	0.25	480	8
ISOCON:SLOPE		COMPARISON		FRACTIONAL CHANGES																																
*CNST AL2O3: 0.97		BIO-LA		-0.00	0.35	-0.00	0.24	-0.18	0.35	1.33	0.82	-0.96	-1.00	1.69	2.23	-0.44	0.17	-1.00	0.37	-1.00	0.32	-0.28	-0.64	-1.00	-1.00	2.36	-0.69	-0.79	2.18	-0.07	-0.97	0.03	0.12	-0.02	5.84	0.57
CNST AL2O3: 0.94		T/A-LA		0.05	-0.10	0.00	0.19	-0.47	0.37	0.16	0.50	-0.26	-0.37	0.64	0.78	-0.13	-0.09	-1.00	0.46	-1.00	-0.25	-0.05	0.28	-0.97	-1.00	-0.08	0.05	-0.33	0.36	0.15	0.11	0.07	-0.19	-0.26	1.09	-0.22
CNST AL2O3: 0.92		AN/GD-LA		0.05	0.16	-0.00	1.54	0.60	1.80	0.52	0.80	-0.97	-0.67	-0.80	0.30	0.78	0.09	0.64	-0.54	0.63	-0.49	-0.16	0.41	0.05	11.39	0.16	-0.09	-0.20	-0.83	0.42	-0.98	0.30	1.43	0.47	7.43	-0.06
ISOCON:SLOPE		COMPARISON		ABSOLUTE CHANGES																																
CNST AL2O3: 0.94		T/A-LA		2.52	-0.06	0.02	1.74	-0.94	2.41	0.03	3.28	-2.55	-0.79	0.74	1.63	-0.02	-0.01	-0.09	81	-0.33	-0.21	-2.02	65.1	-62.0	-0.83	-0.40	3.8	-4.79	14.0	4.2	20.3	10.1	-2.29	-0.30	158	-9.34
*CNST AL2O3: 0.97		BIO-LA		-0.22	0.20	-0.03	2.24	-0.37	2.32	0.26	5.43	-9.65	-2.12	1.97	4.65	-0.06	0.01	-0.09	66.47	-0.33	0.27	-10.5	-149	-64.2	-0.83	12.17	-58.1	-11.3	83.90	-2.15	-186	4.47	1.43	-0.03	814.5	23.61
		SIL-LA																																		
		SIL-ST-LA																																		
CNST AL2O3: 0.92		AN/GD-LA		2.86	0.09	-0.04	14.30	1.21	11.82	0.10	3.97	-9.47	-1.41	-0.93	0.63	0.14	0.01	0.08	-97	0.21	-0.42	-6.02	94.4	3.2	9.49	0.81	-8.0	-2.92	-32.0	12.1	-185	41.0	16.97	0.53	1073	-2.53

NUMBER	STATS	UNIT	ALTN	SIO2	TIO2	AL2O3	FE-T	FE2O3	FEO	MNO	MGO	CAO	NA2O	K2O	H2Ot	CO2t	P2O5	S	BA	AG	BE	CO	CR	CU	LA	NB	NI	PB	RB	SC	SR	V	Y	YB	ZN	ZR
N=2	AVG:	LF'S(APH)	LA	51.30	0.74	16.45	11.30	2.55	7.90	0.23	7.44	10.20	2.25	0.20	1.45	0.25	0.09	0.01	65	0.00	1.05	37.50	255	19.0	0.0	3.5	54.5	14.0	3.0	41.5	150.0	200.0	18.0	1.50	150	49
	STD:	LF'S(APH)	LA	1.20	0.00	0.05	0.60	0.25	0.30	0.05	0.93	0.70	0.85	0.04	0.05	0.05	0.00	0.01	25	0.00	0.25	0.50	15	19.0	0.0	3.5	2.5	1.0	0.0	0.5	40.0	0.0	2.0	0.10	10	5
N=1		LF'S(APH)	BIO	50.9	0.74	17.1	19.7	8.4	10.2	0.59	6.01	0.65	0.2	1.88	3	0.4	0.09	0.02	460	0	0.8	26	110	10.0	1.0	8.0	28.0	14.0	39.0	31.0	17.0	160.0	20.0	1.7	1000	53
N=2	AVG:	LF'S(APH)	T/A	50.40	0.76	15.75	11.80	1.25	9.50	0.21	11.20	4.73	1.75	1.07	3.05	0.20	0.06	0.00	135	0.00	0.40	46.00	426	8.5	1.0	7.0	171.5	10.5	29.5	30.0	139.0	190.0	20.5	2.00	244	59
	STD:	LF'S(APH)	T/A	0.10	0.03	2.95	1.80	0.15	1.50	0.05	2.80	0.19	0.65	0.05	0.95	0.00	0.00	0.00	5	0.00	0.00	12.00	335	1.5	1.0	1.0	138.5	4.5	9.5	1.0	41.0	20.0	8.5	0.70	176	3
N=6	AVG:	LF'S(APH)	AN/GD	51.78	0.85	16.82	14.03	1.48	11.30	0.20	13.38	0.59	0.45	0.43	2.40	0.17	0.06	0.01	77	0.17	1.03	34.00	150	6.3	4.7	6.3	42.7	9.5	18.7	36.7	27.5	176.7	21.8	1.92	345	60
	STD:	LF'S(APH)	AN/GD	2.26	0.05	2.67	0.88	0.37	0.58	0.07	3.05	0.40	0.23	0.33	0.75	0.05	0.03	0.01	39	0.37	0.41	8.21	48	9.4	7.9	5.5	14.1	2.9	14.3	8.6	21.0	22.1	3.1	0.83	124	7
ISOCON:SLOPE		COMPARISON		FRACTIONAL CHANGES																																
*CNST AL203:1.11		BIO-LA		-0.10	-0.10	0.00	0.58	1.96	0.17	1.37	-0.27	-0.94	-0.92	7.50	0.87	0.45	-0.10	2.62	5.40		-0.31	-0.37	-0.61	-0.52		1.07	-0.54	-0.10	10.75	-0.32	-0.90	-0.28	0.13	0.02	5.03	-0.02
CNST AL2O3: 1.102		T/A-LA		-0.04	0.00	0.00	0.02	-0.52	0.18	-0.06	0.48	-0.55	-0.24	4.25	1.06	-0.22	-0.13	-1.00	1.04		-0.63	0.20	0.64	-0.56		0.96	2.09	-0.26	8.65	-0.29	-0.09	-0.12	0.26	0.31	0.60	0.18
CNST AL2O3: 1.09		AN-LA		-0.07	0.05	0.00	0.14	-0.47	0.31	-0.20	0.65	-0.95	-0.82	0.99	0.52	-0.39	-0.15	0.53	0.08		-0.10	-0.17	-0.48	-0.89		0.66	-0.28	-0.38	4.72	-0.19	-0.63	-0.19	0.25	0.17	1.11	0.13
ISOCON:SLOPE		COMPARISON		ABSOLUTE CHANGES																																
CNST AL2O3: 1.10		T/A-LA		-1.86	0.00	0.00	0.28	-1.32	1.42	-0.02	3.55	-5.56	-0.53	0.85	1.54	-0.05	-0.01	-0.01	67.4	0.00	-0.66	7.63	162	-10.7	0.00	3.37	114	-3.70	25.9	-12.1	-13.6	-23.4	4.11	0.46	89.4	8.66
*CNST AL203:1.11		BIO-LA		-5.29	-0.07	0.01	6.51	5.04	1.32	0.31	-2.01	-9.61	-2.07	1.50	1.26	0.11	-0.01	0.01	351	0.00	-0.33	-14.0	-156	-9.96	0.00	3.73	-29	-1.34	32.3	-13.5	-135	-55.4	2.08	0.04	754	-1.09
		SIL-LA																																		
		SIL-ST-LA																																		
CNST AL2O3: 1.09		AN/GD-LA		-3.71	0.04	0.00	1.60	-1.19	2.48	-0.05	4.85	-9.66	-1.84	0.20	0.76	-0.10	-0.01	0.00	5.48	0.00	-0.10	-6.25	-117	-13.2	0.00	2.32	-15.3	-5.27	14.15	-7.80	-125	-37.6	4.06	0.26	167	6.29

*CNST = constant

Table 23. (continued)

NUMBER	STATS	UNIT	ALTN	SIO2	TIO2	AL2O3	FE-T	FE2O3	FEO	MNO	MGO	CAO	NA2O	K2O	H2Ot	CO2t	P2O5	S	BA	AG	BE	CO	CR	CU	LA	NB	NI	PB	RB	SC	SR	V	Y	YB	ZN	ZR
N=2	AVG:	MMF	LA	54.10	0.79	15.45	10.25	2.40	7.05	0.13	5.87	8.64	2.95	0.47	1.55	0.40	0.11	0.02	90	1.00	0.65	30.50	145	23.5	1.5	0.0	27.5	8.5	11.0	31.0	230.0	190.0	13.5	1.20	54	55
	STD:	MMF	LA	0.10	0.03	0.15	0.15	0.20	0.05	0.04	0.32	0.96	0.35	0.27	0.35	0.00	0.00	0.02	10	0.00	0.15	2.50	15	17.5	1.5	0.0	0.5	1.5	7.0	1.0	20.0	10.0	0.5	0.10	37	2
N=1		MMF	T/A	52.70	0.86	16.00	11.40	0.80	9.50	0.13	9.02	5.94	2.40	0.31	1.50	0.10	0.11	0.06	40	1.00	0.60	30.00	98	28.0	1.0	0.0	24.0	8.0	9.0	33.0	210.0	170.0	14.0	1.30	190	62
N=2	AVG:	MMF	AN/GD	51.15	0.80	18.05	14.05	1.25	11.55	0.12	13.00	0.12	0.15	1.34	2.15	0.10	0.12	0.10	265	0.50	0.80	25.00	170	56.0	142.5	8.0	39.5	6.0	18.5	28.5	2.0	200.0	31.5	1.80	570	74
	STD:	MMF	AN/GD	3.65	0.09	0.25	1.65	0.15	1.35	0.05	1.50	0.10	0.05	0.37	0.05	0.00	0.01	0.09	15	0.50	0.40	6.00	60	54.0	137.5	8.0	3.5	2.0	6.5	1.5	2.0	40.0	15.5	0.40	50	1
ISOCON:SLOPE		COMPARISON		FRACTIONAL CHANGES																																
*CNST AL2O3: 1.04		T/A-LA		-0.08	0.08	0.00	0.07	-0.68	0.30	0.00	0.48	-0.34	-0.21	-0.36	-0.07	-0.76	-0.03	2.86	-0.57	-0.03	-0.11	-0.05	-0.35	0.15	-0.36		-0.16	-0.09	-0.21	0.03	-0.12	-0.14	0.00	0.05	2.40	0.09
CNST AL2O3: 1.17		AN/GD-LA		-0.19	-0.13	0.00	0.17	-0.55	0.40	-0.18	0.90	-0.99	-0.96	1.43	0.19	-0.79	-0.07	4.71	1.52	-0.57	0.05	-0.30	0.00	1.04	80.32		0.23	-0.40	0.44	-0.21	-0.99	-0.10	1.00	0.26	8.04	0.14
ISOCON:SLOPE		COMPARISON		ABSOLUTE CHANGES																																
*CNST AL2O3: 1.04		T/A-LA		-3.19	0.05	0.01	0.76	-1.63	2.13	0.00	2.84	-2.90	-0.63	-0.17	-0.10	-0.30	-0.00	0.04	-51.4	-0.03	-0.07	-1.52	-50.3	3.55	-0.53	0.00	-4.32	-0.77	-2.31	0.88	-27.1	-25.8	0.02	0.06	130	4.89
CNST AL2O3: 1.17		AN/GD-LA		-10.3	-0.10	0.00	1.78	-1.33	2.84	-0.02	5.28	-8.53	-2.82	0.67	0.29	-0.31	-0.01	0.07	137	-0.57	0.03	-9.10	0.52	24.4	120	0.00	6.31	-3.36	4.84	-6.60	-228	-18.8	13.46	0.34	434	7.92

NUMBER	STATS	UNIT	ALTN	SIO2	TIO2	AL2O3	FE-T	FE2O3	FEO	MNO	MGO	CAO	NA2O	K2O	H2Ot	CO2t	P2O5	S	BA	AG	BE	CO	CR	CU	LA	NB	NI	PB	RB	SC	SR	V	Y	YB	ZN	ZR
N=4	AVG:	WLH-MA	LA	51.55	0.98	15.78	10.63	2.33	7.48	0.08	5.91	8.11	3.80	1.45	1.85	0.20	0.23	0.12	153	0.0	1.3	34.3	215.0	89.0	0.5	2.8	61.3	8.3	44.3	28.5	275.0	202.5	26.8	2.45	44	69
	STD:	WLH-MA	LA	0.50	0.01	0.23	0.90	0.35	0.73	0.02	0.56	0.79	0.25	0.49	0.18	0.10	0.01	0.07	45	0.0	0.3	8.1	11.2	76.7	0.9	2.9	4.8	1.3	18.1	0.5	33.5	4.3	12.7	1.29	21	5
N=3	AVG:	WLH-MA	AN/GD	47.77	0.98	16.00	12.40	1.33	9.97	0.06	14.73	1.18	1.80	1.63	3.83	0.17	0.21	0.01	147	0.7	0.7	17.0	190.0	4.3	160.3	13.7	74.3	12.7	47.7	28.7	92.0	200.0	105.7	5.27	391	84
	STD:	WLH-MA	AN/GD	3.98	0.04	0.22	4.12	0.61	3.18	0.02	2.05	1.17	1.35	0.99	0.37	0.17	0.04	0.00	90	0.5	0.2	10.6	8.2	1.2	183.7	6.1	17.5	5.2	20.1	1.2	104.7	16.3	109.5	4.79	299	5
ISOCON:SLOPE		COMPARISON		FRACTIONAL CHANGES																																
CNST AL2O3: 1.01		AN/GD-LA		-0.09	-0.01	0.00	0.15	-0.43	0.31	-0.32	1.46	-0.86	-0.53	0.11	1.04	-0.18	-0.06	-0.94	-0.05		-0.45	-0.51	-0.13	-0.95	315.2	3.90	0.20	0.51	0.06	-0.01	-0.67	-0.03	2.89	1.12	7.71	0.21
ISOCON:SLOPE		COMPARISON		ABSOLUTE CHANGES																																
CNST AL2O3: 1.01		AN/GD-LA		-4.45	-0.01	0.00	1.60	-1.01	2.35	-0.03	8.62	-6.94	-2.03	0.16	1.93	-0.04	-0.02	-0.11	-7.89	0.00	-0.60	-17.5	-27.7	-84.7	158	10.7	12.0	4.24	2.75	-0.23	-184	-5.30	77.4	2.74	341	14.40

*CNST = constant

Table 24.

Average and Standard Deviation Data and Mass Balance Calculations for Volcaniclastic Sediments (PCC/LCS, SIV/RGSIV)

NUMBER	STATS	UNIT	ALTN	SIO2	TIO2	AL2O3	FE-T	FE2O3	FEO	MNO	MGO	CAO	NA2O	K2O	H2Ot	CO2t	P2O5	S	BA	AG	BE	CO	CR	CU	LA	NB	NI	PB	RB	SC	SR	V	Y	YB	ZN	ZR
N=8	AVG:	PCC	LA	66.86	0.67	12.03	10.99	2.74	7.44	0.24	1.68	3.86	2.63	0.44	0.95	0.35	0.17	0.14	116	0.3	2.5	5.3	159	34.0	13.3	24.6	3.4	9.4	17.1	19.3	100.9	0.0	105	11.75	243.8	450
	STD:	PCC	LA	2.37	0.05	0.70	1.56	1.20	2.28	0.10	0.60	0.66	0.63	0.43	0.27	0.32	0.03	0.15	57	0.7	0.4	1.4	55	31.2	7.3	5.3	2.2	4.7	18.1	3.0	23.1	0.0	8	1.20	208.0	39
N=3	AVG:	PCC	BIO	65.70	0.63	12.87	7.77	0.70	6.40	0.14	3.96	2.73	2.67	1.39	1.77	0.70	0.14	0.01	277	0.3	3.0	9.3	147	2.0	35.3	30.3	23.3	4.0	115.3	13.9	112.0	22.3	110	12.33	86.7	453
	STD:	PCC	BIO	5.81	0.17	0.26	3.66	0.37	2.97	0.11	2.09	0.47	0.33	0.27	0.54	0.45	0.05	0.01	33	0.5	0.3	6.6	19	1.4	3.7	3.4	29.5	0.6	118.7	6.6	27.5	24.9	17	2.05	61.3	54
N=6	AVG:	PCC	SIL-ST	66.47	0.72	12.02	15.52	4.80	9.58	0.13	2.59	0.40	0.15	1.39	1.55	0.20	0.18	0.16	418	0.0	2.3	7.8	203	40.5	26.7	28.0	2.7	6.6	79.5	18.6	4.3	0.0	114	12.50	162.2	488
	STD:	PCC	SIL-ST	2.16	0.06	0.79	3.92	3.43	2.39	0.05	0.41	0.11	0.13	0.86	0.62	0.15	0.04	0.35	241	0.0	1.5	1.2	85	63.3	3.9	3.2	2.8	4.9	100.8	4.3	4.5	0.0	12	1.26	116.6	54
N=8	AVG:	PCC	T/A	66.14	0.71	12.43	11.33	2.15	8.24	0.27	2.45	2.69	3.60	0.25	0.66	0.19	0.18	0.07	114	0.1	2.4	5.6	123	9.3	20.6	22.1	2.8	8.1	9.3	20.8	98.1	0.0	102	11.63	243.8	481
	STD:	PCC	T/A	1.74	0.09	0.30	1.28	1.33	1.16	0.09	0.34	0.60	0.54	0.15	0.16	0.15	0.04	0.14	58	0.3	0.5	1.9	44	2.6	7.6	6.2	2.2	3.0	5.4	4.1	27.6	0.0	13	1.11	98.7	28
N=13	AVG:	PCC	AN/GD	64.01	0.76	12.79	14.47	3.25	10.10	0.19	4.41	0.90	0.90	0.91	1.62	0.18	0.24	0.06	194	0.4	2.7	8.2	144	39.8	24.9	30.4	4.9	5.8	27.5	20.9	20.0	1.5	128	13.62	604.5	488
	STD:	PCC	AN/GD	7.69	0.24	2.02	5.26	2.56	3.02	0.11	1.49	0.89	0.77	0.69	0.75	0.10	0.16	0.12	129	0.7	1.9	4.0	72	112.8	5.6	4.2	7.8	4.8	22.8	10.2	27.0	5.3	85	7.72	1451.8	101
ISOCON:SLOPE		COMPARISON		FRACTIONAL CHANGES																																	
TI-AL-ZR:1.06		T/A-LA		-0.07	0.00	-0.03	-0.03	-0.26	0.04	0.07	0.38	-0.34	0.29	-0.46	-0.34	-0.49	-0.02	-0.54	-0.08	-0.53	-0.11	0.01	-0.27	-0.74	0.47	-0.15	-0.23	-0.18	-0.49	0.02	-0.10		-0.09	-0.07	-0.06	0.01
TI-AL-ZR:1.01		BIO-LA		-0.03	-0.07	0.06	-0.30	-0.75	-0.15	-0.44	1.35	-0.30	0.01	2.11	0.84	0.98	-0.16	-0.91	1.36	0.32	0.17	0.76	-0.09	-0.94	1.64	0.22	5.85	-0.58	5.67	-0.28	0.10		0.04	0.04	-0.65	-0.00
TI-AL-ZR: 1.06		SIL-ST--LA		-0.06	0.02	-0.05	0.34	0.70	0.22	-0.49	0.46	-0.90	-0.95	1.97	0.55	-0.46	0.00	0.07	2.41	-1.00	-0.14	0.41	0.20	0.13	0.91	0.08	-0.25	-0.31	3.40	-0.07	-0.96		0.02	0.01	-0.37	0.03
TI-AL-ZR:1.10		AN/GD-LA		-0.13	0.04	-0.03	0.20	0.08	0.23	-0.29	1.39	-0.79	-0.69	0.87	0.55	-0.54	0.28	-0.63	0.52	0.40	-0.01	0.43	-0.18	0.07	0.71	0.12	0.33	-0.43	0.46	-0.01	-0.82		0.11	0.05	1.25	-0.01
ISOCON:SLOPE		COMPARISON		ABSOLUTE CHANGES																																	
TI-AL-ZR:1.06		T/A-LA		-4.47	0.00	-0.30	-0.30	-0.71	0.33	0.02	0.64	-1.32	0.77	-0.20	-0.33	-0.17	-0.00	-0.08	-9	-0.1	-0.3	0.1	-43	-25	6	-3.6	-0.6	-1.7	-8	0.3	-10	0.0	-9.1	-0.8	-14	4.0
TI-AL-ZR:1.01		BIO-LA		-1.81	-0.05	0.71	-3.30	-2.04	-1.10	-0.11	2.27	-1.16	0.02	0.93	0.80	0.34	-0.03	-0.13	158	0.1	0.4	4.0	-14	-32	22	5.4	19.7	-5.4	97	-5.5	10	0.0	3.7	0.5	-158	-1.2
		SIL-LA																																			
TI-AL-ZR: 1.06		SIL-ST--LA		-3.92	0.01	-0.65	3.71	1.90	1.64	-0.12	0.77	-3.48	-2.46	0.87	0.52	-0.16	0.00	0.01	260	-0.3	-0.4	2.2	32	4	12	1.9	-0.8	-2.9	58	-1.4	-97	0.0	2.6	0.1	-90	12.4
TI-AL-ZR:1.10		AN/GD-LA		-8.67	0.03	-0.40	2.17	0.21	1.74	-0.07	2.33	-3.04	-1.81	0.38	0.52	-0.19	0.05	-0.09	60	0.1	-0.0	2.2	-29	2	9	3.0	1.1	-4.1	8	-0.3	-83	0.0	11.4	0.6	306	-8.6

NUMBER	STATS	UNIT	ALTN	SIO2	TIO2	AL2O3	FE-T	FE2O3	FEO	MNO	MGO	CAO	NA2O	K2O	H2Ot	CO2t	P2O5	S	BA	AG	BE	CO	CR	CU	LA	NB	NI	PB	RB	SC	SR	V	Y	YB	ZN	ZR
N=10	AVG:	SIV/RGSIV	LA	64.79	0.67	12.80	8.97	2.22	6.07	0.16	2.37	4.52	3.71	0.85	1.25	0.23	0.16	0.14	183	0.10	2.16	22.40	244	69.7	19.5	15.6	100.4	10.3	23.3	13.3	237.4	56.3	73	7.97	199	252
	STD:	SIV/RGSIV	LA	7.04	0.21	2.65	3.38	1.17	2.43	0.11	2.03	2.82	1.08	0.29	0.40	0.21	0.10	0.22	65	0.30	1.11	20.39	331	88.3	14.8	15.1	182.9	6.6	12.5	4.7	165.3	49.7	67	8.11	229	226
N=4	AVG:	SIV/RGSIV	BIO	59.68	0.56	14.35	13.45	4.13	8.40	0.82	5.58	0.69	0.33	1.63	3.03	0.23	0.11	0.22	475	0.00	1.23	19.75	163	64.3	11.0	8.0	62.6	12.5	39.5	15.6	25.0	62.3	31	2.93	1915	158
	STD:	SIV/RGSIV	BIO	4.01	0.04	1.46	3.60	2.21	1.76	0.61	0.90	0.54	0.29	0.43	0.68	0.04	0.01	0.29	111	0.00	0.23	3.03	24	62.6	3.9	2.1	40.0	4.7	7.4	3.6	18.4	22.2	17	1.58	2142	33
N=5	AVG:	SIV/RGSIV	T/A	60.74	0.60	14.28	11.34	2.78	7.72	0.62	5.99	1.87	0.68	1.94	2.34	0.24	0.11	0.09	604	0.00	1.02	21.20	196	48.6	8.2	5.6	44.2	13.6	37.6	20.4	69.6	104.4	23	2.34	1532	126
	STD:	SIV/RGSIV	T/A	6.49	0.12	0.77	4.69	1.83	2.80	0.29	2.44	1.09	0.45	0.76	0.69	0.19	0.00	0.10	267	0.00	0.19	7.25	71	63.4	2.9	5.5	12.7	8.0	18.2	8.0	46.2	39.9	7	0.85	828	38
N=3	AVG:	SIV/RGSIV	AN/GD	61.67	0.62	14.53	11.33	1.50	8.87	0.21	7.64	0.49	0.37	1.42	2.40	0.17	0.13	0.05	367	0.00	1.37	23.67	193	14.3	10.7	5.3	59.3	10.3	25.0	18.7	35.0	105.0	21	1.97	803	122
	STD:	SIV/RGSIV	AN/GD	3.45	0.12	0.83	1.16	0.36	0.93	0.06	2.89	0.26	0.09	0.43	0.24	0.05	0.02	0.04	162	0.00	0.31	4.92	42	9.0	4.6	5.0	19.7	5.9	8.0	6.0	42.6	31.9	14	1.47	775	41
ISOCON:SLOPE		COMPARISON		FRACTIONAL CHANGES																																	
TI-AL:1.01		T/A-LA		-0.07	-0.11	0.10	0.25	0.24	0.26	2.92	1.51	-0.59	-0.82	1.27	0.85	0.03	-0.30	-0.36	2.27	-1.00	-0.53	-0.06	-0.20	-0.31	-0.58	-0.64	-0.56	0.31	0.60	0.52	-0.71	0.84	-0.68	-0.71	6.62	-0.51
TI-AL:0.97		BIO-LA		-0.05	-0.15	0.16	0.55	0.92	0.43	4.35	1.43	-0.84	-0.91	1.23	1.49	0.01	-0.30	0.65	1.68	-1.00	-0.42	-0.09	-0.31	-0.05	-0.42	-0.47	-0.36	0.25	0.75	0.22	-0.89	0.51	-0.58	-0.62	8.92	-0.36
TI-AL:1.02		AN/GD-LA		-0.07	-0.10	0.11	0.24	-0.34	0.43	0.33	2.17	-0.89	-0.90	0.64	0.88	-0.29	-0.23	-0.64	0.96	-1.00	-0.38	0.04	-0.22	-0.80	-0.46	-0.66	-0.42	-0.02	0.05	0.38	-0.86	0.63	-0.72	-0.76	2.96	-0.53
ISOCON:SLOPE		COMPARISON		ABSOLUTE CHANGES																																	
TI-AL:1.01		T/A-LA		-4.65	-0.08	1.34	2.26	0.53	1.57	0.46	3.57	-2.67	-3.04	1.08	1.07	0.01	-0.05	-0.05	415	-0.10	-1.15	-1.41	-48.4	-21.4	-11.4	-10.1	-56.6	3.17	13.9	6.90	-168	47.1	-49.4	-5.65	1318	-128
TI-AL:0.97		BIO-LA		-3.27	-0.10	1.99	4.90	2.03	2.59	0.88	3.38	-3.61	-3.37	1.04	1.87	0.00	-0.05	0.09	307	-0.10	-0.90	-2.04	-78.9	-3.5	-8.2	-7.4	-35.7	2.59	17.4	2.94	-212	28.5	-40.6	-4.95	1775	-90
		SIL-LA																																			
		SIL-ST--LA																																			
TI-AL:1.02		AN/GD-LA		-4.33	-0.07	1.45	2.14	-0.75	2.62	0.05	5.13	-4.04	-3.35	0.55	1.10	-0.07	-0.04	-0.09	178	-0.10	-0.82	0.80	-54.9	-55.6	-9.0	-10.4	-42.2	-0.17	1.2	5.00	-203	46.6	-52.3	-6.04	568	-133

APPENDIX III. Electron Microprobe Analysis

Table 25.

Electron Microprobe Analytical Methods
(Geological Survey of Canada Data)

The electron microprobe at the Geological Survey of Canada was used to quantitatively analyze the composition of silicates from the study area. Sixteen polished thin sections were analyzed using a CAMECA Camebax wavelength dispersive microprobe with four spectrometers. Running conditions were as follows:

Acceleration voltage: 15 kV

Beam Current: 10 μA for Na, Mg, K, and Fe; 30 μA for all other elements

Beam Size: ca. 1-2 μm (spot)

The spectrometers were calibrated with natural silicate standards as follows:

labradorite (Na, Al, Si), orthoclase (K), diopside (Mg, Ca), Rhodonite (Mn, Zn), Rutile (Ti), Chromite (Cr)

Electron Microprobe Analytical Methods
for Data of Thomas, (1991), Appendix B

Silicate mineral compositions of Thomas (1991) were determined using an ARL-SEMQ at Queen's University, fitted with a lithium-drifted silicon detector and using energy dispersive spectrometry. An accelerating potential of 15 kV was used with a beam current of 100nA, a take-off angle of 52.5° and a beam diameter of approximately 10 μm. Spectra were collected for 200 seconds after correction for dead-time.

Analytical quality for ferromagnesium minerals was monitored using synthetic glass (NBS 470), and Kaersutite (USNM 143965) as standards. Small variations in Na2O in biotite was monitored for comparison to analytical error by repeated analysis of low Na2O (0.23%) apatite.

Table 26.
Electron Microprobe Data

SAMPLE #	LITH UNIT	ALTN ZONE	MINERAL	NA2O	K2O	MGO	FEO	AL2O3	SIO2	CAO	TIO2	MNO	CR2O3	ZNO	TOTALS	NA	K	MG	FE	AL	SI	CA	TI	MN	CR	ZN	O
WLO-484	PCC	LA	HBL	1.43	0.00	7.71	22.25	13.83	42.39	10.07	0.79	0.53	0.02	0.12	99.14	0.58	0.00	2.40	3.89	3.40	6.85	2.25	0.12	0.09	0.00	0.02	32.00
WLO-545	PCC	LA	HBL	1.70	0.29	8.82	21.82	14.92	41.13	10.03	0.50	0.25	0.05	0.05	97.56	0.52	0.06	1.82	2.91	2.80	6.55	1.71	0.06	0.03	0.01	0.01	24.00
WLO-545	PCC	LA	HBL	1.65	0.28	8.85	21.23	14.85	40.95	10.02	0.43	0.23	0.00	0.00	98.29	0.52	0.06	1.84	2.66	2.78	6.59	1.73	0.05	0.03	0.00	0.00	24.00
WLO-545	PCC	LA	HBL	1.61	0.34	8.82	21.36	15.01	40.93	10.51	0.47	0.23	0.00	0.10	97.37	0.50	0.07	1.62	2.85	2.82	6.53	1.80	0.06	0.03	0.00	0.01	24.00
WLO-484	PCC	LA	PL	8.16	0.21	0.00	0.00	25.48	60.77	6.79	0.16	0.01	0.00	0.05	101.81	2.78	0.05	0.00	0.00	5.28	10.87	1.28	0.02	0.00	0.00	0.01	32.00
WLO-484	PCC	LA	PL	7.77	0.62	0.02	0.03	25.77	60.29	7.55	0.00	0.00	0.00	0.08	102.33	2.64	0.16	0.00	0.00	5.33	10.58	1.42	0.00	0.00	0.00	0.01	32.00
WLO-545	PCC	LA	PL	6.63	0.52	0.02	0.57	26.45	63.14	4.24	0.02	0.01	0.03	0.00	101.64	1.67	0.09	0.00	0.06	4.05	8.19	0.59	0.00	0.00	0.00	0.00	24.00
WLO-545	PCC	LA	PL	7.97	0.22	0.01	0.11	26.33	59.79	7.45	0.00	0.00	0.01	0.08	101.95	2.04	0.04	0.00	0.01	4.09	7.88	1.05	0.00	0.00	0.00	0.01	24.00
WLO-545	PCC	LA	PL	8.03	0.05	0.00	0.05	25.96	60.14	7.35	0.05	0.04	0.00	0.00	101.68	2.05	0.01	0.00	0.01	4.04	7.93	1.04	0.00	0.00	0.00	0.00	24.00
WLO-545	PCC	LA	GNT	0.00	0.00	2.55	32.14	20.94	37.05	3.97	0.07	2.38	0.00	0.01	99.08	0.00	0.00	0.81	4.35	4.00	6.00	0.69	0.01	0.32	0.00	0.00	24.00
WLO-545	PCC	LA	GNT	0.05	0.01	2.70	32.65	20.86	37.49	3.65	0.04	2.61	0.00	0.01	100.07	0.02	0.00	0.85	4.39	3.95	6.02	0.83	0.00	0.35	0.00	0.00	24.00
WLO-545	PCC	LA	GNT	0.04	0.00	2.71	33.28	21.13	37.04	3.07	0.05	2.58	0.05	0.02	99.99	0.01	0.00	0.85	4.48	4.01	5.97	0.53	0.01	0.35	0.01	0.00	24.00
WLO-484	PCC	LA	GNTcore	0.00	0.33	2.81	33.20	20.81	37.64	3.40	0.12	4.43	0.03	0.08	102.85	0.00	0.09	0.88	5.85	5.17	7.93	0.77	0.02	0.79	0.00	0.00	32.00
WLO-484	PCC	LA	GNTrim	0.03	0.01	2.70	35.90	19.76	35.35	3.59	0.00	4.49	0.04	0.00	101.87	0.01	0.00	0.87	6.52	5.06	7.67	0.84	0.00	0.82	0.01	0.00	32.00
WLO-521	PCC	T/A	GNT	0.04	0.02	3.03	34.42	20.73	37.15	2.27	0.03	2.45	0.04	0.00	100.17	0.01	0.00	0.73	4.64	3.94	5.99	0.39	0.00	0.33	0.00	0.00	24.00
WLO-521	PCC	T/A	GNT	0.00	0.00	3.07	35.49	20.73	37.31	1.51	0.04	2.50	0.01	0.00	100.84	0.00	0.00	0.73	4.77	3.93	6.00	0.26	0.00	0.34	0.00	0.00	24.00
WLO-521	PCC	T/A	PL	9.84	0.03	0.00	0.05	23.36	63.74	4.48	0.03	0.00	0.00	0.01	101.53	2.50	0.00	0.00	0.01	3.61	8.35	0.63	0.00	0.00	0.00	0.00	24.00
WLO-521	PCC	T/A	PL	9.85	0.07	0.01	0.04	23.10	63.91	4.40	0.00	0.06	0.06	0.06	101.56	2.50	0.01	0.00	0.00	3.57	8.37	0.62	0.00	0.01	0.01	0.01	24.00
WLO-521	PCC	T/A	PL	9.47	0.05	0.01	0.10	23.90	64.65	4.49	0.03	0.04	0.05	0.00	102.79	2.37	0.01	0.00	0.01	3.64	8.35	0.62	0.00	0.00	0.01	0.00	24.00
WLO-527	PCC	BIO	PL	9.98	0.28	0.03	0.13	23.06	65.13	3.94	0.01	0.04	0.00	0.00	102.59	2.50	0.05	0.00	0.01	3.52	8.44	0.55	0.00	0.00	0.00	0.00	24.00
WLO-527	PCC	BIO	PL	9.96	0.28	0.03	0.07	23.05	64.43	3.99	0.00	0.03	0.02	0.00	101.85	2.52	0.05	0.01	0.01	3.55	8.41	0.56	0.00	0.00	0.00	0.00	24.00
WLO-527	PCC	BIO	PL	10.16	0.21	0.01	0.04	22.94	65.12	3.96	0.03	0.00	0.04	0.00	102.52	2.55	0.04	0.00	0.00	3.50	8.44	0.55	0.00	0.00	0.00	0.00	24.00
WLO-535	PCC	BIO	PL	11.11	0.05	0.00	0.03	22.30	65.97	2.58	0.02	0.00	0.00	0.05	102.13	2.79	0.01	0.00	0.00	3.41	8.56	0.36	0.00	0.00	0.00	0.01	24.00
WLO-535	PCC	BIO	PL	10.32	0.07	0.01	0.02	21.82	63.70	3.23	0.01	0.03	0.00	0.11	99.30	2.67	0.01	0.00	0.00	3.44	8.51	0.48	0.00	0.00	0.00	0.01	24.00
WLO-535	PCC	BIO	PL	11.01	0.08	0.03	0.00	22.20	66.43	2.77	0.00	0.01	0.00	0.00	102.52	2.75	0.01	0.01	0.00	3.36	8.58	0.38	0.00	0.00	0.00	0.00	24.00
WLO-535	PCC	BIO	PL	10.97	0.04	0.02	0.05	22.38	66.91	2.43	0.00	0.02	0.00	0.00	102.82	2.73	0.01	0.00	0.01	3.89	8.60	0.33	0.00	0.02	0.00	0.00	24.00
WLO-527	PCC	BIO	BIO	0.04	8.94	7.63	24.72	17.66	33.78	0.18	1.53	0.17	0.00	0.08	94.95	0.01	1.96	2.01	3.56	3.58	5.81	0.03	0.20	0.03	0.00	0.01	24.00
WLO-527	PCC	BIO	BIO	0.07	9.53	8.05	25.11	18.09	35.40	0.03	1.56	0.14	0.00	0.18	98.12	0.02	2.07	2.04	3.58	3.23	6.03	0.00	0.20	0.02	0.00	0.02	24.00
WLO-527	PCC	BIO	BIO	0.13	8.70	7.79	24.68	16.66	34.15	0.30	1.43	0.18	0.03	0.16	94.18	0.04	1.92	2.01	3.58	3.40	5.92	0.06	0.19	0.02	0.00	0.02	24.00
WLO-535	PCC	BIO	BIO	0.62	8.03	10.62	20.66	17.73	36.09	0.00	1.75	0.02	0.00	0.04	95.75	0.20	1.69	2.82	2.88	3.45	5.97	0.00	0.22	0.00	0.00	0.00	24.00
WLO-535	PCC	BIO	BIO	0.34	8.02	10.30	20.73	18.01	35.22	0.02	1.73	0.03	0.00	0.06	94.47	0.11	1.72	2.57	2.91	3.56	5.91	0.00	0.22	0.00	0.00	0.01	24.00
WLO-535	PCC	BIO	BIO	0.73	8.10	10.38	20.59	18.11	35.96	0.12	1.74	0.05	0.05	0.00	95.83	0.23	1.71	2.55	2.84	3.52	5.94	0.02	0.22	0.01	0.01	0.00	24.00
WLO-580	PCC	BIO	BIO	0.15	7.94	6.90	25.22	19.41	33.30	0.19	1.49	0.00	0.01	0.06	94.66	0.05	1.74	1.76	3.62	3.92	5.71	0.03	0.19	0.00	0.00	0.01	24.00
WLO-580	PCC	BIO	BIO	0.14	7.89	6.30	22.85	20.13	30.07	0.26	1.37	0.01	0.03	0.08	89.12	0.04	1.83	1.71	3.48	4.32	5.47	0.05	0.19	0.00	0.00	0.01	24.00
WLO-580	PCC	BIO	BIO	0.29	9.11	6.42	24.68	18.84	34.01	0.00	2.02	0.02	0.02	0.13	95.53	0.10	1.98	1.63	3.52	3.79	5.80	0.00	0.26	0.00	0.00	0.02	24.00
WLO-580	PCC	BIO	BIO	0.21	8.75	5.77	25.16	19.15	34.08	0.21	1.89	0.05	0.02	0.18	95.45	0.07	1.90	1.47	3.59	3.85	5.81	0.04	0.24	0.01	0.00	0.02	24.00
WLO-580	PCC	BIO	CHL	0.01	0.00	8.48	33.34	23.25	22.92	0.03	0.12	0.00	0.00	0.10	88.25	0.00	0.00	2.37	5.24	5.15	4.31	0.01	0.02	0.00	0.00	0.01	24.00
WLO-535	PCC	BIO	GNT	0.00	0.01	3.83	37.88	21.11	37.49	0.78	0.01	0.70	0.01	0.00	101.81	0.00	0.00	0.91	5.03	3.95	5.95	0.13	0.00	0.09	0.00	0.00	24.00
WLO-535	PCC	BIO	GNT	0.02	0.01	3.92	37.70	21.07	37.50	0.53	0.03	0.58	0.00	0.00	101.37	0.01	0.00	0.93	5.02	3.95	5.97	0.09	0.00	0.08	0.00	0.00	24.00
WLO-535	PCC	BIO	GNT	0.03	0.00	3.89	38.29	21.02	37.10	0.89	0.04	0.70	0.00	0.20	100.16	0.01	0.00	0.93	4.88	3.96	5.96	0.15	0.00	0.10	0.00	0.02	24.00
WLO-580	PCC	BIO	GNT	0.00	0.00	1.96	39.49	20.81	36.79	0.85	0.02	0.55	0.04	0.00	100.51	0.00	0.00	0.47	5.36	3.96	5.98	0.15	0.00	0.07	0.01	0.00	24.00
WLO-580	PCC	BIO	GNT	0.00	0.01	1.92	39.89	20.89	37.26	0.85	0.05	0.60	0.00	0.05	101.53	0.00	0.00	0.48	5.36	3.96	6.00	0.15	0.01	0.08	0.00	0.01	24.00
WLO-580	PCC	BIO	GNT	0.09	0.00	2.00	39.86	21.11	36.71	1.13	0.02	0.59	0.00	0.07	101.59	0.03	0.00	0.48	5.37	4.01	5.91	0.20	0.00	0.08	0.00	0.01	24.00

Table 26. (continued)
Electron Microprobe Data

SAMPLE #	LITH UNIT	ALTN ZONE	MINERAL	NA2O	K2O	MGO	FEO	AL2O3	SIO2	CAO	TIO2	MNO	CR2O3	ZNO	TOTALS	NA	K	MG	FE	AL	SI	CA	TI	MN	CR	ZN	O
WLO-560	PCC	BIO	SP	0.52	0.01	1.15	20.45	56.01	0.08	0.00	0.00	0.01	0.00	20.32	98.52	0.16	0.00	0.31	3.07	11.87	0.01	0.00	0.00	0.00	0.00	2.70	24.00
WLO-580	PCC	BIO	SP	0.57	0.00	1.14	21.40	55.55	0.02	0.00	0.00	0.00	0.05	19.71	98.45	0.20	0.00	0.31	3.23	11.81	0.00	0.00	0.00	0.00	0.01	2.63	24.00
WLO-580	PCC	BIO	SP	0.61	0.03	1.00	17.87	55.29	0.02	0.00	0.02	0.00	0.00	23.57	98.42	0.22	0.01	0.27	2.71	11.82	0.00	0.00	0.00	0.00	0.00	3.16	24.00
WLO-535	PCC	BIO	SP	0.03	0.00	2.09	14.42	52.92	27.17	0.02	0.64	0.03	0.03	1.13	98.47	0.01	0.00	0.45	1.75	9.07	3.95	0.00	0.07	0.00	0.00	0.12	24.00
WLO-532	PCC	SIL-ST	BIO	1.29	8.58	0.47	2.30	37.33	19.33	0.00	0.28	0.00	0.03	0.00	99.60	0.34	1.50	0.10	0.27	6.05	6.79	0.00	0.03	0.00	0.00	0.00	24.00
WLO-532	PCC	SIL-ST	BIO	0.02	4.49	9.40	26.18	19.68	28.65	0.03	0.94	0.05	0.03	0.00	89.48	0.01	1.04	2.54	3.97	4.20	5.19	0.01	0.13	0.01	0.00	0.00	24.00
WLO-532	PCC	SIL-ST	BIO	1.41	8.72	0.41	2.36	36.78	48.39	0.00	0.30	0.00	0.00	0.00	98.34	0.38	1.55	0.08	0.28	6.05	8.76	0.00	0.03	0.00	0.00	0.00	24.00
WLO-532	PCC	SIL-ST	BIO	0.13	6.62	7.20	23.90	18.78	33.83	0.00	1.66	0.02	0.00	0.05	94.19	0.04	1.89	1.84	3.43	3.80	5.81	0.00	0.21	0.00	0.00	0.01	24.00
WLO-532	PCC	SIL-ST	BIO	0.20	8.93	7.60	22.23	18.70	34.21	0.02	1.51	0.01	0.00	0.00	93.40	0.01	1.96	1.95	3.20	3.79	5.88	0.00	0.19	0.00	0.00	0.00	24.00
WLO-832	PCC	SIL-ST	BIO	0.41	8.52	9.39	20.98	19.24	35.96	0.13	1.07	0.00	0.04	0.12	95.85	0.13	1.80	2.31	2.90	3.74	5.94	0.02	0.13	0.00	0.00	0.01	24.00
WLO-832	PCC	SIL-ST	BIO	0.23	7.80	9.66	21.32	18.17	35.11	0.00	1.23	0.02	0.02	0.00	93.34	0.07	1.64	2.44	3.02	3.63	5.95	0.00	0.16	0.00	0.00	0.00	24.00
WLO-832	PCC	SIL-ST	BIO	0.47	8.50	9.60	20.87	18.71	35.49	0.02	1.33	0.04	0.00	0.03	95.05	0.15	1.81	2.39	2.91	3.68	5.92	0.00	0.17	0.01	0.00	0.00	24.00
WLO-532	PCC	SIL-ST	CHL	0.00	0.02	9.55	31.63	21.96	23.26	0.00	0.18	0.12	0.01	0.01	86.63	0.00	0.01	2.70	5.01	4.90	4.43	0.00	0.03	0.02	0.00	0.00	24.00
WLO-532	PCC	SIL-ST	CHL	0.07	0.02	9.31	33.09	21.87	23.48	0.00	0.11	0.09	0.00	0.02	87.64	0.03	0.00	2.82	5.23	4.82	4.43	0.00	0.02	0.01	0.00	0.00	24.00
WLO-532	PCC	SIL-ST	CHL	0.01	0.03	9.32	32.39	22.18	23.22	0.01	0.15	0.09	0.00	0.00	87.39	0.00	0.01	2.63	5.12	4.94	4.39	0.00	0.02	0.01	0.00	0.00	24.00
WLO-532	PCC	SIL-ST	GNT	0.00	0.01	2.62	39.22	20.70	36.92	1.04	0.06	0.75	0.00	0.02	101.34	0.00	0.00	0.63	5.28	3.93	5.95	0.18	0.01	0.10	0.00	0.00	24.00
WLO-532	PCC	SIL-ST	GNT	0.01	0.00	1.92	39.51	20.69	37.17	0.79	0.00	1.24	0.00	0.00	101.33	0.00	0.00	0.48	5.33	3.93	6.00	0.14	0.00	0.17	0.00	0.00	24.00
WLO-532	PCC	SIL-ST	GNT	0.01	0.01	1.09	14.24	54.53	26.83	0.01	0.51	0.08	0.03	0.54	97.87	0.00	0.00	0.24	1.73	9.35	3.90	0.00	0.06	0.01	0.00	0.06	24.00
WLO-532	PCC	SIL-ST	GNT	0.00	0.00	2.59	39.27	21.05	36.64	0.55	0.01	0.71	0.07	0.00	100.89	0.00	0.00	0.82	5.31	4.01	5.92	0.10	0.00	0.10	0.01	0.00	24.00
WLO-832	PCC	SIL-ST	GNT	0.06	0.01	2.75	38.36	21.21	36.60	0.46	0.00	0.41	0.04	0.10	99.99	0.02	0.00	0.66	5.21	4.06	5.94	0.08	0.00	0.06	0.01	0.01	24.00
WLO-832	PCC	SIL-ST	GNT	0.00	0.01	2.78	37.60	21.68	36.52	0.63	0.02	0.43	0.00	0.00	99.68	0.00	0.00	0.67	5.10	4.14	5.92	0.11	0.00	0.06	0.00	0.00	24.00
WLO-832	PCC	SIL-ST	GNT	0.01	0.01	3.14	38.26	20.97	37.09	0.81	0.06	0.38	0.02	0.05	100.59	0.00	0.00	0.75	5.15	3.98	5.97	0.10	0.01	0.05	0.00	0.01	24.00
WLO-532	PCC	SIL-ST	ST	0.04	0.00	0.76	12.82	54.78	26.75	0.01	0.45	0.08	0.06	1.08	96.82	0.01	0.00	0.17	1.57	9.48	3.92	0.00	0.05	0.01	0.01	0.12	24.00
WLO-532	PCC	SIL-ST	ST	0.07	0.00	1.06	14.48	55.99	25.39	0.01	0.60	0.09	0.00	1.08	98.78	0.02	0.00	0.23	1.76	9.58	3.69	0.00	0.07	0.01	0.00	0.12	24.00
WLO-532	PCC	SIL-ST	ST	0.04	0.01	0.78	13.73	54.52	27.33	0.00	0.43	0.03	0.00	0.94	97.81	0.01	0.00	0.17	1.57	9.48	3.92	0.00	0.05	0.01	0.01	0.12	24.00
WLO-832	PCC	SIL-ST	ST	0.05	0.01	1.71	14.59	53.54	27.15	0.00	0.49	0.02	0.00	0.81	98.36	0.01	0.00	0.37	1.77	9.17	3.95	0.00	0.05	0.00	0.00	0.09	24.00
WLO-832	PCC	SIL-ST	ST	0.05	0.03	1.43	14.76	54.04	27.25	0.00	0.67	0.02	0.01	0.86	99.12	0.01	0.01	0.31	1.78	9.19	3.93	0.00	0.07	0.00	0.00	0.09	24.00
WLO-832	PCC	SIL-ST	ST	0.09	0.00	1.69	14.89	53.49	27.34	0.00	0.56	0.02	0.00	0.85	98.93	0.03	0.00	0.36	1.80	9.13	3.96	0.00	0.06	0.00	0.00	0.09	24.00
WLO-532	PCC	SIL-ST	ST	0.00	0.00	1.18	14.19	54.38	27.25	0.00	0.55	0.07	0.00	0.80	98.42	0.00	0.00	0.25	1.72	9.28	3.94	0.00	0.06	0.01	0.00	0.09	24.00
WLO-482	PCC	AN/GD	BIO	0.26	7.43	12.43	17.33	19.32	35.49	0.22	1.20	0.04	0.00	0.11	93.63	0.08	1.57	3.06	2.39	3.76	5.86	0.04	0.15	0.01	0.00	0.01	24.00
WLO-482	PCC	AN/GD	BIO	0.16	8.41	12.31	17.50	18.42	36.54	0.10	1.17	0.07	0.04	0.14	94.86	0.05	1.76	3.01	2.40	3.58	6.00	0.02	0.14	0.01	0.00	0.02	24.00
WLO-482	PCC	AN/GD	BIO	0.27	8.65	11.52	17.75	18.56	36.82	0.01	1.33	0.06	0.00	0.13	95.11	0.09	1.81	2.81	2.43	3.59	6.04	0.00	0.16	0.01	0.00	0.02	24.00
WLO-790	PCC	AN/GD	BIO	0.42	8.41	12.89	17.76	17.42	37.11	0.00	1.20	0.01	0.00	0.13	95.34	0.13	1.78	3.14	2.43	3.36	6.07	0.00	0.15	0.00	0.00	0.02	24.00
WLO-790	PCC	AN/GD	BIO	0.34	8.34	12.15	18.92	17.29	36.64	0.03	1.05	0.03	0.04	0.08	94.90	0.11	1.76	2.99	2.62	3.37	6.06	0.00	0.13	0.00	0.00	0.01	24.00
WLO-858	PCC	AN/GD	BIO	0.49	8.30	14.99	15.45	16.51	38.48	0.03	1.00	0.04	0.01	0.04	95.35	0.15	1.71	3.60	2.08	3.14	6.21	0.01	0.12	0.01	0.00	0.00	24.00
WLO-858	PCC	AN/GD	BIO	0.65	7.96	14.88	15.13	16.53	38.73	0.00	1.15	0.03	0.03	0.01	95.10	0.20	1.64	3.57	2.04	3.14	6.24	0.00	0.14	0.00	0.00	0.00	24.00
WLO-858	PCC	AN/GD	BIO	0.33	8.65	15.13	15.50	16.29	38.22	0.00	1.05	0.05	0.01	0.09	95.31	0.10	1.79	3.85	2.10	3.11	6.19	0.00	0.13	0.01	0.00	0.01	24.00
WLO-482	PCC	AN/GD	CDT	0.14	0.00	6.15	4.70	32.96	49.22	0.02	0.00	0.13	0.00	0.13	93.44	0.04	0.00	1.29	0.55	5.48	6.94	0.00	0.00	0.01	0.00	0.01	24.00
WLO-482	PCC	AN/GD	CDT	0.31	0.01	8.89	7.41	33.33	49.05	0.00	0.02	0.09	0.02	0.12	99.26	0.08	0.00	1.80	0.84	5.33	6.65	0.00	0.00	0.01	0.00	0.01	24.00
WLO-482	PCC	AN/GD	CDT	0.30	0.01	9.00	7.49	33.17	48.77	0.03	0.02	0.09	0.01	0.07	98.95	0.08	0.00	1.83	0.85	5.32	6.64	0.00	0.00	0.01	0.00	0.01	24.00
WLO-482	PCC	AN/GD	CDT	0.33	0.00	9.15	7.46	33.18	48.94	0.00	0.03	0.07	0.03	0.11	99.30	0.09	0.00	1.85	0.85	5.30	6.64	0.00	0.00	0.01	0.00	0.01	24.00
WLO-790	PCC	AN/GD	CDT	0.24	0.00	8.65	7.73	32.93	48.78	0.02	0.00	0.02	0.00	0.07	98.44	0.06	0.00	1.78	0.88	5.31	6.67	0.00	0.00	0.00	0.00	0.01	24.00
WLO-790	PCC	AN/GD	CDT	0.24	0.01	8.78	8.09	33.74	48.70	0.02	0.05	0.06	0.00	0.02	99.71	0.06	0.00	1.77	0.92	5.38	6.59	0.00	0.00	0.01	0.00	0.00	24.00
WLO-858	PCC	AN/GD	CDT	0.22	0.00	9.62	6.72	33.06	49.12	0.02	0.02	0.05	0.05	0.02	98.90	0.06	0.00	1.94	0.76	5.28	6.86	0.00	0.00	0.01	0.01	0.00	24.00
WLO-858	PCC	AN/GD	CDT	0.28	0.00	9.52	6.63	33.09	49.72	0.03	0.02	0.09	0.04	0.00	99.41	0.07	0.00	1.91	0.75	5.25	6.70	0.00	0.00	0.01	0.00	0.00	24.00
WLO-858	PCC	AN/GD	CDT	0.24	0.00	9.40	6.75	33.07	49.43	0.05	0.00	0.11	0.02	0.00	99.08	0.06	0.00	1.90	0.76	5.27	6.89	0.01	0.00	0.01	0.00	0.00	24.00

Table 26. (continued)
Electron Microprobe Data

SAMPLE #	LITH UNIT	ALTN ZONE	MINERAL	NA2O	K2O	MGO	FEO	AL2O3	SIO2	CAO	TIO2	MNO	CR2O3	ZNO	TOTALS	NA	K	MG	FE	AL	SI	CA	TI	MN	CR	ZN	O
WLO-482	PCC	AN/GD	GNT	0.08	0.00	4.37	35.02	21.30	37.39	0.94	0.02	1.90	0.04	0.15	101.22	0.03	0.00	1.04	4.65	3.99	5.94	0.18	0.00	0.28	0.00	0.02	24.00
WLO-482	PCC	AN/GD	GNT	0.04	0.10	4.88	34.79	21.21	37.49	0.98	0.04	1.98	0.03	0.03	101.55	0.01	0.02	1.15	4.60	3.95	5.93	0.17	0.00	0.28	0.00	0.00	24.00
WLO-482	PCC	AN/GD	GNT	0.00	0.00	4.54	33.53	21.28	37.26	0.96	0.04	2.94	0.00	0.08	100.61	0.00	0.00	1.08	4.47	3.99	5.94	0.16	0.00	0.40	0.00	0.01	24.00
WLO-790	PCC	AN/GD	GNT	0.09	0.01	4.21	35.42	21.36	37.45	1.52	0.04	0.59	0.08	0.06	100.82	0.03	0.00	1.00	4.71	4.00	5.95	0.28	0.00	0.08	0.01	0.01	24.00
WLO-790	PCC	AN/GD	GNT	0.01	0.02	3.63	35.55	25.10	34.15	1.63	0.02	0.60	0.04	0.06	100.81	0.00	0.00	0.86	4.75	4.73	5.48	0.28	0.00	0.08	0.01	0.01	24.00
WLO-482	PCC	AN/GD	AN/GD	1.87	0.01	10.27	25.98	22.48	38.23	0.18	0.22	0.48	0.02	0.14	99.83	0.56	0.00	2.35	3.34	4.07	5.88	0.03	0.03	0.06	0.00	0.02	24.00
WLO-482	PCC	AN/GD	AN/GD	1.89	0.00	10.20	25.92	17.68	40.82	0.17	0.23	0.48	0.00	0.11	97.51	0.58	0.00	2.39	3.41	3.28	6.42	0.03	0.03	0.06	0.00	0.01	24.00
WLO-482	PCC	AN/GD	AN/GD	1.94	0.02	10.04	26.09	17.80	40.73	0.19	0.24	0.44	0.03	0.12	97.65	0.59	0.00	2.35	3.43	3.30	6.40	0.03	0.03	0.06	0.00	0.01	24.00
WLO-482	PCC	AN/GD	AN/GD	1.76	0.01	10.20	26.39	17.04	41.26	0.17	0.18	0.58	0.04	0.07	97.71	0.54	0.00	2.39	3.47	3.16	6.49	0.03	0.02	0.08	0.01	0.01	24.00
WLO-790	PCC	AN/GD	AN/GD	2.17	0.03	8.93	27.45	19.11	39.35	0.32	0.19	0.18	0.01	0.07	97.81	0.67	0.01	2.11	3.83	3.56	6.22	0.05	0.02	0.02	0.00	0.01	24.00
WLO-790	PCC	AN/GD	AN/GD	2.16	0.00	9.21	27.81	18.05	40.08	0.32	0.15	0.19	0.03	0.03	98.01	0.68	0.00	2.17	3.87	3.36	6.33	0.05	0.02	0.02	0.00	0.00	24.00
WLO-858	PCC	AN/GD	AN/GD	1.83	0.02	12.30	24.50	14.40	43.15	0.43	0.16	0.47	0.00	0.00	97.25	0.55	0.00	2.87	3.20	2.65	6.75	0.07	0.02	0.06	0.00	0.00	24.00
WLO-858	PCC	AN/GD	AN/GD	1.71	0.00	12.87	25.16	13.70	43.72	0.42	0.15	0.44	0.02	0.09	98.28	0.51	0.00	2.96	3.26	2.51	6.78	0.07	0.02	0.06	0.00	0.01	24.00
WLO-858	PCC	AN/GD	AN/GD	1.62	0.00	13.54	25.29	11.36	45.96	0.42	0.15	0.39	0.00	0.17	98.90	0.48	0.00	3.10	3.25	2.06	7.07	0.07	0.02	0.05	0.00	0.02	24.00
WLO-858	PCC	AN/GD	AN/GD	1.67	0.04	12.92	25.20	12.96	45.00	0.43	0.14	0.41	0.01	0.17	98.95	0.50	0.01	2.96	3.24	2.35	6.92	0.07	0.02	0.05	0.00	0.02	24.00
WLO-482	PCC	AN/GD	ST	0.07	0.00	1.51	9.36	51.99	27.34	0.02	0.65	0.10	0.00	3.92	94.96	0.02	0.00	0.34	1.17	9.15	4.08	0.00	0.07	0.01	0.00	0.43	24.00
WLO-482	PCC	AN/GD	ST	0.09	0.01	1.98	12.11	52.07	27.32	0.04	0.66	0.10	0.00	3.99	98.37	0.02	0.00	0.43	1.48	8.98	4.00	0.01	0.07	0.01	0.00	0.43	24.00
WLO-482	PCC	AN/GD	ST	0.26	0.00	9.03	7.61	33.24	48.93	0.00	0.02	0.15	0.01	0.04	99.28	0.07	0.00	1.83	0.86	5.31	6.64	0.00	0.00	0.02	0.00	0.00	24.00
WLO-790	PCC	AN/GD	ST	0.05	0.00	2.12	14.07	53.32	27.16	0.04	0.57	0.00	0.00	1.15	98.47	0.01	0.00	0.46	1.71	9.12	3.94	0.01	0.06	0.00	0.00	0.12	24.00
WLO-790	PCC	AN/GD	ST	0.08	0.02	2.17	13.85	52.72	27.79	0.03	0.67	0.03	0.00	1.14	98.50	0.02	0.00	0.47	1.68	9.01	4.03	0.00	0.07	0.00	0.00	0.12	24.00
WLO-790	PCC	AN/GD	ST	0.06	0.01	2.20	13.95	52.81	27.06	0.03	0.69	0.08	0.00	0.86	97.74	0.02	0.00	0.48	1.70	9.09	3.95	0.00	0.08	0.01	0.00	0.10	24.00
WLO-858	PCC	AN/GD	ST	0.05	0.01	2.29	14.68	51.95	27.37	0.01	1.15	0.12	0.00	1.00	98.61	0.01	0.00	0.50	1.79	8.91	3.98	0.00	0.13	0.01	0.00	0.11	24.00
WLO-858	PCC	AN/GD	ST	0.02	0.03	2.23	14.78	52.71	27.43	0.00	1.06	0.07	0.02	0.96	99.30	0.01	0.00	0.48	1.79	8.97	3.96	0.00	0.11	0.01	0.00	0.10	24.00
WLO-226	CLR	LA	HBL	1.09	0.31	6.86	22.59	9.71	43.88	10.36	0.69	0.19	0.01	0.10	95.59	0.48	0.09	2.22	4.11	2.49	9.49	2.41	0.11	0.04	0.00	0.02	32.00
WLO-228	CLR	LA	HBL	1.97	0.39	6.30	22.97	9.84	42.97	10.67	0.91	0.14	0.02	0.00	96.18	0.83	0.11	2.04	4.18	2.52	9.35	2.49	0.15	0.03	0.00	0.00	32.00
WLO-226	CLR	LA	HBL	1.98	0.33	6.35	23.55	9.29	43.22	10.55	0.90	0.24	0.03	0.00	96.43	0.83	0.09	2.06	4.29	2.38	9.41	2.46	0.15	0.04	0.01	0.00	32.00
WLO-226	CLR	LA	PL	9.58	0.11	0.01	0.17	22.76	68.21	2.98	0.03	0.01	0.04	0.01	103.90	3.14	0.02	0.00	0.02	4.53	11.52	0.54	0.00	0.00	0.01	0.00	32.00
WLO-226	CLR	LA	PL	10.17	0.10	0.00	0.05	21.45	68.11	2.76	0.01	0.02	0.00	0.07	100.74	3.45	0.02	0.00	0.01	4.42	11.55	0.52	0.00	0.00	0.00	0.01	32.00
WLO-226	CLR	LA	PL	8.60	0.18	0.00	0.22	22.86	67.53	3.07	0.01	0.01	0.00	0.00	102.60	2.91	0.02	0.00	0.03	4.60	11.52	0.56	0.00	0.00	0.00	0.00	32.00
WLO-486	CCLR	AN/GD	PL	9.90	0.09	0.03	0.00	23.49	64.02	4.25	0.00	0.01	0.00	0.00	101.79	2.51	0.01	0.01	0.00	3.61	8.36	0.59	0.00	0.00	0.00	0.00	24.00
WLO-486	CCLR	AN/GD	PL	9.74	0.03	0.00	0.04	23.68	63.63	4.44	0.00	0.00	0.00	0.06	101.63	2.47	0.01	0.00	0.00	3.65	8.33	0.62	0.00	0.00	0.00	0.01	24.00
WLO-486	CCLR	AN/GD	PL	9.32	0.03	0.00	0.06	24.24	64.28	4.71	0.02	0.00	0.02	0.04	102.69	2.34	0.00	0.00	0.01	3.69	8.31	0.65	0.00	0.00	0.00	0.00	24.00
WLO-489	CCLR	AN/GD	PL	10.61	0.05	0.02	0.10	21.95	65.90	2.50	0.02	0.00	0.00	0.12	101.27	2.68	0.01	0.00	0.01	3.38	8.60	0.35	0.00	0.00	0.00	0.01	24.00
WLO-489	CCLR	AN/GD	PL	10.76	0.05	0.00	0.05	22.40	66.16	2.67	0.03	0.02	0.00	0.00	102.13	2.70	0.01	0.00	0.01	3.42	8.57	0.37	0.00	0.00	0.00	0.00	24.00
WLO-489	CCLR	AN/GD	PL	10.81	0.04	0.00	0.07	21.91	65.56	2.44	0.00	0.00	0.00	0.00	100.82	2.75	0.01	0.00	0.01	3.39	8.60	0.34	0.00	0.00	0.00	0.00	24.00
WLO-513	CCLR	AN/GD	PL	11.64	0.06	0.01	0.19	21.07	66.94	1.58	0.00	0.00	0.01	0.16	101.67	2.94	0.01	0.00	0.02	3.23	8.71	0.22	0.00	0.00	0.00	0.02	24.00
WLO-513	CCLR	AN/GD	PL	11.33	0.07	0.00	0.05	20.71	66.76	1.50	0.03	0.01	0.01	0.00	100.48	2.88	0.01	0.00	0.00	3.20	8.78	0.21	0.00	0.00	0.00	0.00	24.00
WLO-788	CCLR	AN/GD	PL	10.49	0.07	0.00	0.04	22.71	65.85	3.47	0.00	0.00	0.00	0.00	102.63	2.62	0.01	0.00	0.00	3.46	8.51	0.48	0.00	0.00	0.00	0.00	24.00
WLO-788	CCLR	AN/GD	PL	10.45	0.05	0.00	0.01	22.91	65.59	3.43	0.07	0.01	0.00	0.04	102.56	2.62	0.01	0.00	0.00	3.49	8.48	0.48	0.01	0.00	0.00	0.00	24.00
WLO-788	CCLR	AN/GD	PL	10.61	0.04	0.00	0.18	22.89	65.79	3.53	0.03	0.02	0.03	0.05	103.16	2.65	0.01	0.00	0.02	3.47	8.47	0.49	0.00	0.00	0.00	0.00	24.00

Table 26. (continued)
Electron Microprobe Data

SAMPLE #	LITH UNIT	ALTN ZONE	MINERAL	NA2O	K2O	MGO	FEO	AL2O3	SIO2	CAO	TIO2	MNO	CR2O3	ZNO	TOTALS	NA	K	MG	FE	AL	SI	CA	TI	MN	CR	ZN	O
WLO-488	CCLR	AN/GD	BIO	0.41	7.64	12.55	19.04	17.05	35.68	0.24	1.05	0.10	0.00	0.09	93.83	0.13	1.63	3.13	2.67	3.36	5.97	0.04	0.13	0.01	0.00	0.00	24.00
WLO-788	CCLR	AN/GD	BIO	0.23	9.02	10.91	19.90	17.56	35.80	0.07	1.16	0.00	0.04	0.10	94.78	0.07	1.93	2.72	2.78	3.46	5.99	0.01	0.15	0.00	0.00	0.01	24.00
WLO-513	CCLR	AN/GD	CDT	0.28	0.04	8.20	7.78	33.02	46.50	0.02	0.01	0.09	0.08	0.04	98.06	0.07	0.01	1.68	0.89	5.35	8.87	0.00	0.00	0.01	0.01	0.00	24.00
WLO-513	CCLR	AN/GD	CDT	0.33	0.02	8.35	7.52	32.76	48.38	0.01	0.03	0.14	0.04	0.04	97.62	0.09	0.00	1.72	0.87	5.33	8.87	0.00	0.00	0.02	0.00	0.00	24.00
WLO-486	CCLR	AN/GD	CHL	0.00	0.00	12.11	29.04	23.08	23.95	0.00	0.06	0.02	0.04	0.05	88.34	0.00	0.00	3.30	4.44	4.97	4.38	0.00	0.01	0.00	0.01	0.01	24.00
WLO-489	CCLR	AN/GD	CHL	0.07	0.16	9.96	30.30	18.40	27.81	0.24	0.13	0.24	0.04	0.17	87.53	0.03	0.04	2.76	4.70	4.02	5.16	0.05	0.02	0.04	0.01	0.02	24.00
WLO-513	CCLR	AN/GD	CHL	0.00	0.01	13.94	24.52	22.22	24.30	0.04	0.11	0.04	0.03	0.03	85.23	0.00	0.00	3.85	3.80	4.85	4.50	0.01	0.01	0.01	0.00	0.00	24.00
WLO-486	CCLR	AN/GD	GNT	0.00	0.00	3.59	35.66	20.95	37.17	2.05	0.08	1.08	0.00	0.11	100.66	0.00	0.00	0.88	4.78	3.95	5.95	0.35	0.01	0.15	0.00	0.01	24.00
WLO-488	CCLR	AN/GD	GNT	0.00	0.00	3.65	35.94	20.91	36.69	1.15	0.00	1.17	0.02	0.04	99.58	0.00	0.00	0.88	4.87	3.99	5.95	0.20	0.00	0.16	0.00	0.00	24.00
WLO-486	CCLR	AN/GD	GNT	0.06	0.01	3.53	34.93	21.06	37.05	1.76	0.00	1.09	0.00	0.08	99.58	0.02	0.00	0.85	4.71	4.00	5.98	0.30	0.00	0.15	0.00	0.01	24.00
WLO-489	CCLR	AN/GD	GNT	0.01	0.02	4.25	35.40	21.20	37.34	0.47	0.01	1.36	0.01	0.02	100.10	0.00	0.00	1.02	4.74	4.00	5.98	0.08	0.00	0.18	0.00	0.00	24.00
WLO-489	CCLR	AN/GD	GNT	0.00	0.00	3.73	36.26	20.99	37.20	0.41	0.02	1.37	0.00	0.12	100.08	0.00	0.00	0.90	4.88	3.98	5.99	0.07	0.00	0.19	0.00	0.01	24.00
WLO-489	CCLR	AN/GD	GNT	0.03	0.00	4.12	34.57	21.02	37.07	0.47	0.04	1.29	0.00	0.03	98.64	0.01	0.00	0.99	4.69	4.02	6.01	0.08	0.01	0.18	0.00	0.00	24.00
WLO-788	CCLR	AN/GD	GNT	0.09	0.02	3.45	37.68	20.68	37.86	0.82	0.00	0.91	0.00	0.01	101.33	0.03	0.00	0.82	5.03	3.89	6.01	0.14	0.00	0.12	0.00	0.00	24.00
WLO-788	CCLR	AN/GD	GNT	0.04	0.00	3.51	37.97	21.11	37.50	0.87	0.02	0.66	0.01	0.17	102.05	0.01	0.00	0.83	5.04	3.95	5.95	0.15	0.00	0.12	0.00	0.02	24.00
WLO-788	CCLR	AN/GD	GNT	0.01	0.01	3.68	37.33	20.89	37.37	1.11	0.06	0.85	0.01	0.04	101.35	0.00	0.00	0.88	4.98	3.93	5.96	0.19	0.01	0.12	0.00	0.00	24.00
WLO-486	CCLR	AN/GD	AN/GD	2.06	0.00	9.92	26.92	15.87	41.53	0.24	0.16	0.27	0.02	0.04	97.01	0.63	0.00	2.35	3.57	2.97	6.59	0.04	0.02	0.04	0.00	0.00	24.00
WLO-488	CCLR	AN/GD	AN/GD	2.15	0.02	10.07	26.39	16.43	41.23	0.23	0.13	0.28	0.03	0.17	97.10	0.66	0.00	2.38	3.50	3.07	6.53	0.04	0.02	0.03	0.00	0.02	24.00
WLO-486	CCLR	AN/GD	AN/GD	1.97	0.03	10.43	27.35	15.46	41.85	0.28	0.18	0.23	0.09	0.05	97.89	0.60	0.01	2.45	3.61	2.87	6.60	0.05	0.02	0.03	0.01	0.01	24.00
WLO-489	CCLR	AN/GD	AN/GD	2.30	0.00	9.37	27.01	19.12	39.25	0.11	0.17	0.40	0.00	0.01	97.73	0.70	0.00	2.21	3.57	3.58	6.21	0.02	0.02	0.05	0.00	0.00	24.00
WLO-489	CCLR	AN/GD	AN/GD	2.21	0.01	9.14	26.45	19.53	38.97	0.12	0.19	0.34	0.00	0.09	97.05	0.68	0.00	2.16	3.51	3.68	6.19	0.02	0.02	0.05	0.00	0.01	24.00
WLO-513	CCLR	AN/GD	AN/GD	2.33	0.01	8.67	25.53	19.21	38.62	0.07	0.14	0.34	0.01	0.09	95.01	0.73	0.00	2.09	3.45	3.66	6.25	0.01	0.02	0.05	0.00	0.01	24.00
WLO-513	CCLR	AN/GD	AN/GD	2.18	0.01	8.44	25.70	19.23	38.65	0.12	0.13	0.39	0.02	0.12	95.20	0.68	0.00	2.03	3.47	3.66	6.27	0.02	0.02	0.05	0.00	0.01	24.00
WLO-513	CCLR	AN/GD	AN/GD	2.25	0.03	8.84	25.02	19.04	39.19	0.08	0.13	0.35	0.06	0.01	94.99	0.70	0.01	2.12	3.37	3.61	6.31	0.01	0.02	0.05	0.01	0.00	24.00
WLO-788	CCLR	AN/GD	AN/GD	2.33	0.04	8.42	28.78	18.93	36.77	0.14	0.20	0.17	0.00	0.03	97.62	0.72	0.01	2.00	3.84	3.56	6.16	0.02	0.02	0.02	0.00	0.00	24.00
WLO-788	CCLR	AN/GD	AN/GD	2.25	0.01	8.49	28.19	18.66	39.15	0.16	0.17	0.19	0.01	0.09	97.35	0.70	0.00	2.02	3.78	3.51	6.25	0.03	0.02	0.03	0.00	0.01	24.00
WLO-788	CCLR	AN/GD	AN/GD	2.25	0.01	8.66	29.00	18.81	39.58	0.13	0.19	0.13	0.03	0.00	98.58	0.69	0.00	2.04	3.83	3.46	6.25	0.02	0.02	0.02	0.00	0.00	24.00
WLO-513	CCLR	AN/GD	ST	0.00	0.00	1.94	14.36	52.09	27.34	0.02	0.92	0.08	0.00	0.49	97.25	0.00	0.00	0.42	1.78	9.01	4.01	0.00	0.10	0.01	0.00	0.05	24.00
WLO-513	CCLR	AN/GD	ST	0.02	0.01	2.02	13.64	35.16	26.70	0.00	0.42	0.10	0.00	0.50	78.56	0.01	0.00	0.55	2.09	7.59	4.89	0.00	0.06	0.02	0.00	0.07	24.00
WLO-513	CCLR	AN/GD	ST	0.06	0.00	1.94	13.24	52.09	27.49	0.01	0.69	0.07	0.03	0.58	96.20	0.02	0.00	0.43	1.63	9.06	4.06	0.00	0.08	0.01	0.00	0.06	24.00

Table 27.
Selected Representative Electron Microprobe Data of Thomas (1991)

SAMPLE #	LITH UNIT	ALTN ZONE	MINERAL	N	NA2O	K2O	MGO	FEO	AL2O3	SIO2	CAO	TIO2	MNO	TOTALS	NA	K	MG	FE	AL	SI	CA	TI	MN	O
660004	LF*	LA	HBL	*	0.91	0.84	9.74	18.69	10.29	44.93	11.98	0.63	0.32	98.22	0.27	0.13	2.27	2.44	1.89	7.02	2.01	0.07	2.44	24.00
660023	MMF	LA	HBL	*	1.55	1.28	4.94	24.79	11.97	40.04	11.05	0.84	1.25	97.73	0.50	0.27	1.21	3.41	2.32	6.59	1.95	0.09	0.17	24.00
660005	WLH-FWF	LA	HBL	*	1.59	0.20	11.26	15.51	12.85	44.27	11.26	0.51	0.21	97.78	0.47	0.04	2.58	2.00	2.33	6.82	1.86	0.06	0.03	24.00
660067	WLH-FWF	LA	HBL	*	1.22	0.80	10.80	16.41	10.06	44.71	12.07	0.56	0.14	98.85	0.37	0.16	2.50	2.39	1.84	6.95	2.01	0.07	0.02	24.00
660014	LF*	LA	BIO	*	0.11	9.55	9.26	23.64	15.66	35.53	0.02	2.25	0.28	96.50	0.04	2.05	2.33	3.33	3.15	5.98	0.00	0.28	0.04	24.00
660125	MMF	LA	BIO	*	0.00	8.08	11.91	22.52	16.76	35.48	0.02	1.72	0.12	96.69	0.00	1.70	2.94	3.11	3.27	5.87	0.00	0.21	0.02	24.00
660024	QFF	LA	BIO	*	0.08	9.35	4.76	28.76	16.89	34.76	0.00	1.94	0.52	96.88	0.02	2.05	1.22	4.13	3.38	5.98	0.00	0.25	0.08	24.00
660010	WLH-FWF	LA	BIO	*	0.05	4.27	12.01	24.17	15.62	31.96	1.04	2.78	0.14	92.13	0.01	0.95	3.12	3.52	3.20	5.56	0.19	0.36	0.02	24.00
660018	LF*	BIO	BIO	*	0.83	7.42	20.56	8.20	15.23	40.56	0.00	0.63	0.03	93.53	0.25	1.49	4.83	1.08	2.83	6.40	0.00	0.07	0.00	24.00
660049	QFF	BIO	BIO	*	0.40	9.40	21.10	5.52	17.67	40.21	0.02	0.74	0.00	95.07	0.12	1.85	4.86	0.71	3.22	6.22	0.00	0.09	0.00	24.00
660072	QFF	BIO	BIO	*	0.25	9.03	20.99	5.74	18.15	39.77	0.01	0.88	0.03	94.85	0.07	1.78	4.84	0.74	3.16	6.15	0.07	0.10	0.00	24.00
660109	QFF	BIO	BIO	*	0.47	9.29	20.35	6.78	16.75	40.02	0.00	0.78	0.02	94.42	0.14	1.86	4.75	0.89	3.09	6.30	0.00	0.09	0.00	24.00
660018	WLH-FWF	BIO	BIO	*	0.27	8.70	18.28	11.60	16.03	37.90	0.03	0.88	0.02	93.81	0.08	1.79	4.41	1.57	3.05	6.13	0.01	0.11	0.00	24.00
660040	LF*	BIO	CHL	*	0.10	0.12	17.56	21.56	16.16	27.97	0.15	0.02	0.15	85.89	0.04	0.03	4.73	3.26	3.87	5.05	0.03	0.00	0.02	24.00
660072	LF*	BIO	CHL	*	0.25	9.03	20.99	5.74	18.15	39.77	0.01	0.88	0.03	94.85	0.07	1.78	4.64	0.74	3.16	6.15	0.00	0.10	0.00	24.00
660067	LF*	AN/GD	BIO	*	0.12	6.16	17.23	12.60	15.96	39.26	0.00	1.11	0.05	94.57	0.04	1.67	4.11	1.68	3.01	6.28	0.00	0.13	0.01	24.00
660125	LF*	AN/GD	BIO	*	0.79	7.63	20.34	8.71	14.85	40.78	0.00	0.67	0.00	93.98	0.24	1.53	4.77	1.15	2.78	6.42	0.00	0.10	0.00	24.00
660042	MMF	AN/GD	BIO	*	0.74	7.33	16.42	10.94	15.54	39.46	0.00	0.79	0.07	93.48	0.23	1.50	4.40	1.47	2.93	6.32	0.00	0.10	0.01	24.00
660042	MMF	AN/GD	BIO	*	0.74	7.33	16.42	10.94	15.54	39.46	0.00	0.79	0.07	93.48	0.23	1.50	4.40	1.47	2.93	6.32	0.00	0.10	0.01	24.00
660067	WLH-FWF	AN/GD	BIO	*	0.00	7.98	15.58	14.00	16.35	37.58	0.05	0.95	0.08	92.69	0.00	1.68	3.82	1.93	3.17	6.19	0.01	0.12	0.01	24.00
660080	LF*	AN/GD	CHL	*	0.05	0.01	17.14	23.36	22.45	25.31	0.00	0.07	0.00	88.43	0.02	0.00	4.52	3.48	4.68	4.48	0.00	0.01	0.00	24.00
660078	MMF	AN/GD	CHL	*	0.00	0.04	22.38	16.80	22.93	26.92	0.02	0.03	0.02	88.96	0.00	0.01	5.65	2.35	4.58	4.56	0.00	0.00	0.00	24.00
660113	WLH-FWF	AN/GD	CHL	*	0.00	0.03	22.61	15.72	22.48	26.65	0.00	0.16	0.03	87.73	0.00	0.01	5.77	2.25	4.53	4.56	0.00	0.02	0.00	24.00
660069	LF*	AN/GD	AN/GD	*	0.20	0.00	21.21	18.41	2.50	53.53	0.29	0.05	0.11	96.30	0.06	0.00	4.77	2.32	0.44	8.07	0.05	0.01	0.01	24.00
660110	LF*	AN/GD	AN/GD	*	0.00	0.07	19.67	20.35	1.55	55.59	0.07	0.07	0.09	97.63	0.00	0.01	4.38	2.55	0.27	8.30	0.01	0.01	0.01	24.00
660042	MMF	AN/GD	AN/GD	*	0.12	0.06	18.88	20.45	2.70	52.23	0.39	0.03	0.23	95.14	0.04	0.01	4.35	2.64	0.49	8.07	0.06	0.00	0.03	24.00
660113	WLH-FWF	AN/GD	AN/GD	*	0.00	0.02	20.38	20.94	1.96	53.27	0.16	0.00	0.12	96.81	0.00	0.00	4.61	2.66	0.35	8.08	0.03	0.00	0.02	24.00

* LF undivided: FSP (feldspar)-phyric vs. APH (aphyric)
** reported composition is average of N mineral analyses per sample